

UNCLASSIFIED

AD NUMBER

ADB029580

LIMITATION CHANGES

TO:

Approved for public release; distribution is unlimited.

FROM:

Distribution authorized to U.S. Gov't. agencies only; Test and Evaluation; 05 FEB 1978. Other requests shall be referred to Manufacturing Technology Division, Air Force Materials Laboratory, Wright-Patterson AFB, OH 45433.

AUTHORITY

AFWAL ltr, 6 Oct 1981

THIS PAGE IS UNCLASSIFIED

**THIS REPORT HAS BEEN DELIMITED  
AND CLEARED FOR PUBLIC RELEASE  
UNDER DOD DIRECTIVE 5200.20 AND  
NO RESTRICTIONS ARE IMPOSED UPON  
ITS USE AND DISCLOSURE.**

**DISTRIBUTION STATEMENT A**

**APPROVED FOR PUBLIC RELEASE;  
DISTRIBUTION UNLIMITED.**

NTZ

AFML-TR-77-185 ✓

VOLUME I

②  
LEVEL

AD B 0 2 9 5 8 0

# VERIFICATION OF PRODUCTION HOLE QUALITY

METCUT RESEARCH ASSOCIATES INC.  
CINCINNATI, OH 45209

NOVEMBER 1977

TECHNICAL REPORT AFML-TR-77-185  
FINAL REPORT AUGUST 1975-SEPTEMBER 1977

DDC  
RECORDED  
AUG 29 1978  
A

ADJ NU.  
DDC FILE COPY

*Distribution limited to U.S. Government agencies only;  
Test and Evaluation Data: 5 February 1978. Other  
requests for this document must be referred to the  
Manufacturing Technology Division, Air Force Materials  
Laboratory, Wright-Patterson Air Force Base, Ohio 45433*

78 08 28 115

AIR FORCE MATERIALS LABORATORY  
AIR FORCE WRIGHT AERONAUTICAL LABORATORIES  
AIR FORCE SYSTEMS COMMAND  
WRIGHT-PATTERSON AIR FORCE BASE, OHIO 45433

NOTICES

When Government drawings, specifications, or other data are used for any purpose other than in connection with a definitely related Government procurement operation, the United States Government thereby incurs no responsibility for any obligation whatsoever; and the fact that the Government may have formulated, furnished, or in any way supplied the said drawings, specifications, or other data, is not to be regarded by implication or otherwise as in any manner licensing the holder or any other person or corporation, or conveying any rights or permission to manufacture, use or sell any patented invention that may in any way be related thereto.

Copies of this report should not be returned unless return is required by security considerations, contractual obligations, or notice on a specific document.

This final report was submitted by Metcut Research Associates Inc., Cincinnati, Ohio, under Contract No. F33615-75-C-5173, Manufacturing Methods Project 760-5, "Verification of Production Hole Quality". Mr. William A. Harris, AFML/LTM, was the laboratory monitor.

This technical report has been reviewed and is approved for publication.

ACCESSION BY	
BY	DATE
DATE	DATE
UNCLASSIFIED	<input type="checkbox"/>
RESTRICTED	<input checked="" type="checkbox"/>
DISTRIBUTION AVAILABILITY STATEMENTS	
CLASS.	AVAIL. STATE. OR SPECIAL
B	

*William A. Harris*  
WILLIAM A. HARRIS  
Project Engineer

FOR THE COMMANDER

*H. A. Johnson*  
H. A. JOHNSON  
Chief, Metals Branch  
Manufacturing Technology Division



Unclassified

SECURITY CLASSIFICATION OF THIS PAGE (When Data Entered)

<b>19 REPORT DOCUMENTATION PAGE</b>		READ INSTRUCTIONS BEFORE COMPLETING FORM	
<b>1</b> REPORT NUMBER	<b>2</b> GOVT ACCESSION NO.	<b>3</b> RECIPIENT'S CATALOG NUMBER	
AFML TR-77-185 Vol. 1	1	9 Kept.	
<b>4</b> TITLE (and Subtitle)		<b>5</b> TYPE OF REPORT & PERIOD COVERED	
6 VERIFICATION OF PRODUCTION HOLE QUALITY Volume I.		Final 1 Aug 1975 - 31 Jul 1977	
<b>6</b>		<b>14</b>	<b>7</b> PERFORMING ORG. REPORT NUMBER
			978-22800-5
<b>8</b> AUTHOR(s)		<b>9</b> CONTRACT OR GRANT NUMBER(s)	
10 William P. Koster, John B. Kohls, and John T. Cammett (Metcut Research), B.L. Cornell (Lockheed-Georgia Company)		15 F33615-75-C-5173	
<b>7</b> PERFORMING ORGANIZATION NAME AND ADDRESS		<b>10</b> PROGRAM ELEMENT, PROJECT, TASK AREA & WORK UNIT NUMBERS	
Metcut Research Associates Inc. 3980 Rosslyn Drive Cincinnati, OH 45209		760-5	
<b>11</b> CONTROLLING OFFICE NAME AND ADDRESS		<b>10</b> REPORT DATE	
Air Force Materials Laboratory Air Force Systems Command Wright-Patterson Air Force Base, OH 45433		11 Nov 1977	
<b>14</b> MONITORING AGENCY NAME & ADDRESS (if different from Controlling Office)		<b>11</b> NUMBER OF PAGES	
12 246p.		232	
		<b>15</b> SECURITY CLASS. (of this report)	
		Unclassified	
		<b>15a</b> DECLASSIFICATION/DOWNGRADING SCHEDULE	
<b>16</b> DISTRIBUTION STATEMENT (of this Report)			
Distribution limited to U.S. Government agencies only; Test and Evaluation Data; 5 February 1978. Other request for this document must be referred to the Manufacturing Technology Division Air Force Materials Laboratory, Wright-Patterson Air Force Base, Ohio 45433.			
<b>17</b> DISTRIBUTION STATEMENT (of the abstract entered in Block 20, if different from Report)			
<b>18</b> SUPPLEMENTARY NOTES			
<b>19</b> KEY WORDS (Continue on reverse side if necessary and identify by block number)			
surface integrity, hole quality, tapered fastener, interference, perpendicularity, bellmouthing, barrelling, ovality, surface finish, rifling, axial scratch, chatter, plastic deformation, tears, laps			
<b>20</b> ABSTRACT (Continue on reverse side if necessary and identify by block number)			
Definitive surface integrity information identifying and ranking the importance of hole quality variables on the performance of tapered interference fit fasteners has been developed. This report summarizes the fatigue behavior of open hole specimens and low load transfer specimens containing a variety of metallurgical and geometric hole quality variables. Limited crack growth behavior is also reported.			

Unclassified

SECURITY CLASSIFICATION OF THIS PAGE (When Data Entered)

22.7 2.00

28 115

1/5

## FOREWORD

This final technical report covers all work performed under Contract F33615-75-C-5173 entitled "Verification of Production Hole Quality". This project was accomplished under the technical direction of W.A. Harris of the Metals Branch (LTM), Manufacturing Technology Division, Air Force Materials Laboratory, Wright-Patterson Air Force Base, Ohio. The effort was performed during the period 1 August 1975 through 31 July 1977 and was released by the authors in September 1977. The effort dealt with the quality requirements for an interference fit tapered fastener system, and was oriented toward a specific application within the C-5A aircraft program. The material and fastener design selected were chosen because that combination was one considered for extensive use in future wing structure developments of the C-5A aircraft.

The subject contract was placed with Metcut Research Associates Inc. of Cincinnati, Ohio. Metcut chose as its principal subcontractor the Lockheed-Georgia Company of Marietta, Georgia. Metcut provided the overall technical direction of the program as well as the facilities for manufacturing all test specimens and performing all of the fatigue tests reported herein. The Lockheed-Georgia Company provided engineering direction and support for the analysis of the data which resulted from the effort.

At Metcut, the program was under the supervision of Dr. William P. Koster. John B. Kohls, Dr. John T. Cammett and L.R. Gatto also contributed to the effort. Activities at the Lockheed-Georgia Company were managed by C.G. Trevillion and supported by H.S. Gibson, B.L. Cornell and P.G. Dodd who performed much of the detailed numerical analysis.

This program was a continuation of the effort in the surface integrity/surface quality area which has been supported by the Air Force Materials Laboratory for the past eight years to provide information which will lead to the cost effective manufacturing of aerospace hardware by the American industrial sector.

The final technical report on this contract is being prepared in two volumes. Volume I is the final summary report on all work performed including the necessary tables to document the procedures and the results obtained. Volume II contains the complete inspection reports on all specimens manufactured under this contract.

TABLE OF CONTENTS

<u>Section</u>		<u>Page</u>
I	INTRODUCTION	1
II	OBJECT OF PROGRAM	3
III	SCOPE OF PROGRAM	4
	1. Program Constants	4
	2. Program Variables	5
IV	CONCLUSIONS	9
	1. General Conclusions	9
	2. Detailed Conclusions	11
	3. Relaxation of Hole Quality Specifications	13
	4. Significance to the Aerospace Industry	13
	5. Taper Blade Cutter Conclusion	13
V	RECOMMENDATIONS	14
	1. Supplemental Work	14
	2. Other Fastener Systems	14
	3. Other Structural Materials	14
VI	PROCEDURES	15
	1. Test Material Documentation	15
	2. Specimen Manufacture and Assembly	20
	3. Production of Hole Quality Variables	35
	4. Measurement of Hole Quality Level	54
	5. Fatigue Testing Methods	75
	6. Statistical Evaluation of Fatigue Test Data	78
	7. Fractography	79
VII	DISCUSSION AND EVALUATION	83
	1. Open Hole Specimens	83
	2. LLT Testing - Dogbone/Strap Specimens	95
	3. LLT Testing - Reverse Dogbone Specimens	128
	4. Discussion: Crack Growth Testing	139
	5. Fracture Mechanics Analysis	145
	APPENDIX	191

## LIST OF TABLES

<u>Table No.</u>		<u>Page</u>
1	Material Documentation	152
2	Fatigue Data Summary: Test Series 1	153
3	Machining Conditions Used for Milling the Specimens	154
4	Manufacturing, Inspection and Fatigue Summary: Low Load Transfer Baseling (Dogbone/Strap)	155
5	Manufacturing, Inspection and Fatigue Summary: Test Series 9, Surface Roughness	156
6	Manufacturing, Inspection and Fatigue Summary: Test Series 10	159
7	Manufacturing, Inspection and Fatigue Summary: Test Series 11	160
8	Manufacturing, Inspection and Fatigue Summary: Test Series 12	161
9	Manufacturing, Inspection and Fatigue Summary: Test Series 2, Interference Level	162
10	Manufacturing, Inspection and Fatigue Summary: Test Series 7, Perpendicularity	164
11	Manufacturing, Inspection and Fatigue Summary: Test Series 8, Barrelling	165
12	Manufacturing, Inspection and Fatigue Summary: Test Series 17, Ovality	167
13	Manufacturing, Inspection and Fatigue Summary: Test Series 18, Burrs	168
14	Manufacturing, Inspection and Fatigue Summary: Test Series 19	170
15	Alpha Beta Factor - Dogbone Plus Strap Test Data	173

LIST OF TABLES (continued)

<u>Table No</u>		<u>Page</u>
16	Manufacturing, Inspection and Fatigue Summary: Test Series 20/21	174
17	Manufacturing, Inspection and Fatigue Summary: Test Series 22	176
18	Alpha Beta Factor - Reverse Dogbone Test Data	178
19	Alpha Beta Factor - Combined Data	179
20	Summary of Load Transfer Data on Dogbone/ Strap Specimens	180
21	Summary of Load Transfer Data on Reverse Dogbone Specimens	182
22	Fatigue Precracking Results	186
23	Cyclic Life Results, Precracked Specimens	187
24	Fatigue Crack Propagation Results - Open Hole Specimens - Series 4	188

LIST OF ILLUSTRATIONS

<u>Figure No.</u>		<u>Page</u>
1	Cross Section of Extruded Solid Shape per Drawing No. 900102	16
2	Structure of Test Material Al-7175- T73511	17
3	Fatigue Strength of Test Material	19
4	Parent Metal Specimen (PM)	21
5	Low Load Transfer Dogbone/Strap Specimen (LLT)	22
6	Open Hole Specimen (OH)	23
7	Zero Load Transfer Specimen (ZLT)	24
8	Reverse Dogbone Specimen (RD)	25
9	Photograph of As-Received Extrusion of the 7175 Aluminum Test Material	26
10	Layout of Specimen Identification as it Relates to Location in Extrusions	28
11	Fixture Used for Drilling and Reaming of Specimen	31
12	Fixture Used for Drilling and Reaming of Specimen with a Strap in Place	32
13	Reaming of Dogbone/Strap Specimen as an Assembly	33
14	Sketch Showing Protrusion Height	36
15	Rollout of Bluing Pin to Permit Graphical Integration of Percent Bearing Contact	38
16	Air Gage for Measurement of Diametral Surface Deviation	39
17	Capacitance Gage to Measure Percent Bearing Between the Taper-Lok and Surface of the Hole	41

LIST OF ILLUSTRATIONS (continued)

<u>Figure No.</u>		<u>Page</u>
18	Variables in Reaming Used to Obtain Range of Interference Levels	43
19	Variation in Manufacturing Procedures to Produce a Non-Perpendicular Hole	45
20	Variations in Manufacturing Procedures to Produce Bellmouthing	46
21	Variations in Manufacturing Procedures to Produce Barrelling	47
22	Variations in Manufacturing Procedures to Produce Ovality	49
23	Sketch Showing Rifling at Intersection of Fay Surface	50
24	Sketch Showing Axial Scratch at Intersection of Fay Surface	53
25	Illustration of Chatter Produced by a Left-Hand Spiral Reamer	55
26	Optical Photographs of Holes From Test Series 9 Showing Typical Appearance of Surfaces	58
27	Scanning Electron Micrograph Showing Taper Reamed Surfaces at the 32 AA Level (Test Series 9)	59
28	Scanning Electron Micrograph Showing Taper Reamed Surface at the 63 AA Level (Test Series 9)	59
29	Scanning Electron Micrograph Showing Taper Reamed Surface at the 125 AA Level (Test Series 9)	60
30	Scanning Electron Micrograph Showing Taper Reamed Surface at the 250 AA Level (Test Series 9)	60
31	Cross Section Photomicrograph Showing Typical Taper Reamed Surface at the 32 AA Level (Test Series 9)	61
32	Cross Section Photomicrograph Showing Typical Taper Reamed Surface at the 63 AA Level (Test Series 9)	61

LIST OF ILLUSTRATIONS (continued)

<u>Figure No.</u>		<u>Page</u>
33	Cross Section Photomicrograph Showing Typical Taper Reamed Surface at the 125 AA Level (Test Series 9)	62
34	Cross Section Photomicrograph Showing Typical Taper Reamed Surface at the 250 AA Level (Test Series 9)	62
35	Optical Photograph of Hole Showing Typical Appearance of Rifling (Test Series 10)	64
36	Scanning Electron Micrographs Showing Typical Rifling (Test Series 10)	65
37	Cross Section Photomicrograph Showing Typical Rifling (Test Series 10)	66
38	Optical Photograph of Hole Showing Typical Appearance of Axial Scratch (Test Series 11)	67
39	Scanning Electron Micrographs Showing Typical Axial Scratch (Test Series 11)	68
40	Cross Section Photomicrograph Showing Typical Axial Scratch (Test Series 11)	69
41	Optical Photograph of Hole Showing Typical Appearance of Chatter (Test Series 12)	70
42	Scanning Electron Micrographs Showing Typical Chatter (Test Series 12)	71
43	Cross Section Photograph Showing Typical Chatter Condition (Test Series 12)	72
44	Optical Photograph of Hole Showing Typical Appearance of Tears/Laps/Plastic Deformation (Test Series 12)	73
45	Scanning Electron Micrographs Showing Typical Tears/Laps/Plastic Deformation (Test Series 12)	74
46	Cross Section Photomicrograph Showing Tears/Laps/Plastic Deformation (Test Series 12)	76
47	Closed Loop, Servo-Controlled Hydraulic Testing Machine	77
48	Code Established for Identifying Specimen Failure Nucleation Sites	80
49	Scanning Electron Micrographs Showing Failure Origin and Fatigue Progression Typical of Failures Originating at Different Areas of the Test Specimens	82



LIST OF ILLUSTRATIONS (continued)

<u>Figure No.</u>		<u>Page</u>
50	Fatigue Strength of Open Hole Specimens	84
51	Fatigue Summary of Open Hole Specimens	86
52	Survival Probability of Open Hole Specimens - Surface Roughness	90
53	Survival Probability of Open Hole Specimens - Rifling	91
54	Survival Probability of Open Hole Specimens - Axial Scratches	92
55	Survival Probability of Open Hole Specimens - Chatter and Tears/Laps/Plastic Deformation	93
56	Composite: Survival Probability of Open Hole Specimens	94
57	Fatigue Strength of Dogbone/Strap Specimens	96
58	Fatigue Summary of Dogbone/Strap Testing: Interference and Burrs - 22 ksi	98
59	Fatigue Summary of Dogbone/Strap Specimens	100
60	Fatigue Summary of Dogbone/Strap Testing	101
61	Fatigue Summary of Dogbone/Strap Testing Combined Variables	103
62	Alpha Beta Analysis of Dogbone/Strap Specimens	108
63	Survival Probability of Dogbone/Strap Specimens - Interference	110
64	Survival Probability of Dogbone/Strap Specimens - Perpendicularity (22 ksi)	111
65	Survival Probability of Dogbone/Strap Specimens - Perpendicularity (25 ksi)	112
66	Survival Probability of Dogbone/Strap Specimens - Bellmouthing (22 ksi)	113
67	Survival Probability of Dogbone/Strap Specimens - Bellmouthing (25 ksi)	114

LIST OF ILLUSTRATIONS (continued)

<u>Figure No.</u>		<u>Page</u>
68	Survival Probability of Dogbone/Strap Specimens - Barrelling (22 ksi)	115
69	Survival Probability of Dogbone/Strap Specimens - Barrelling (25 ksi)	116
70	Survival Probability of Dogbone/Strap Specimens - Ovality	117
71	Composite: Survival Probability of Dogbone/Strap Specimens	118
72	Survival Probability of Dogbone/Strap Specimens - Exit Burrs	119
73	Survival Probability of Dogbone/Strap Specimens - Increased Roughness	120
74	Survival Probability of Dogbone/Strap Specimens - Increased Roughness and Rifling	121
75	Survival Probability of Dogbone/Strap Specimens - Increased Roughness and Axial Scratches	122
76	Survival Probability of Dogbone/Strap Specimens - Increased Roughness and Ovality	123
77	Composite: Survival Probability of Dogbone/Strap Specimens (Increased Roughness)	125
78	Alpha Beta Analysis: All Dogbone/Strap Specimens - 50% Confidence	126
79	Alpha Beta Analysis: All Dogbone/Strap Specimens - 95% Confidence	127
80	Fatigue Summary of Reverse Dogbone Testing - Combined Variables	129
81	Alpha Beta Analysis of Reverse Dogbone Specimens	132
82	Alpha Beta Analysis: Reverse Dogbone Specimens - 50% Confidence	133
83	Alpha Beta Analysis: Reverse Dogbone Specimens - 95% Confidence	134

LIST OF ILLUSTRATIONS (continued)

<u>Figure No.</u>		<u>Page</u>
84	Alpha Beta Analysis: Reverse Dogbone Specimens - 50% Confidence	135
85	Alpha Beta Analysis: Reverse Dogbone Specimens - 95% Confidence	136
86	Alpha Beta Analysis: All Reverse Dogbone Specimens - 50% Confidence	137
87	Alpha Beta Analysis: All Reverse Dogbone Specimens - 95% Confidence	138
88	Combined Alpha Beta Analysis of All Specimens - 50% Confidence	140
89	Combined Alpha Beta Analysis of All Specimens - 95% Confidence	141
90	Schematic Illustration of Fastener Hole/Crack Geometry for Fatigue Crack Propagation Specimens	142
91	Specimen Cyclic Life as a Function of Initial Crack Length on Fay Surface	146
92	Verification of Production Hole Quality - Correlation of Test Data With Analysis	148

LIST OF ABBREVIATIONS

AA	=	Arithmetic Average
LLT	=	Low-Load Transfer
OH	=	Open Hole
PM	=	Parent Metal
R	=	Stress Ratio (minimum/maximum level of cyclic stress)
ZLT	=	Zero Load Transfer
$\alpha$	=	Hole Finish Factor
$\beta$	=	Hole Filling Factor

## SECTION I

### INTRODUCTION

Techniques used for joining have always held a key role in the design and fabrication of aircraft structures. Whenever holes are placed in components for the purpose of joining them together with bolts or similar mechanical fasteners, the stress concentration resulting from these holes significantly reduces the dynamic load which the components can safely carry. It is sometimes possible to reduce the importance of these stress concentrations by locating the holes in areas which are not critically stressed. But as a practical matter, the requirements for fasteners are so numerous and their placement in most structures so widespread that means must be used to mitigate the fatigue strength degradation due to holes and the related stress concentration. Accordingly, many varieties of "fatigue enhancement" fasteners have been developed. Some of these involve prestressing the bolt region in compression or strengthening this area by cold working so that tensile cyclic loads can better be resisted. Interference fit fasteners, on the other hand, are designed to preload the region around the hole in such a way that the range of cyclic stress to which the metal is subjected will be reduced.

Experience has shown that the performance of interference fit tapered fasteners is highly dependent upon the preparation of the holes into which they are placed. If the quality of the hole resulting from a production situation is in some way inadequate, the resulting structure may suffer a degradation in fatigue strength as exhibited by shortened operating life. Therefore, adequate controls must be exercised to assure the hole quality demanded by the fastener system to achieve optimum fatigue strength. On the other hand, it is conceivable that certain features of hole quality such as finish, roundness, straightness, etc., could be overspecified for a particular fastener system. In this instance the cost necessary to produce the structure would be unnecessarily high and the development of suitable engineering data could lead to intelligent cost reduction.

The purpose of the subject program was to determine the relative importance of each of several variations in hole quality with respect to the performance of interference fit fasteners. To make this program directly meaningful to current Air Force systems, Metcut chose to work with the Lockheed-Georgia Company, as a subcontractor and to use a material/fastener system of current importance. This decision resulted in the selection of Al 7175-T73511 extrusions in the form of integrally stiffened panels and fastened with

a nominally 5/16 in. diameter Taper-Lok fastener. This particular combination of material/fastener represents over 80% of the fasteners projected for use by Lockheed-Georgia in providing the new center and inner wing structures for the C-5A aircraft. Using technology developed under this contract, specimens were also fabricated and tested for an ongoing AGARD program.

The effort undertaken was intended to identify those variables in hole quality which are significant in terms of structural life and also to identify those which are not. Auxilliary effort was devoted to the evaluation of a tapered blade cutter for producing the required fastener holes. This cutter was advanced as an alternative to separate drilling and reaming operations. The information gathered during the course of the program should be helpful in establishing fabrication procedures which will permit the production of fastened assemblies having maximum reliability but without the expenditure of unnecessary cost. While this effort would directly support a possible forthcoming activity at the Lockheed-Georgia Company, the information produced is judged to also be of value to other aerospace firms which are employing interference fit fastener systems.

## SECTION II

### OBJECT OF PROGRAM

The object of this program was to develop hole quality criteria and related data which will facilitate the adoption of cost effective specifications for the fabrication of high strength assemblies using interference fit fasteners. Four specific objectives of the program were:

- (1) To establish quantitative hole quality data for an extruded aluminum alloy.
- (2) To identify the ranking or order of hole quality characteristics as a function of the effect on fastener life of fatigue critical interference fit fastener systems and joints.
- (3) To evaluate the performance of a tapered blade cutter in producing tapered holes suitable for fastener installation in a single operation.
- (4) To develop, fabricate and test specimens for an ongoing AGARD program (a technical summary of this work is contained in the Appendix of this report).

## SECTION III

### SCOPE OF PROGRAM

#### 1. Program Constants

##### Material:

Aluminum alloy 7175-T73511 in the extrusion form, conforming to the applicable GELAC (Lockheed-Georgia Company) specification

##### Material Thickness:

5/16 in. as tested, with minimum of .050 in. material removal from the as-extruded surface

##### Material Surface Treatment:

Shot peened per STP51-501, Revision G\*  
Anodize per STP58-208, Revision E\*  
Coating per STP59-505, Revision C\*

##### Fastener:

Alloy Steel (8740) Taper-Lok, 5/16 in. diameter, 100° countersink flush head in a 5/8 in. fastened assembly. Fastener to be wet installed with sealant per STP56-107. Revision F.\*

##### Evaluation - Destructive:

Fatigue testing at room temperature, nominally 900-1800 cycles/minute, R = 0.1 and -.33. Metallography before and after testing, residual stress profile determination using x-ray diffraction.

##### Evaluation - Nondestructive:

Surface roughness, hole metrology and hole bearing using both mechanical and capacitance techniques.

##### Correlation Analysis:

Determine fatigue crack growth rate on specimens containing artificially produced corner flaws. Correlate crack growth behavior with discrepant specimens to determine equivalent initial flaw size of discrepant conditions.

---

\* STP XXX = Specification of the Lockheed-Georgia Company



## 2. Program Variables

Certain variables of hole quality were introduced into the program as indicated below:

### Mechanical Variables:

Hole size, perpendicularity, bellmouthing, barrelling, ovality, bearing, and exit burr.

### Surface Integrity Variables in Hole Quality:

Roughness, rifling, axial scratches, chatter marks, plastic deformation, tears and laps.

Details concerning the range and limiting values of the program variables are as indicated below:

### Test Series 1

Parent metal specimens without fastener holes comparing the as-milled to the milled plus shot peened condition; 20 specimens.

### Test Series 2

Low-load transfer (dogbone/strap) specimens comparing five levels of interference fit fasteners, five specimens at each level. The levels of diametral interference were .0005, .0023, .0035, .0048 and .0060 inches.

Note: Test Series 3 was eliminated during program negotiations.

### Test Series 4

Open hole specimens having a crack oriented normal to the load line initiated in the fastener hole prior to fatigue testing; three specimens.

### Test Series 5

Zero load transfer (modified dogbone with sectioned strap) specimens. A crack oriented normal to the load line initiated in a dogbone fastener hole prior to fatigue testing and having a fastener installed with a neat fit (zero interference); three specimens.

#### Test Series 6

Low-load transfer (dogbone/strap) specimens having a crack oriented normal to the load line initiated in the fastener hole of the dogbone. The fastener was installed with a neat fit (zero interference); three specimens.

#### Test Series 7

Low-load transfer (dogbone/strap) specimens evaluating a 3° nonperpendicular centerline. This angle of deviation was normal to the load line. This condition was evaluated at two levels of interference, the first being the minimum allowable interference per the controlling specification and the second level being the maximum allowable interference, .0023 in. and .0048 inches, respectively. Each level or condition contained ten specimens each.

#### Test Series 8

Low-load transfer (dogbone/strap) specimens - bell-mouthing. This condition was evaluated at two levels of interference, the minimum and maximum values allowable per the controlling specifications. Ten specimens each level.

Low-load transfer (dogbone/strap) specimens - barrelling. As in bellmouthing, this variable was evaluated at two levels of interference, the minimum and maximum values allowable per the controlling specification. Ten specimens each level.

#### Test Series 9

Open hole specimens - surface roughness. Four levels of surface roughness were evaluated, 32, 63, 125 and 250 microinches AA. Five specimens were tested at levels 32 and 125 AA. Eight specimens were tested at level 63 and ten specimens at level 250 AA. The controlling specification identifies 63 microinches as the maximum acceptable level.

#### Test Series 10

Open hole specimens - rifling. Rifling with a spiral groove approximately .005 in. to .007 in. deep at the exit of the hole. Ten specimens were evaluated.

### Test Series 11

Open hole specimens - scratches. An axial scratch approximately .005 in. to .007 in. deep was located 90 degrees to the load line; ten specimens were evaluated.

### Test Series 12

Open hole specimens - chatter. Chatter was visually observed to maintain a constant level. Ten specimens were evaluated.

Open hole specimens - tears and laps plus plastic deformation. This discrepant variable was evaluated at one level of deformation, approximately .002 in.; ten specimens were evaluated.

Note: Test Series 13 through 16 were eliminated during program negotiations.

### Test Series 17

Low-load transfer (dogbone/strap) specimens - ovality. The oval hole was oriented such that lack of interference would occur 90 degrees to the load line. The amount of ovality was between .005 in. and .007 in.; ten specimens were evaluated.

### Test Series 18

Low-load transfer (dogbone/strap) specimens - burrs. Four different groups of five specimens each were evaluated. These four levels were with and without burrs on the exit of the hole at two levels of interference; minimum and maximum specification limits. The average burr height was between .015 in. and .020 inches.

### Test Series 19

Low-load transfer (dogbone/strap) specimens. This series was a combination of various discrepant variables from the earlier portion of the program. Constant in this test series was a roughness height reading of between 100 and 125 microinch AA. Four different conditions were evaluated: (1) surface roughness value alone; (2) surface roughness plus an axial scratch; (3) surface roughness plus rifling and (4) surface roughness plus ovality. Each of these four combinations was evaluated at both the minimum and maximum interference specification value. There were five specimens for each condition; a total of 40 specimens for this test series.

### Test Series 20 and 21

Low-load transfer (reverse dogbone) specimens. This was a combination of variables similar to Test Series 19. Surface roughness of 100 to 125 microinch AA and a mid-level (.0035 in.) of interference were constants. Four combinations were evaluated: (1) surface roughness by itself; (2) surface roughness plus scratches; (3) surface roughness plus rifling, and (4) surface roughness plus ovality. Ten specimens were evaluated each combination, a total of 40 specimens.

### Test Series 22

Low-load transfer (reverse dogbone) specimens. Surface roughness and the mid-level of interference were constant throughout this test series. Three combinations were tested: (1) surface roughness by itself; (2) surface roughness plus scratch; and (3) surface roughness plus ovality. Ten specimens per each condition; a total of thirty specimens. The difference between this test series and Series 20/21 was the mode of testing. The stress ratio (R) for Test Series 22 was -0.33, indicating that the minimum component of the cyclic load was compressive. (All other tests were run at  $R = +0.1$ ).

### Test Series 23

Low-load transfer (reverse dogbone) specimens. These specimens are to be spectrum tested at a later date. In manufacturing, surface roughness in the range of 100-125 AA and the mid-range of interference were held as constants. The four levels manufactured were: (1) surface roughness by itself; (2) surface roughness plus ovality; (3) surface roughness plus barrelling; and (4) surface roughness plus rifling. Five specimens are planned for each level; a total of 20 specimens.

## SECTION IV

### CONCLUSIONS

This program has examined the effect of various conditions and hole quality discrepancies on the fatigue performance capabilities of a tapered interference fit fastener system. The conditions evaluated were basically related to hole quality levels which might logically occur in a production environment. In broad summary relative to the practice of producing holes, certain conclusions have been reached or implied as a result of the testing accomplished in this program. These conclusions are based solely on the test results obtained within the parameters selected for use in this program. Specific applicability of these results to the C-5A program, however, can be determined only after currently planned tests using a spectrum loading regime are completed and evaluated by cognizant structures engineering.

#### 1. General Conclusions

The broad conclusions may be drawn that a surface roughness of 125 AA or better is similar in behavior insofar as fatigue is concerned; that burrs at the nut side exit of the hole do not have detrimental effects on joint fatigue life; that lack of hole axis perpendicularity within 3° of normal to the load path is of no concern to joint fatigue life; that hole ovality is of serious concern and is detrimental to joint fatigue strength; that bellmouthing and barrelling are of concern, but to a lesser extent than ovality; and that there is a limiting size or extent at which scratches, rifling, chatter, plastic deformation, tears and laps, etc., may not be of serious detriment to joint fatigue life.

A tabular summary of these findings along with an indication of their impact on current manufacturing specifications at the Lockheed-Georgia Company is tabulated on the following page:

<u>Condition</u>	<u>Detrimental Effect</u>			<u>Spec. Change</u>
	<u>None</u>	<u>Moderate</u>	<u>Severe</u>	
Surface Finish 125 AA or better 125-250 AA	X		X	Revised 63 AA to 125 AA
Interference .0023-.0048	X			No Change
Exit Burrs	X			N/C, Removal Not Required
Perpendicularity	X			N/C, Remaining Within 2°
Bellmouthing, Barrelling, Ovality (.006")			X	N/C, None Allowed
Axial Scratches (.006") Open Hole Joint		X	X	N/C, None Allowed N/C, None Allowed
Rifling (.006") Open Hole Joint	X		X	N/C, None Allowed N/C, None Allowed
Chatter, Etc.		X		N/C, None Allowed

The ranking order of hole quality characteristics as determined by effect on fatigue life of fastened joints is summarized below. The ranking is based on an alpha beta analysis for three different levels of survival probability and confidence; the most detrimental effect is at the top of each column:

(50,50)*	(99,50)	(99,95)
Barrelling	Ovality	Bellmouthing
Ovality	Bellmouthing	Ovality
Bellmouthing	Barrelling	Scratches
Scratches	Scratches	Barrelling
Rifling	Rifling	Rifling
Perpendicularity	Perpendicularity	Perpendicularity

\*(Survival Probability, Confidence)

## 2. Detailed Conclusions

Interference: Joint fatigue life performance is roughly equivalent from minimum specification interference to maximum specification interference where holes have no discrepancies. This conclusion is based on performance of all applicable test series. However, test data indicates that low interference installations are prone to a higher amount of scatter than high interference installations.

Perpendicularity: Test results indicate that there are no reductions in joint fatigue life for up to 3° misalignment from the centerline of the hole relative to perpendicularity with the joint sheet surface when the plane of angle is normal to the loading direction. In view of the nature of the effects of misalignment coincident with the direction of loading, a more involved test would be required to determine the effects of joint fatigue life of transferring load pickup from one fastener to another because of various degrees of misalignment. No testing was included in this area and therefore the conclusions on the direction normal to loading cannot be expanded to include misalignment coincident to loading.

Bellmouthing: Testing indicates that bellmouthing has a serious detrimental effect on joint fatigue life at the minimum specified interference. At maximum specified interference, however, the detrimental effect is much smaller.

Barrelling: Testing indicates that barrelling has a serious detrimental effect on joint fatigue life.

Ovality: Ovality has a highly detrimental effect on joint fatigue life; it is more serious than any other single condition evaluated.

Exit Burr: Due to the absence of failures associated with exit burrs, i.e., burrs at the nut side of the hole, a conclusion is drawn that the presence of hole exit burrs has no detrimental effect on joint fatigue life. Burrs at the faying surface, however, were not evaluated.

Surface Roughness: Failure modes of specimens with a hole surface roughness of 125 AA and lower were disassociated with surface roughness. Failures of 250 AA

specimens were directly related to the hole surface roughness. Therefore, the conclusion is drawn that a 125 AA or lower roughness yields similar results for the tapered fastener, but a finish rougher than 125 AA must be avoided.

Rifling: Testing indicated that rifling has a seriously detrimental effect on fatigue life of open holes. Specimens with fasteners installed, however, indicate that rifling of the magnitude tested had no effect. The magnitude of rifling was similar for open hole and installed fastener testing. Apparently the interference of the pin reduces the detrimental effects of rifling of the magnitude used. Further testing could identify the magnitude of rifling which would be detrimental even with fastener interference. The current conclusion must be that rifling may have a detrimental effect.

Axial Scratches: Again open hole testing indicated that axial scratches are seriously detrimental. With fasteners installed, scratches had a detrimental effect of low magnitude though a slightly greater effect than rifling. Further testing would establish at what magnitude or depth the scratch would be seriously detrimental. The current conclusion must be that any scratches in an axial direction may have a detrimental effect on joint fatigue life.

Chatter, Plastic Deformation, Tears and Laps: Open hole testing indicated relatively low detrimental effect of these conditions of the magnitude tested on fatigue life. These data suggest that these conditions must be considered detrimental to fatigue life.

Crack Growth Tests: Neat fit tests were run on open hole, zero load transfer and low-load transfer specimens. All load transfer specimens had fasteners installed to a neat fit. Incremental crack measurements were made for the open hole specimens only. The shape of the growth curves obtained are similar to the analytical curves. In all cases, the cycles to failure were greater than predicted by analysis, the ratio varying from 1.24 to 2.90 with an average of 1.80. In general, the cycles to failure show considerable scatter with longer initial crack lengths providing longer lives than shorter initial crack lengths in some cases. Therefore, no realistic conclusions can be drawn.



3. Relaxation of Hole Quality Specifications

This effort has identified the potential for relaxing certain hole quality specifications. For example, it appears from the data developed that hole surface roughness as great as 125 AA is as satisfactory for fastener performance as holes having a roughness of 63 AA or better and therefore, specifications requiring 63 AA could be relaxed to 125 AA. Some of the other factors indicate a possibility of relaxing; rifling, for example. However, additional testing will be necessary to quantify or further refine the acceptable extent of these conditions prior to effecting reductions in requirements.

4. Significance to the Aerospace Industry

This program has served to characterize and quantify the effects of several hole quality variables as they relate to the fatigue performance of a tapered interference fit fastener system. Prior to the execution of this program, the effects of many of these hole quality variables were subject to conjecture, but without supporting data. The program has, in summary, served to identify possible areas for cost reduction which will provide maximum quality/performance available at the minimum necessary manufacturing costs.

5. Taper Blade Cutter Conclusion

The 5/16 in. taper blade cutter produced holes which would be unacceptable in a production environment because of excessive chatter. This judgement is based on visual appearance only; no evaluation was made by fatigue testing. The holes were, however, of good metallurgical quality in that the surfaces were free of tears, laps and plastic deformation.

## SECTION V RECOMMENDATIONS

Based on the data observed and the general outcome of this program, additional effort in the hole quality area is suggested in order to provide a significant addition to the technology available in this manufacturing area.

### 1. Supplemental Work

In order to enhance the value of the data developed in this program, certain additional testing using the same material/fastener system is recommended as follows:

- a. Complete the spectrum loading fatigue tests on reverse dogbone specimens containing controlled quality levels which were manufactured as Test Series 23 under this program.
- b. Run additional tests evaluating the effect of surface roughness, by covering the range of 32 to 500 AA. This effort, using the dogbone/strap specimens is suggested to clarify anomalies present in the existing data and also to provide more complete definition of fastener behavior as effected by roughness.
- c. Explore greater depths of scratching and rifling in order to better define the maximum level of these discrepancies which can be tolerated by this fastener system.
- d. Repeat crack growth tests using the fastener installed at both minimum and maximum specification interference levels. This information would supplement that now available in identifying the true capabilities of the Taper-Lok fastener with respect to crack retardation.

### 2. Other Fastener Systems

A program similar to the one described in this report but using straight shank fatigue enhancement fit fasteners would serve to characterize the effects of various hole quality variables on the performance of this type of fastener system.

### 3. Other Structural Materials

Preliminary programs evaluating the effect of hole quality variables in structural materials other than aluminum should be considered. Specifically, evaluation of both titanium and high strength steel as structural alloys should be considered.

SECTION VI

PROCEDURES

1. Test Material Documentation

This program used aluminum alloy 7175-T73511 for all test specimens. This alloy is a modification of 7075 in which the chemistry is closely controlled. The T-73511 condition designates an extruded material which has been stretched and overaged. This processing/heat treatment procedure resulted in a high level of stress corrosion resistance and fracture toughness of the alloy but with some loss in strength when compared to maximum strength levels available.

The material was ordered as 30.5 in. long sections of an extruded solid shape per Lockheed-Georgia Company Drawing No. 900102 as sketched in Figure 1. This extruded shape is a nonproduction configuration which simulates a number of C-5A wing panel configurations. Such panels are typically extruded in lengths of 42 feet or greater. This material was ordered from Alcoa and produced at their extrusion plant in Lafayette, Indiana. All material was ultrasonically inspected per MIL-I-8950B, Class A.

Chemistry

The chemical composition of this alloy is given below in comparison to the applicable Lockheed-Georgia Company specification.

	<u>Specification</u>		<u>Metcut Analysis</u>
	<u>Max.</u>	<u>Min.</u>	
Si	.15		.14
Fe	.2		<.02
Cu	.2	1.2	1.52
Mn	.1		<.02
Mg	2.9	2.1	2.29
Cr	.3	.18	.2
Zn	6.1	5.1	5.13
Ti	.1		.025
Others	.05 ea.		<.01
	.15 total		

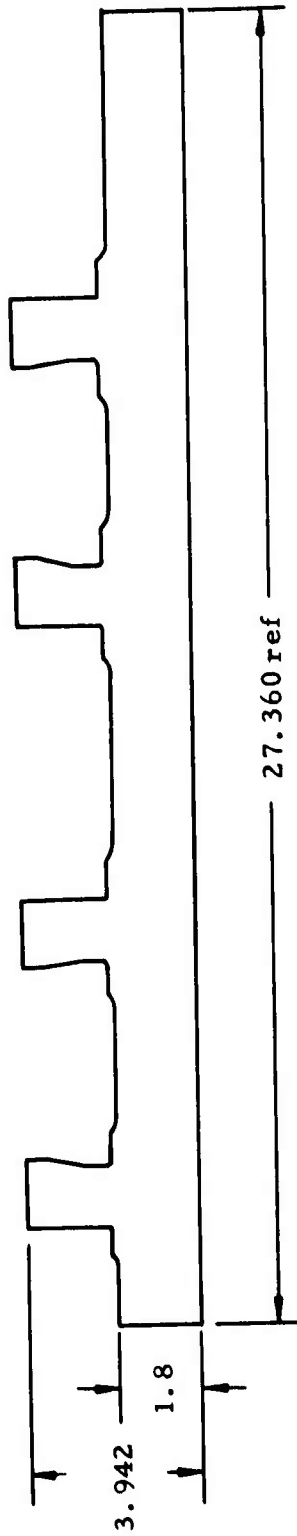


Figure 1 - CROSS SECTION OF EXTRUDED SOLID SHAPE PER DRAWING NO. 900102

### Microstructure

A photomicrograph showing the basic structure of this alloy is shown in Figure 2 below:

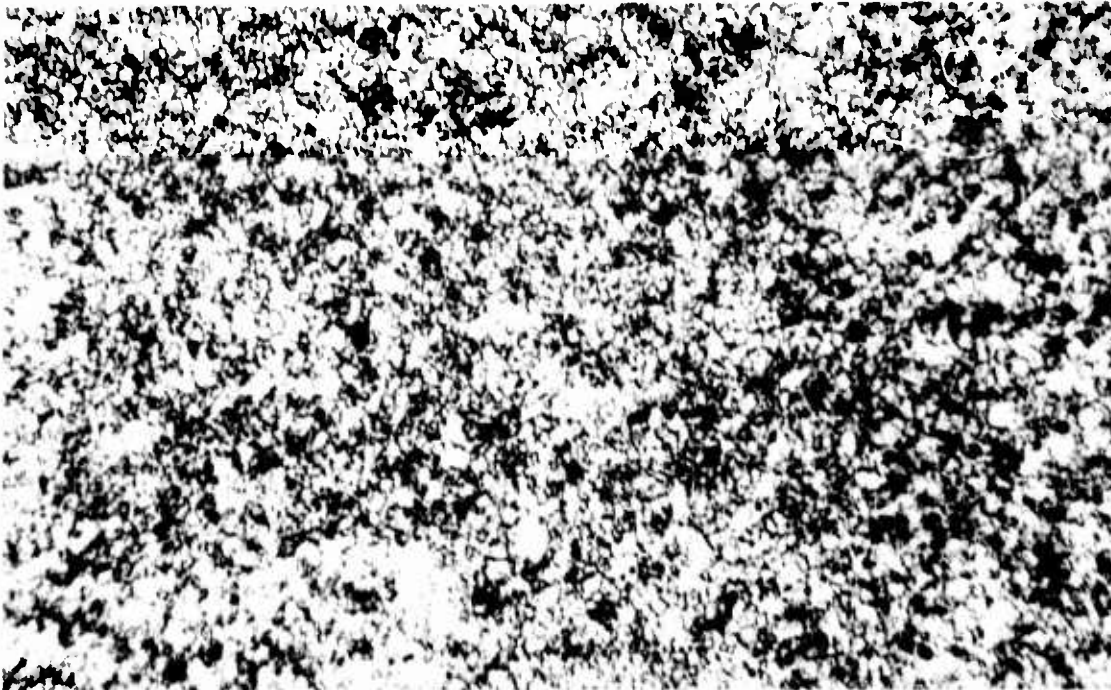


Plate: 20663

Mag: 300X

Figure 2 - STRUCTURE OF TEST MATERIAL AL 7175-T73511

### Mechanical Properties

Mechanical properties of the material supplied were also verified in relation to the requirements of the preliminary Lockheed-Georgia Company specification. All specimens were made in the longitudinal direction from the panel extrusions.

Tensile tests were performed using specimens having a gage length of 2 in. and a diameter of .505 in. All tests were conducted at room temperature. A summary of the tensile properties obtained in comparison with specification values is shown on the following pages. All of the test data are summarized in Table 1.

<u>Location</u>	<u>Orientation</u>	<u>U.T.S.</u> <u>(ksi)</u>	<u>.2% Y.S.</u> <u>(ksi)</u>	<u>Elong.</u> <u>(%)</u>	<u>R.A.</u> <u>(%)</u>
Near Ribs	Longitudinal	74.5	64.2	12.9	39
	Transverse	72.4	61.4	10.7	26
Flat Side	Longitudinal	75.8	65.3	12.7	42
	Transverse	74.6	64.2	11.8	33
Preliminary Specification Minimums	Longitudinal	69.0	59.0	9.0	--
	Transverse	63.0	52.0	4.0	--

### Fatigue Strength

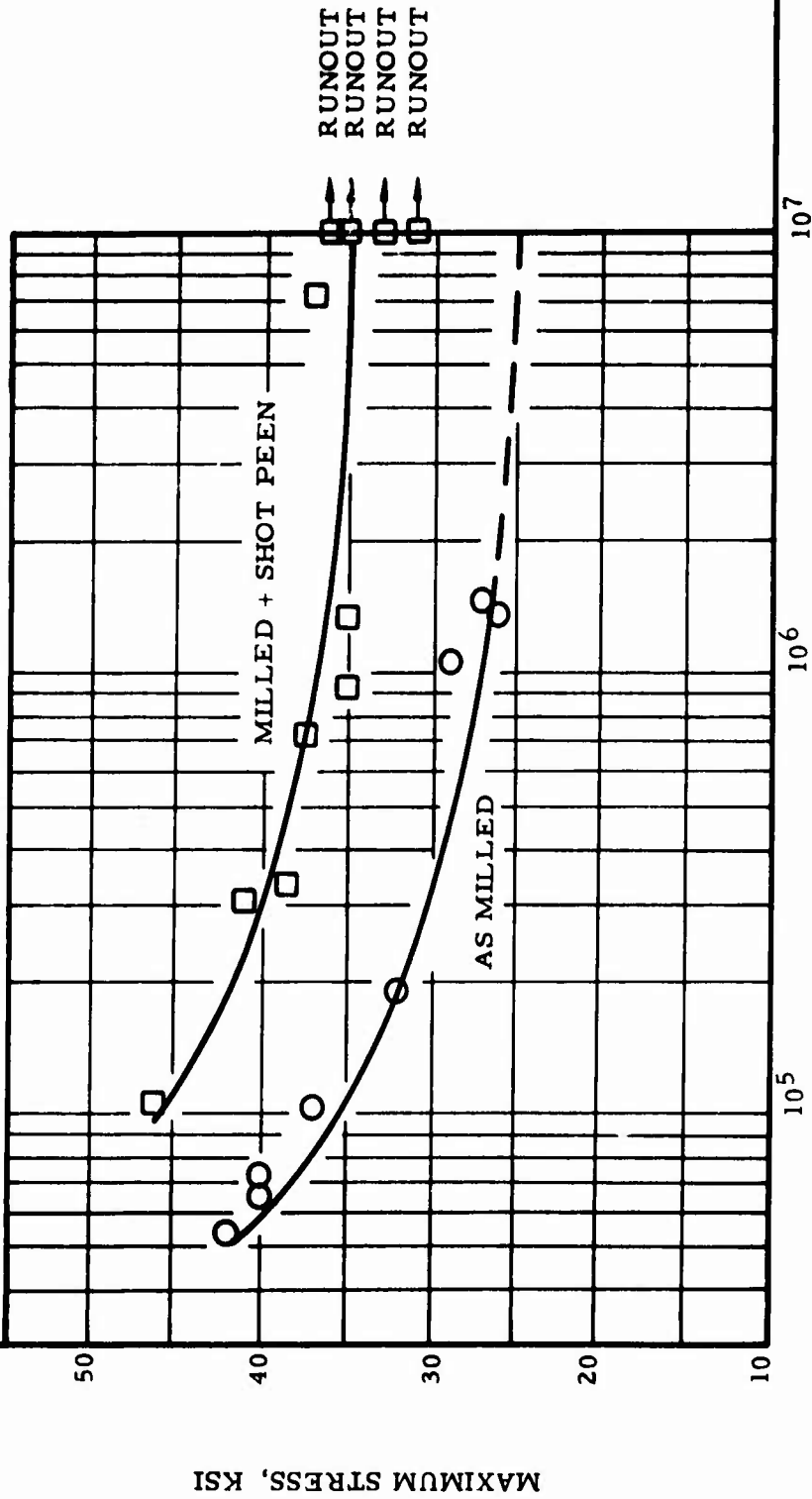
Fatigue testing of the parent metal was done to obtain the basic properties of the material and was performed on unnotched specimens in the tension-tension mode at  $R = 0.1$  and at testing speeds ranging from 900 to 1800 cycles per minute. Perhaps it should be noted here that the R value used in setting up fatigue tests is the ratio of the minimum to the maximum stress. At an R value of 0.1, for example, and for a test whose maximum stress is reported as 35,000 psi, the minimum stress would be 3500 psi. Similarly, at an R value of -0.33, the minimum stress would be 11,500 psi in compression. Tests were performed in closed loop, servo-controlled hydraulic test equipment and in this particular case, the force was cycled between the minimum and maximum values prescribed for each test using a sinusoidal wave form.

Testing for material documentation was confined to Test Series 1 (Table 2) which covers the evaluation of the basic material in both the as-face milled condition and also in the milled plus shot peened condition.

A plot of the data developed is shown in Figure 3. Note that the endurance limit associated with both of these surface finishing conditions is somewhat different, as would be expected from surface integrity considerations. In the as-milled condition, using the particular conditions chosen for these specimens (Table 3), endurance limit is estimated to be about 25,000 psi at  $10^7$  cycles. As may also be seen in Figure 3, the fatigue strength at  $10^7$  cycles for the shot peened surface, which surface condition was used for the balance of the program, is about 35,000 psi. (The peening conditions are noted in Section VI.2.b). All of the fatigue data shown in Figure 3 have been corrected for stress concentration

FATIGUE BEHAVIOR OF 7175-T73511 ALUMINUM ALLOY

MODE: AXIAL, R = 0.1  
 FREQUENCY: AS MILLED, 7-30 Hz, MILLED + PEEN, 20-30 Hz  
 ORIENTATION: LONGITUDINAL  
 TEMPERATURE: 75°F



CYCLES TO FAILURE

FIGURE 3 - FATIGUE STRENGTH OF TEST MATERIAL

effects in the samples and normalized to the  $K_t = 1$  condition. By strain gage measurement, the surface stress at the gage length/fillet intersection was determined to be 10% higher than the normal test stress. This correction was applied to those tests in which failure initiated at this location. A complete summary of this fatigue data is contained in Table 2.

2. Specimen Manufacture and Assembly

a. Test Specimens

Several different fatigue test specimens were used during the course of this program. These are illustrated in Figures 4 through 8. All were .3125 in. thick, duplicating the application to design requiring the use of 5/16 in. thick panels for testing. The various test specimens to be used are as identified below; the test series are described in Section III.

<u>Figure No.</u>	<u>Type Specimen</u>	<u>Test Series</u>
4	Parent Metal	1
5	Low-Load Transfer (dogbone/strap)	2,6,7,8, 17,18,19
6	Open Hole	4,9,10,11,12
7	Zero Load Transfer (dogbone-split setup)	5
8	Low Load Transfer (reverse dogbone)	20,21,22,23

b. General Specimen Manufacturing and Finishing Procedures

Coupon Machining

The material was received as described in Section VI.1. A photograph of an as-received extrusion section, 30.5 in. in length, is seen in Figure 9. A sketch showing the orientation which was established for all specimens is presented in



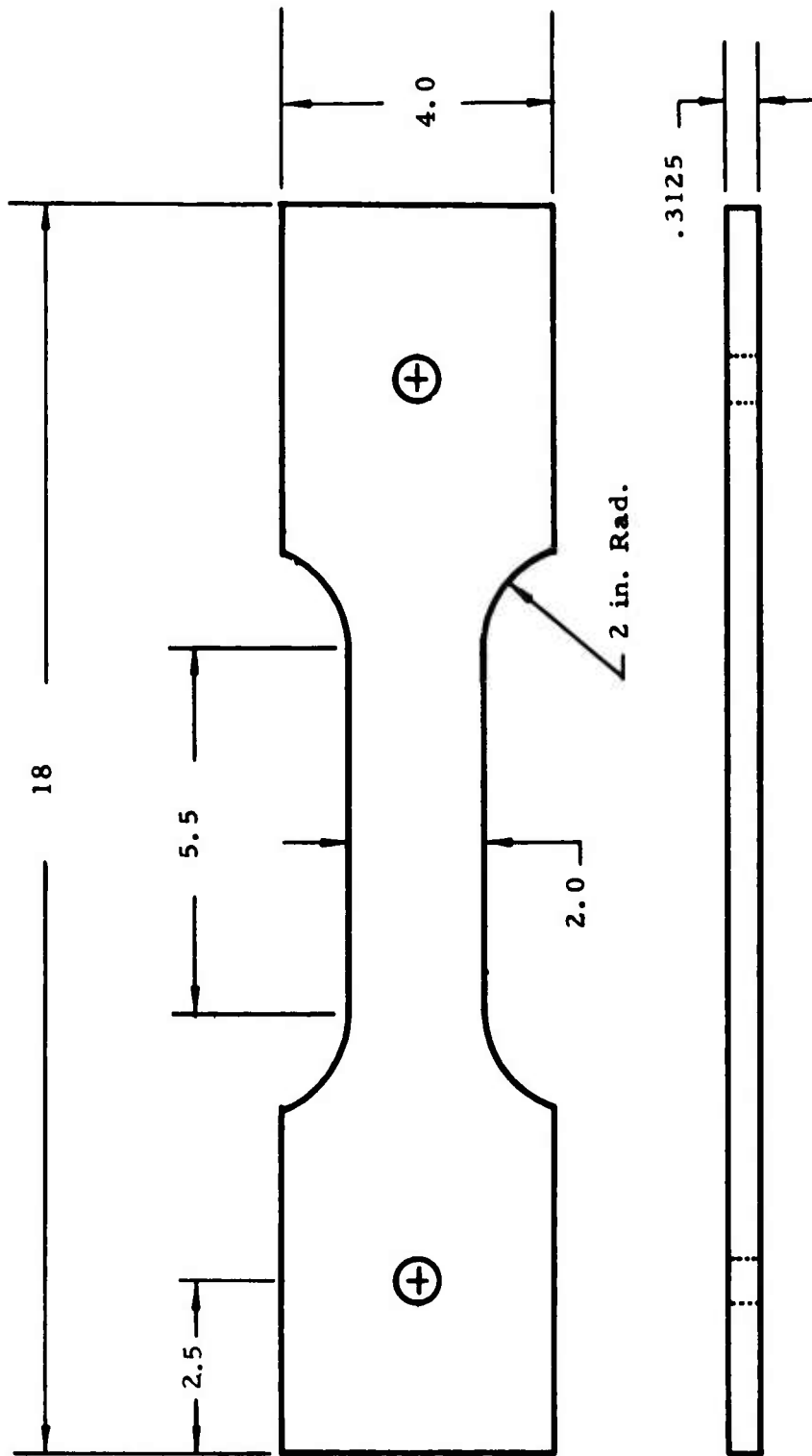


Figure 4 - PARENT METAL SPECIMEN (PM)

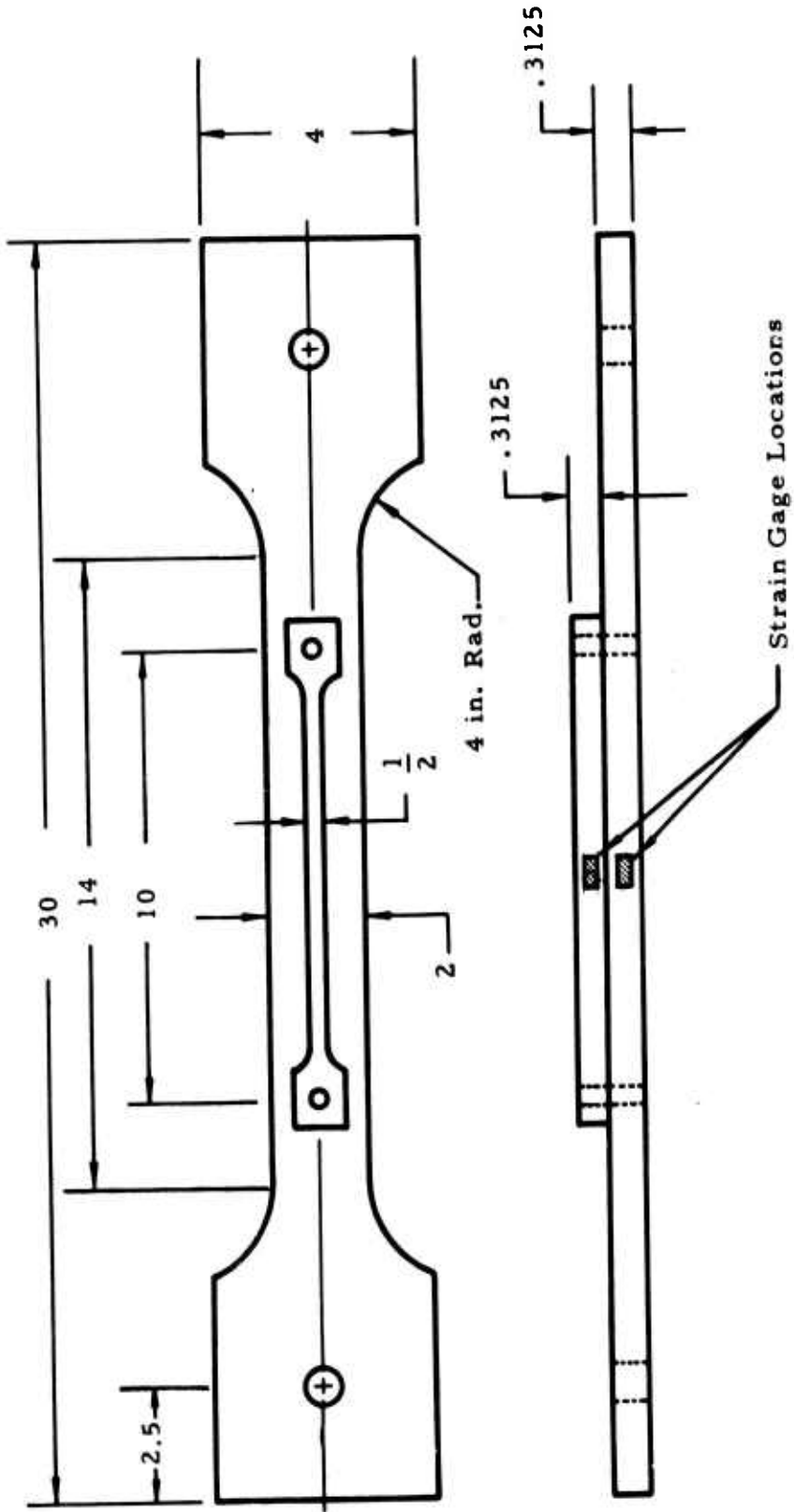


Figure 5 - LOW LOAD TRANSFER DOGBONE-STRAP SPECIMEN (LLT)

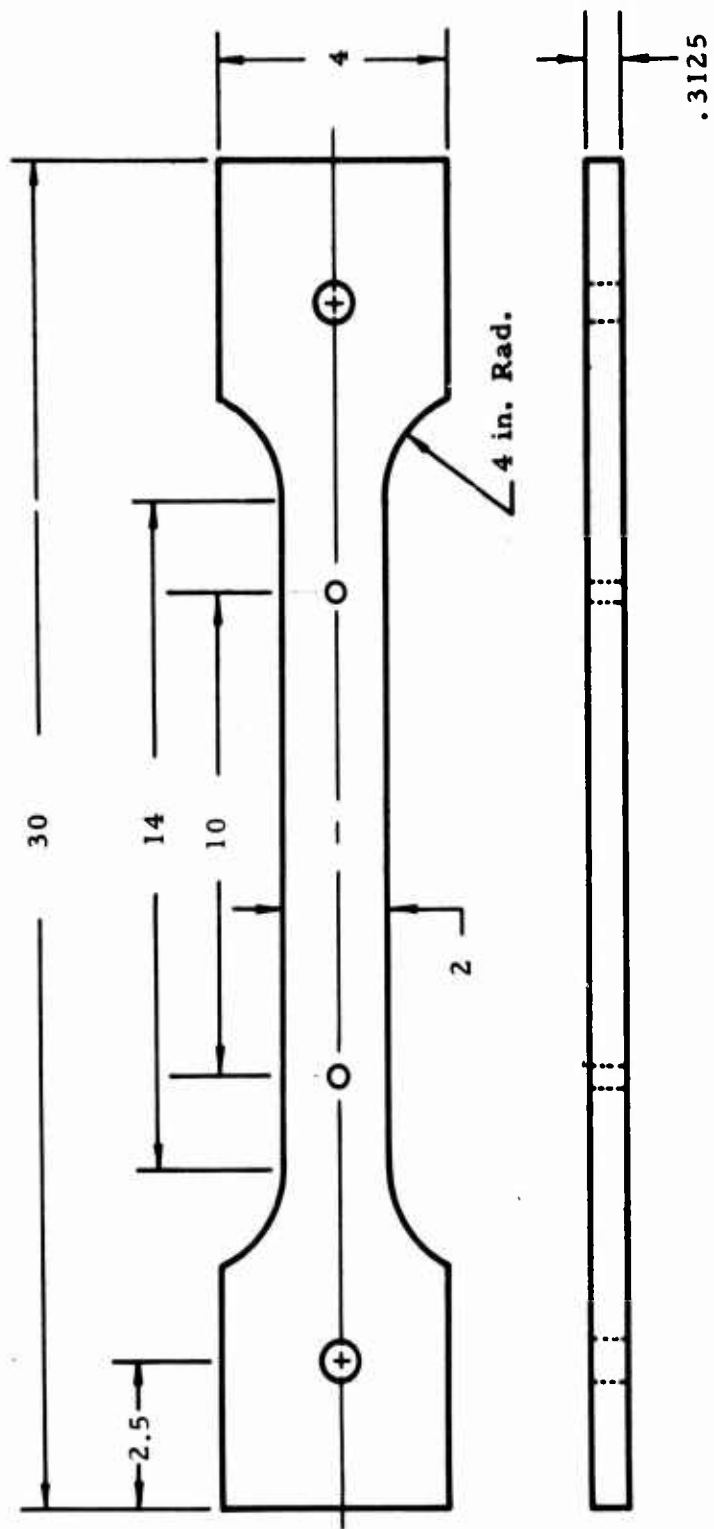


Figure 6 - OPEN HOLE SPECIMEN (OH)

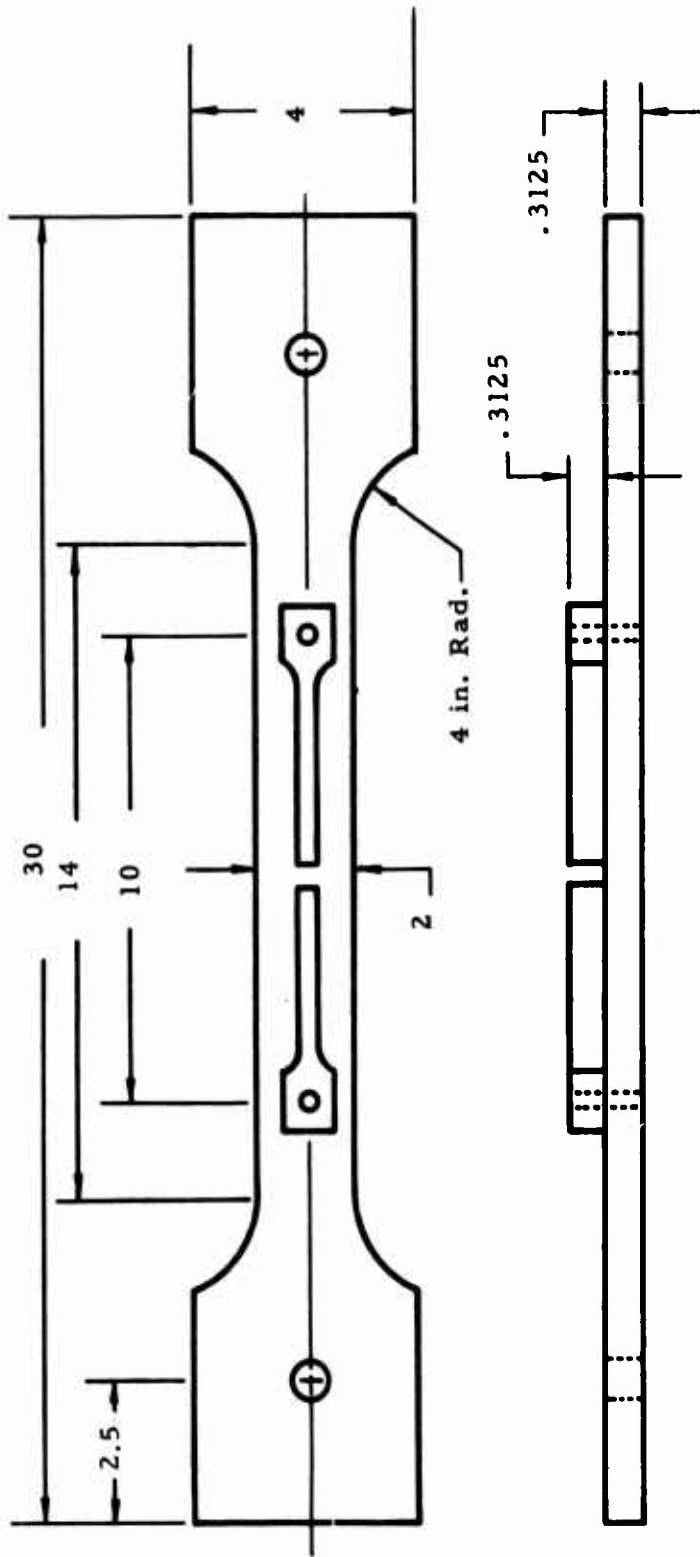


Figure 7 - ZERO LOAD TRANSFER SPECIMEN (ZLT)

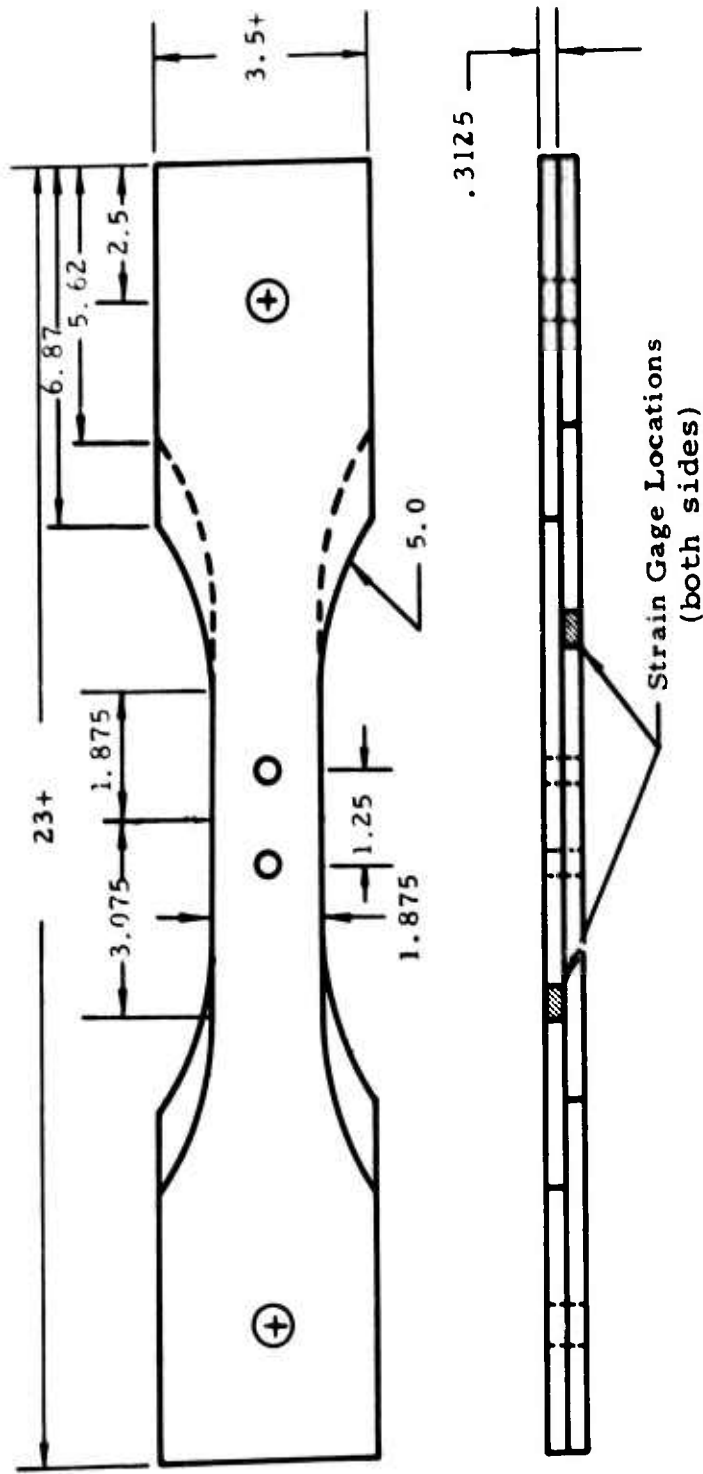


Figure 8 - REVERSE DOGBONE SPECIMEN (RD)

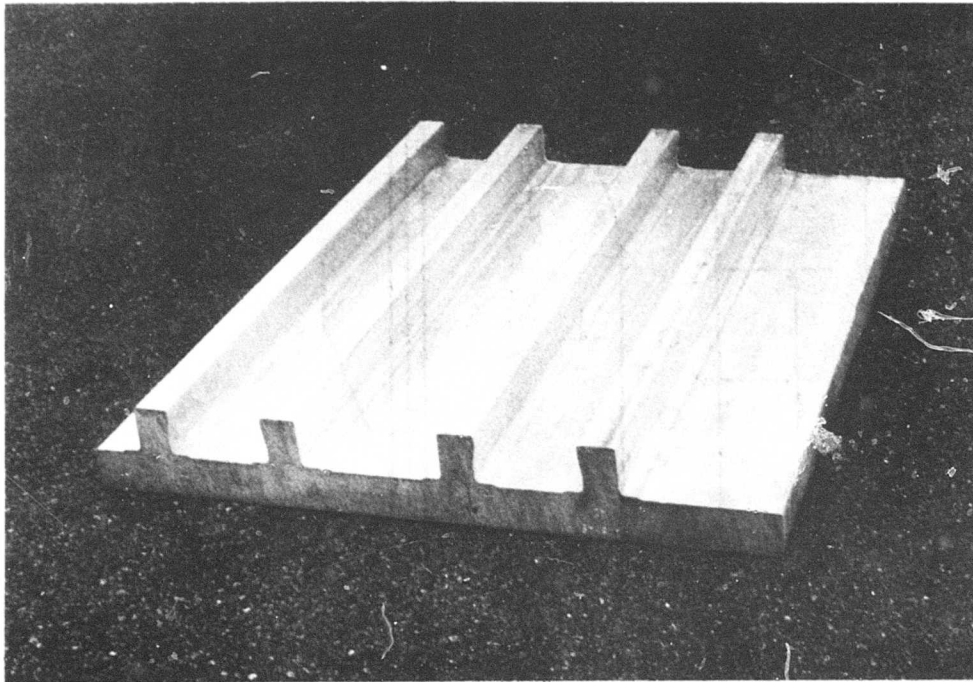


Plate: 6651

Figure 9 - PHOTOGRAPH OF AS-RECEIVED EXTRUSION  
OF THE 7175 ALUMINUM TEST MATERIAL

Figure 10. Each extrusion was cut along the 30.5 in. dimension into six slices. Each slice, numbered 1 through 6, was then cut into four separate coupons. These were identified as top, top center, bottom center, and bottom. Although all the material was from a single heat, the identification was maintained so that each coupon could be identified with respect to the extrusion section from which it came. A typical coupon identification is as follows: 2D4TC. This number or identification shows that the particular coupon came from skid No. 2, Section D, the fourth slice in the top center location.

After the coupons were identified and cut out, initial blanking occurred. The coupons were machined into 5/16 in. x 4 in. x 30 in. rectangular blanks. This machining was performed per the conditions given in Table A3. After blanking, the specimens were then ready to be contoured into the final configuration. This contouring was performed per the conditions shown in Table 3.

After contouring, the coupon then went through a series of processing steps in preparation for taper hole drilling. This processing sequence was as follows:

- Shot peening per Standard STP 51-501, Revision G;
- Anodizing per Standard STP 58-208, Revision E;
- Coating per Standard STP 59-505, Revision C.

Following processing, the coupons were ready for tapered hole drilling and reaming. When dogbone/strap and reverse dogbone specimens were manufactured, drilling and taper reaming was accomplished on the specimen pair with the mating pieces clamped together in final position.

#### Shot Peening

Shot peening was to be accomplished to the gage section of all specimens except a small portion of those designated for Test Series 1 which were to be evaluated in the as-milled condition. Shot peening was accomplished in accordance with Lockheed-Georgia Company Specification STP51-501, Revision G. With reference to aluminum alloys in the thickness range involved in this program, the specification called for a saturation peening intensity of .006A-.012A. For purposes of achieving control and consistency in the subject program, the range of peening parameters was chosen as follows:

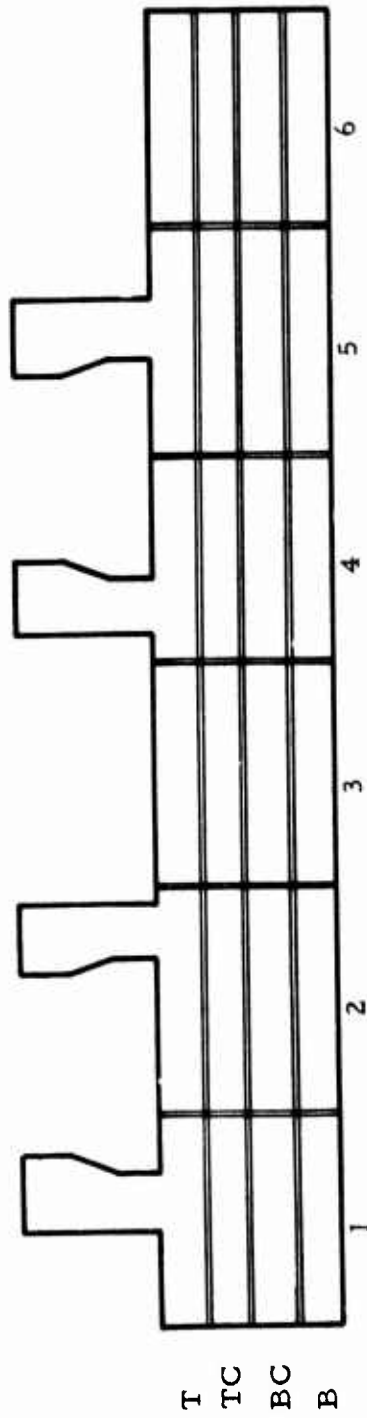


Figure 10 - LAYOUT OF SPECIMEN IDENTIFICATION AS IT RELATES TO LOCATION IN EXTRUSIONS



Peening Intensity: .008A-.010A  
Coverage: 100%  
Shot Size: S110

During peening, each specimen was clamped into a fixture where it was supported at each end outside of the locating holes. Using the fixture, the specimen was rotated at a speed of approximately 60-70 rpm. It received the discharge of two nozzles which translated parallel to the specimen axis at a rate of 1.5 feet per minute for a total of three minutes. In the particular fixturing used, this set of parameters produced the 100% visual coverage required by the specification. After the specimen was removed from the fixture, the ends which had previously been masked by the rotating fixture were then peened using manual control.

Shot peening of all test specimens was accomplished by The Metal Improvement Company, a division of the Curtiss-Wright Corporation, at their Cincinnati facility.

#### Anodizing

After peening, all specimens were subjected to sulfuric acid anodizing which was performed in accordance with Lockheed-Georgia Company Specification STP58-208, Revision E. A type I non-died coating was applied which was specified to have a minimum thickness of 0.0002 in. The anodizing requirements were as follows:

Min. Anodic Coating Weight (mg/sq.ft.): 1000  
Steady Voltage, DC: 6-24  
Anodic Current Density (amps/sq.ft.): 12 min.  
Solution Temperature: 68-72 degrees

After anodizing, all samples were rinsed thoroughly with cold water, then in sodium bicarbonate solution and finally in a demineralized water. Samples were then sealed by immersion in a 4-6% dichromate bath for 15-20 minutes, followed by both spray and immersion rinses in hot, demineralized water. Final drying was accomplished with forced air.

The anodizing operation was accomplished by Smith Electrochemical Company, Carthage, Ohio.

### Coating

A clear polyurethane coating was applied to the gage sections of all specimens after anodizing. This was done in accordance with Lockheed-Georgia Company Specification STP59-505, Revision C, which is equivalent to MIL-C-27725. To avoid the possibility of reducing friction in the grip areas of the specimens, the coating was masked from those regions.

Coating was accomplished by Alpine Products Inc., Dayton, Ohio.

### Fastener Installation

The drilling and taper reaming of the dogbone/strap specimen was accomplished in a special fixture. The fixture was constructed to assure the proper relative positioning of the mating coupons which make up the specimen assembly, to provide for the accurate positioning of the tapered hole, and also to provide adequate rigidity for the drilling and reaming operations. A photograph of this fixture, without specimen coupons in place, is shown in Figure 11. Note that the fixture used a variety of pins, spring loaded pins, and stops in order to locate and support the specimens. The fixture was designed so that, after drilling and reaming, the fastener would enter from the dogbone side of the specimen assembly and the nut would be on the strap side. It should be noted that in the case of the dogbone/strap configuration the strap must be under the dogbone during the drilling operation and since it is smaller than the dogbone, means had to be provided for properly positioning these two coupons.

A photograph of the dogbone/strap fixture with the strap in place is shown in Figure 12. Note that the strap is positioned by two stops and corresponding spring loaded pins. A photograph of a dogbone coupon placed over a strap in the same fixture is shown in Figure 13. The dogbone is positioned by means of a round pin at one end and a diamond pin at the other. The round versus diamond configuration allows for slight variation in distance between pin holes in the dogbone coupon. As shown in Figure 13, the specimen is clamped in the fixture ready for the drilling and subsequent reaming operations to be performed.

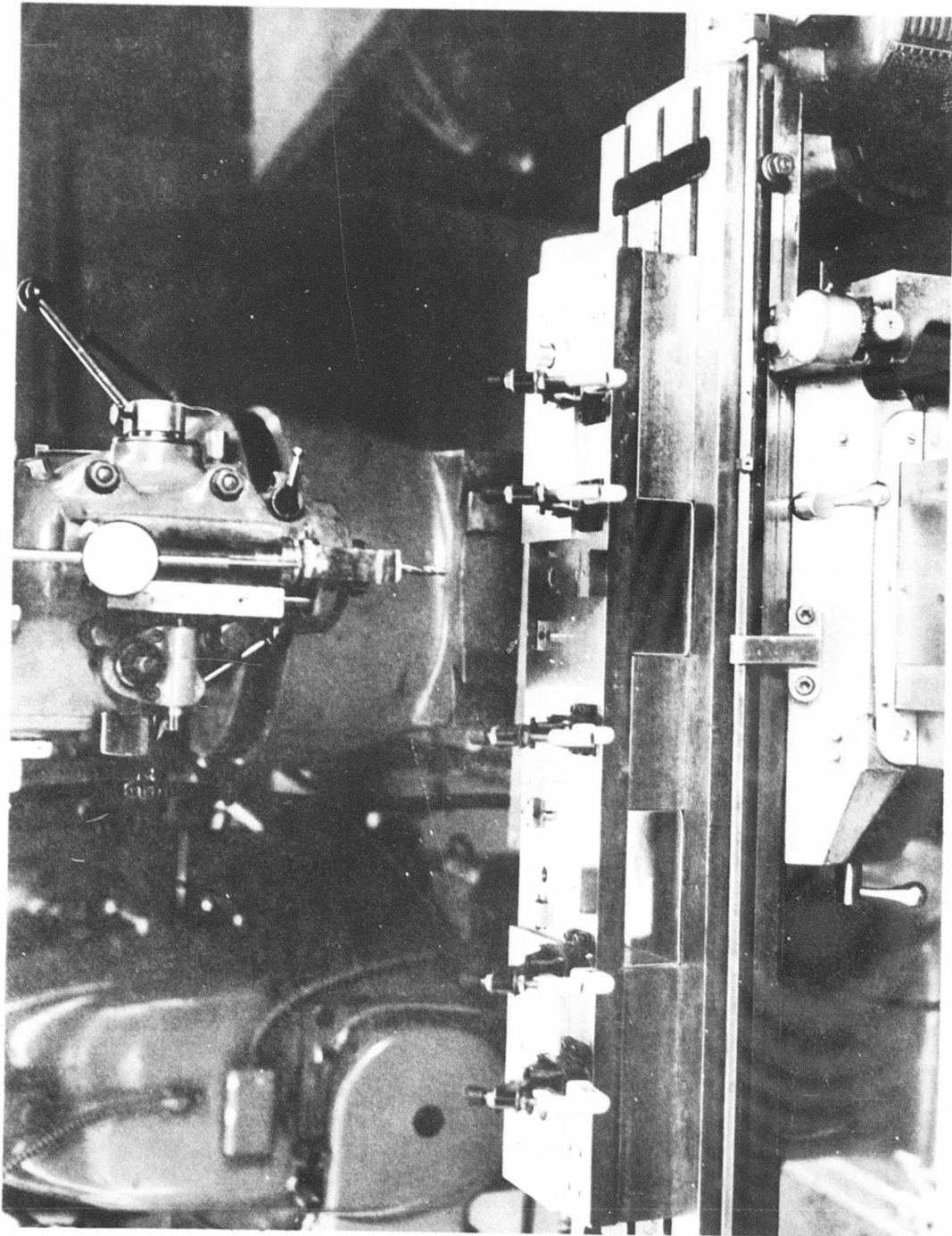


Plate: 6625

Figure 11 - FIXTURE USED FOR DRILLING AND REAMING OF SPECIMEN

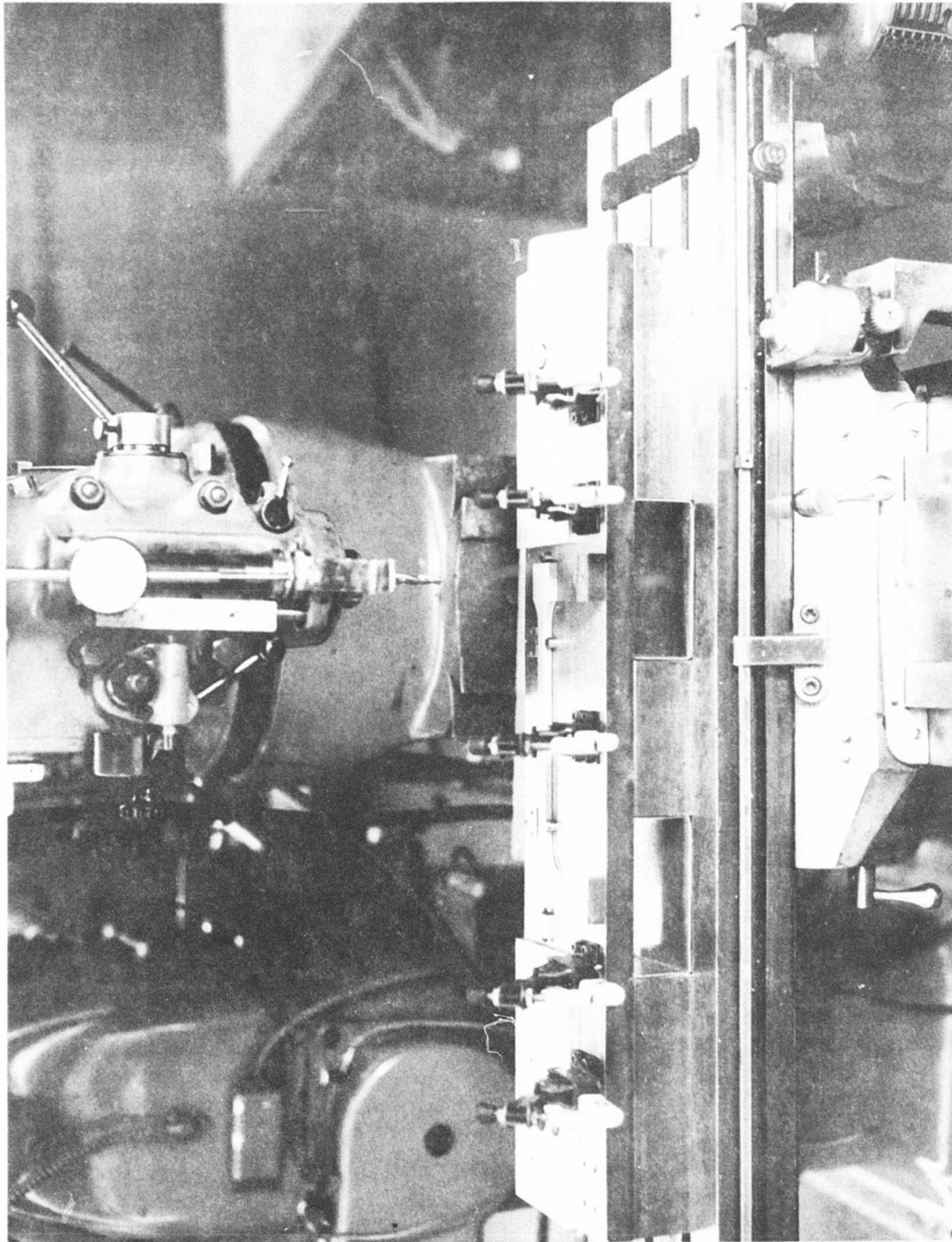


Plate: 6624

Figure 12 - FIXTURE USED FOR DRILLING AND REAMING OF SPECIMEN WITH A STRAP IN PLACE

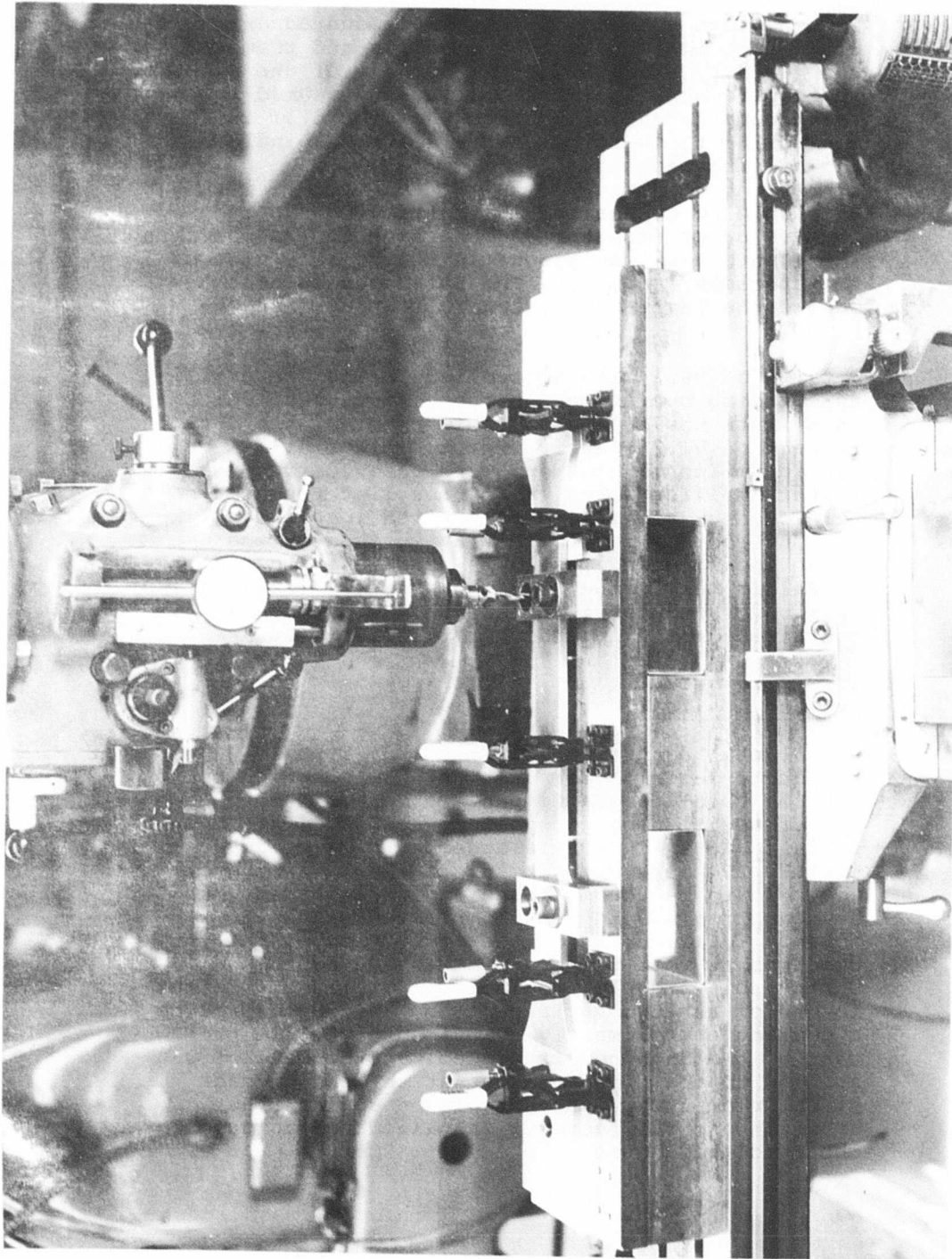


Plate: 6623

Figure 13 - REAMING OF DOGBONE/STRAP SPECIMEN AS AN ASSEMBLY

The specimen assembly fixture was mounted on a Bridgeport milling machine. Drills and reamers were held by a collet in the spindle of the machine. The depth control of the drilled and reamed holes was accomplished through the use of a dial indicator monitoring the vertical travel of the spindle of the milling machine.

It should be emphasized again that the tapered reamers enter from the dogbone side of the specimen. The countersink was placed in the dogbone side of the specimen assembly. The nuts used to seat and secure the Taper-Lok fasteners rest against the strap.

Details of variables controlled during the drilling and reaming operations on these specimens, which constitute the nucleus of this program, are detailed in Section VI.3 of this report. After drilling was accomplished, coupons were removed from the fixturing illustrated in Figures 11 through 13 and were cleaned and inspected. After inspection, sealant was applied to the fay surface of the strap specimen and fasteners were inserted and installed making the specimen assembly ready for testing. Details of the assembly procedure are contained in the Appendix of this report.

#### Sealant Application

A sealant, identified as PR-1431-G, Type I, (Products Research Corporation) was supplied by the Lockheed-Georgia Company to be applied to each set of specimen coupons before assembly. This sealant had an indicated assembly time of approximately 20 hours which means that all working or movement to be accomplished once the sealant has been applied should be accomplished within 20 hours. Total curing or tack-free time of the specimen at room temperature was 120 hours. During this program, sealant was applied by Metcut to one of the two surfaces to be joined to produce a coating approximately .015 in. thick. In the case of the dogbone/strap specimen the sealant was applied to the two tab areas at the end of each strap. The strap was then placed against the specimen and the fastener installed and torqued to the specified level.



3. Production of Hole Quality Variables

a. Tapered Hole Procedures

All tapered holes in the specimens were located and drilled on a Bridgeport milling machine. The Bridgeport was equipped with a Trav-A-Dial for reading table location in the longitudinal direction and a dial indicator for locating the spindle in the vertical direction.

After the fixture had been properly aligned with the milling machine spindle, a dummy specimen of the same alloy and same thickness was drilled and reamed to permit the adjustment of the spindle depth stop to produce a hole having the proper protrusion and countersink depth.

After the spindle depth stop had been properly set, two more holes were drilled and reamed. These holes were inspected for protrusion, surface finish and bearing using the procedures explained in the succeeding paragraphs.

When two satisfactory holes had been produced in the dummy material, a specimen was then mounted in the fixture and the two tapered holes were drilled, reamed and inspected using the same procedures that were used to produce the verification practice holes.

The amount of interference between the fastener and the tapered hole was determined by measuring the distance the fastener head protrudes from the specimen's surface when it is pressed firmly into the hole with thumb pressure. A sketch showing the protrusion height is shown in Figure 14.

The fasteners used during this program are Group I fasteners. Group I tapered holes having the following amounts of interferences and protrusions were produced:

<u>Interference</u>	<u>Protrusion</u>
.0005"	.024"
.0023"	.110"
.0035"	.168"
.0048"	.230"
.0060"	.288"

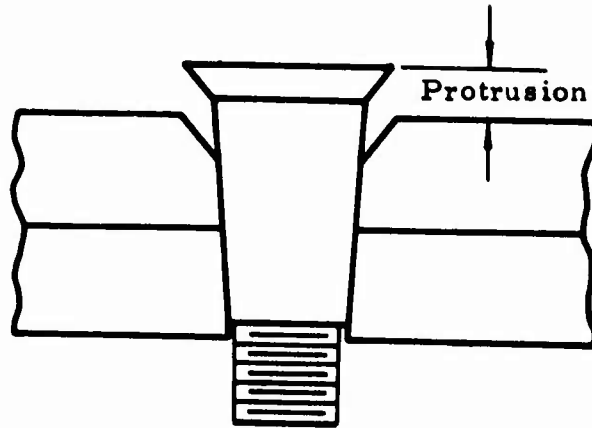


Figure 14 - SKETCH SHOWING PROTRUSION HEIGHT

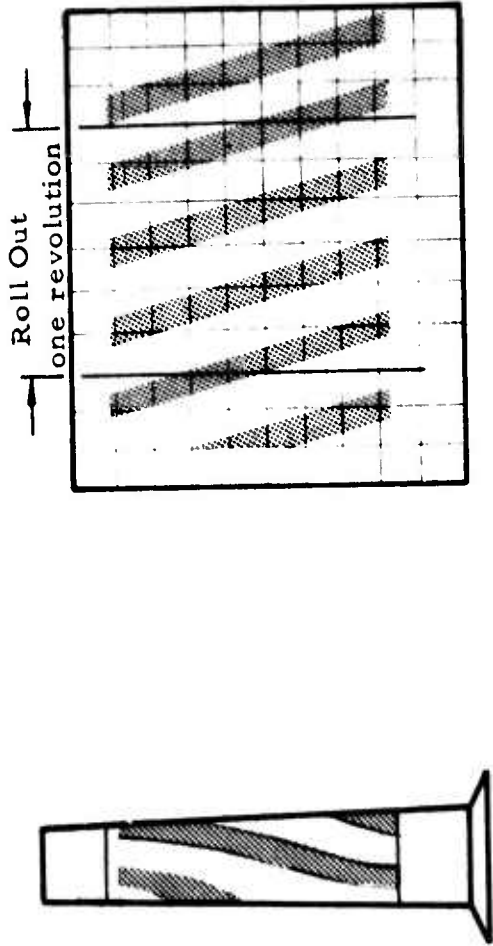


The surface roughness of the tapered hole was measured in the axial direction using a Clevite Surfanalyzer instrument. This measurement was recorded for each hole on a manufacturing report. (Manufacturing reports for each specimen are contained in Volume II of this report). The countersink and tapered surface were also visually inspected for scratches, rifling and chatter marks.

Holes were checked for bearing, ovality, bell-mouthing, barrelling, rifling, and roughness by use of a bluing pin. The bluing pin test is fairly common in the fastener industry and for this program the procedure used was as follows: The bluing pin was coated with a thin uniform coating of Prussian Blue using the fingertips or a cheesecloth swab. The hole was previously cleaned of all chips and cutting lubricant that may have remained after drilling. The blued pin was then pressed firmly into the hole with thumb pressure and the protrusion of the head was measured. The pin was then driven into the hole approximately .050" with a plastic mallet or hammer. The pin was then knocked out of the hole and caught in such a way so as not to smear the bluing. The pin was then rolled on a piece of coordinate paper to make a permanent record of the bearing surface. A sketch of a bluing pattern and rollout are shown in Figure 15.

Hole contour was checked with an Omark Industries Air Gage equipped with a multiple-orifice tapered probe as shown in Figure 16. After inserting the probe into the hole, the surface was inspected at various axial positions by reading the output of the various orifices. Radial deviations could be measured by rotating the probe to any desired angular position. With this data the contour of the hole at various axial positions could be plotted.

The procedure for using the air gage was to insert it into a master tapered hole and set the indicator on zero. The probe was then inserted into the hole that was to be inspected and the output of each orifice was recorded at 45° increments of probe rotation. For the 5/8 in. thick specimen, the first six orifices were used.



Note: Areas of Contact Will Have Less Bluing Than Areas of No Contact

Figure 15 - ROLLOUT OF BLUING PIN TO PERMIT GRAPHICAL INTEGRATION OF PERCENT BEARING CONTACT

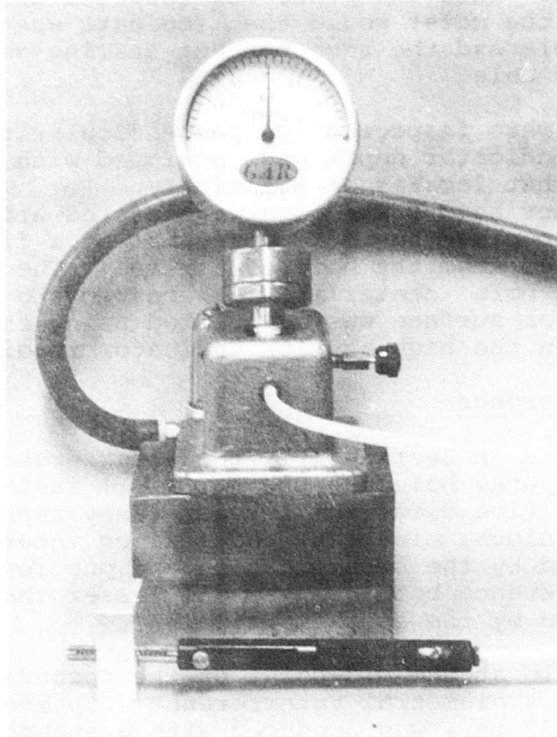


Plate: 6549

Figure 16 - AIR GAGE FOR MEASUREMENT OF  
DIAMETRAL SURFACE DEVIATION

The percent bearing of the holes was checked with an Omark Industries Taper-Lok Electronic Gage (Figure 17) that distinguishes tapered hole characteristics by measuring the capacitance established between the hole and the tapered probe. A single reading identifying average hole characteristics was obtained.

The probe was first inserted into a master tapered hole of a known percent bearing and the meter was nulled. When the probe was inserted into the test hole, the meter would then indicate whether or not the hole had the same percent bearing as the master hole.

Holes were inspected for perpendicularity using a dial indicator depth gage equipped with a special base that locates on a flush type Taper-Lok fastener head. The gage was rotated around the head keeping the indicator point at a fixed distance from the hole centerline. The angularity of the hole centerline with respect to the fastener surface was calculated using the difference between the high and low indicator readings.

b. Interference

As noted in Section III, the interference between the tapered hole and the Taper-Lok fastener was set at five different levels. They represented the minimum, mid-point and maximum interference allowed by the specification and one level of interference both greater and lesser than that allowed by the specification.

The hole at the mid-point of the specification, having a diametral interference with the fastener of .0035 in., was produced with a standard reamer. The tool had an integral countersink. The next larger hole, having an interference of .0023 in. was produced by slightly opening up a standard hole with an oversize tapered reamer. The still larger hole, having the interference of .0005 in., was produced by still another oversize reamer. In the case of the .0023 in. and .0005 in. interference holes, the countersink blend radius which was placed in the coupon by the original cut of the standard reamer, was slightly cut into by the oversize reamer. The extent of this cut, however,

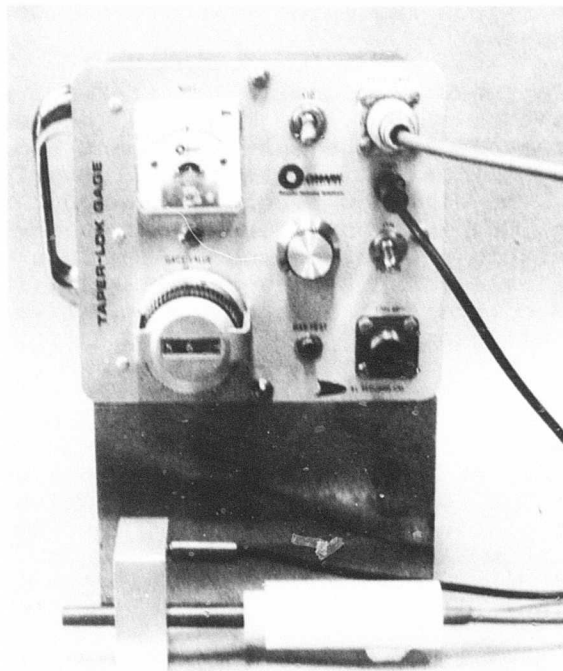


Plate: 6550

Figure 17 - CAPACITANCE GAGE TO MEASURE  
PERCENT BEARING BETWEEN THE  
TAPER-LOK AND SURFACE OF THE  
HOLE

was of the order of .0015 in. on the radius of the fastener. This cut was considered small compared to the radius between the tapered hole and the countersink of .040 in.  $\pm$  .010 in. as produced by the standard tool with integral countersink.

The minimum size hole having the maximum interference of .0060 in. was produced by a specially ground tapered reamer. The .0048 in. interference hole was produced by following up that operation with an oversize reamer enlarging the hole slightly so as to reduce the interference from .0060 in. to .0048 inches.

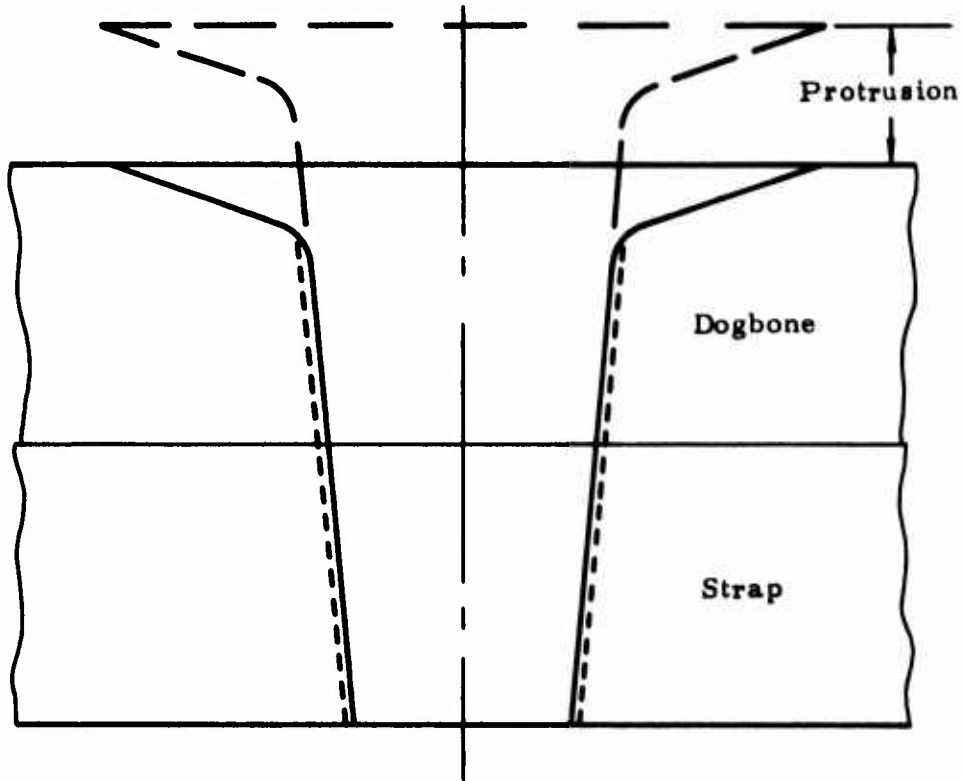
By developing variations in interference using this two-tool method, the flushness between the fastener heads and the test specimens remained within specification limits at all interference levels. The limit on flushness was .002 in. below flush to .004 in. above flush. It was felt that this variable should be produced in this way so that the relationship between Taper-Lok fastener head and countersink in the test panel was the same in all cases.

A sketch and description of how these holes having various levels of interference were produced is shown in Figure 18. The principal means of measurement and inspection of this hole quality variable was by measurement of protrusion of the fastener placed manually into the test hole. This is also shown in Figure 18.

c. Perpendicularity

On specimens where perpendicularity was not a test variable, the fastener centerline was to be held to within 0.5 degrees of the true perpendicular position. A lack of perpendicularity of 3° had been selected as the level for studying this parameter as a discrepant condition. These holes were produced in manufacturing by tilting the head on the milling machine which carries the drill and reamer. The hole entered the test specimen at its centerline. The inclination was perpendicular to the axis of loading of the specimen.

This quality variable and method of producing it was considered typical of the production situation where the operator does not have his fixturing,



- Cut with standard geometry reamer to obtain holes which will produce .0035 and .0060" interference with installed fastener
- Cut with oversize reamer to reduce levels of interference to .0005, .0023, and .0045"
- Fastener in position to measure protrusion, hence interference

Figure 18 - VARIABLES IN REAMING USED TO OBTAIN RANGE OF INTERFERENCE LEVELS

namely the drill cage, placed firmly against the panel to be drilled. In such a situation, loss of perpendicularity was a result of the inclination of the cutting tool. While the entrance of the hole had the correct edge distance, the exit of the hole resulted in a slightly reduced edge distance.

Interference of artificially inclined holes was measured by means of protrusion at the centerline of the fastener and a plane perpendicular to that in which the inclination was produced. The lack of perpendicularity actually achieved was measured by taking readings with a depth indicator on the head of the fastener at 90 degree increments around the fastener head.

d. Bellmouthing

Bellmouthing was produced as a two-tool operation. By using reamers of controlled geometry, the conditions were produced repeatedly in several different specimen sets. The initial reamed hole was put in by a controlled reamer which cut oversize at the exit side of the hole and also in the region where the hole/countersink intersection should be located. A standard cutter was then introduced to produce the proper taper where the hole was not already oversize. The resulting hole was within specification limits at the face surface, but lacked interference at the countersink/hole intersection and at the exit. The metal removed successively by these two cutters is shown schematically in Figure 20.

This type of hole discrepancy was considered to be similar to that which would be produced by an operator should he become unsteady with his power tool during the drilling or reaming operation. We chose a two-tool method of producing the discrepancy so that it could be uniformly reproduced.

e. Barrelling

Like the bellmouthing operation just described, the barrelling condition was also produced by successive cuts of two different tools. As shown in Figure 21, the first reaming operation was performed with a standard reamer which produced the tapered hole of the proper contour along with



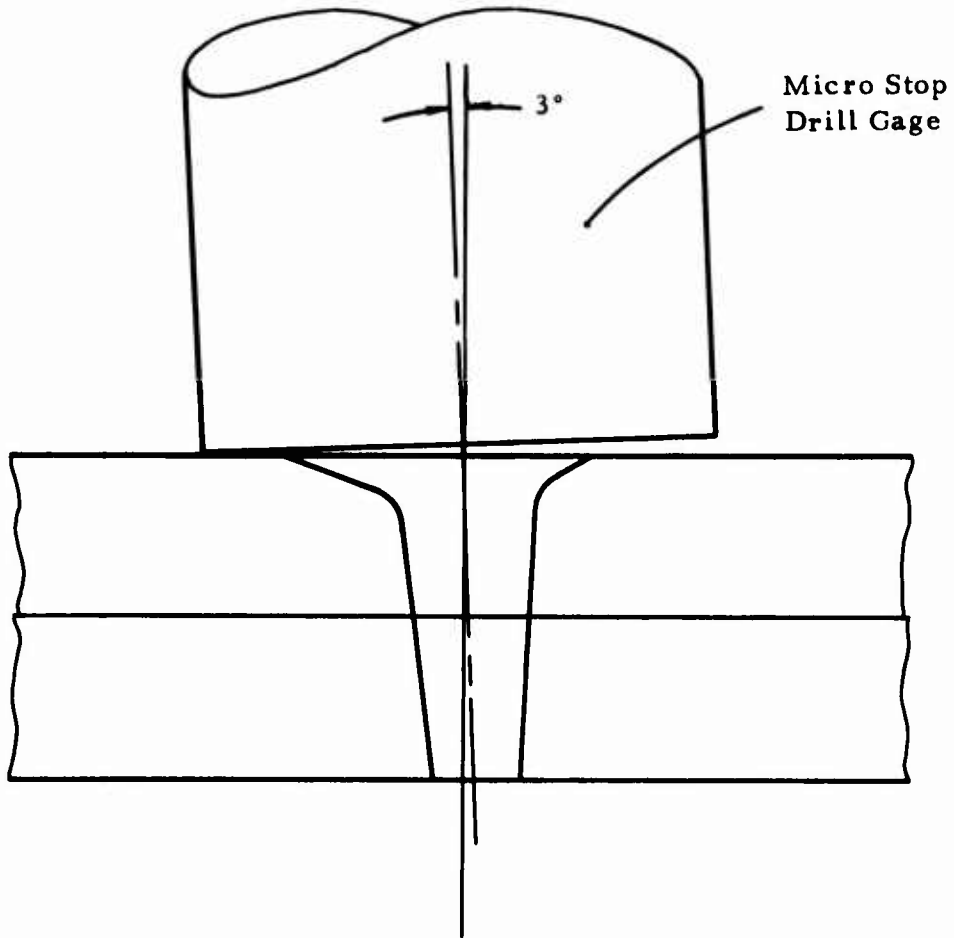
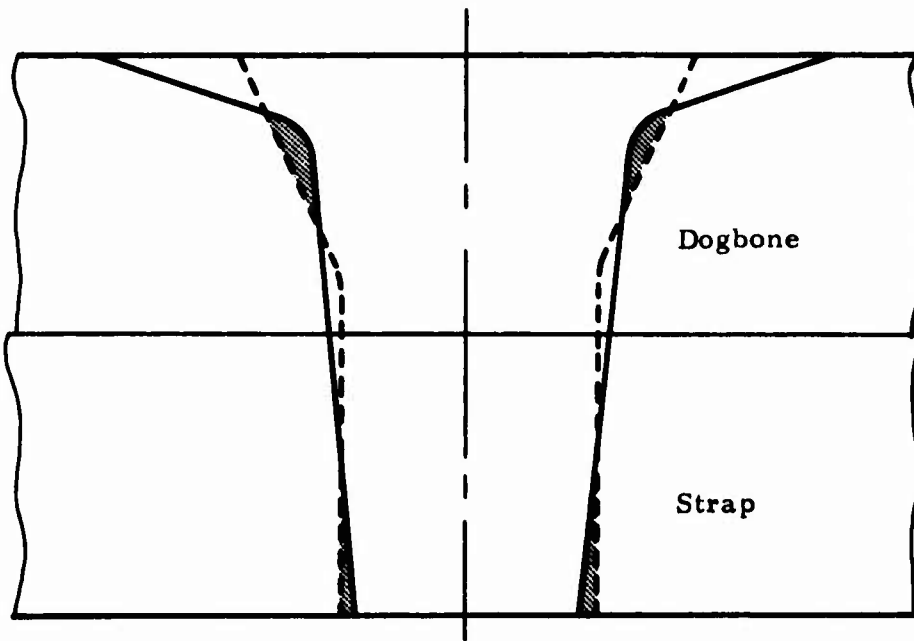


Figure 19 - VARIATION IN MANUFACTURING PROCEDURES  
TO PRODUCE A NON-PERPENDICULAR HOLE




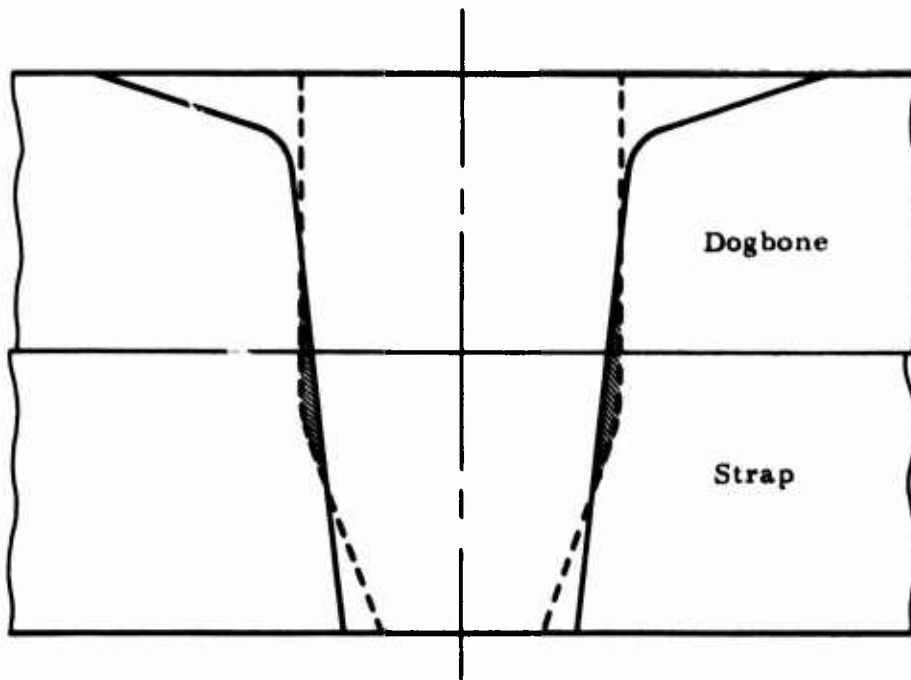
- Cut of Control Reamer
- Cut of Standard Reamer
-  Areas where inadequate interference is produced, resulting in bellmouthing

Figure 20 - VARIATIONS IN MANUFACTURING PROCEDURES TO PRODUCE BELLMOUTHING




- Cut of control reamer
- Cut of standard reamer
-  Areas where inadequate interference is produced, resulting in barrelling

Figure 21 - VARIATIONS IN MANUFACTURING PROCEDURES TO PRODUCE BARRELLING

the integral countersink. This was followed with a cutter ground in such a way as to produce a larger hole than standard in the region of the fay surface. As shown in Figure 21, this hole had proper bearing of the tapered fastener at all areas except in the center of the tapered region which coincided with the fay surface of the specimen.

This hole discrepancy can occur during manufacturing when the chips do not clear themselves from the cutter. On the assembly line, holes have been drilled and reamed in structures which have a layer of sealant at the fay surface. This sealant tends to retain the chips on the reamer in the plane of the fay surface, causing the reamer to cut oversize in that area.

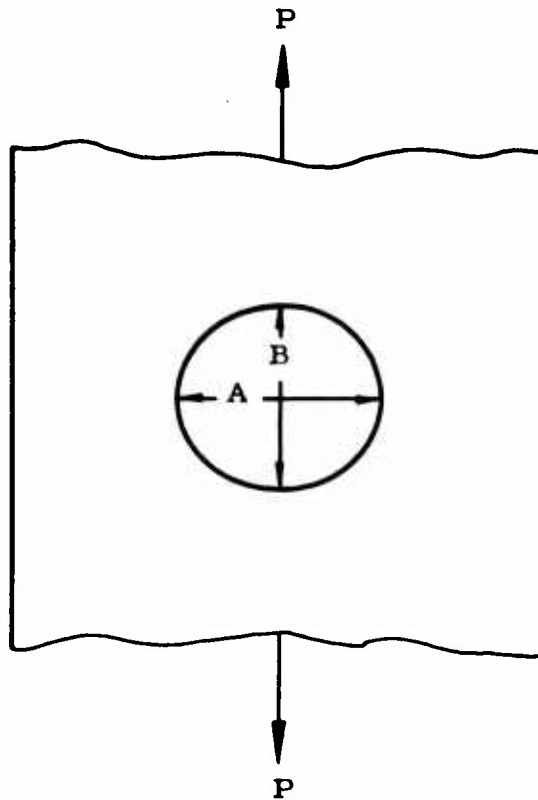
The barrelled holes were inspected in two steps. The first inspection occurred after the use of the controlled reamer by lowering the indicator on the machine tool spindle into the hole and reading the diameter at prescribed depths. Second, interference in the entrance and exit areas was measured using a protrusion pin as discussed in Section VI.3.b.

f. Ovality

Ovality may occur when drilling and reaming a hole on a vertical surface in the event that the weight of the power tool is allowed to dwell excessively on the cutter. This discrepancy was not frequently found by itself. When it occurred, it was usually in combination with other defects, notably barrelling and bellmouthing.

In this study, ovality was produced by translation of the milling machine table with the reamer engaged in the workpiece. As shown in Figure 23, the larger diameter of the oval hole was perpendicular to the loading axis. An increase in diameter of .004 in. was achieved in the transverse direction.

This discrepancy was inspected by tramping the hole in the specimen with an indicator in the milling machine spindle. The fay surfaces of the specimens were similarly checked while they were disassembled before sealing.



P = direction of loading  
A = diameter of hole 90° to loading axis  
B = diameter of hole parallel to loading axis  
A to be .004-.006" greater than B

Figure 22 - VARIATIONS IN MANUFACTURING PROCEDURE  
TO PRODUCE OVALITY

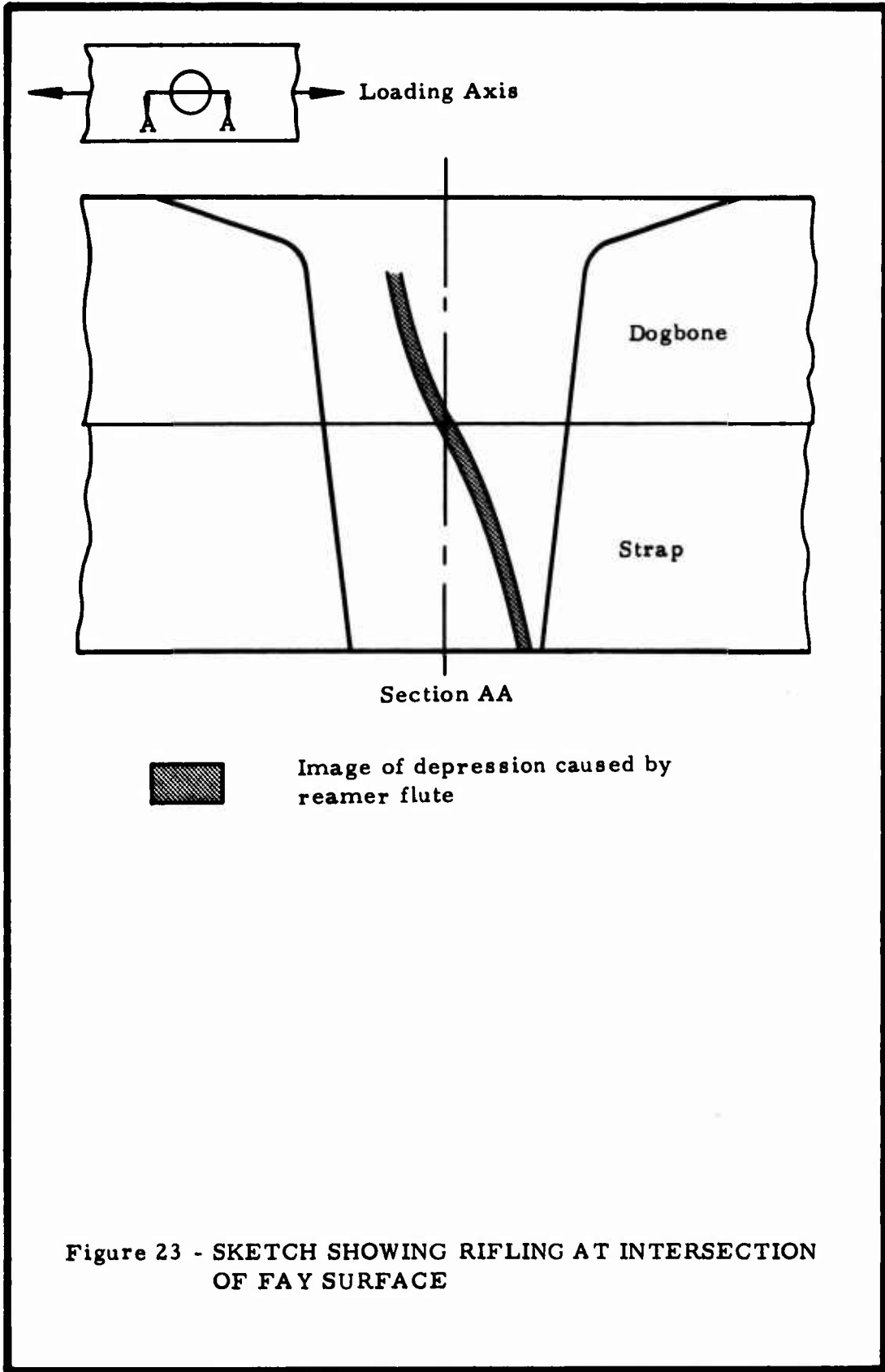


Figure 23 - SKETCH SHOWING RIFLING AT INTERSECTION OF FAY SURFACE

g. Exit Burr

In drilling 5/16 in. diameter holes under the conditions used for this program, an exit burr ranging in height from .015 in. to .020 in. was a normal result. In most of the test series of this program, this burr was not removed. The washer-nut had a recess area in front of the threads to allow the burr to remain unaltered after clamp-up. In a case where the effect of the exit burr was to be studied, (Test Series 18), this exit burr was removed on one series of control samples so that the fatigue behavior without the burr could be compared to the balance of the specimens. The burr was removed with a hand chamfer tool.

Burr height was measured with a series of feeler gages. The measurement was indicated by the thickness of the gage. When placed next to the burr, it permitted a second feeler to slide across the gage and the burr without interference.

h. Surface Roughness

Surface roughness was measured with a stylus type surface roughness gage (Surfindicator) parallel to the axis of the hole, and was varied from 32 to 250 microinches AA. Holes having this range of roughness were produced by allowing aluminum to pick up or build up on a series of reamers and then using these reamers to finish the surface of the test holes. The pickup on the reamer was produced by cutting under conditions which induced buildup on the margin of the cutter. These conditions were high cutting speed and a light feed rate. By controlling the amount of buildup on the cutter, it was possible to produce the desired range of surface roughness.

In producing samples for the surface roughness study, significant amounts of pickup were allowed to develop, resulting in a substantial increase in surface roughness over that which would normally be encountered in a production environment.

i. Rifling

Rifling was defined as the image or impression of the flutes of a reamer being embossed into the surface of the reamed hole. This condition

occurred when a drill motor was stalled in a hole during a reaming operation. This condition was produced by forcing a two-flute tapered reamer into a standard reamed hole (which had already been inspected and found satisfactory with respect to interference and bearing). The reamer was forced into the hole using the spindle downfeed on the milling machine; the reamer was free to rotate but no torque was applied. The reamer was positioned prior to forcing it into the hole so that the flute intersected the fay surface at 90 to the loading axis of the specimen. This configuration is shown in Figure 23.

For this program, the depth of the resulting impression in the wall of the tapered reamed hole was between .005 in. and .010 inches. The width of the impression depended upon the geometry of the reamer flute used. Beyond the dimensional characteristics of the hole as reamed, inspection of the rifled groove was made by replication using a silicone rubber plug and by means of a binocular microscope to examine the indentation at the fay surface. An optical comparator was used to measure the dimensions of the rubber replicate.

j. Axial Scratch

Axial scratches may accidentally be produced in tapered holes either from withdrawing a stalled drilling/reaming tool or through the misuse of a positioning clamp. For our purposes, one axial scratch .005 in. to .007 in. deep was simulated by introducing a V-notch in the side of the hole, 90 degrees from the axial centerline of the test specimen. A small boring bar was ground so as to produce a 45 degree V-notch in the hole surface when the bar was withdrawn through the hole. The sketch in Figure 24 shows the placement of the notch. To create the simulated scratch, the boring bar was withdrawn in the same direction that the drill or reamer would be withdrawn, starting the notch at the exit side of the hole and continuing it up the wall of the hole until it intersected the countersink.

In addition to documenting the hole prior to the introduction of the axial scratch, the final condition was observed using a silicone rubber replicate and also the binocular microscope, as described for making measurements of the rifled condition in Section VI.3.i.



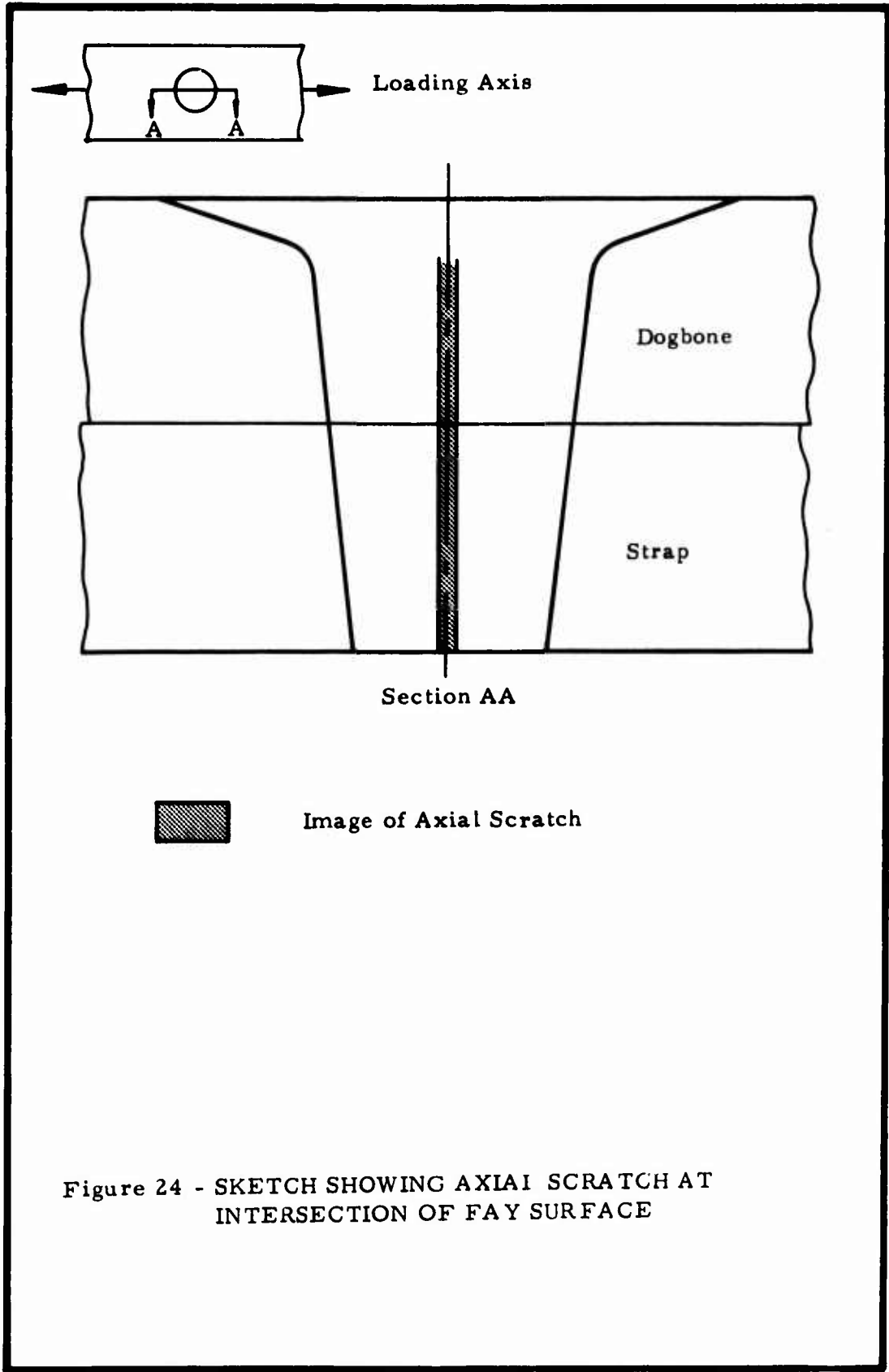


Figure 24 - SKETCH SHOWING AXIAL SCRATCH AT INTERSECTION OF FAY SURFACE

k. Chatter

Chatter is a surface condition characterized by a microscopic roughening or jaggedness of the machine surface resulting from the lack of rigidity between the cutting tool and the workpiece. This condition could be consistently produced in reamed samples in the laboratory by loosening the retaining clamps of the fixture and using a left-hand spiral reamer during the finishing operation.

A typical appearance of a reamed hole in which chatter is present is shown in Figure 25. During the course of this program, the chatter condition itself was inspected visually.

l. Plastic Deformation, Tears and Laps

Worn or dull tooling can produce tears, laps, and associated plastic deformation in a reaming operation. This condition was produced in the laboratory by reaming hundreds of holes without cleaning or resharpening of the tool. When the reamer reached the condition of wear desired, it was used to accomplish the finish reaming operation in the test specimens.

In addition to dimensional requirements, inspection of this condition was by visual observation of the surface and metallographic inspection of a cross section of a hole produced under the same conditions as the test specimens. Metallographic cross sections were used to indicate the extent of plastic deformation and give an estimate of the frequency of tears and laps.

4. Measurement of Hole Quality Level

a. Inspection of Holes

Holes were inspected and conditions documented to the extent noted below. Data is summarized in Tables 4 through 8. Complete inspection sheets on each specimen are contained in Volume II of this report.

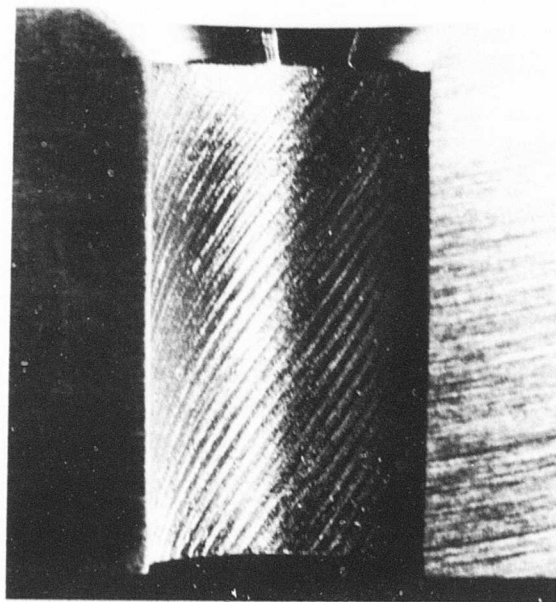


Plate: 6626

Mag: 5X

Figure 25 - ILLUSTRATION OF CHATTER PRODUCED  
BY A LEFT-HAND SPIRAL REAMER

### Inspection at Metcut

Each taper reamed hole was inspected at Metcut in the following manner:

- Protrusion was measured with a height gage as a means of measuring the interference between the fastener and the hole surface.
- Perpendicularity was calculated from measurements of the height of the fastener head as described in Section VI.3.c.
- Burr height was measured by feeler gages as described in Section VI.3.g.
- An air gage was used to determine conformance of the hole at up to five stations of depth and at 45 degree increments around its periphery. The entire matrix of readings was recorded.
- Comparator and dial indicators were used to indicate the extent of bellmouthing, barrelling, depth of rifling, and scratches.
- Readings taken with a capacitance gage supplied by the Briles Fastener Corporation were recorded.
- Silicone rubber replicas were taken of some of the hole surfaces.
- The percentage of bearing was determined by tapping a tapered pin which was coated with Prussian blue into each hole. The impression was transferred from the pin so that it was visually documented with each specimen and presented with the test data. This item was performed by Metcut immediately before final assembly of the test specimens. Inspection performed by Lockheed-Georgia Company as noted below preceded the bluing and assembly operation.

### Inspection at Lockheed-Georgia Company

Two specimens representing each of the various test series were sent to Lockheed-Georgia Company after inspection by Metcut. The primary purpose for this phase was to give Lockheed-Georgia Company the opportunity to work with the segmented capacitance gage which they are developing for tapered reamed holes.

b. Metallography

In manufacturing several series of test specimens, trial coupons were initially drilled and reamed with flaws introduced as required. These coupons were then checked with respect to roughness, flaw depth, hole taper, etc., in order to be certain that the desired condition was being achieved and that it could be reproduced from hole to hole. Once it was established that manufacturing parameters were properly established, holes for each of the test series were then produced in the necessary number of specimen blanks. Coupons relating to each set of specimens were set aside for metallographic examination as covered by this section of the report.

Optical photographs of the surfaces of holes exhibiting variations in surface roughness for Test Series 9 are shown in Figure 26. These photographs, reproduced at a magnification of 15X, were taken on samples of holes which had been sectioned to permit the examination. Scanning electron micrographs of these same four surfaces at both 50X and 200X are shown in Figures 27 through 30. These micrographs show, in much greater detail, the change in characteristics of the surface with increased roughness.

Microstructures of test coupons were also examined to determine the extent of subsurface plastic deformation, possible changes in microhardness and other features that might be related to a particular set of drilling/reaming parameters. Samples were sectioned from coupons and mounted for metallographic examination using standard techniques developed for the study of surface integrity effects. These techniques involve the use of an epoxy mounting material charged with alumina particles. This procedure results in a metallographic mount considerably harder than the material of the sample being examined, thus permitting excellent retention of surface edges and providing the opportunity to examine the surface region in detail.

Photomicrographs of the cross sections of hole surfaces from Test Series 9 are included in this report as Figures 31 through 34. The appearance of these photomicrographs is consistent with the increase in surface roughness from 32 AA to 250 AA.

32 AA

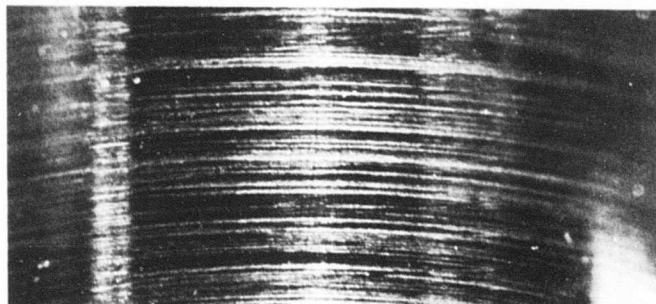


Plate: 6679

63 AA

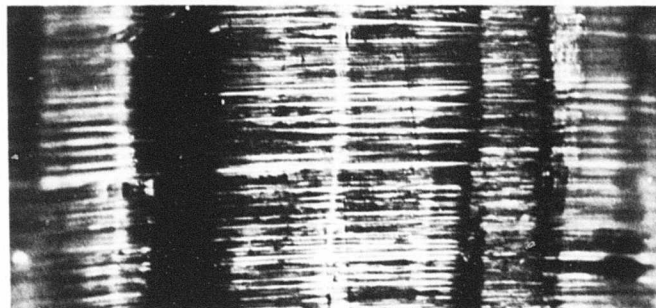


Plate: 6802

125 AA

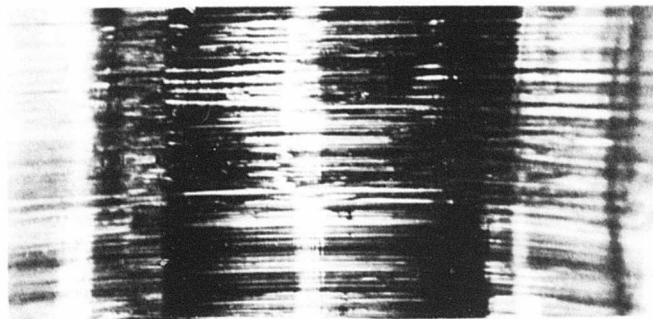


Plate: 6803

250 AA

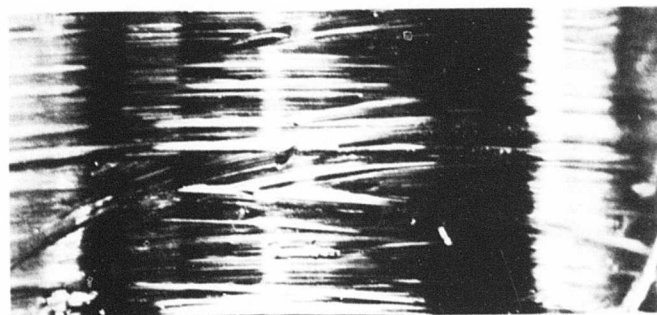


Plate: 6804

Mag: 15X

Figure 26 - OPTICAL PHOTOGRAPHS OF HOLES FROM TEST SERIES 9 SHOWING TYPICAL APPEARANCE OF SURFACES

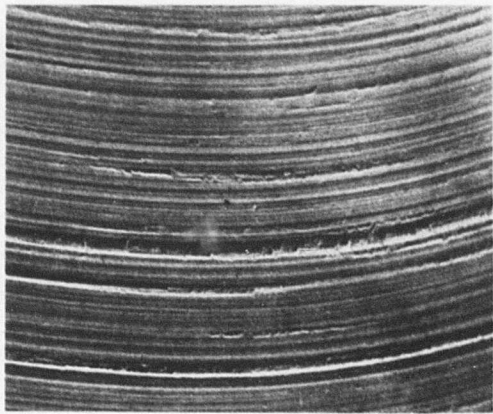


Plate: 6941

Mag: 50X

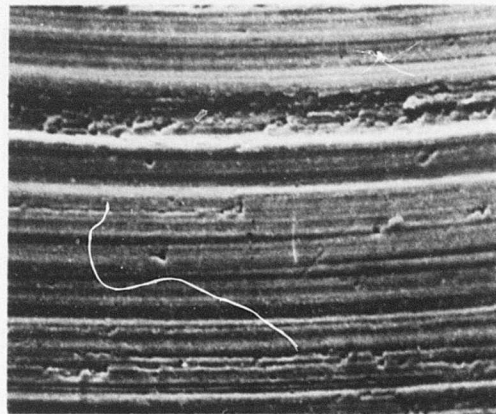


Plate: 6957

Mag: 200X

Figure 27 - SCANNING ELECTRON MICROGRAPH SHOWING  
TAPER REAMED SURFACES AT THE 32 AA  
LEVEL (TEST SERIES 9)

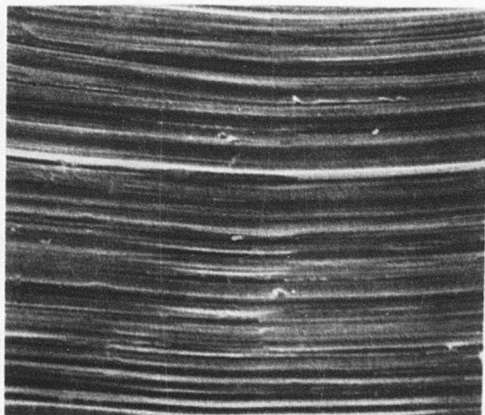


Plate: 6942

Mag: 50X

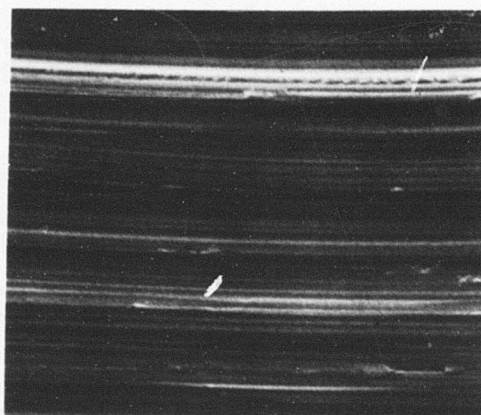


Plate: 6958

Mag: 200X

Figure 28 - SCANNING ELECTRON MICROGRAPH SHOWING  
TAPER REAMED SURFACE AT THE 63 AA  
LEVEL (TEST SERIES 9)



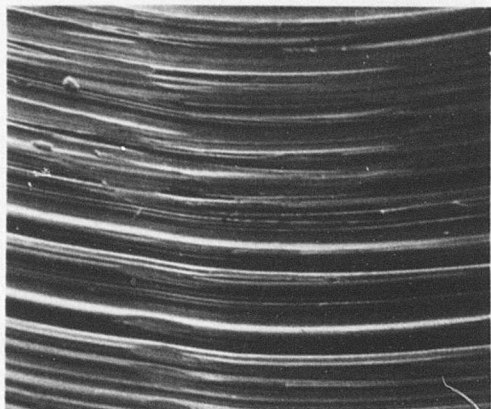


Plate: 6943

Mag: 50X

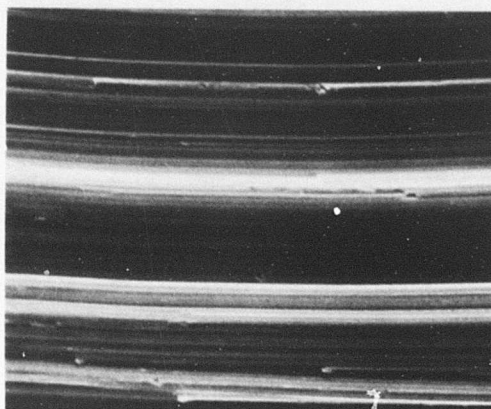


Plate: 6959

Mag: 200X

Figure 29 - SCANNING ELECTRON MICROGRAPH SHOWING  
TAPER REAMED SURFACE AT THE 125 AA  
LEVEL (TEST SERIES 9)

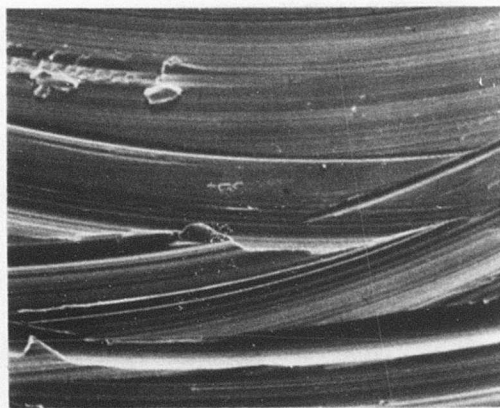


Plate: 6944

Mag: 50X

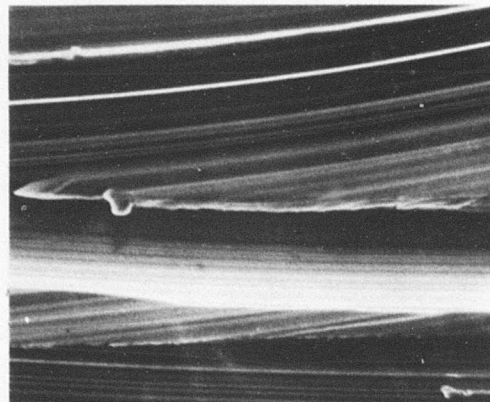


Plate: 6960

Mag: 200X

Figure 30 - SCANNING ELECTRON MICROGRAPH SHOWING  
TAPER REAMED SURFACE AT THE 250 AA  
LEVEL (TEST SERIES 9)



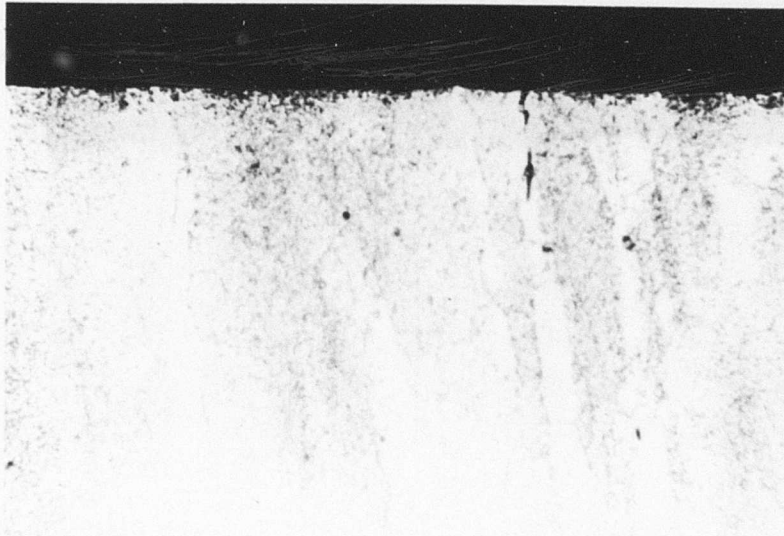


Plate: 21069

Mag: 1000X

Figure 31 - CROSS SECTION PHOTOMICROGRAPH SHOWING  
TYPICAL TAPER REAMED SURFACE AT THE  
32 AA (TEST SERIES 9)

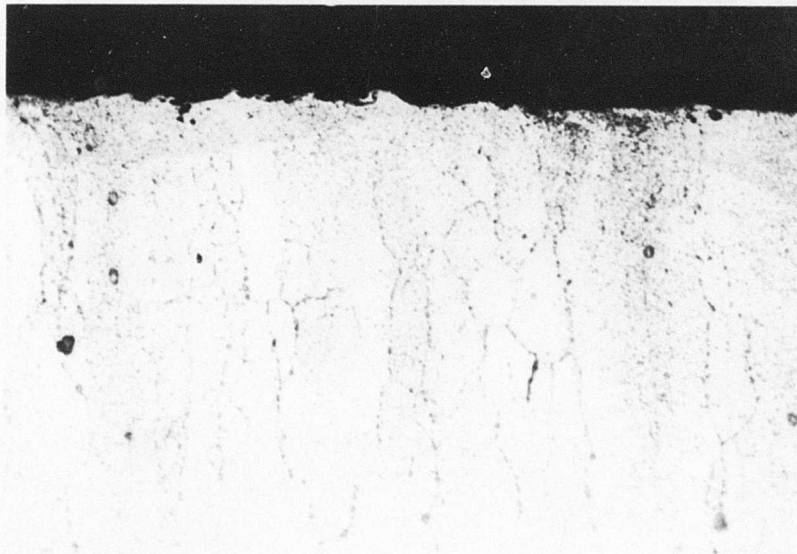


Plate: 21070

Mag: 1000X

Figure 32 - CROSS SECTION PHOTOMICROGRAPH SHOWING  
TYPICAL TAPER REAMED SURFACE AT THE  
63 AA LEVEL (TEST SERIES 9)

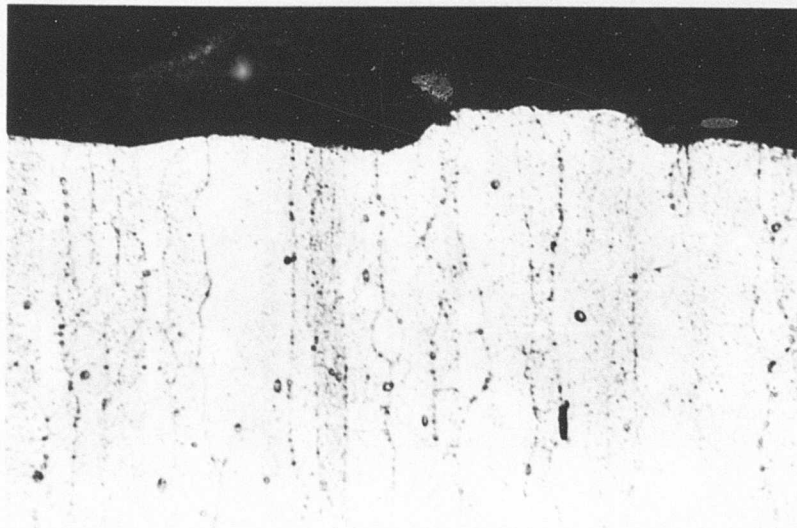


Plate: 21505

Mag: 1000X

Figure 33 - CROSS SECTION PHOTOMICROGRAPH SHOWING  
TYPICAL TAPER REAMED SURFACE AT THE  
125 AA LEVEL (TEST SERIES 9)

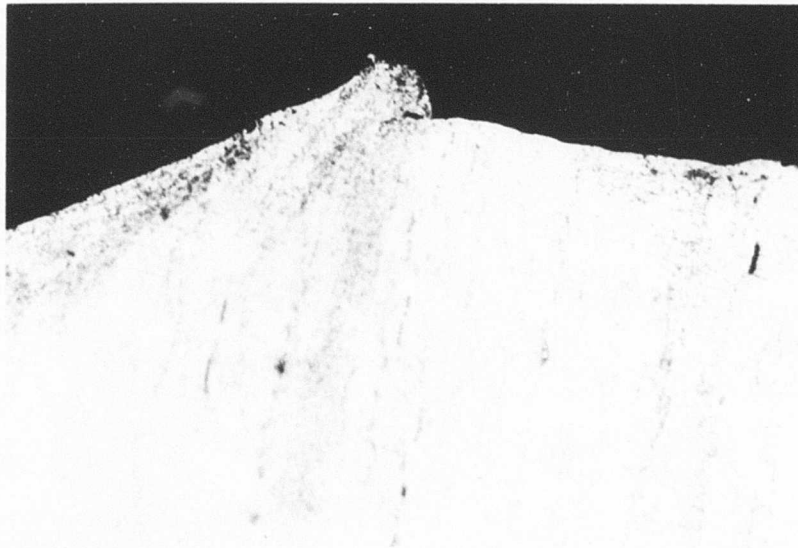


Plate: 21506

Mag: 1000X

Figure 34 - CROSS SECTION PHOTOMICROGRAPH SHOWING  
TYPICAL TAPER REAMED SURFACE AT THE  
250 AA LEVEL (TEST SERIES 9)

Note also the increase in plastic deformation at the surface with increasing surface roughness; this is particularly evident in Figure 34 which depicts the 250 AA sample. When microhardness of these samples was initially checked using a 100-gram load, Knoop data converted to Rockwell B values indicated a slight softening in the first .001 in. of the reamed surface. Subsequent checking and rechecking with lower load readings in the 50-gram range indicated that no consistent hardness change was present. The specimens made for this program exhibited a hardness range of Rockwell B 79-82.

An optical photograph at 15X showing the appearance of the type of rifling covered in this program is illustrated in Figure 35. Scanning electron micrographs at both 50X and 200X showing this defect are contained in Figure 36. An optical photomicrograph showing the appearance of a cross section of one of the rifling grooves is shown in Figure 37. The presence of some plastically deformed material on the periphery of the groove is quite evident in this illustration.

The condition identified as axial scratching, Test Series 11, is illustrated in Figure 38. This consists of a hole initially having a finish of approximately 63 AA to which axial scratches have been added. Scanning electron micrographs of a typical scratch are shown in Figure 39. An optical photomicrograph taken at 1000X shows a typical cross section of this defect in Figure 40.

Chatter, one of the conditions covered by Test Series 12, is illustrated in Figure 41. This illustration is an optical macrograph taken at 15X. Scanning electron micrographs also illustrating the chatter condition are shown in Figure 42. Figure 43 is a cross section photomicrograph of a chatter surface. Note the surface undulations and the waves of plastically deformed material at the surface.

The tears/laps/plastic deformation condition also covered by Test Series 12 is illustrated in Figure 44. The companion scanning electron micrographs are shown in Figure 45. A cross section of this

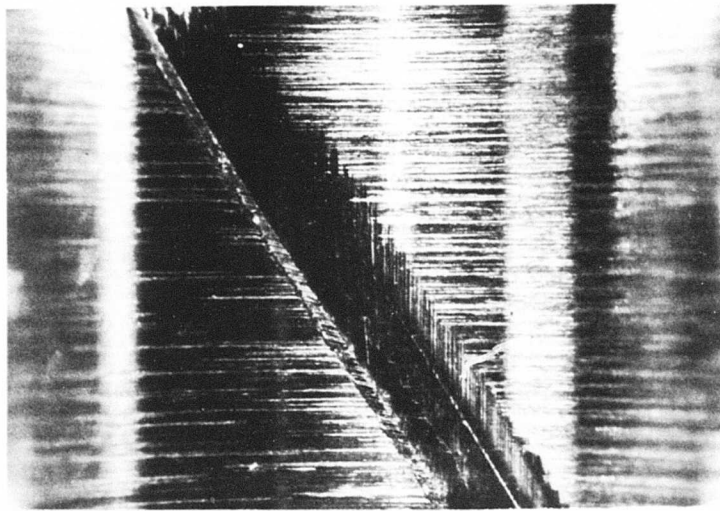


Plate: 6799

Mag: 15X

Figure 35 - OPTICAL PHOTOGRAPH OF HOLE SHOWING  
TYPICAL APPEARANCE OF RIFLING  
(TEST SERIES 10)

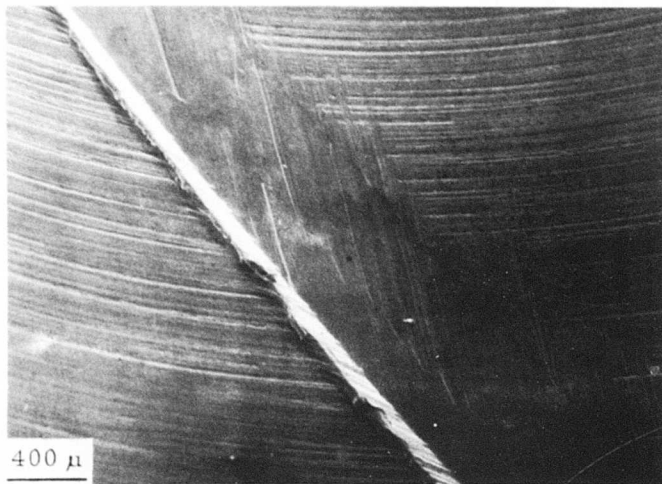


Plate: 6961

Mag: 50X

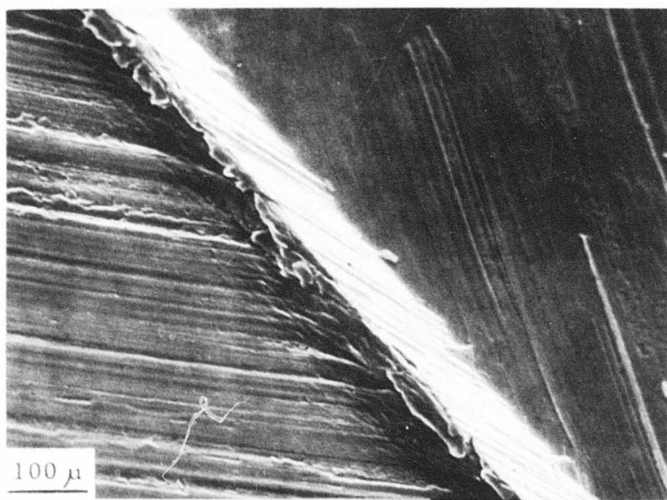


Plate: 6950

Mag: 200X

Figure 36 - SCANNING ELECTRON MICROGRAPHS  
SHOWING TYPICAL RIFLING  
(TEST SERIES 10)

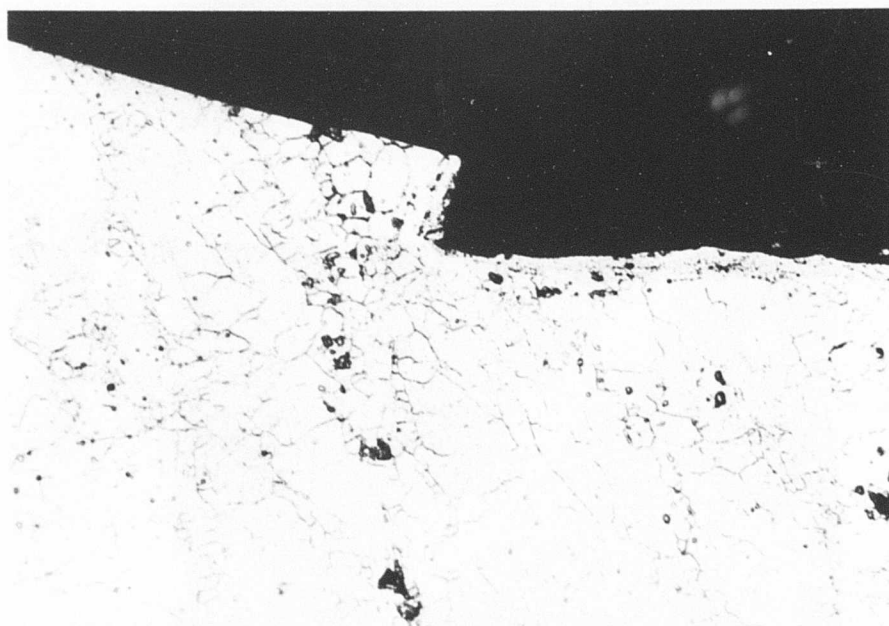


Plate: 21072

Mag: 300X

Figure 37 - CROSS SECTION PHOTOMICROGRAPH SHOWING  
TYPICAL RIFLING (TEST SERIES 10)



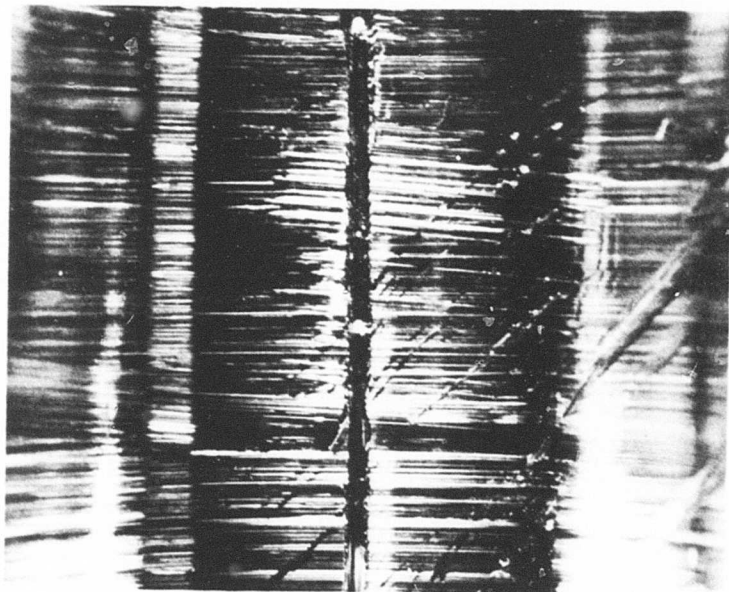


Plate: 6798

Mag: 15X

Figure 38 - OPTICAL PHOTOGRAPH OF HOLE SHOWING  
TYPICAL APPEARANCE OF AXIAL SCRATCH  
(TEST SERIES 11)

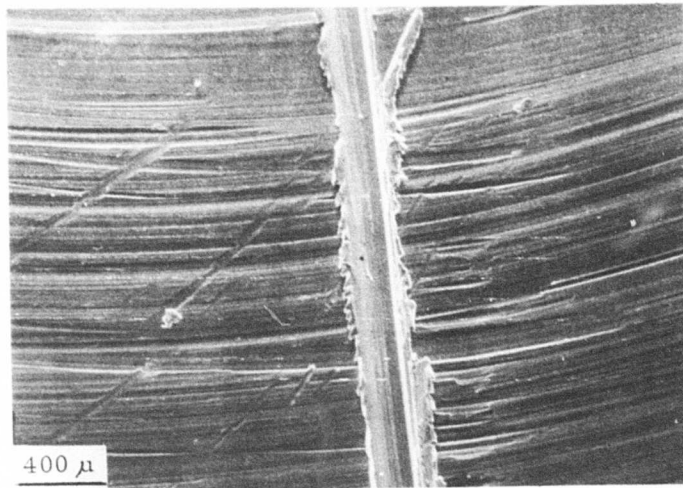


Plate: 6962

Mag: 50X

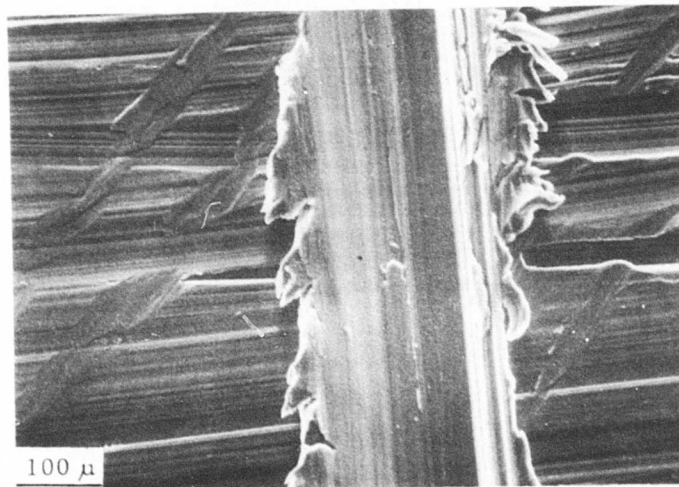


Plate: 6954

Mag: 200X

Figure 39 - SCANNING ELECTRON MICROGRAPHS  
SHOWING TYPICAL AXIAL SCRATCH  
(TEST SERIES 11)



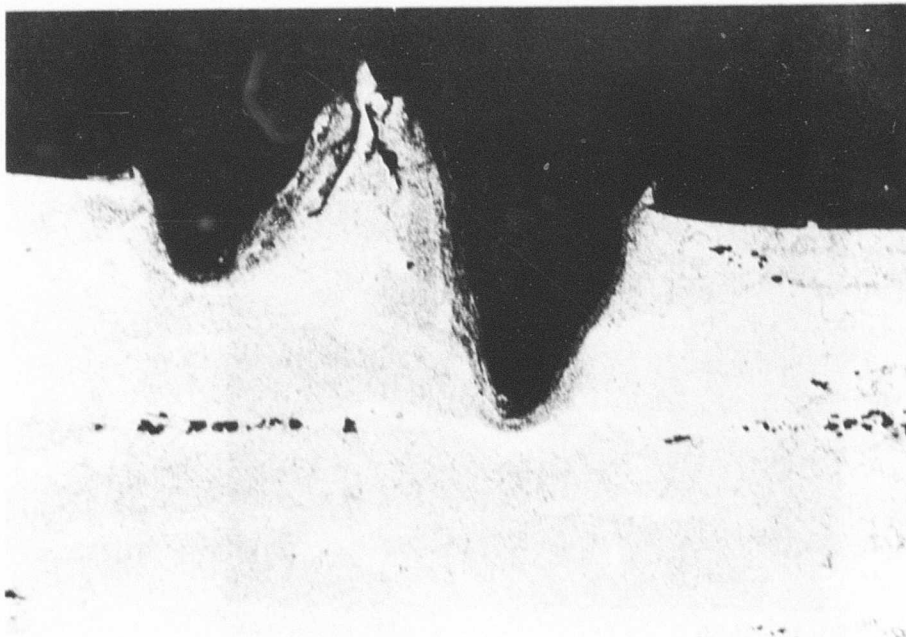


Plate: 21073

Mag: 300X

Figure 40 - CROSS SECTION PHOTOMICROGRAPH SHOWING  
TYPICAL AXIAL SCRATCH (TEST SERIES 11)

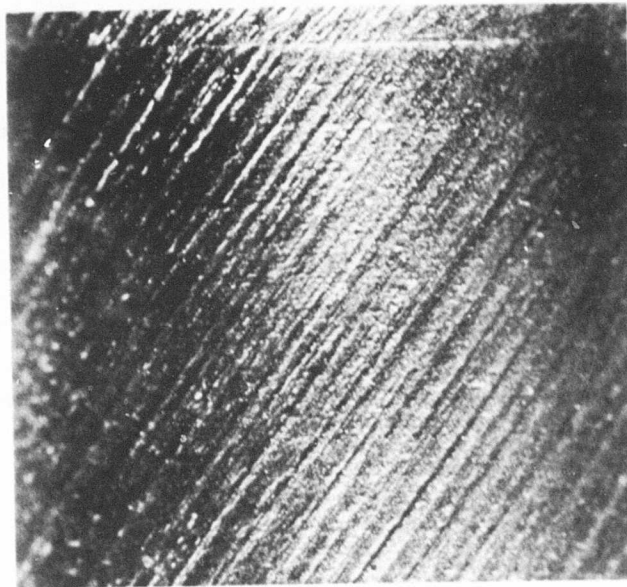


Plate: 6800

Mag: 15X

Figure 41 - OPTICAL PHOTOGRAPH OF HOLE  
SHOWING TYPICAL APPEARANCE  
OF CHATTER (TEST SERIES 12)

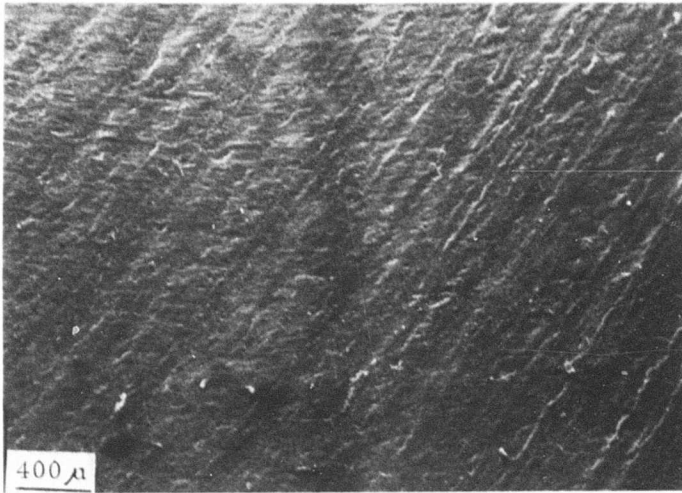


Plate: 6963

Mag: 50X

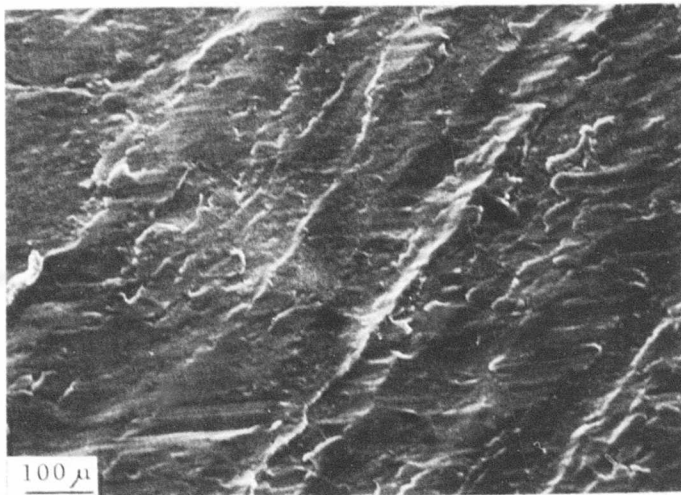


Plate: 6953

Mag: 200X

Figure 42 - SCANNING ELECTRON MICROGRAPHS  
SHOWING TYPICAL CHATTER  
(TEST SERIES 12)

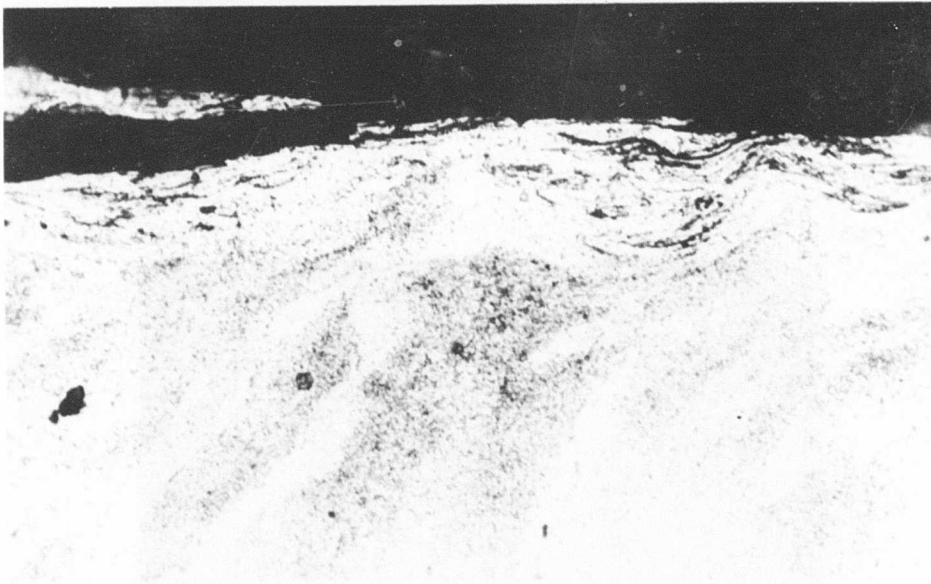


Plate: 21071

Mag: 1000X

Figure 43 - CROSS SECTION PHOTOGRAPH SHOWING  
TYPICAL CHATTER CONDITION  
(TEST SERIES 12)

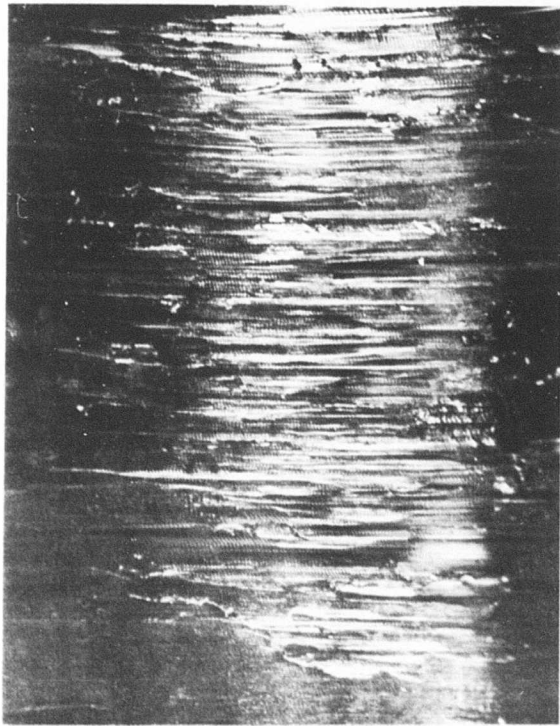


Plate: 6301

Mag: 15X

Figure 44 - OPTICAL PHOTOGRAPH OF HOLE SHOWING  
TYPICAL APPEARANCE OF TEARS/LAPS/  
PLASTIC DEFORMATION (TEST SERIES 12)

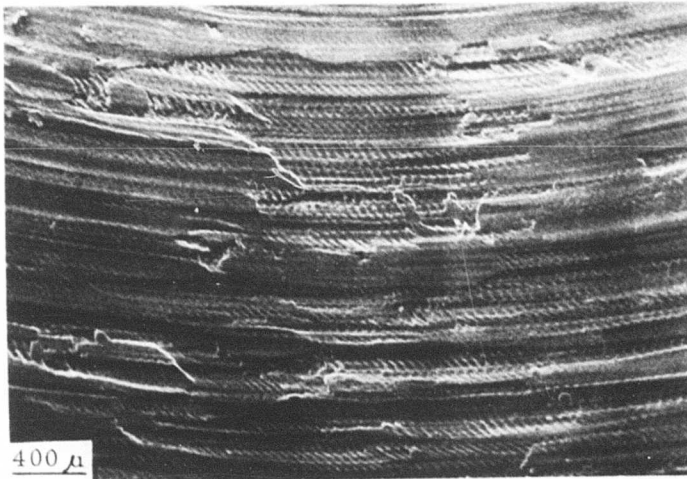


Plate: 6964

Mag: 50X

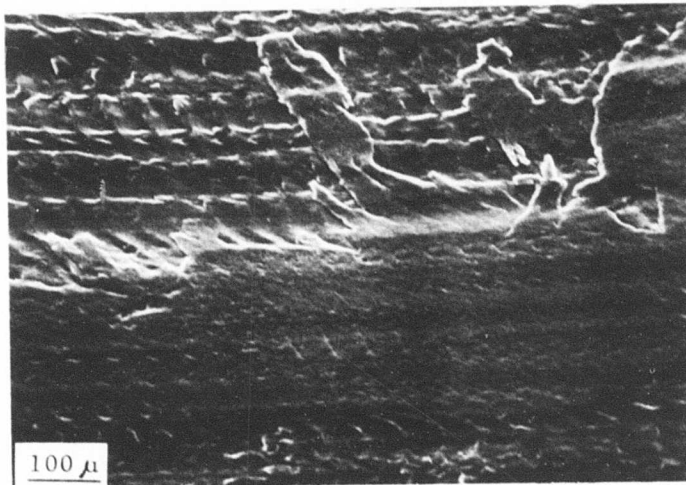


Plate: 6952

Mag: 200X

Figure 45 - SCANNING ELECTRON MICROGRAPHS  
SHOWING TYPICAL TEARS/LAPS/  
PLASTIC DEFORMATION (TEST SERIES 12)

condition at 1000X is shown in Figure 46. The tears/laps/plastic deformation condition is produced by using a reamer which has become loaded, contains a built-up edge or is otherwise effectively "dulled". This condition is intended to produce a fairly high level of working or plastic deformation at the surface along with some tears and laps or smears of redeposited metal. The extent of the severity of the plastic deformation produced in this test series is quite clearly shown in Figure 46. Even in this situation, however, no detectable microhardness change could be related to the highly deformed areas.

## 5. Fatigue Testing Methods

As indicated previously, testing under this program was accomplished in closed-loop servo controlled hydraulic test equipment. Most of the testing was carried out at  $R = 0.1$  and a cyclic speed of 20 to 30 Hz. Limited testing on reverse dogbone specimens was done at  $R = -0.33$ . A photograph of the machine and related equipment used for these tests is shown in Figure 47. In this particular illustration, strain gages are in place on the neutral bending axes of both the dogbone and the strap parts of a low load transfer specimen. These gages were used for determining load transfer levels.

On two or more specimens in each test group, the strain gaged assembly as shown in Figure 47 was continuously monitored by an oscilloscope during the course of the test. The peak cyclic strain measured on both the dogbone and strap or on both dogbones, as was the case, was recorded at intervals. These peak strain levels were used to calculate load transfer and also to observe whether or not the percentage of load transfer changed during the course of the test. Load transfer in this program is defined as that fraction of total load applied to the specimen which is transferred through the fasteners from one component of the specimen to the other. In the case of the dogbone/strap specimens, the calculation is:

$$LT = \frac{\epsilon_a \times A_a}{\epsilon_b \times A_b \times \epsilon_a \times A_a}$$

where  $LT$  = decimal value of load transfer,  $\epsilon_a$  and  $\epsilon_b$  are strains measured in the strap and dogbone, respectively, and  $A_a$  and  $A_b$  are cross sectional areas of the strap and dogbone taken midway between the test



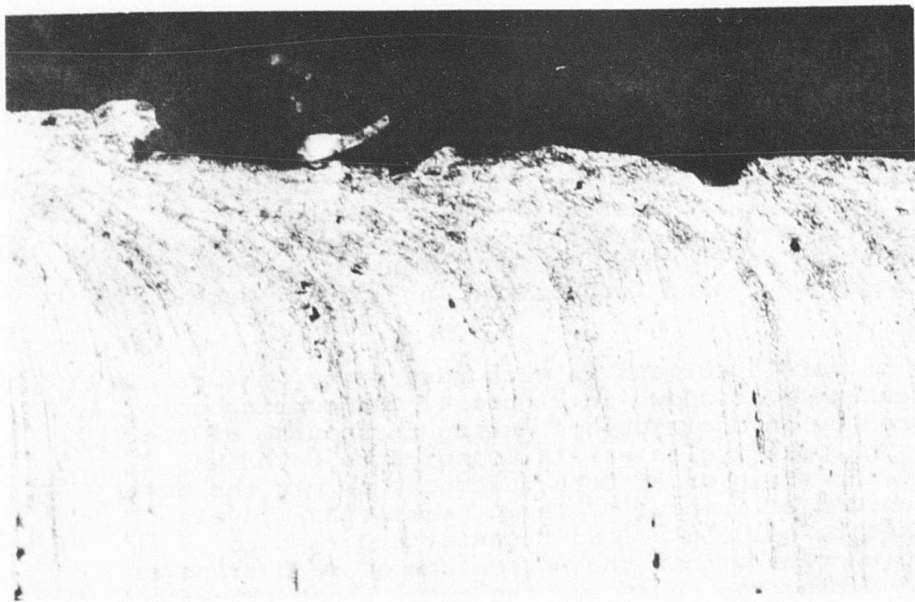


Plate: 21504

Mag: 300X

Figure 46 - CROSS SECTION PHOTOMICROGRAPH SHOWING  
TEARS/LAPS/PLASTIC DEFORMATION  
(TEST SERIES 12)



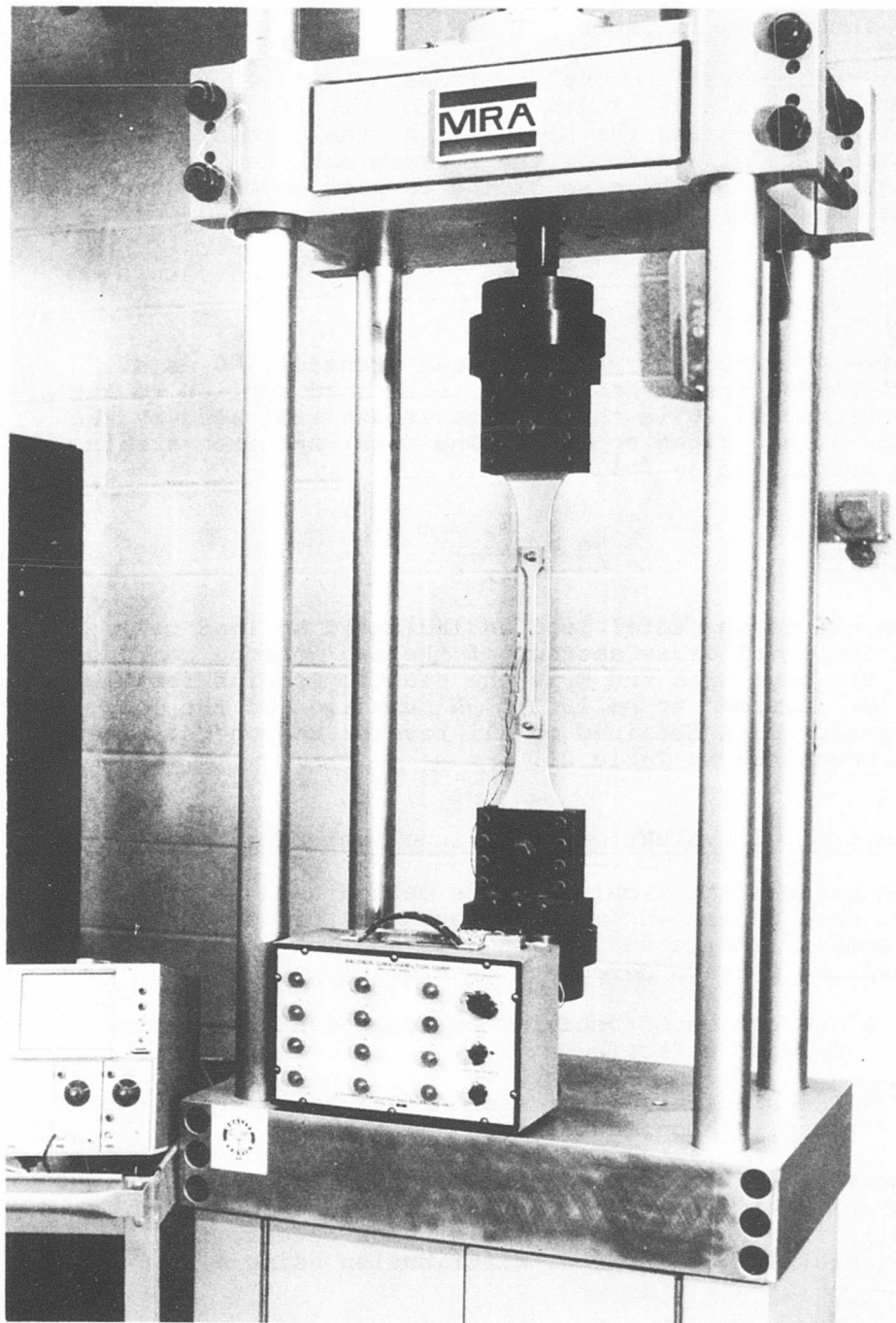


Plate: 6654

Figure 47- CLOSED LOOP, SERVO-CONTROLLED HYDRAULIC TESTING MACHINE

holes. Load transfer data for all dogbone specimens is summarized in Table 20.

For the reverse dogbone specimens, a different calculation is required. This is due to both the nature of this specimen and the placement of the strain gages which were selected for the reverse dogbone tests. (See Figure 8). In the case of the reverse dogbone specimens, the calculation is:

$$LT = \frac{\epsilon_0 - \epsilon_g}{\epsilon_0}$$

Where LT = decimal value of load transfer,  $\epsilon_0$  is a calculated strain based upon total load applied to the specimen and  $\epsilon_g$  is the average strain indicated by the four strain gages applied. The total specimen strain is calculated as follows:

$$\epsilon_0 = \frac{\Sigma}{A \times E}$$

where  $\Sigma$  is the total load as indicated by load cell, A is the total cross section of the two dogbone components in the gage area and E is the elastic modulus for the alloy (assumed to be 10.3). A summation of the load transfer data obtained on all reverse dogbone specimens is contained in Table 21.

## 6. Statistical Evaluation of Fatigue Test Data

The basic statistical analysis method used to evaluate the data generated by this program is presented in the Appendix. The method outlined is applied to the data sampling of each defect to determine:

- The projected behavior of the parent population on each defect.
- The significance of each defect relative to the baseline configuration.

The method assumes the test data sampling fits a "log-normal distribution". The log of the dependent variable ( $X_j$ ), from the test sampling of each defect, is correlated to the normal distribution using a

"linear regression analysis." This analysis directly yields a sample correlation coefficient ( $r_{xu}$ ) and, using the other quantities calculated, the analysis is adapted to include the effect of confidence level.

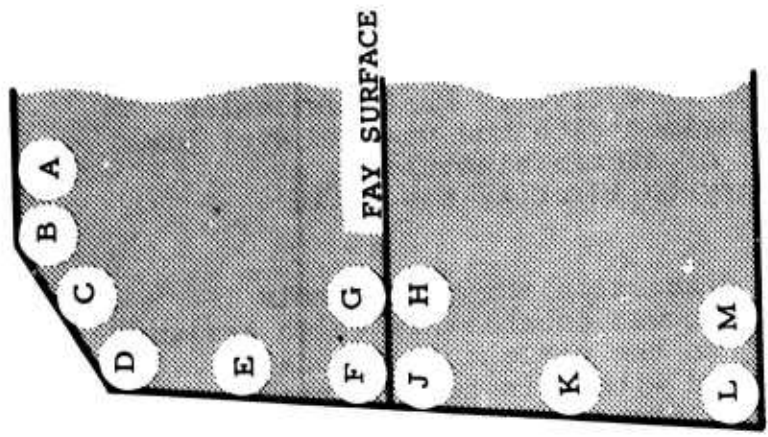
The calculated value of  $r_{xu}$  for the sampling may or may not be statistically significant. This can be examined by subjecting the sample  $r_{xu}$  to a significance test. This test considers the null hypothesis that there is zero correlation between the log of the dependent variable and a normal distribution at a given level of significance. The test determines the absolute critical value of  $r_{xu}$ ; if the sample  $r_{xu}$  is greater than the determined critical value, we reject (at that level of significance) the null hypothesis that the variables have zero correlation. In other words, if the null hypothesis that zero correlation exists were true, a sample  $r_{xu}$  greater than the critical value would only occur with a probability less than the specified level of significance. The test is an equal-tails test since we are interested in both positive and negative correlation.

At a 1% level of significance, the typical critical value of  $r_{xu}$  is approximately .800. This critical value is based on two variables and a minimum of ten data points. If the sample  $r_{xu}$  values calculated are greater than this critical .800 value, then it can be said that a definite statistical correlation exists for the data evaluated.

## 7. Fractography

Following fatigue testing, each failed specimen was examined in order to determine, if possible, the primary origin of failure. Having this information was important, since the nucleation site of the failure provides an indication as to whether or not the interference fit fastener was effective in that particular test. Failures were examined with the unaided eye, low power magnifying glass, or stereo binoculars, as appropriate and necessary to identify the failure origin.

In order to facilitate discussion throughout this report, a system of coding was established which assigned letters "A" through "M" to the various locations of failure origins associated with this test program. This code is described by Figure 48. A brief definition of these failure sites is also indicated on that figure.



Centerline  
of Tapered  
Hole

- A - Entrance Surface
- B - Intersection With Fastener Head
- C - Under Fastener Head
- D - Intersection of Countersink and Hole
- E - Tapered Hole Surface
- F - Exit Corner
- G - Fay Surface
- H - Entrance Corner
- J - Tapered Hole Surface
- K - Exit Corner
- L - Exit Surface
- M - Runout (Removed From Test Without Failure)

Figure 48 - CODE ESTABLISHED FOR IDENTIFYING SPECIMEN FAILURE  
NUCLEATION SITES

Typical fractographs of the failure origins have been recorded using scanning electron microscopy and are illustrated in Figure 49. A failure at the "B" location as shown in Figure 49 is typically caused by fretting between the test material and the head of the fastener. The failure at location "D" is sometimes found at the intersection between the countersink and the tapered surface of the hole resulting from lack of interference at this point or a stress concentration related to the discontinuity. Failures along the tapered surface, as represented by location "E", again are usually associated with lack of interference between the fastener and the structural material into which it is placed. In the case of open hole testing, detrimental hole quality will result in a failure originating in this region. The majority of failures in specimens occurred either at locations "F" or "G" in the free surface (exit surface in the case of open hole specimens) or at the corresponding locations at the exit of the specimen ("L" and "M", Figure 48). A failure occurring at location "F" is what would be expected if an open hole specimen were being tested and if the quality of the hole itself were not sufficiently detrimental to the fatigue strength of the specimen to have an effect. In other words, the stress concentration is such that from geometric considerations, location "F" is the weakest point of the specimen and the anticipated origin of failure. When the fastener is installed, however, and if interference is adequate, failures at location "F" should be inhibited and driven to location "G". An examination of the data contained in the tables at the end of this report shows rather clearly that the majority of failures of specimens containing fasteners was observed at the "G", "H" or "M" locations (Figure 48) except in those situations where the hole quality detracted from fastener performance.

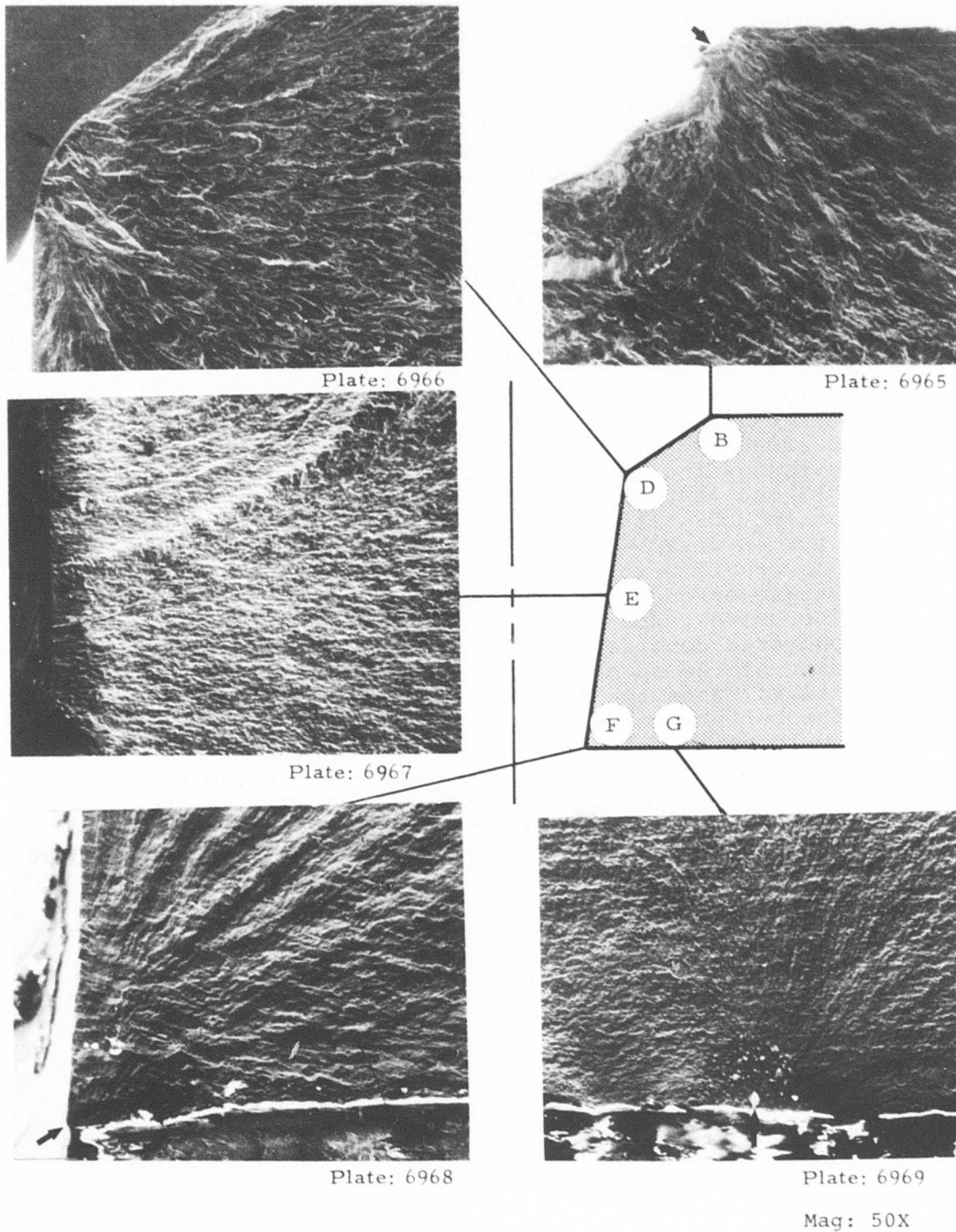


Figure 49 - SCANNING ELECTRON MICROGRAPHS SHOWING FAILURE ORIGIN AND FATIGUE PROGRESSION TYPICAL OF FAILURES ORIGINATING AT DIFFERENT AREAS OF THE TEST SPECIMENS

## SECTION 7

### DISCUSSION AND EVALUATION

Testing on this program fell into three different groups, each related to one of the three different types of specimens used. The open hole testing was carried out for the purpose of identifying the effects of several hole quality variables separated from the effects of the fastener being present. The low-load transfer tests run with the dogbone/strap specimen had the purpose of assessing the influence of detrimental variables identified during the open hole testing and also of assessing the effect of geometric consideration such as interference, ovality, barrelling, etc. The third group of tests, also low-load transfer in nature but using a reverse dogbone specimen, was intended to identify the effects of significant combinations of variables identified with the preceding types of specimens.

This report contains a discussion and evaluation of the fatigue tests developed on Test Series 1 through 22. The specimens for Test Series 23 were manufactured to include the variables shown in Section 3 of this report. These specimens are, however, to be subsequently tested at a laboratory source other than Metcut using C-5A flight spectrum conditions. The results of these tests will be available at a later date.

#### 1. Open Hole Specimens

##### a. Fatigue Testing

Tests on all open hole specimens (Series 9 through 12) were conducted at 1800 cycles per minute and a stress ratio of  $R = 0.1$ . The maximum cyclic stress was determined initially on specimens from Series 9 having a surface roughness of 63 AA or better (per current Lockheed-Georgia Company specifications) by developing the S/N curve shown in Figure 50. From this curve, a selection was made of 16,500 psi as that peak stress which would yield an average specimen life of between  $5 \times 10^5$  and  $10^6$  cycles. Individual test results are contained in Table 4.

Groups of nominally ten specimens exhibiting each of the variables to be covered for the open hole tests (Series 9 through 12) were then all exposed to fatigue loading at a peak stress of 16,500 psi. These groups consisted of different surface roughness levels averaging 32, 63, 125 and 250 AA

FATIGUE BEHAVIOR OF OPEN HOLE SPECIMENS  
7175-T73511 ALUMINUM ALLOY

MODE: AXIAL,  $R = 0.1$   
FREQUENCY: 30 Hz

ORIENTATION: LONGITUDINAL  
TEMPERATURE: 75°F

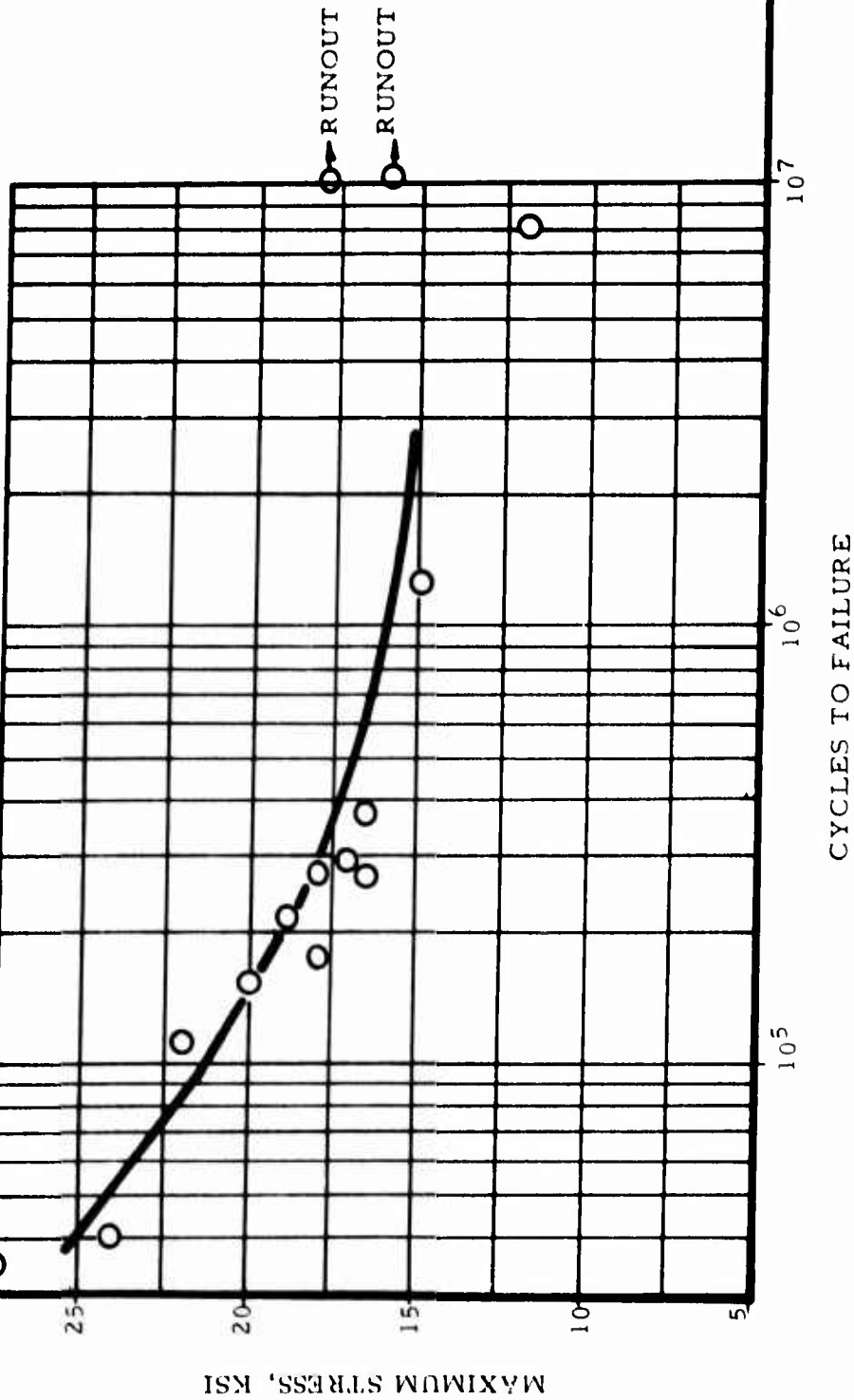


Figure 50 - FATIGUE STRENGTH OF OPEN HOLE SPECIMENS



(Test Series 9), rifling (Test Series 10), axial scratches (Test Series 11), and both chatter and tears/ laps/plastic deformation (Test Series 12). While the nominal baseline anticipated a failure at  $10^6$  cycles or less, a runout level of  $2 \times 10^6$  cycles was established which would permit discontinuance of a test after two million cycles in the event that failure did not occur.

A summary of all of the open hole fatigue testing results is contained in Figure 51. This figure illustrates, for each condition at each stress level, a bar indicating the range of lives exhibited by the specimens in that group. Each vertical line within the bar indicates the life at which a single specimen failed. The number in the box at the right side of the bar indicates the number of runouts exhibited by that group. Mean values and standard deviations are also indicated for each data set.

It will be noted that the specimens having the 63 AA level failed slightly below the baseline expectation which had been previously established with specimens of the same condition. Both the 32 AA and 125 AA samples performed somewhat better. The 250 AA samples, however, while exhibiting one runout and one relatively high life test, also experienced a number of relatively short life failures, suggesting that an increase in roughness to the 250 AA level causes a degradation in fatigue strength. Both rifling and axial scratches have definite and significant detrimental effects on fatigue strength, as again may be seen in Figure 51. The chatter and tears/laps/plastic deformation conditions appear to have some detrimental effect although they are much less significant than the rifling and axial scratch conditions.

An evaluation of this fatigue data is contained in Section VII.1.c of this report. Individual listings of each specimen and results for Test Series 9 through 12 are contained in Tables 5 through 8.

b. Fractography

Each failed fatigue specimen was examined to determine the primary origin of failure as explained in Section VI.6. A summary of the fractographic data developed for the open hole portion of this program, Test Series 9 through 12, is summarized below. The coding used for this summary is indicated in Figure 48:

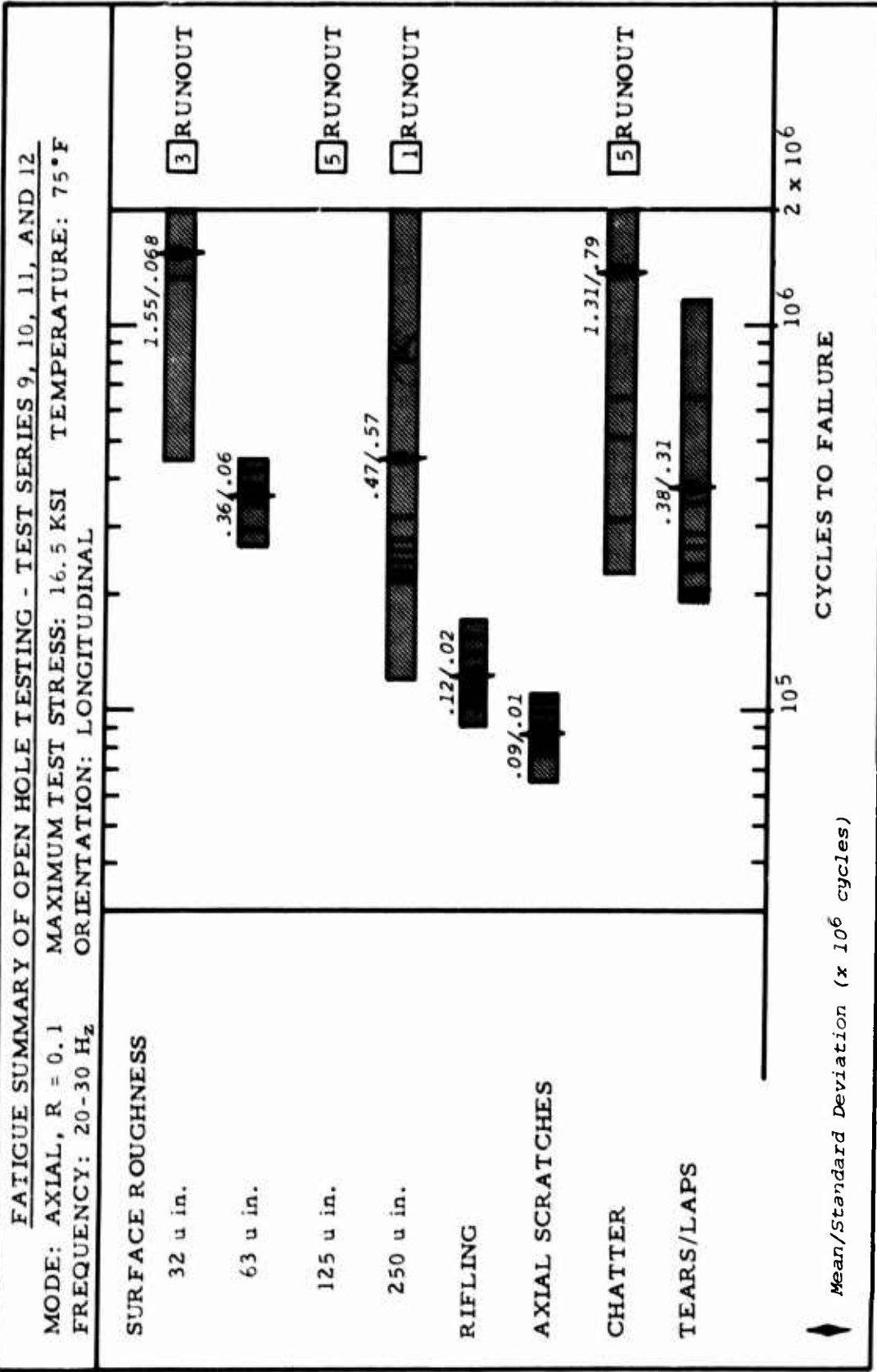


FIGURE 51 - FATIGUE SUMMARY OF OPEN HOLE TESTING

<u>Test Series</u>	<u>Failure Origins Per Figure 48</u>
9 (finish)	
32 AA	3 at F, 7RO
63 AA	1 at D, 4 at E, 12 at F
125 AA	10 RO
250 AA	6 at E, 3 at F, 1RO
10 (rifling)	1 at D, 8 at E, 1 at F
11 (scratches)	6 at D, 4 at E
12 (chatter, etc)	Tears/Laps 4 at E, 6 at F Chatter 5 at F, 5RO

In reviewing this data, we will first consider the testing which dealt with variations in surface roughness, Series 9. Many of the failures in this group occurred at the hole exit location, "F", or were designated as runouts, "RO". Both types of behavior are attributable to specimen geometry and not to a detrimental effect relatable to surface roughness. Specimens having a roughness of approximately 125 AA gave a similar indication and had an indicated fatigue strength as high as the 32 AA specimens. In this instance, all ten of the 125 AA specimens were tested to runout; no failures occurred. The 250 AA specimens showed a visible degradation in fatigue strength in that six of the ten tested failed in the "E" region. Failures in this location indicate that a degradation in fatigue properties due to the surface condition within the hole is sufficiently large to overcome the stress concentration at the exit. So it can be clearly said that the 250 AA finish level does result in a fatigue strength loss. The performance of the 63 AA specimens is somewhat anomalous when compared to the 32 AA and 125 AA specimens. Four of the 63 AA specimens exhibited failures in the "E" location and one in the "D" location. This outcome was puzzling when the tests were being run, resulting in the total number of tests at the 63 AA level being increased from ten (as originally scheduled) to seventeen. Nevertheless, the anomalous condition continues and should be verified or checked further by additional testing.

Specimens from Test Series 10, which evaluated the rifling condition, showed a significant degradation in fatigue strength due to rifling. Eight of the ten specimens tested failed in location "E" with the ninth failing at location "D". The specimens containing axial scratches, Test Series 11, also indicated a fatigue degradation due to this

artificially induced defect. Six of the ten specimens tested failed at location "D", with the remaining four failing at location "E".

Test Series 12 consisted of 20 specimens, ten evaluating a chatter condition and ten evaluating tears/laps/plastic deformation. Of the groups evaluating chatter, five failed at location "F" and the other five were runouts, having been removed from test after an excess of two million cycles without failure. The specimens containing tears/laps, however, did exhibit a modest fatigue degradation in that four of the ten specimens in this group failed at location "E", indicating a sensitivity to the condition of the surface on the side of the taper reamed hole.

If one compared the fractographic evidence covered in this section with the fatigue data contained in Section VII.1.a, excellent agreement is observed. Specimens which exhibited either runouts or failures in location "F" all behaved like the standard or baseline group of specimens which contained no intentional flaws. Those test series which exhibited the large number of failures at locations "D" and "E", happened to be the same groups of specimens that exhibited low levels of fatigue life. From this comparison, it can be concluded that both cyclic life and origin of fracture can be considered as valid criteria for judging the significance of various potentially detrimental conditions on the cyclic resistance of an open hole specimen.

c. Evaluation

Four series of open hole tests are covered by this evaluation; the specific quality variables and the associated test series numbers are:

Surface Roughness 32-250 AA	Test Series 9
Rifling	Test Series 10
Axial Scratches	Test Series 11
Chatter; Tears/Laps/Plastic Deformation	Test Series 12

The specimens were tested to failure or to  $2 \times 10^6$  cycles, whichever occurred first; the following data were recorded:

Cycles to failure (if failure occurred)  
Maximum stress  
Which hole failed (if failure occurred)  
Location of failure in the hole

The complete recorded data are listed in Tables 5 through 8. The data evaluation is performed using the statistical analysis method outlined in Section VI.6. Throughout the analysis, cycles to failure are taken as the dependent variable.

After a preliminary investigation of the data, it was decided that only the pertinent data run at a maximum stress of 16,500 psi would be evaluated. The results of the statistical analysis are summarized in Figures 52 through 56.

### Interpretation

Review of the test data generated for the various induced flaws or discrepancies did not yield definitive results. It was anticipated that a correlation could be established and that the different hole qualities could be grouped into a simplified criterion which would then be related to a well-documented initial flaw condition.

The scatter and the inconsistencies noted in the data, particularly with regard to surface finish effects, were discouraging. It was anticipated that a definite progression of degradation of fatigue life would be evident as changes were made to the hole quality finish. Based on the data obtained, the fatigue life of a tapered hole in 7175-T73511 aluminum alloy is approximately the same for finishes of 32, 63, and 125 AA, but shows definite reduction as 250 AA is approached. This is based on two considerations: the 32 and 125 AA fatigue lives were approximately equal and the modes of failure of 32, 63 and 125 AA specimens were corner failures while those of 250 AA specimens were hole surface associated failures. This latter finding indicates that somewhere between 125 AA and 250 AA the surface roughness becomes a factor in failure mode and location. No statistical correlation could be established between cycles to failure and surface roughness. The corresponding sample correlation for this case is  $r_{xu} = 0.5038$  which is less than the critical value of .800 discussed in

LINEAR REGRESSION ANALYSIS - OPEN HOLE SPECIMENS  
 TEST SERIES 9: SURFACE ROUGHNESS

PEAK STRESS: 16,500 PSI  
 $R = 0.1$   
 $r_{xu} = 0.8568$

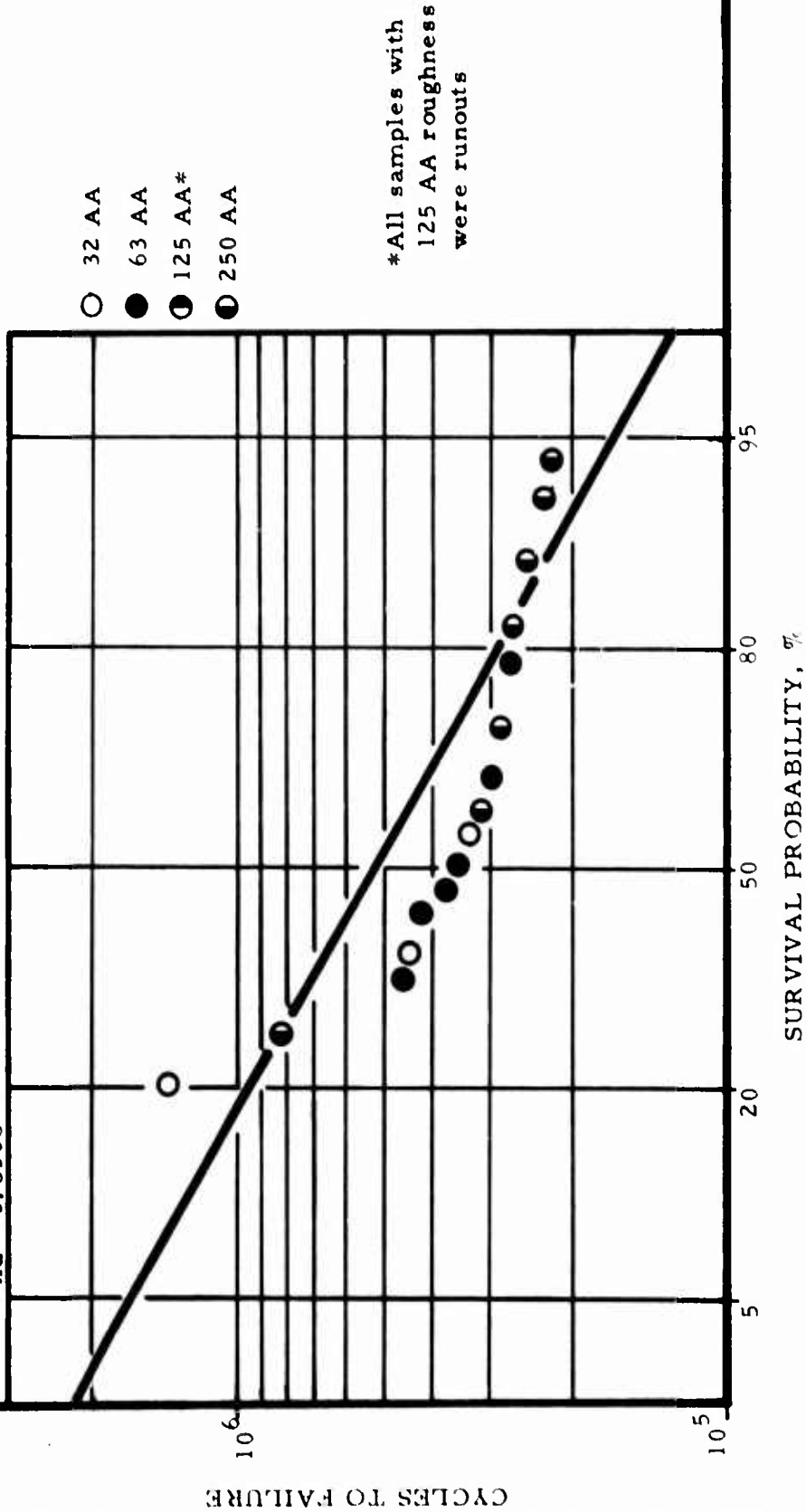


Figure 52 - SURVIVAL PROBABILITY OF OPEN HOLE SPECIMENS - SURFACE ROUGHNESS

LINEAR REGRESSION ANALYSIS - OPEN HOLE SPECIMENS  
TEST SERIES 10: RIFLING

PEAK STRESS: 16,500 PSI  
 $R = 0.1$   
 $r_{xu} = 0.9939$

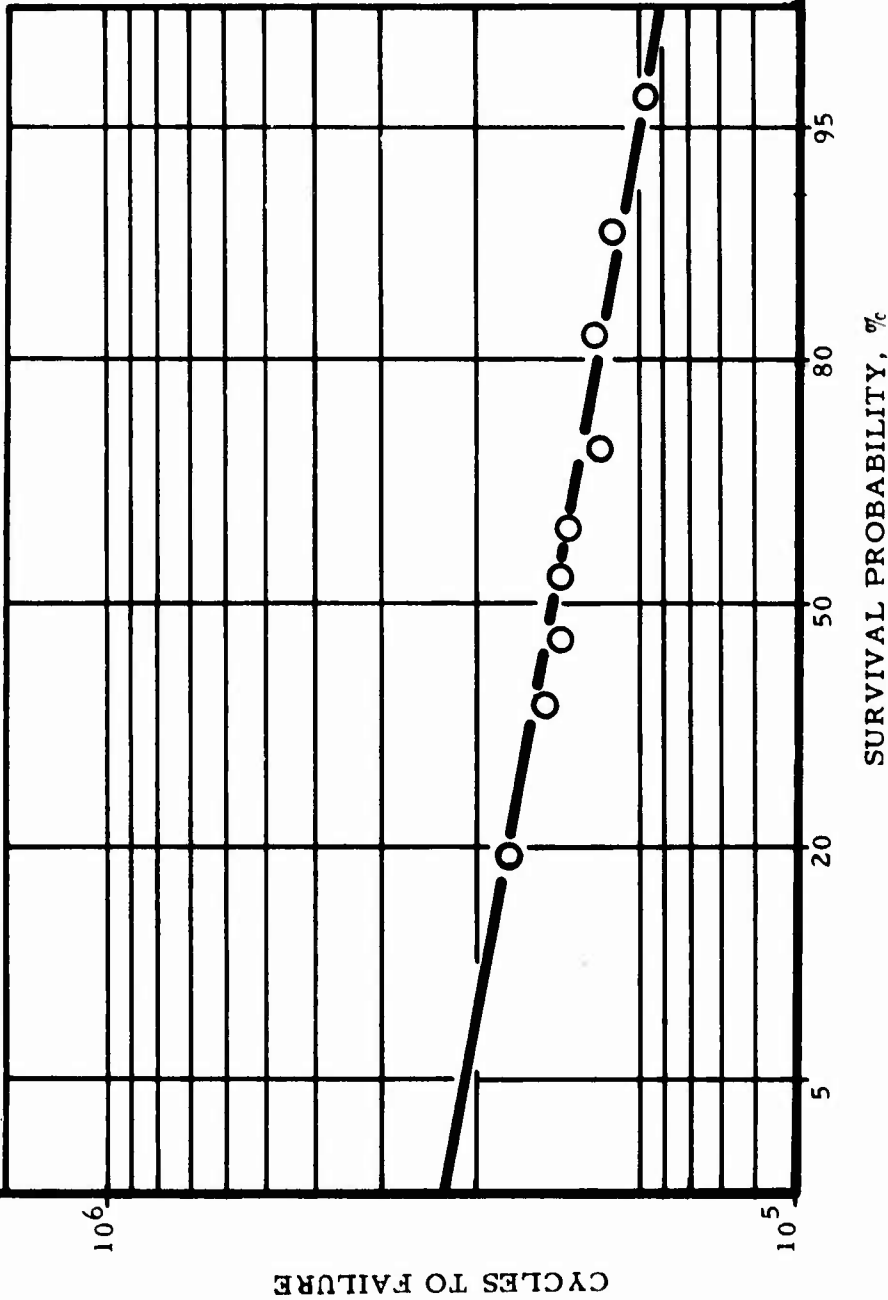


Figure 53 - SURVIVAL PROBABILITY OF OPEN HOLE SPECIMENS - RIFLING

LINEAR REGRESSION ANALYSIS - OPEN HOLE SPECIMENS  
 TEST SERIES 11 - AXIAL SCRATCHES

PEAK STRESS: 16,500 PSI

R: 0.1

$r_{xu} = 0.9871$

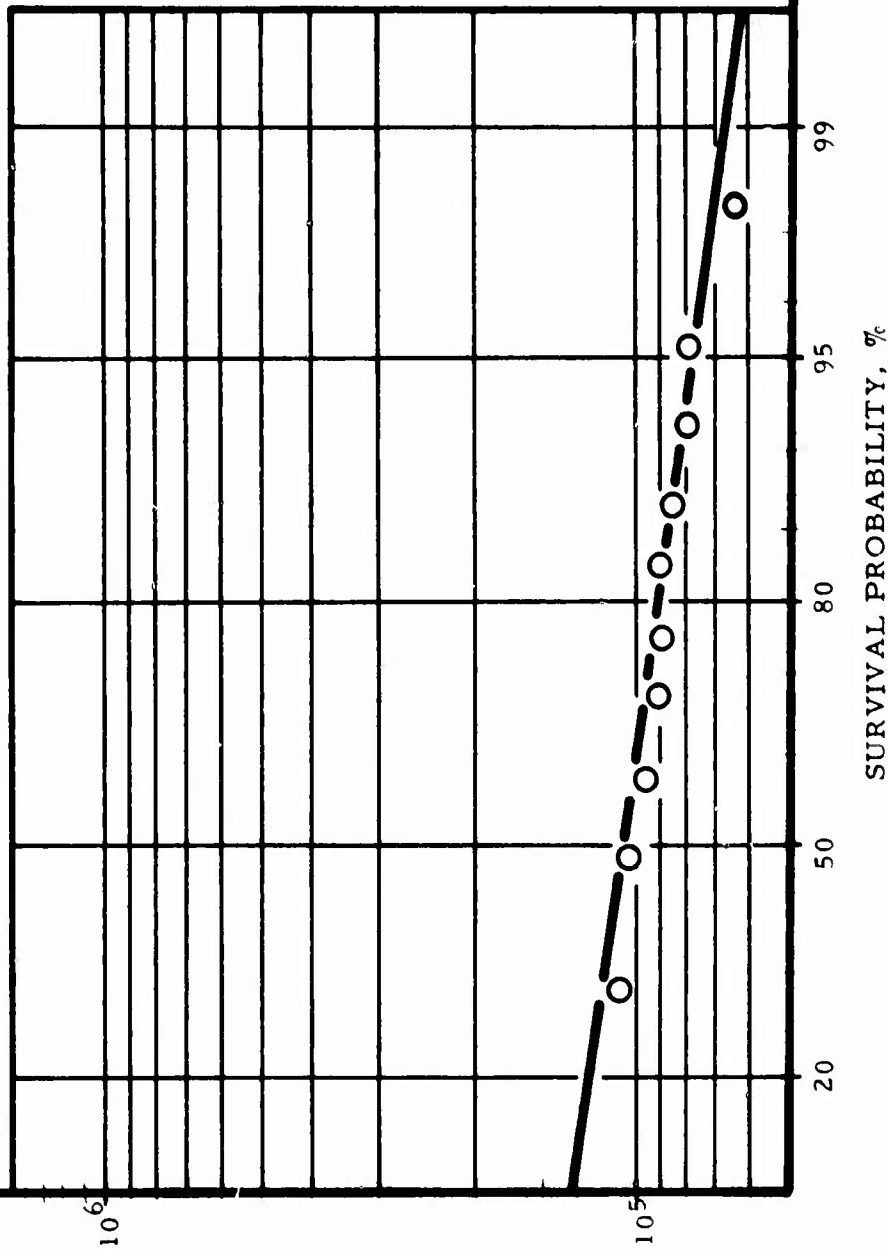


Figure 54 - SURVIVAL PROBABILITY OF OPEN HOLE SPECIMENS - AXIAL SCRATCHES



LINEAR REGRESSION ANALYSIS - OPEN HOLE SPECIMENS  
 TEST SERIES 12: CHATTER AND TEARS/LAPS/PLASTIC DEFORMATION

PEAK STRESS: 16,500 PSI

$R = 0.1$

$r_{xu} = 0.9206$

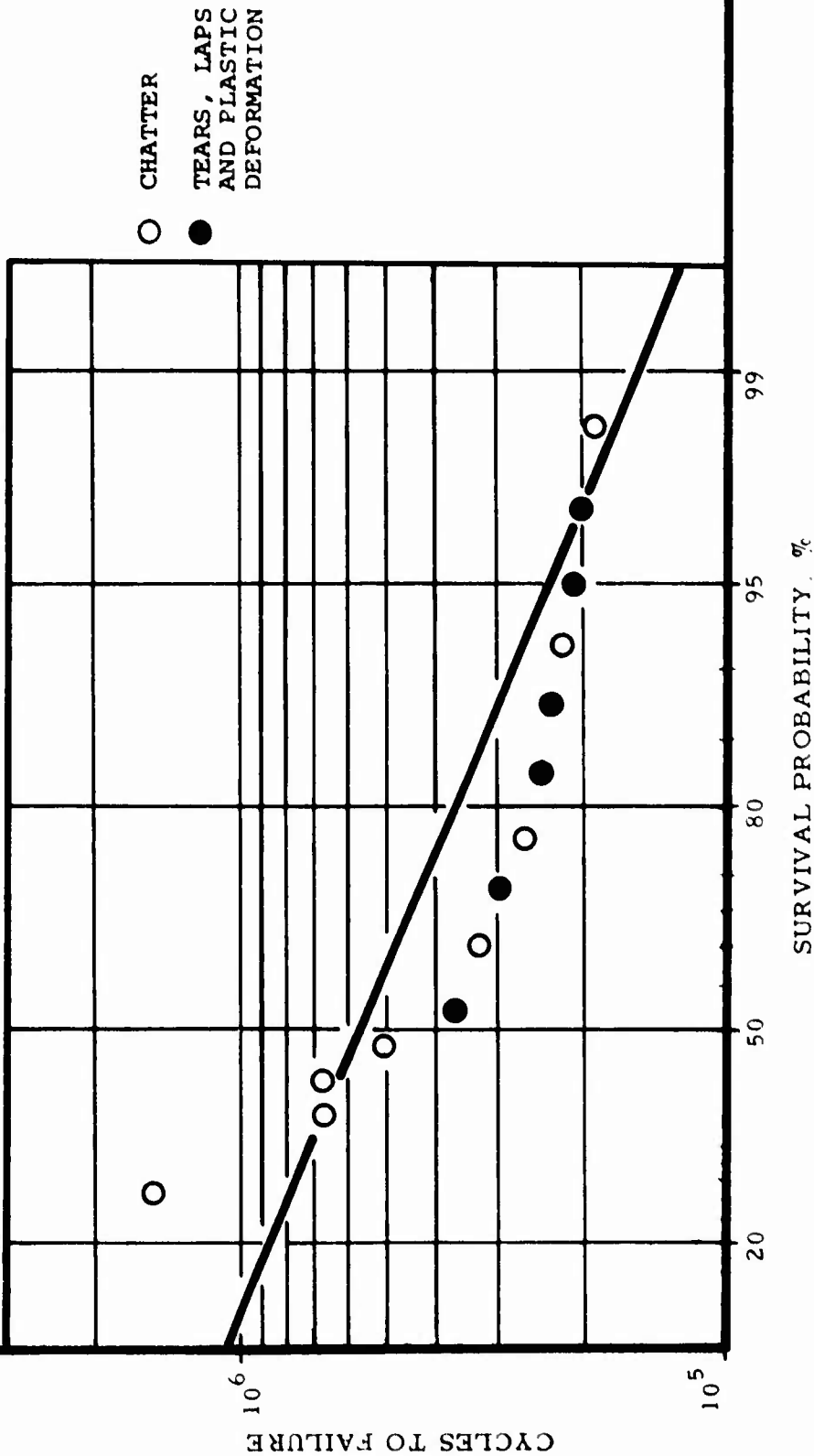


Figure 55 - SURVIVAL PROBABILITY OF OPEN HOLE SPECIMENS - CHATTER AND TEARS/LAPS/PLASTIC DEFORMATION

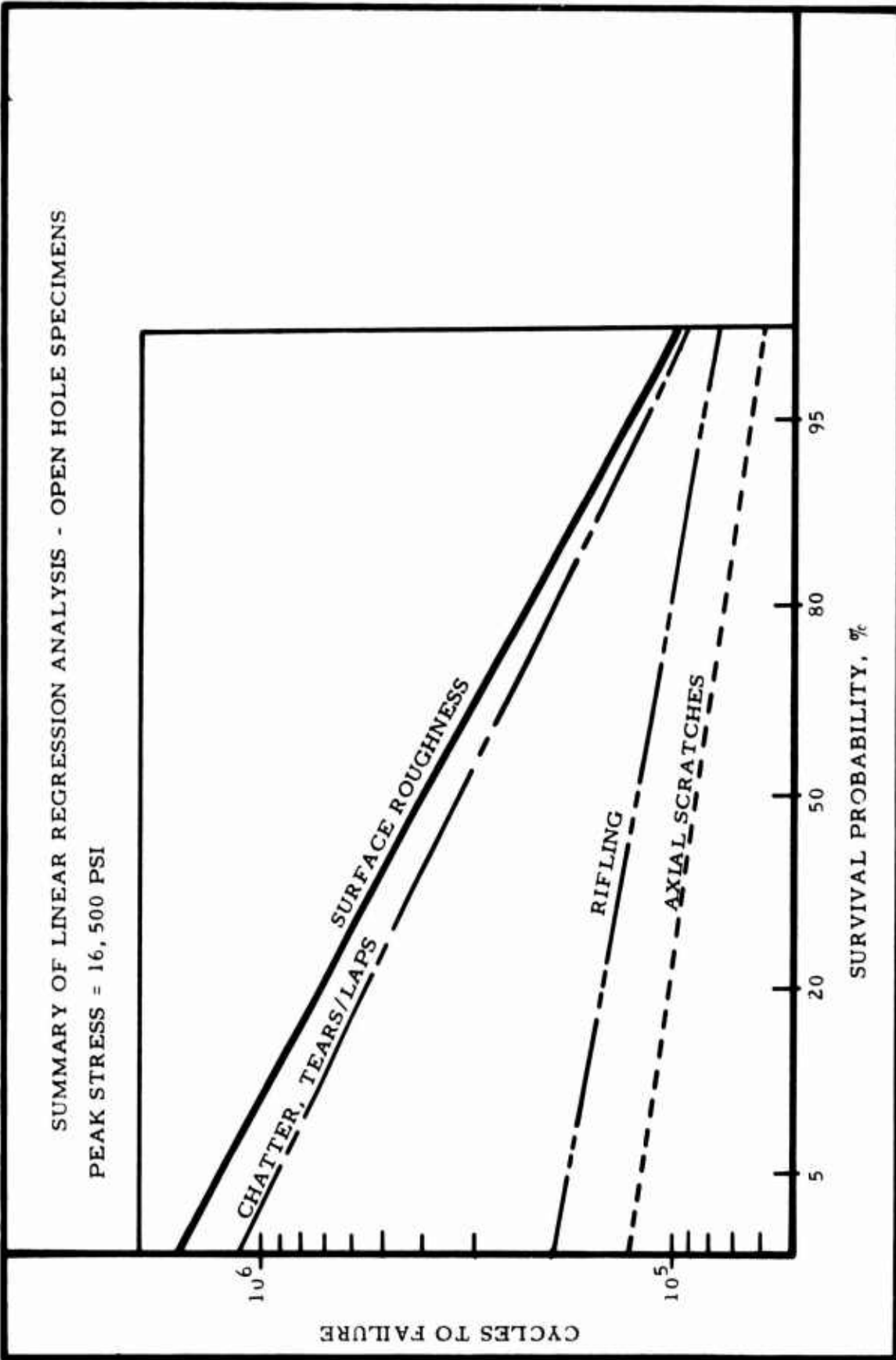


Figure 56 - COMPOSITE: SURVIVAL PROBABILITY OF OPEN HOLE SPECIMENS

Section VI.6. Therefore, the statistical correlation analysis presented was made pooling all surface roughness data.

Intentional variations in hole quality such as scratches, rifling, chatter, and plastic deformation were assessed as to their fatigue performance. It was hoped that this group of discrepancies could be reduced to a common denominator, which could then be related to an existing criterion. Statistical analysis of the test data concluded that the discrepancies cannot be assumed to be of the same statistical population. Therefore, each discrepancy will have to be assessed relative to its individual performance in specific applications as they arise.

## 2. LIT Testing - Dogbone/Strap Specimens

### a. Fatigue Testing

Tests on all (8, 17, 18 and 19) were conducted at a stress ratio of  $R = 0.1$  and for the most part at cyclic speeds between 1200 and 1800 cycles per minute. The specimen, described by Figure 5, produced a load transfer in the range of 13-15%. In the initial stages of this program, a few tests were run at slower test speeds; however, this factor is not considered to be a significant variant in this program. In the early stages of testing, the S/N curve shown in Figure 57 was developed. This was done so that the maximum cyclic or peak stress which would yield a life of between 0.5 and 1.0 million cycles on the standard or baseline specimens could be identified. From the data shown in Figure 57, this maximum stress was selected as 22,000 psi for the testing of all remaining dogbone/strap specimens.

Groups of approximately ten specimens representing each of the dogbone/strap variables were then scheduled for testing at this stress level. Initially, the scatter was somewhat larger than expected in that a number of specimens exhibited lives well in excess of one million cycles. Subsequently, as the dogbone/strap testing proceeded,

FATIGUE BEHAVIOR OF DOGBONE/STRAP SPECIMENS  
7175-T73511 ALUMINUM ALLOY

MODE: AXIAL, R = 0.1  
FREQUENCY: 20 Hz  
ORIENTATION: LONGITUDINAL  
TEMPERATURE: 75°F

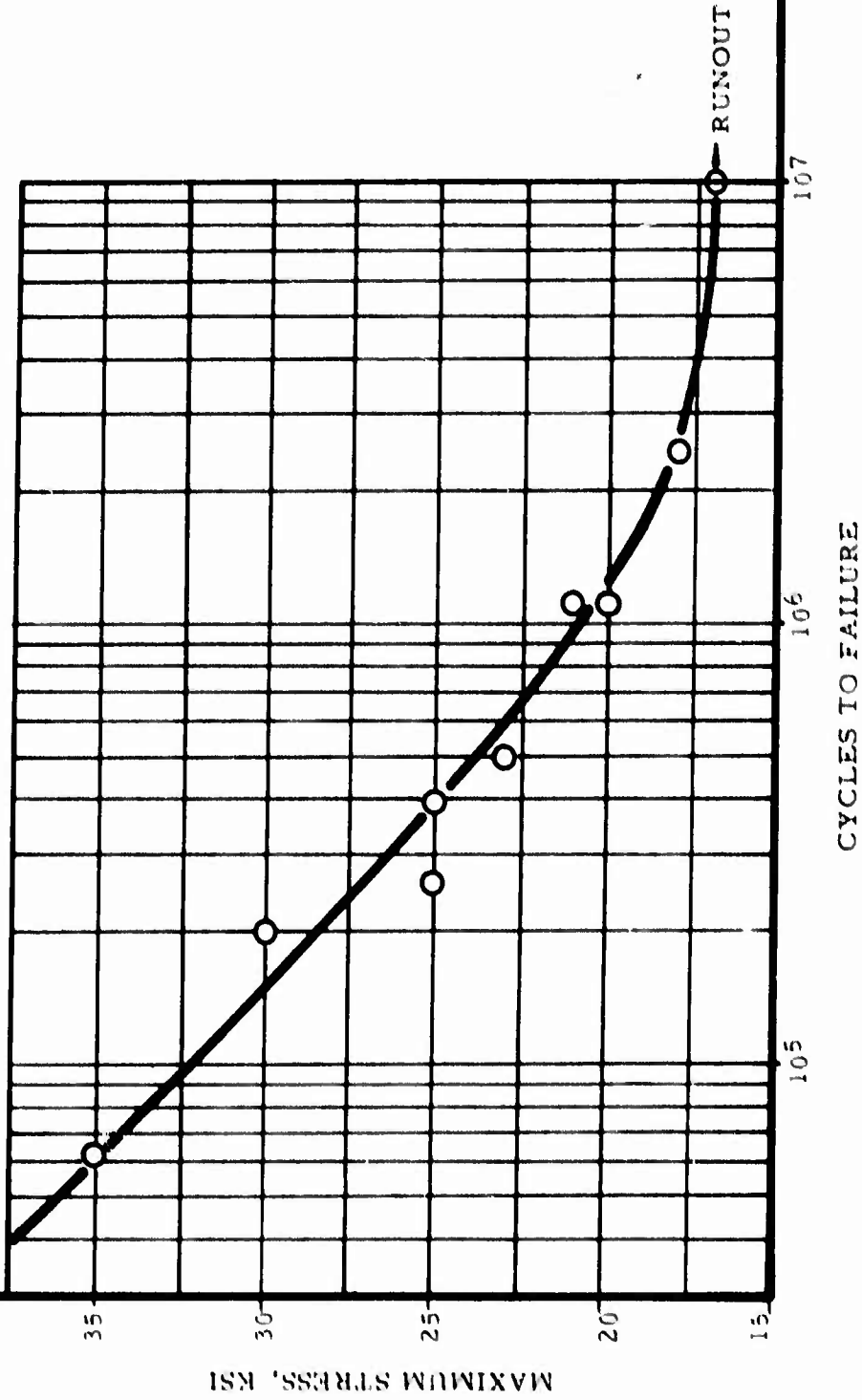


Figure 57 - FATIGUE STRENGTH OF DOGBONE/STRAP SPECIMENS

it was decided to reallocate the specimens representing each variable into two groups of five, one group to be tested at 22,000 and the other group at 25,000 psi.

A summary of the low-load transfer fatigue testing with the dogbone/strap specimens is contained in Figures 58, 59, 60 and 61. In each of these figures, the horizontal bars indicate the range of lives exhibited by specimens in each of the indicated groups and the vertical lines within each bar indicate the lives at which the various specimens in that group failed. Mean values and standard deviations are also included. As explained previously, the number in the box at the right side of the bar, where present, indicates the number of runouts exhibited by that test group.

Referring to Figure 58, note that specimens in which the fastener interference was .0035 in. or .0048 in. (the mid- and maximum interference allowable per the applicable Lockheed-Georgia Company specification), demonstrated maximum fatigue life. The .0060 in. level of interference, which is in excess of the specification, showed a small but statistically insignificant drop in fatigue strength. On the other hand, the specimen having less than the minimum allowable interference, .0005 in., exhibited a relatively low fatigue life. In three of five test results, the specimens having .0023 in. interference, which is the minimum allowed by the specification, also exhibited cyclic life less than the average for the group. At first glance, it would appear that the minimum level of interference is associated with less than substandard fatigue performance. When, however, these data are analyzed statistically and when data from other test series (particularly 7 and 18) which cover interference as a variable are included, it will then be seen that the fatigue behavior of dogbone/strap specimens having fastener interference of about .0023 in. falls in the same range as that of specimens having higher levels of fastener interference.

Test Series 18, which is also summarized in Figure 58, was the first series run on this program using the dogbone/strap specimen design. This group of specimens was run first in order to determine whether the balance of the low-load

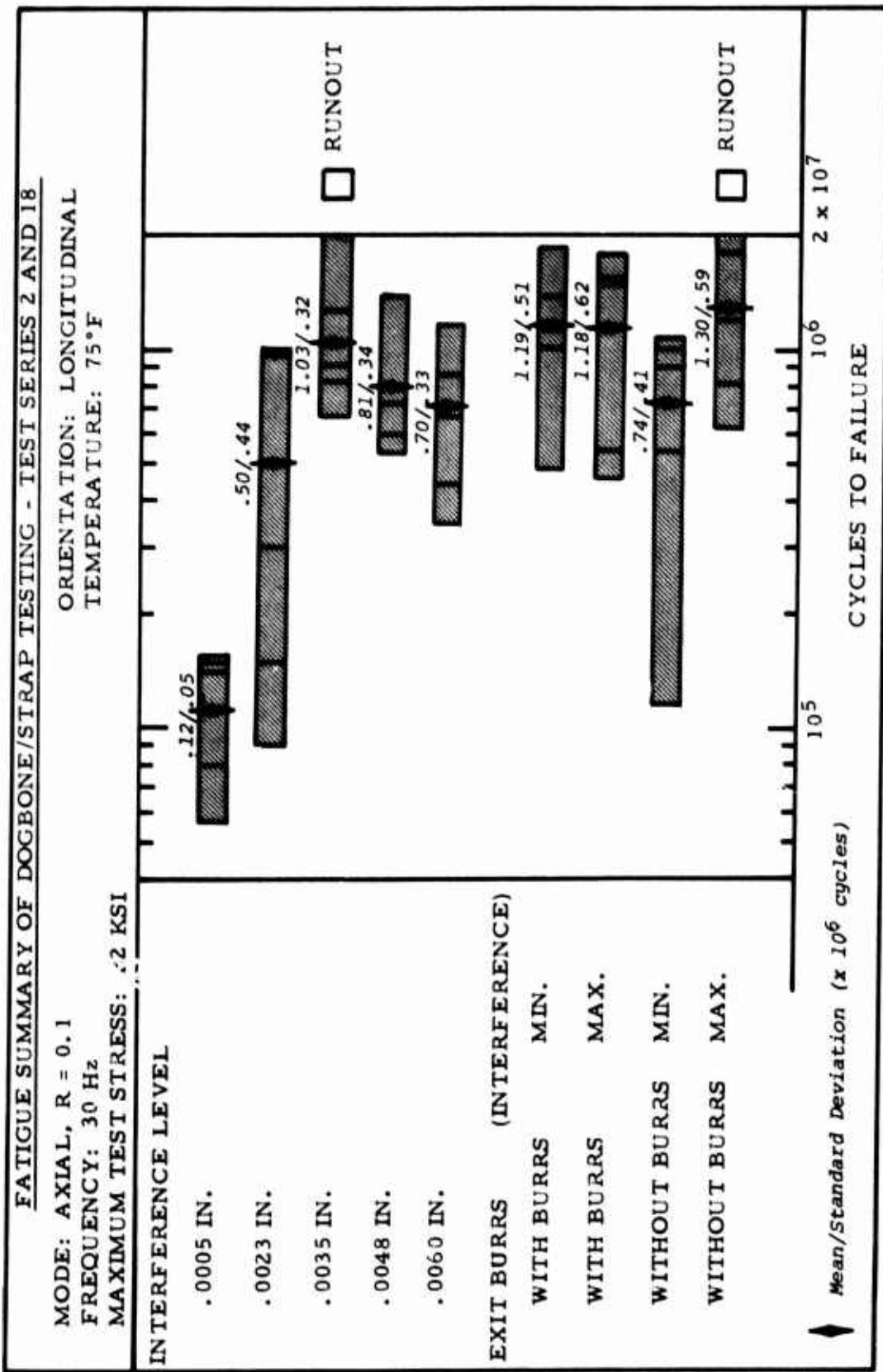


Figure 58 - FATIGUE SUMMARY OF DOGBONE/STRAP TESTING: INTERFERENCE AND BURRS - 22 KSI

transfer specimens would be run with or without the exit burrs which occurred during specimen manufacturing. (In some circles, the presence of exit burrs is considered to promote a loss of fatigue strength, although the applicability of this comment depends upon specimen design and the number of other factors). As far as this particular program was concerned, and as can be readily seen in Figure 58, the presence of the exit burrs had no detrimental effect on fatigue strength. One of the twenty specimens tested exhibited a somewhat shorter fatigue life than the rest of the group but this behavior is not statistically significant. Burrs were therefore not removed on all specimens of the other test series.

Test Series 7, 8 and 17, which evaluated perpendicularity, bellmouthing, barrelling and ovality involved fatigue testing at both 22,000 and 25,000 psi. A summary of the fatigue results on these groups of specimens is presented in Figures 59 and 60. Tests involving perpendicularity, Series 7, showed the same general range of fatigue behavior as the baseline or reference specimens summarized in Figure 58. In the case of bellmouthing, the specimens at the minimum interference level exhibited fatigue degradation in some of the samples but the scatter in test results was quite high. In the case of the bellmouthed specimens having maximum fastener interference, this fatigue behavior was similar to that exhibited by the nondiscrepant specimens. Both barrelling and ovality, as also shown in Figure 59, were associated with marked degradation in fatigue life. These particular hole quality discrepancies resulted in an average fatigue life of roughly 100,000 cycles, compared to an average baseline or reference fatigue life approaching one million cycles.

The data presented in Figure 60 summarizes fatigue behavior resulting from testing at a peak stress of 25,000 psi, compared to the 22,000 psi summarized in Figure 59. Here again, the same general behavior was obtained. Significant fatigue degradation was associated with bellmouthing at the minimum fastener interference level and with ovality and also with barrelling at both interference levels.

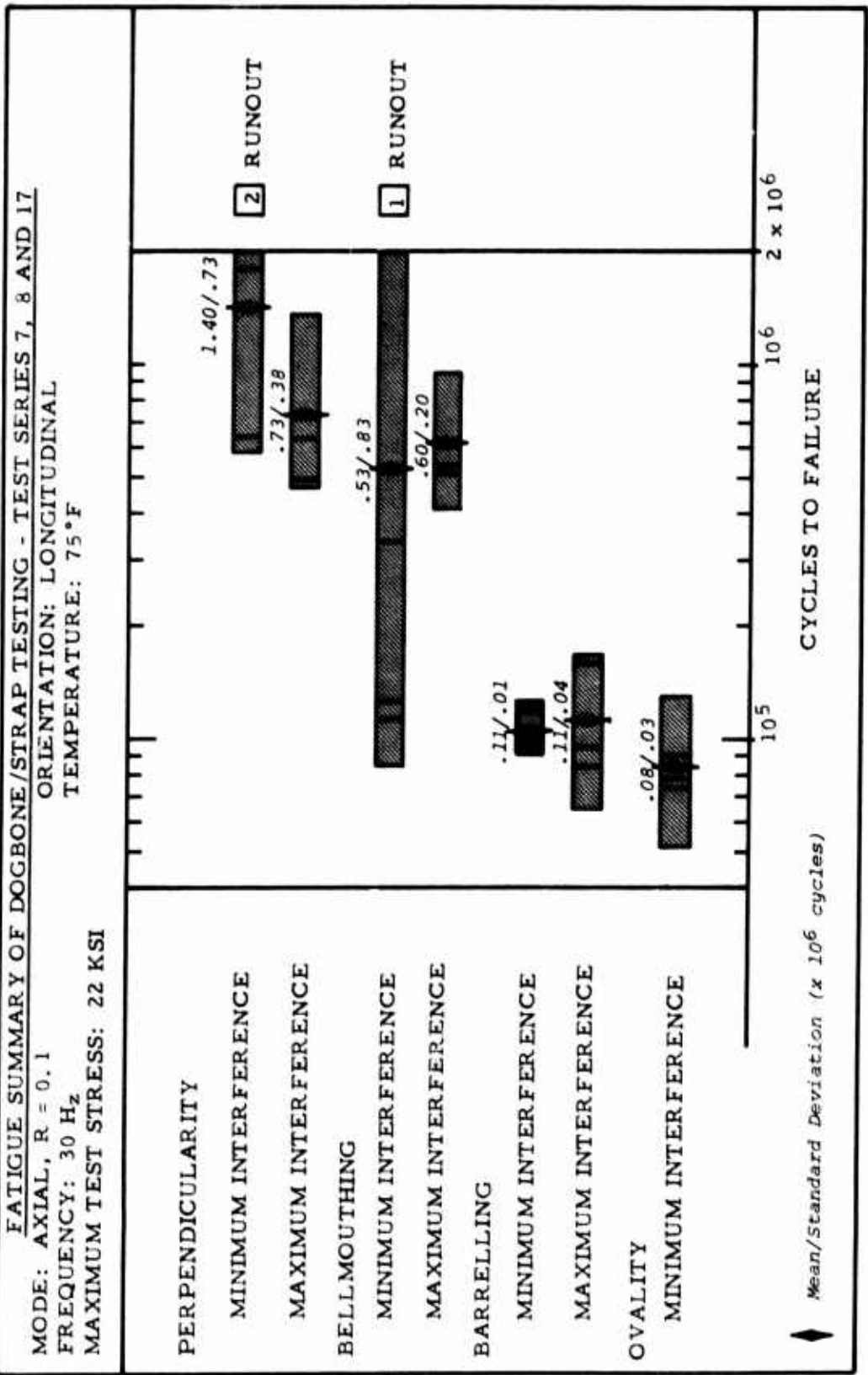


FIGURE 59 - FATIGUE SUMMARY OF DOGBONE/STRAP TESTING



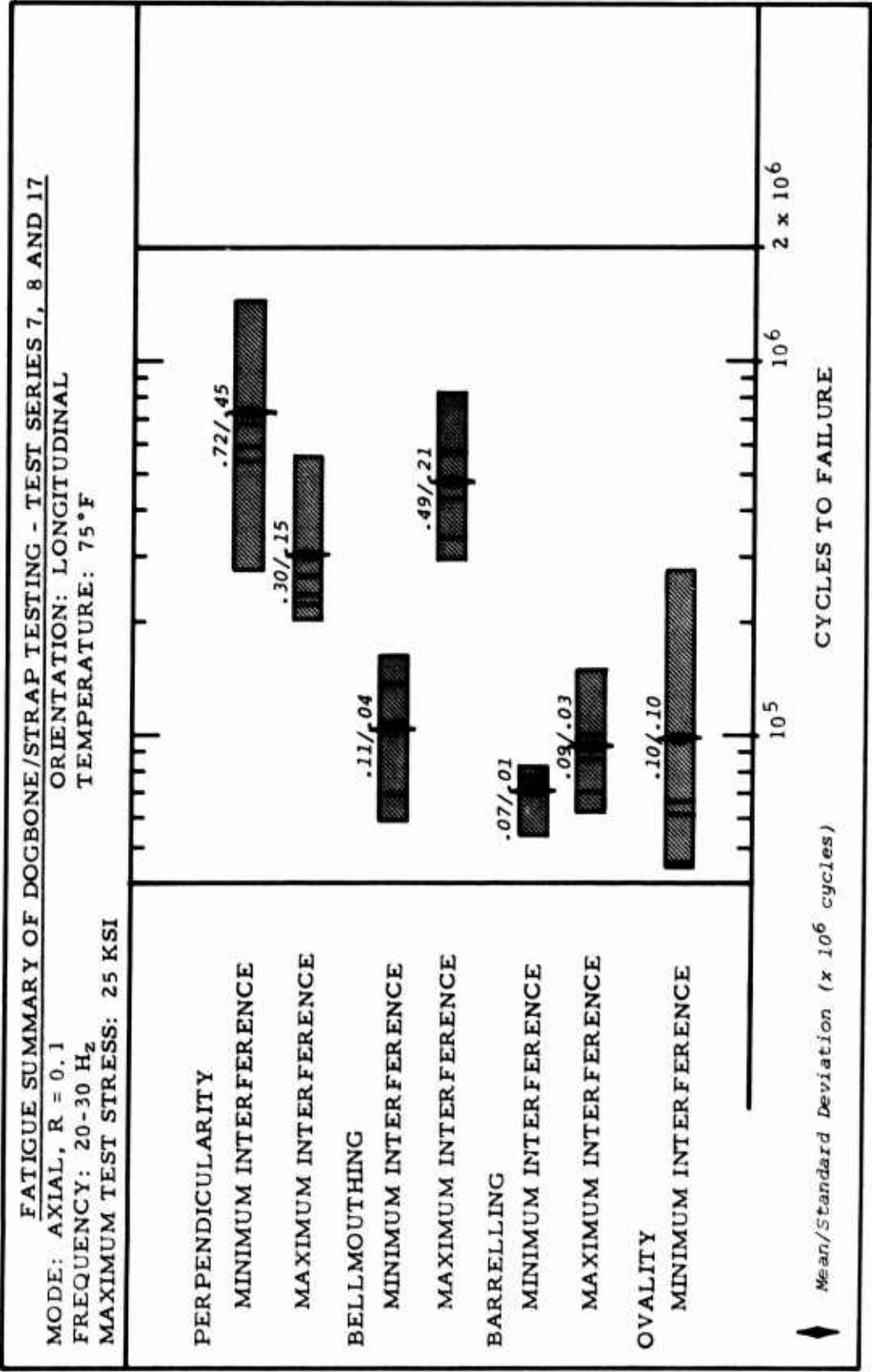


FIGURE 60 - FATIGUE SUMMARY OF DOGBONE/STRAP TESTING

Test Series 19 was concerned with the interactive effect of both hole quality and discrepancies which were intentionally introduced. In this test series, all holes were finished to the 100/125 AA level; both the minimum and maximum specification interference levels were evaluated. As can be seen in Figure 61, holes containing both an axial scratch and rifling behaved no differently than the test hole which was free of an intentional defect. Ovality of holes, however, resulted in a significant degradation in fatigue life. These findings were consistent with the results produced by the other dogbone/strap test series run on this program.

A summary of the fractographic observations on the dogbone/strap specimens is presented in the following section of this report. An evaluation of fatigue data associated with these specimens is contained in Section VII.2.c. Individual listings of each specimen from Test Series 2, 7, 8, 17, 18 and 19, including both specimen inspection report and summary of fatigue behavior, are contained in Tables 9 through 14.

b. Fractography

Each failed specimen was again examined, as was the case with open hole specimens, to determine the origin of the failure. A summary of the fractographic data obtained for these specimens, using the scheme for coding described in Figure 48 of this report, is summarized below:

<u>Test Series</u>	<u>Failure Origins per Figure 48</u>
2 (Interference)	
.0005 in. interference	5 at F
.0023	1 at A, 3 at F, 1 at G
.0035	1 at A, 1 at C, 3 at G
.0048	1 at A, 1 at F, 3 at G
.0060	1 at F, 3 at G
7 (Perpendicularity)	
Min. Interference	1 at E, 1 at F, 7 at G
Max. Interference	10 at G
8 (Bellmouthing)	
Min. Interference	1 at B, 8 at F
Max. Interference	2 at B, 1 at C, 7 at G

FATIGUE SUMMARY OF DOGBONE/STRAP TESTING - COMBINED VARIABLE, TEST SERIES 19

MODE: AXIAL, R = 0

FREQUENCY: 25-30 Hz

MAXIMUM TEST STRESS: 22 KSI

ORIENTATION: LONGITUDINAL

TEMPERATURE: 75°F

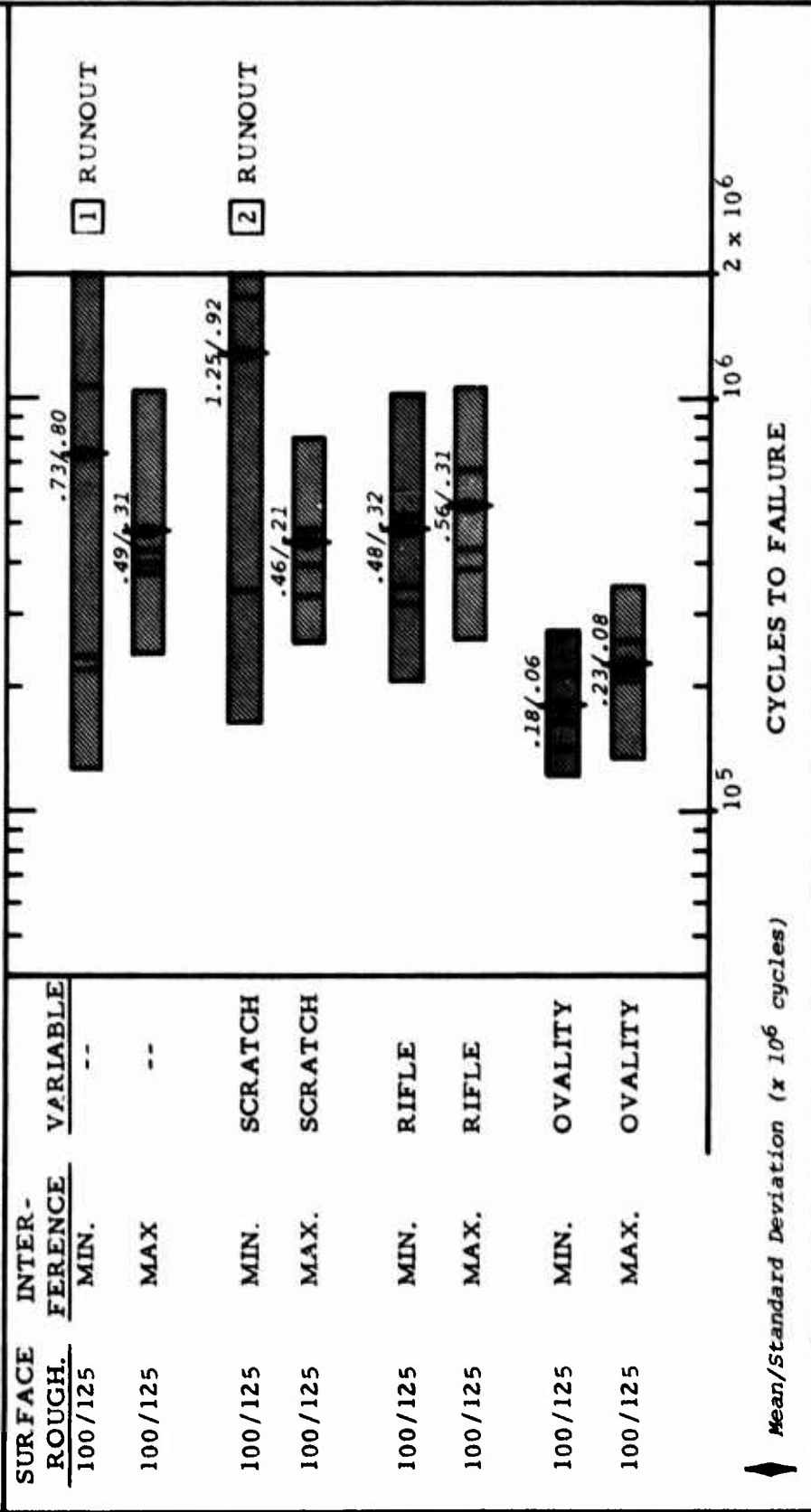


FIGURE 61 - FATIGUE SUMMARY OF DOGBONE/STRAP TESTING COMBINED VARIABLE

<u>Test Series</u>	<u>Failure Origins per Figure 48</u>
8 (Barrelling)	
Min. Interference	10 at F
Max. Interference	10 at F
17 (Ovality)	10 at F
18 (Burrs)	
Min. Interference	2 at B, 1 at C, 1 at E, 3 at F, 1 at G
Max. Interference	1 at B, 2 at F, 7 at G
19 (125 AA plus defect)	
(None)	
Min. Interference	1 at B, 1 at E, 3 at F
Max. Interference	1 at F, 4 at G (Scratch)
(Scratch)	
Min. Interference	3 at F
Max. Interference	2 at B, 3 at G
(Rifling)	
Min. Interference	3 at E, 2 at F
Max. Interference	1 at B, 1 at F, 3 at G
(Ovality)	
Min. Interference	5 at F
Max. Interference	5 at F

In reviewing the above data in relation to the failure orientations coded in Figure 48, it should again be noted that the failures of the dogbone/strap specimen will normally occur at locations A, B, C or G. On the other hand, should the level of interference be inadequate or should the discrepancies in the hole such as scratches or rifling be contributing to poor performance, hole failures at locations D, E and F would then be expected. Failures along the hole surface in this region result from inadequate prestressing from the fastener to overcome the stress concentration attributable either to the hole geometry or to the presence of some discrepant condition.

Considering this, note that in the case of Test Series 2, in which the level of interference was varied, specimens having interference at the mid-specification level and higher levels, all exhibited predominant failures at location G. The group of specimens having substandard interference all exhibited failures at location F. This is consistent with expectations. Specimens having the minimum

specification interference of .0023 in. exhibited several failures at location F which is not completely consistent with the data or with the expected behavior of this configuration.

In the case of Test Series 7 which evaluated perpendicularity, all of the specimens having maximum interference between the tapered hole and the fastener exhibited failures at location G. Most of the specimens having minimum interference produced failures at this same point. From the fractographic examination, one would readily conclude that perpendicularity to the extent covered by this program ( $3^\circ$  normal to the direction of loading) is not detrimental to the fatigue performance of this particular fastener system.

Test Series 8 evaluated both barrelling and bell-mouthing. At all interference levels, bellmouthing led to failures at the exit corner of the specimen, location F. This failure location indicated that the fastener was not effective in inhibiting fatigue in this specimen configuration. This observation was consistent with the low level of fatigue life exhibited by the group of specimens which covered barrelling as a variable. In the case of the samples containing bellmouthing, seven of those tested at the maximum fastener interference level included failures at location G at the minimum interference level eight of those tested failed at location F. These findings indicated that the high level of interference was effective in overcoming the bellmouthed condition studied, while the minimum interference level was not. These findings were also consistent with the observed fatigue behavior.

In the case of the evaluation of the exit burrs using Test Series 18, specimens having maximum interference exhibited predominant failure at location G. Specimens having a minimum interference exhibited a mixed mode of failure nucleation sites apparently without any relation to the presence or absence of burrs.

Test Series 19 considered the interactive effect of several variables at the 125 AA finish level. In general terms, these samples contained fracture orientation consistent with fatigue performance. At both interference levels, ovality produced a

minimum fatigue life and all specimens consistently failed at location F. The other variables produced a spread in fatigue strength which was also consistent with the range of failure nucleation sites observed in these specimens.

In summary, therefore, it may be concluded that the fractographic behavior of the dogbone/strap specimen is consistent with the fatigue behavior of this same group of specimens and that these criteria may be used together or separately as a means of assessing the influence of hole quality variations on joint fatigue performance.

c. Evaluation

Six series of low-load transfer dogbone/strap specimens containing specific defects were manufactured and fatigue tested in the tension-tension mode. The specific defects, the maximum applied stress, and the associated test series number were as follows:

<u>Defect</u>	<u>Stress (ksi)</u>	<u>Test Series</u>
Interference	22	2
Perpendicularity	22 and 25	7
Barrelling and Bellmouthing	22 and 25	8a,b,c,d
Ovality	22 and 25	17
Burrs	22	18
Baseline (100-125 AA hole surface roughness), scratches, rifling, and ovality; one-half at minimum interference = .0023"; one-half at maximum interference = 0.0048"	22	19

Figure 5 illustrates the specimen used for these test series. Manufacturing details are contained in Section VI.3 of this report. Recorded data on specimen quality and fatigue performance is contained in Tables 9 through 14.

The data evaluation is performed using the statistical analysis method outlined in Section VI.6. The analysis is presented for two dependent variables: (1) cycles to failure and (2)  $1/\alpha\beta$ .

Cycles to failure is a well known dependent variable and requires no further explanation. In the dependent variable,  $1/\alpha\beta$ , the  $\alpha\beta$  term is an empirical factor used by the Lockheed-Georgia Company in their "Joint Fatigue Analysis Method". This analysis method accounts for axial stress, fastener load transfer, fastener tilting and joint fretting. But at the present time it cannot directly account for hole finish and hole filling or interference. The effects of hole finish ( $\alpha$ ) and hole filling ( $\beta$ ) must be determined by test. Since it is difficult to separate the two effects the factors are combined and referred to as  $\alpha\beta$ . The  $\alpha\beta$  factor is applied in the analysis very much like a stress concentration factor would be applied, an increase in the  $\alpha\beta$  factor like an increase in the stress concentration factor, will produce a decrease in fatigue life.

To determine the test demonstrated values of  $\alpha\beta$ , the specimen is first analyzed using the Joint Fatigue Analysis Method for various assumed values of  $\alpha\beta$ . From the results of this analysis, a curve of  $\alpha\beta$  versus cycles to failure is then plotted, Figure 62. Entering Figure 62 with the test cycles to failure, a test demonstrated value of  $\alpha\beta$  can be obtained for each specimen.

Expressing the test results in terms of  $\alpha\beta$  permits the ranking of the various hole defects to be established in a manner meaningful to the design process. Once a design value of  $\alpha\beta$  is determined for a given defect, a Joint Fatigue Analysis can be performed to ascertain its effect on aircraft life.

The test demonstrated values of  $\alpha\beta$  are listed in Tables 9 through 14. A more detailed description of the "Joint Fatigue Analysis Method" and the  $\alpha\beta$  factor may be found in Reference (1).

#### Results - Dependent Variable: Cycles to Failure

The reduced results for Test Series 2 which considered the variable of fastener interference

- (1) B.L. Cornell and L.G. Darby, "Correlation of Analysis and Test Data to the Effect of Fastener Load Transfer on Fatigue", AISS Paper No. 74-983, AIAA 6th Aircraft Design Flight and Operating Meeting, Los Angeles, CA, August 12-14, 1974.

ALPHA BETA ANALYSIS OF  
DOGBONE/STRAP SPECIMENS

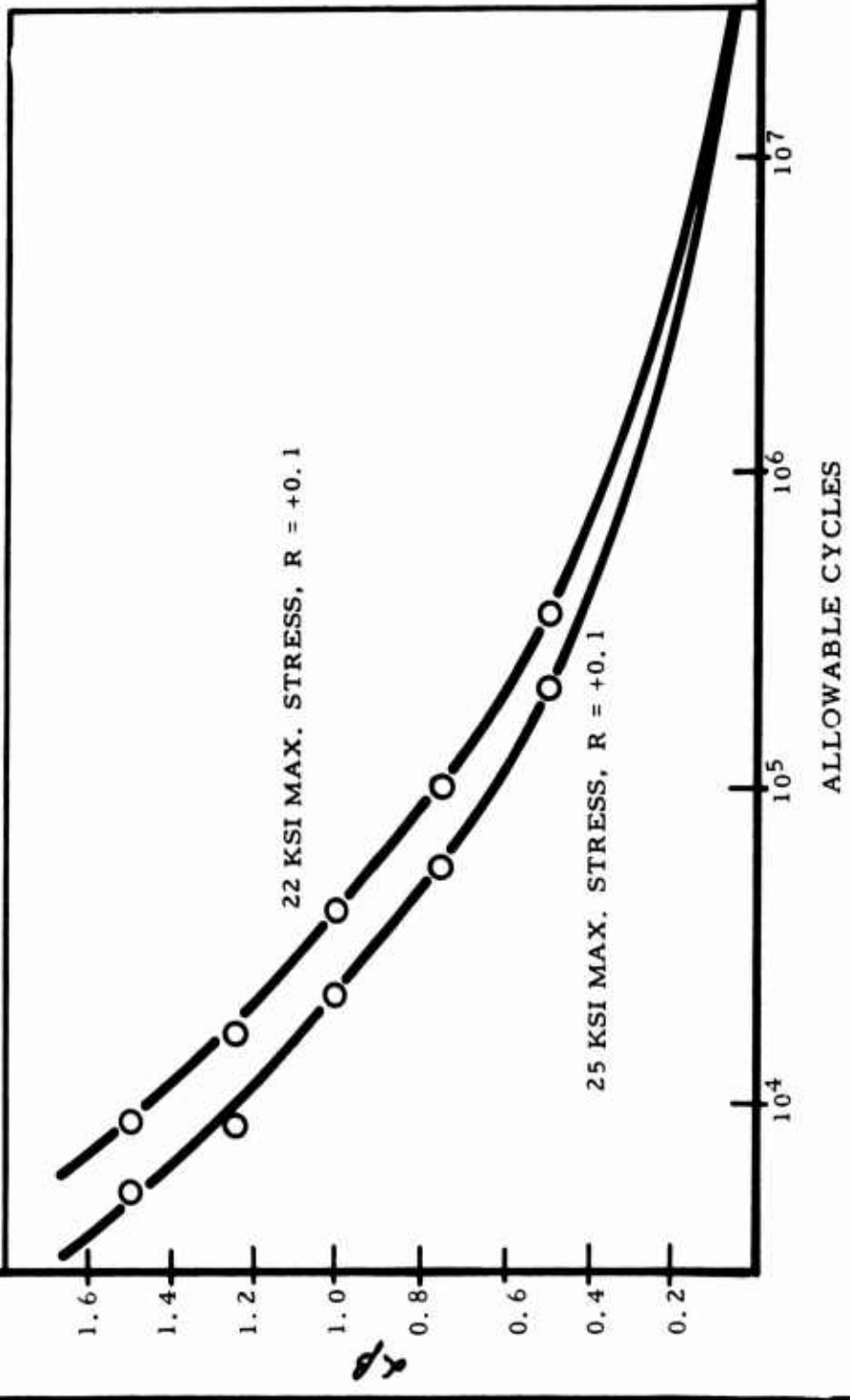


Figure 62 - ALPHA BETA ANALYSIS OF DOGBONE/STRAP SPECIMENS



with a 63 AA surface roughness are presented in Figure 63. Analysis of this data, shows no significant change in fatigue performance by varying the fastener interference within the range investigated. A similar trend is apparent for all tests performed. The pooling of data for all interference values for a given test series gives sample correlation coefficients greater than the critical .800 value.

There is also a practical reason for pooling the interference data. In a production environment it is not possible to control the exact interference of each fastener. All we know is that the interference should be to the specification requirements. So pooling the interference data more realistically represents the actual aircraft behavior.

The reduced results for Test Series 7 (Perpendicularity) are presented in Figures 64 and 65. Figures 66 through 69 present the reduced results for Test Series 8 (Bellmouthing and Barrelling). Figure 70 presents the reduced results for Test Series 17 (Ovality).

In Figure 71, the results of the linear regression analysis for Test Series 2, 7, 8 and 17 are presented for comparison. Relative to the baseline, ovality has the most adverse effect on fatigue followed by barrelling and bellmouthing. The condition of perpendicular deviation appears to enhance the fatigue life. However, it must be recognized that the direction of perpendicular deviation was normal to the load direction. The same results may not be true for all directions of this defect.

The reduced results for Test Series 18 (Exit Burrs) are presented in Figure 72. The analysis shows no adverse effect on fatigue life due to the presence of exit burrs. Since the origin of failure always occurred at the faying surface, the faying surface is still the most critical location.

Figures 73 through 76 present reduced results for Test Series 19. The hole defects for this series were the defects which were shown to be most critical in previous tests in the program. All

LINEAR REGRESSION ANALYSIS - DOGBONE/STRAP SPECIMENS  
 TEST SERIES 2: INTERFERENCE

PEAK STRESS: 22 KSI  
 $r_{xu} = .9170$

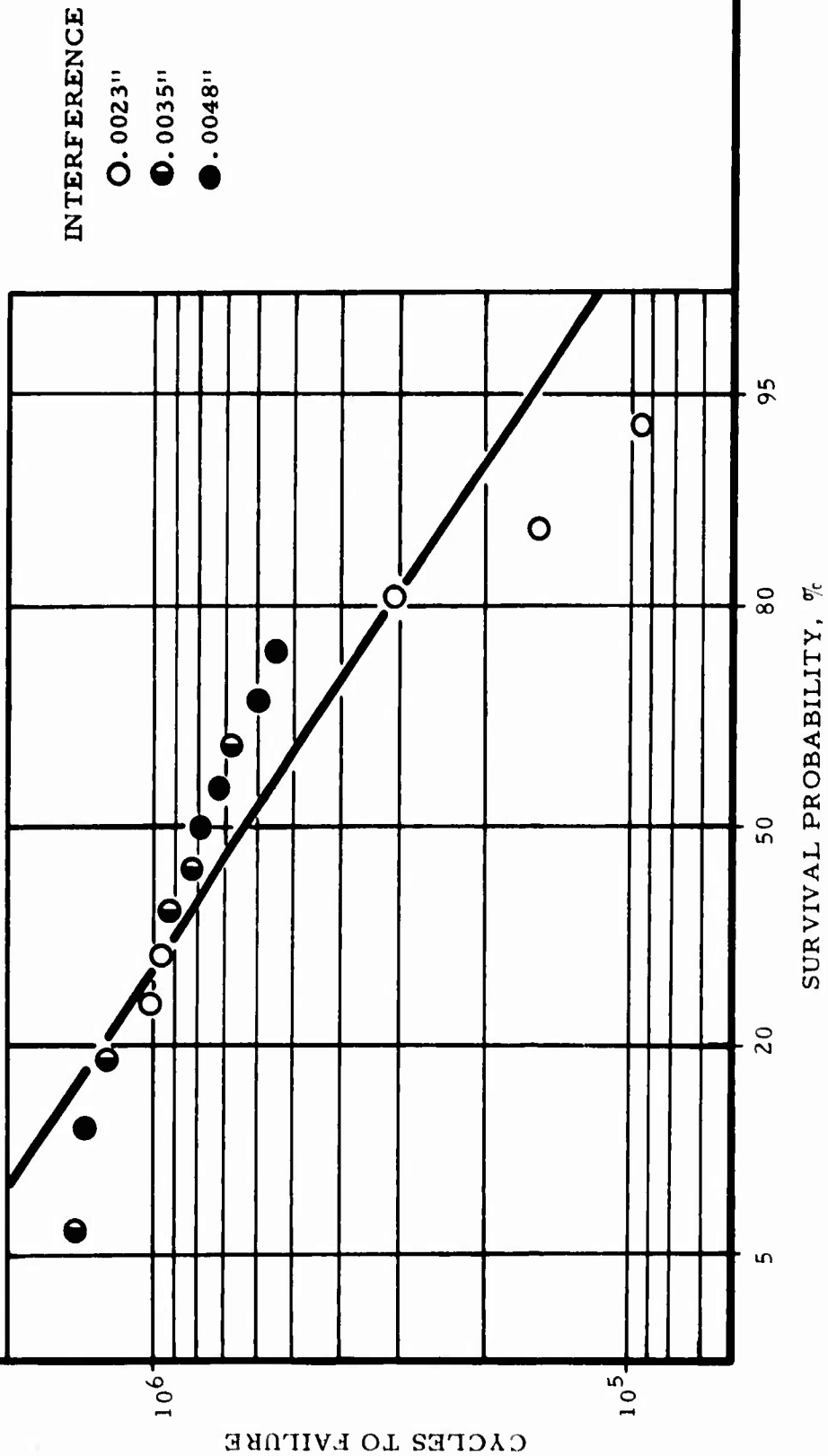


Figure 63 - SURVIVAL PROBABILITY OF DOGBONE/STRAP SPECIMENS - INTERFERENCE

LINEAR REGRESSION ANALYSIS OF DOGBONE/STRAP SPECIMENS  
 TEST SERIES 7: PERPENDICULARITY

PEAK STRESS: 22 KSI  
 $r_{xu} = .9320$

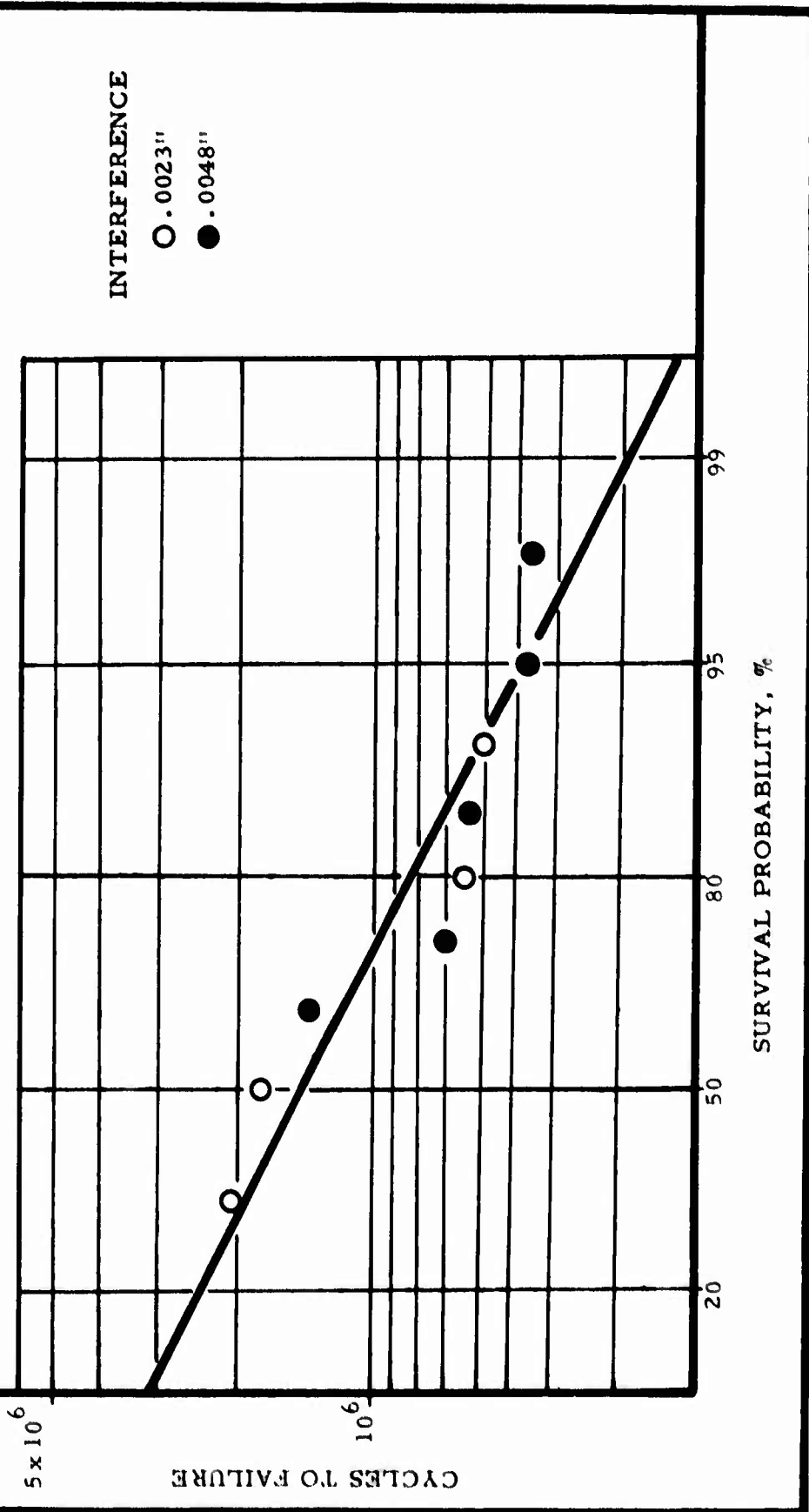


Figure 64 - SURVIVAL PROBABILITY OF DOGBONE/STRAP SPECIMENS - PERPENDICULARITY (22 KSI)

LINEAR REGRESSION ANALYSIS - DOGBONE/STRAP SPECIMENS  
 TEST SERIES 7: PERPENDICULARITY

PEAK STRESS: 25 KSI  
 $r_{xy} = .9453$

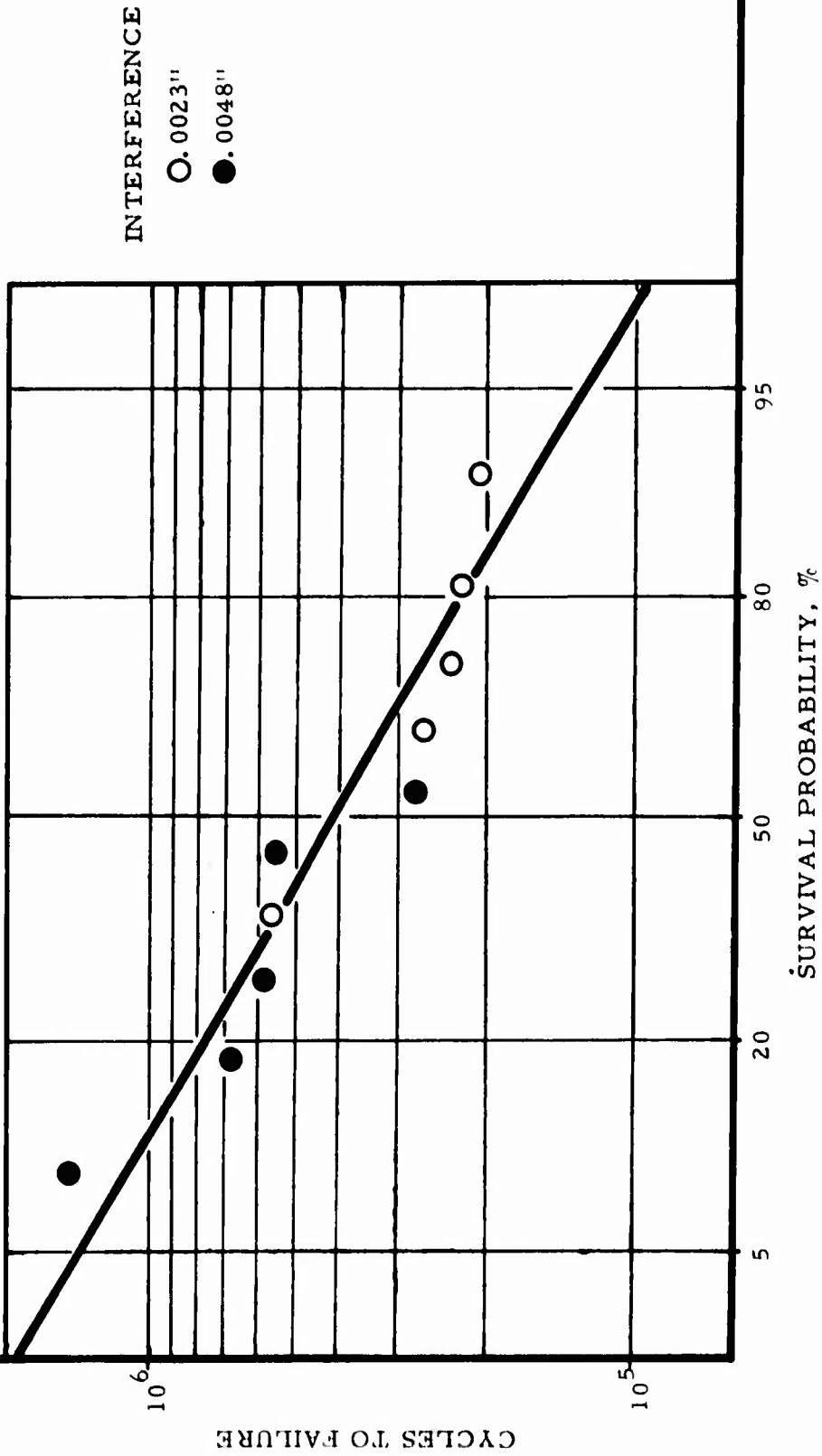


Figure 65 - SURVIVAL PROBABILITY OF DOGBONE/STRAP SPECIMENS - PERPENDICULARITY (25 KSI)

LINEAR REGRESSION ANALYSIS - DOGBONE/STRAP SPECIMENS  
 TEST SERIES 8A, B: BELLMOUTHING

PEAK STRESS: 22 KSI  
 $r_{xu} = 0.9717$

INTERFERENCE

- .0023"
- .0048"

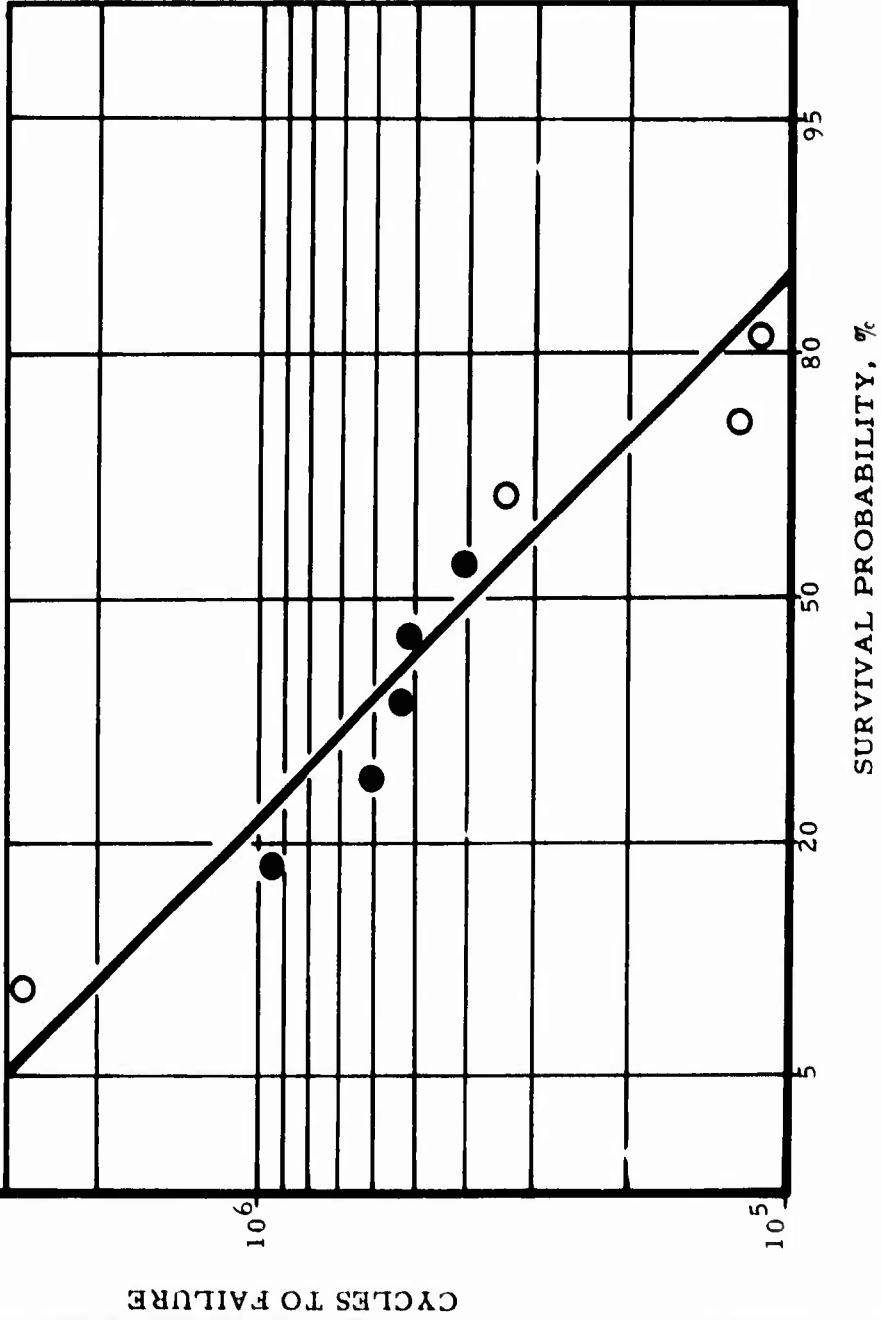


Figure 66 - SURVIVAL PROBABILITY OF DOGBONE/STRAP SPECIMENS - BELLMOUTHING (22 KSI)

LINEAR REGRESSION ANALYSIS - DOGBONE/STRAP SPECIMENS  
 TEST SERIES 8A, B: BELLMOUTHING

PEAK STRESS: 25 KSI  
 $r_{xu} = 0.9791$

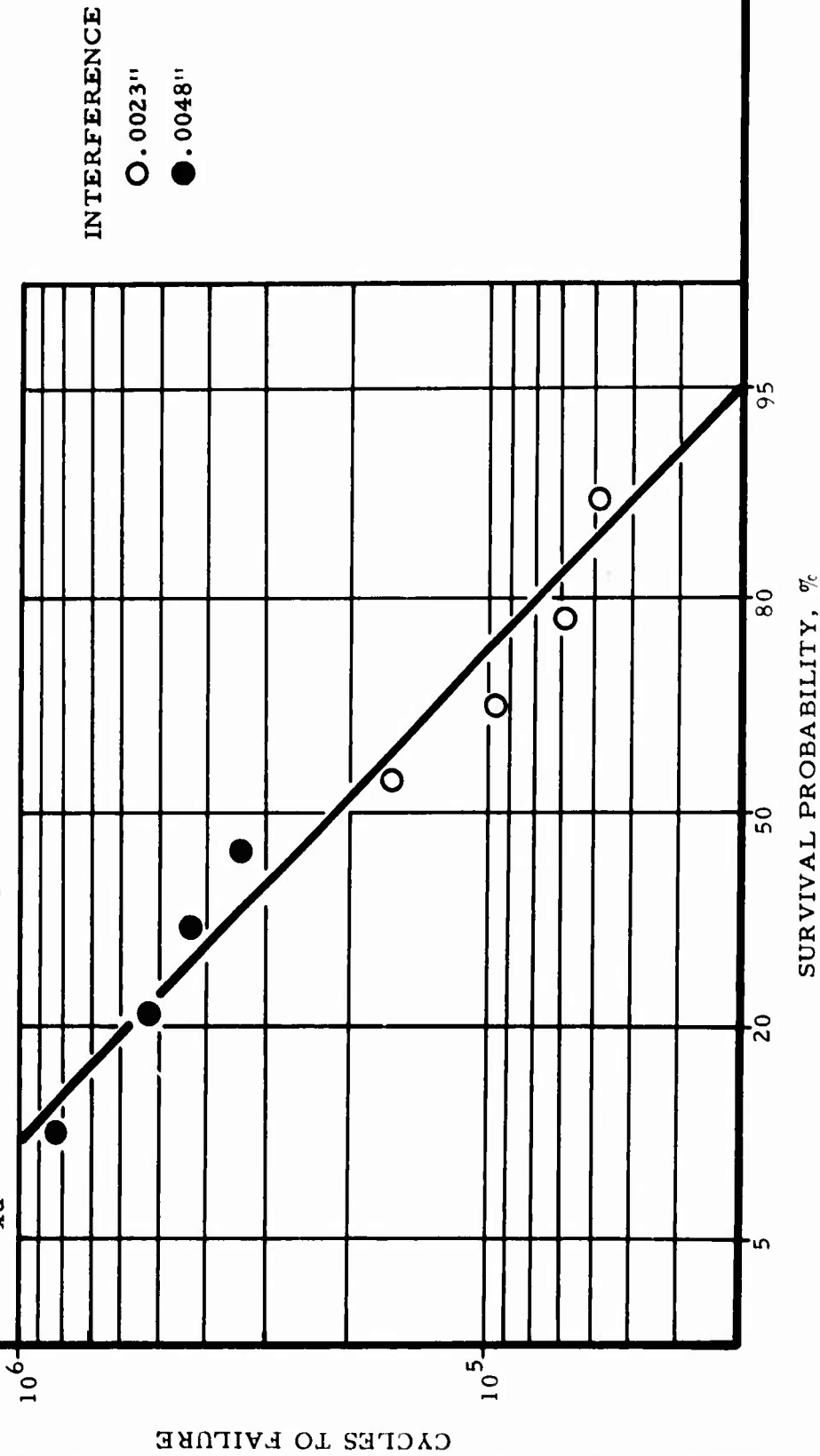


Figure 67 - SURVIVAL PROBABILITY OF DOGBONE/STRAP SPECIMENS - BELLMOUTHING (25 KSI)

LINEAR REGRESSION ANALYSIS - DOGBONE/STRAP SPECIMENS  
 TEST SERIES 8C, D: BARRELLING

PEAK STRESS: 22 KSI  
 $r_{xu} = 0.9743$

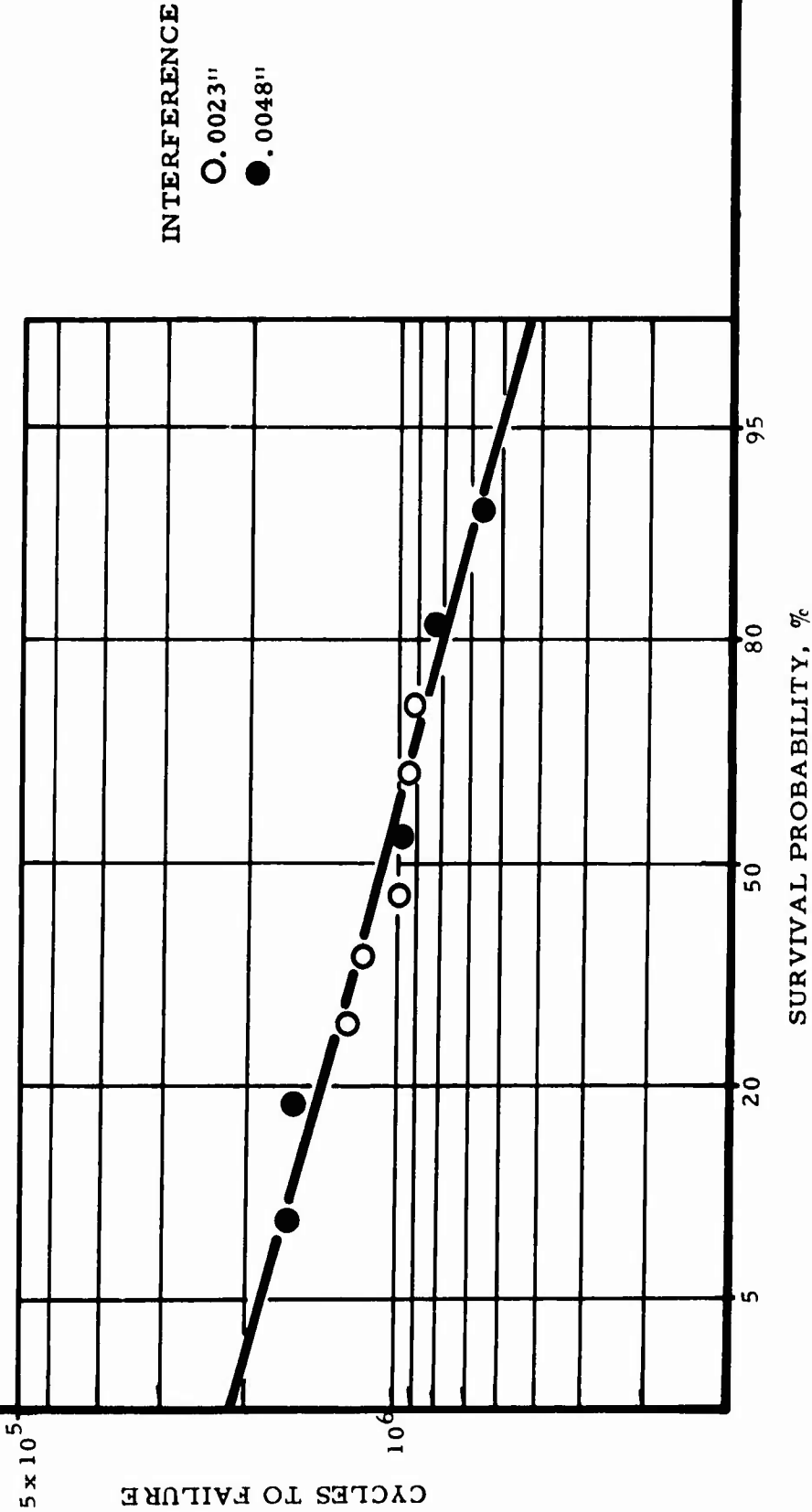


Figure 68 - SURVIVAL PROBABILITY OF DOGBONE/STRAP SPECIMENS - BARRELLING (22 KSI)

LINEAR REGRESSION ANALYSIS - DOGBONE/STRAP SPECIMENS  
 TEST SERIES 8C, D: BARRELLING

PEAK STRESS: 25 KSI  
 $r_{xu} = 0.9231$

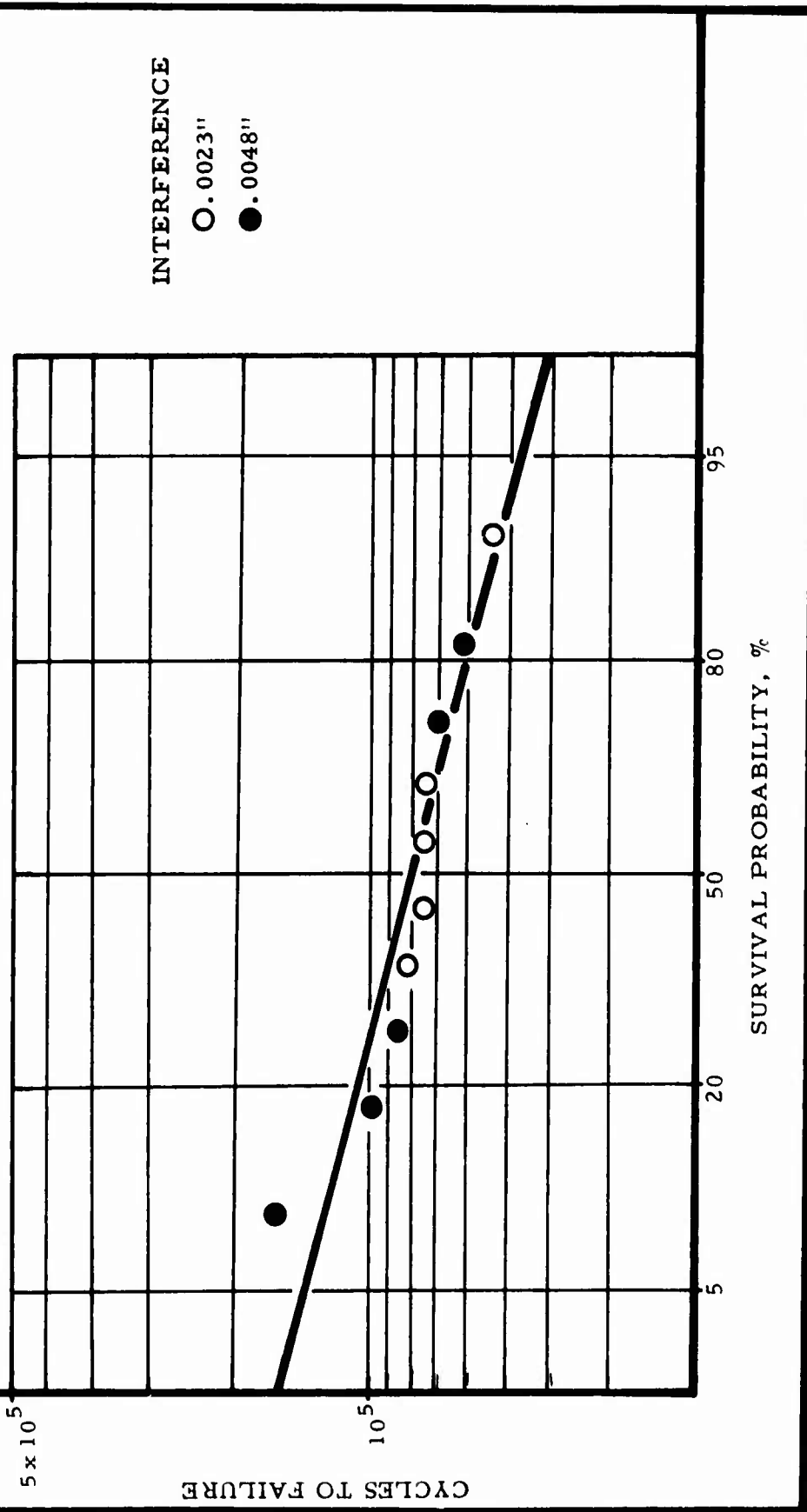


Figure 69 - SURVIVAL PROBABILITY OF DOGBONE/STRAP SPECIMENS - BARRELLING (25 KSI)



LINEAR REGRESSION ANALYSIS - DOGBONE/STRAP SPECIMENS  
 TEST SERIES 17: OVALITY

○ PEAK STRESS: 22 KSI  
 $r_{xu} = 0.9782$

● PEAK STRESS: 25 KSI  
 $r_{xu} = 0.8546$

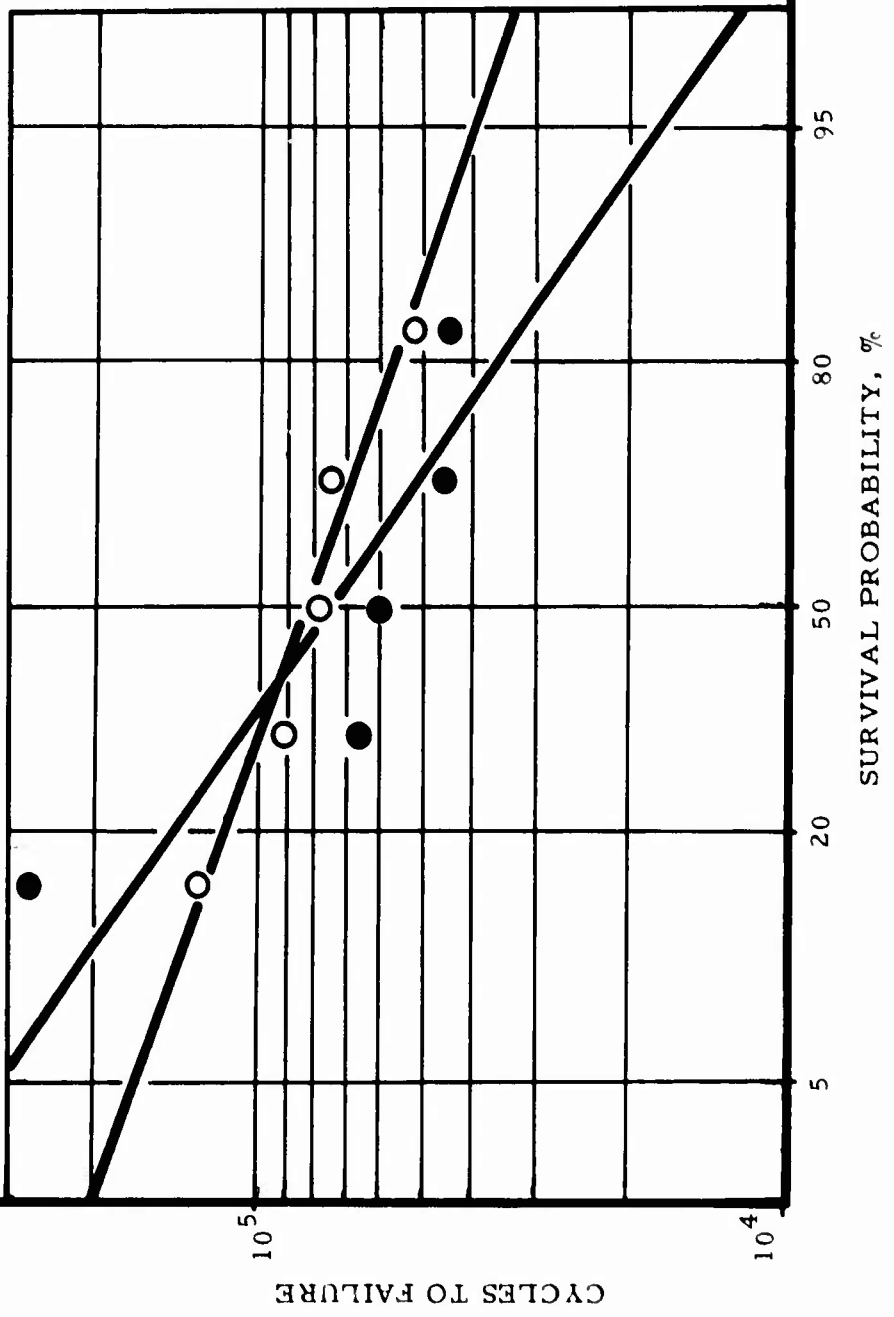


Figure 70 - SURVIVAL PROBABILITY OF DOGBONE/STRAP SPECIMENS - OVALITY

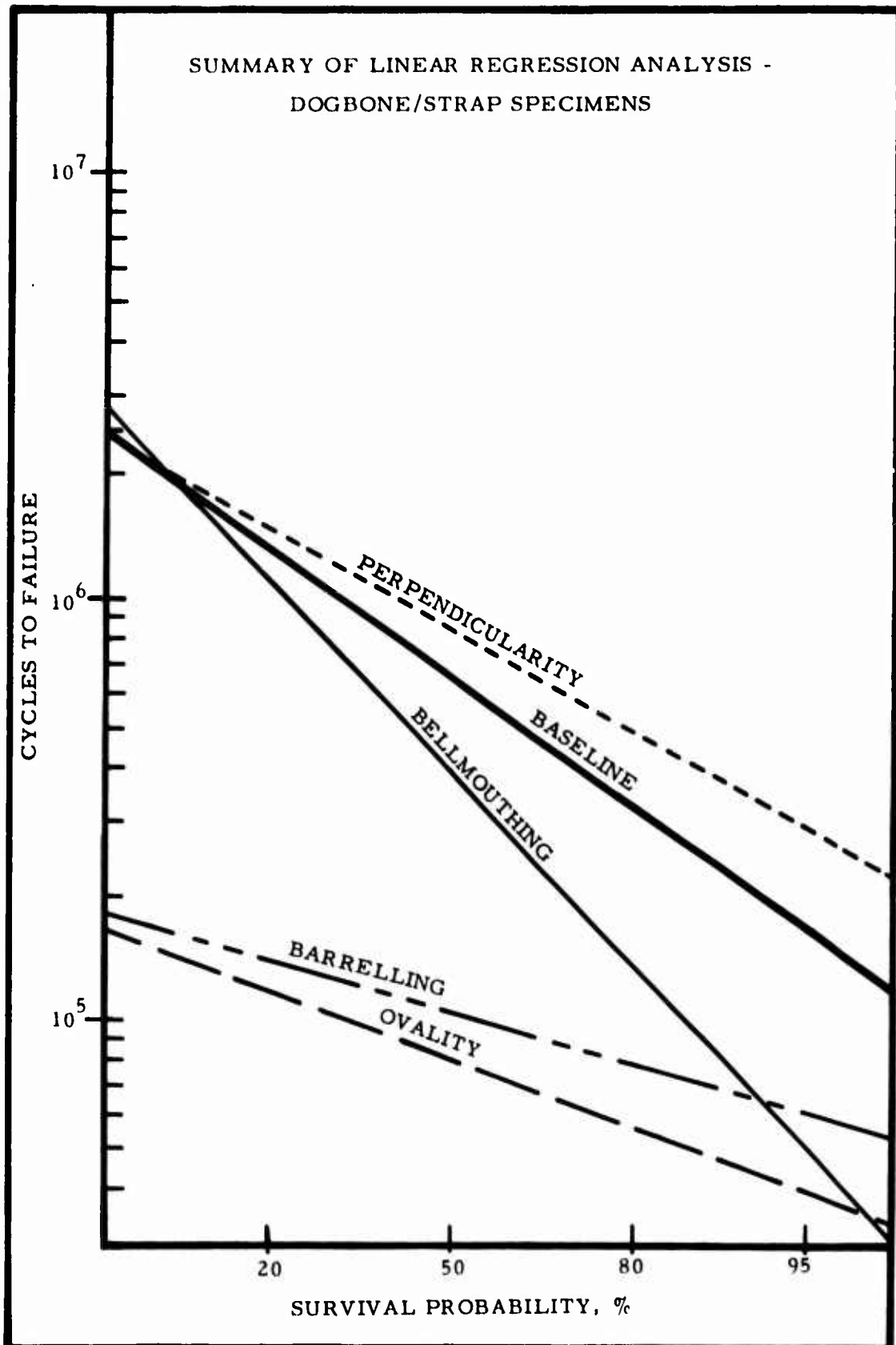


Figure 71 - COMPOSITE: SURVIVAL PROBABILITY OF DOGBONE/STRAP SPECIMENS

LINEAR REGRESSION ANALYSIS - DOGBONE/STRAP SPECIMENS  
 TEST SERIES 18: EXIT BURRS

PEAK STRESS: 22 KSI  
 $r_{xu} = 0.9457$

○ WITH BURRS  
 ● BURRS REMOVED

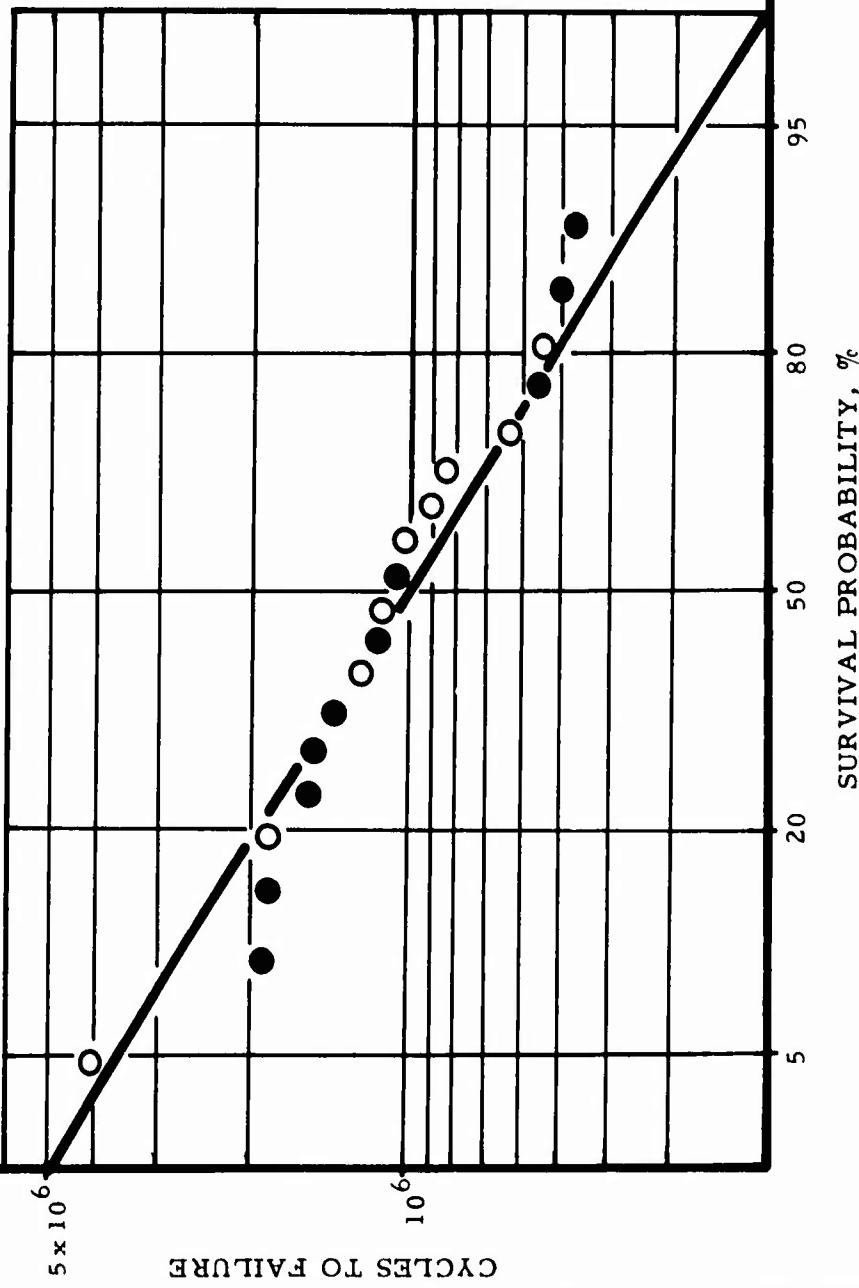


Figure 72 - SURVIVAL PROBABILITY OF DOGBONE/STRAP SPECIMENS - EXIT BURRS

LINEAR REGRESSION ANALYSIS - DOGBONE/STRAP SPECIMENS  
 TEST SERIES 19: INCREASED ROUGHNESS (125 AA)

PEAK STRESS: 22 KSI  
 $r_{xu} = 0.8995$

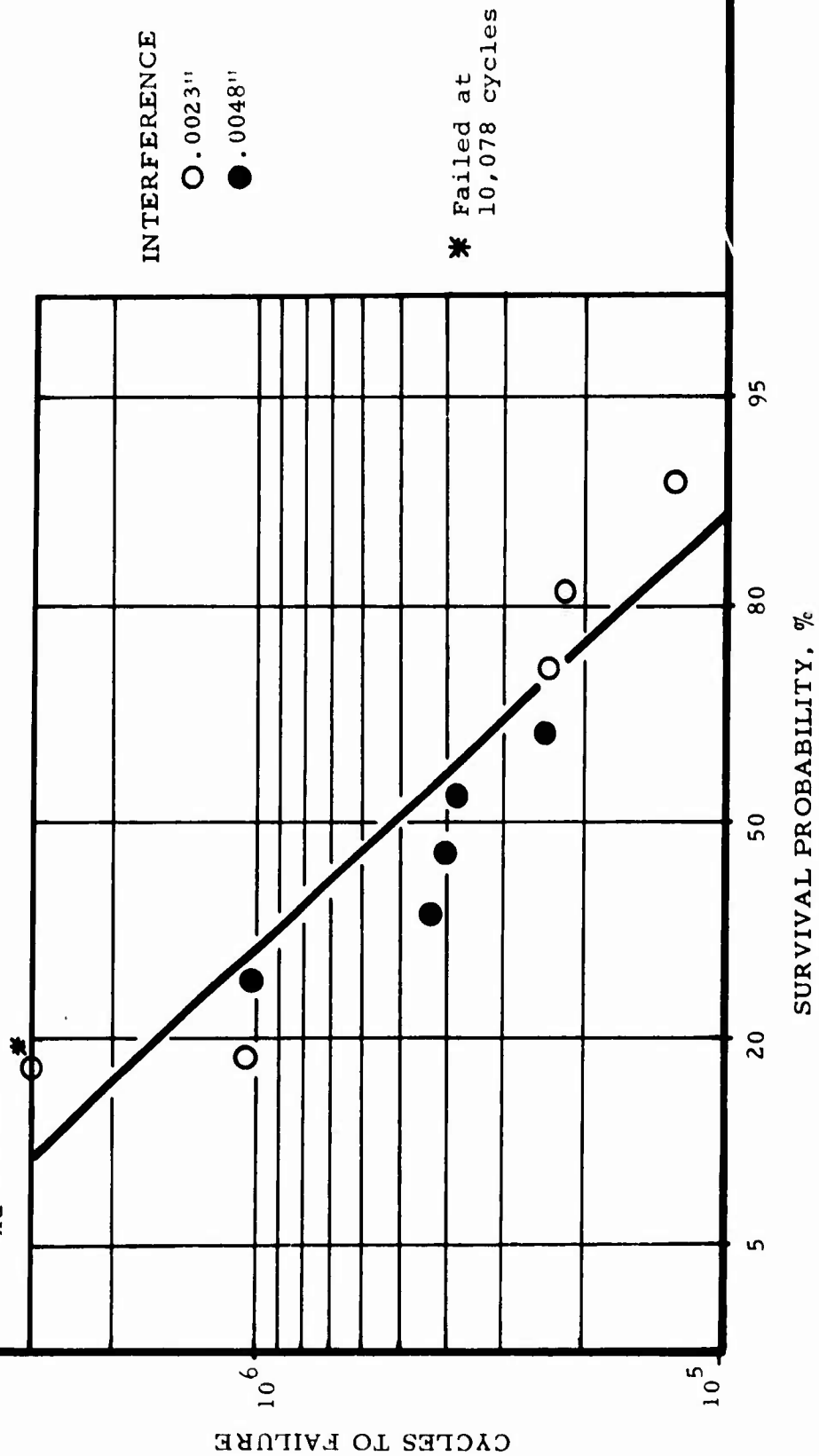


Figure 73 - SURVIVAL PROBABILITY OF DOGBONE/STRAP SPECIMENS - INCREASED ROUGHNESS

LINEAR REGRESSION ANALYSIS - DOGBONE/STRAP SPECIMENS  
 TEST SERIES 19: INCREASED ROUGHNESS (125 AA) AND RIFLING

PEAK STRESS: 22 KSI  
 $r_{xu} = 0.9824$

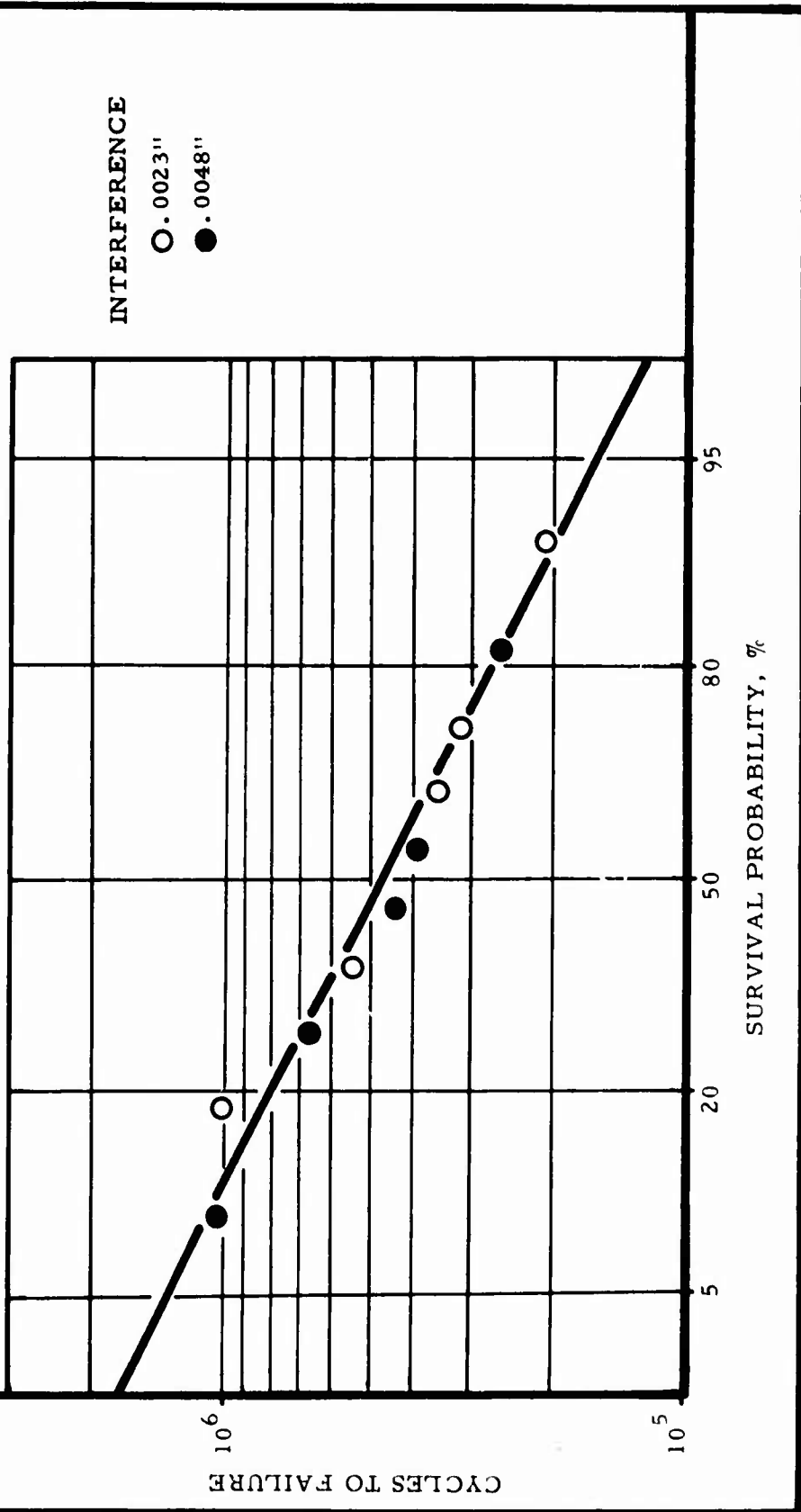


Figure 74 - SURVIVAL PROBABILITY OF DOGBONE/STRAP SPECIMENS - INCREASED ROUGHNESS AND RIFLING

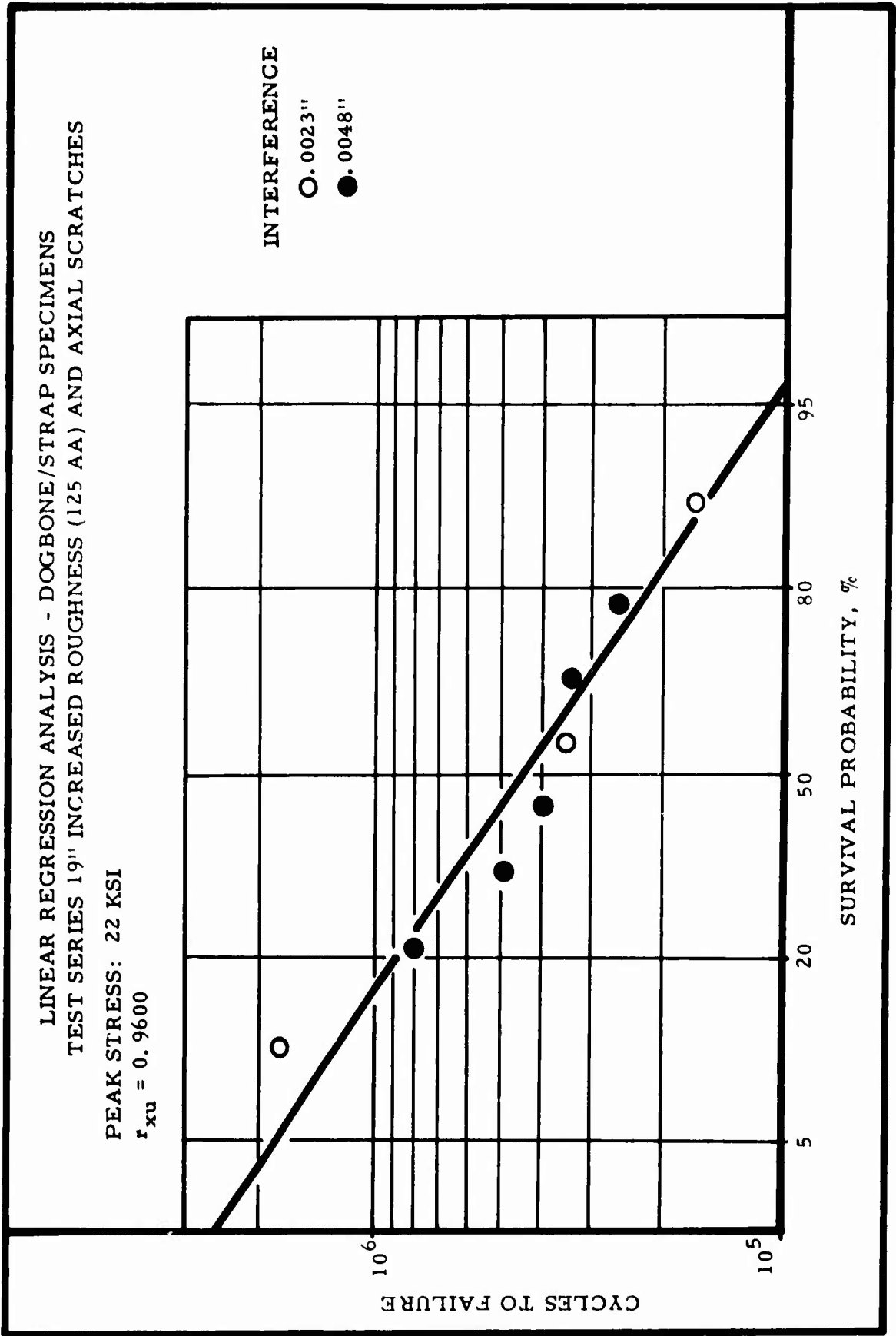


Figure 75 - SURVIVAL PROBABILITY OF DOGBONE/STRAP SPECIMENS - INCREASED ROUGHNESS AND AXIAL SCRATCHES

LINEAR REGRESSION ANALYSIS - DOGBONE/STRAP SPECIMENS  
 TEST SERIES 19: INCREASED ROUGHNESS (125 AA) AND OVALITY

PEAK STRESS: 22 KSI  
 $r_{xu} = 0.9877$

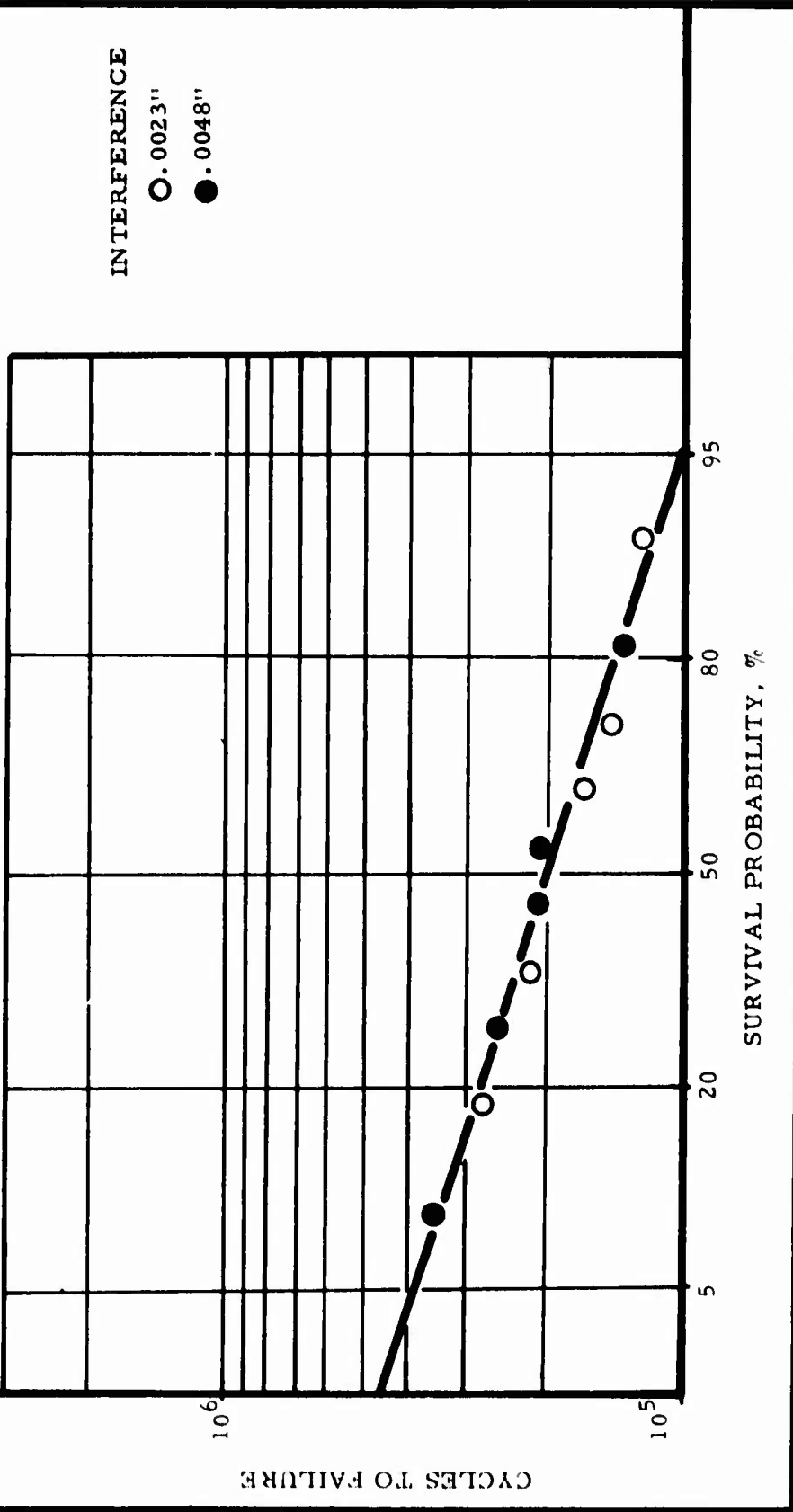


Figure 76 - SURVIVAL PROBABILITY OF DOGBONE/STRAP SPECIMENS - INCREASED ROUGHNESS AND OVALITY

hole surface roughnesses in this series were in the 100-125 AA range. A summary of the linear regression analysis is presented in Figure 77 for comparison. Consistent with previous results, ovality has the most adverse effect on fatigue. The effect of an axial scratch and rifling is shown to be a function of survival probability. For survival probabilities less than 50%, they have an adverse effect on fatigue; greater than 50% a beneficial effect.

Results - Dependent Variable:  $(1/\alpha \beta)$

Applying the method described in Section VII.2.c, Figures 78 and 79 and Table 15 present the results of reducing the test data in terms of  $\alpha \beta$ . The baseline results are obtained by pooling the test data from Test Series 2 and 19. The variables for Test Series 2 and 19 are in essence the same except for hole surface roughness. Test Series 2 has a 63 AA surface roughness while Test Series 19 has a 100-125 AA surface roughness. The sample correlation coefficient ( $r_{xu}$ ) of 0.9811 indicates that varying the surface roughness within the range of 63-125 AA has no significant effect on fatigue.

Figure 78 presents results using confidence  $P_C = 50\%$  and Figure 79 for  $P_C = 95\%$ . In Table 15, the values of  $\alpha \beta$  for 50,50 (Percent Survival Probability, Percent Confidence), 99,50, and 99,95 are presented. Of the three values of  $\alpha \beta$  shown, the 99,95 value is the most significant. Test experience on the C-5A aircraft has shown that the 99,95 value for  $\alpha \beta$  is required when using element test results to predict full scale test performance. To illustrate the significance of  $\alpha \beta$ , Table 15 also presents the equivalent cycles to failure using the data presented in Figure 78. Based on the 99,95 value of  $\alpha \beta$ , the ranking of the hole defects at the levels studied in this program and starting with the most severe, is as follows:

Ovality  
Bellmouthing  
Axial Scratch  
Barrelling  
Rifling  
Perpendicular Deviation ( $3^\circ$ )



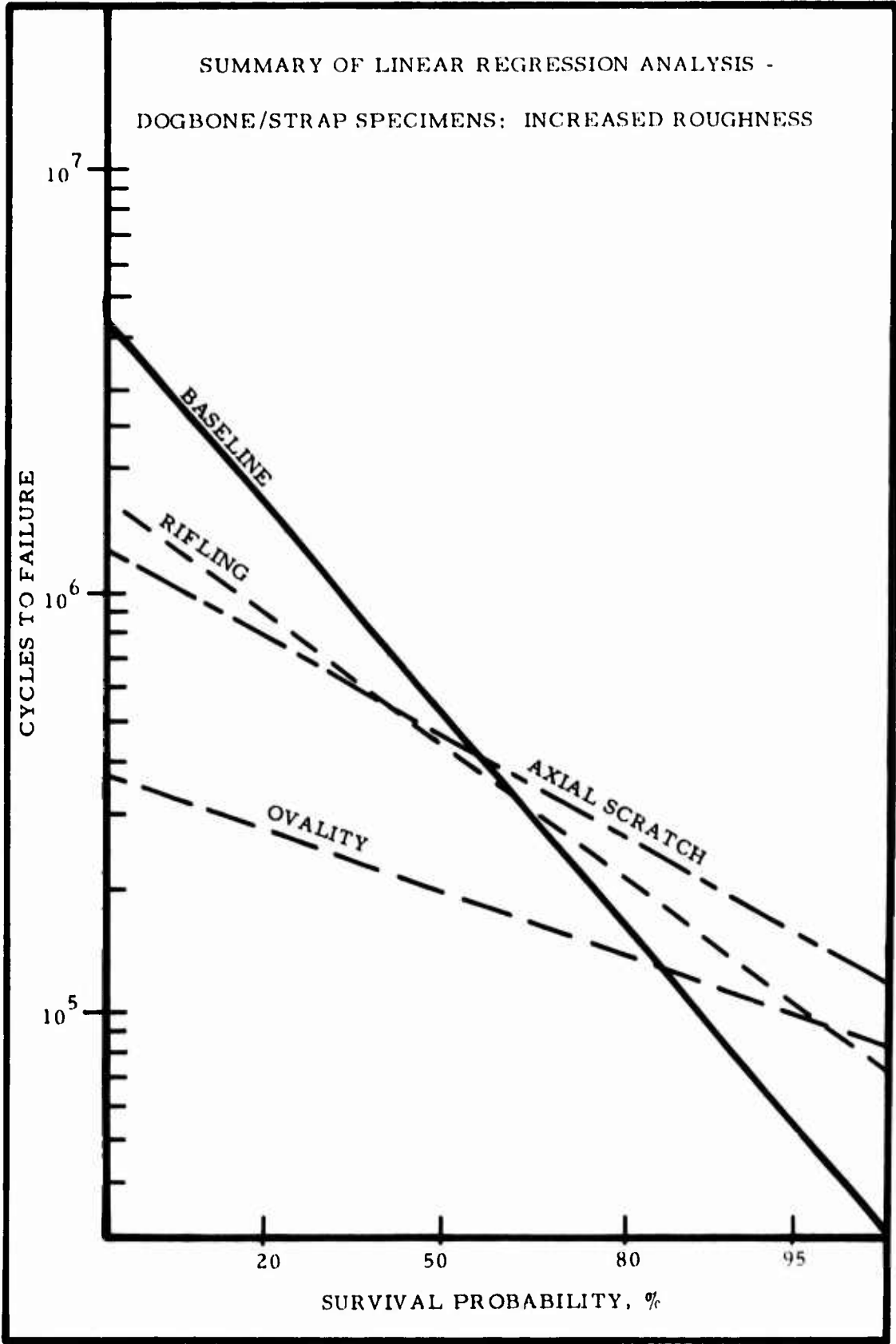


Figure 77 - COMPOSITE: SURVIVAL PROBABILITY OF DOGBONE/STRAP SPECIMENS (INCREASED ROUGHNESS)

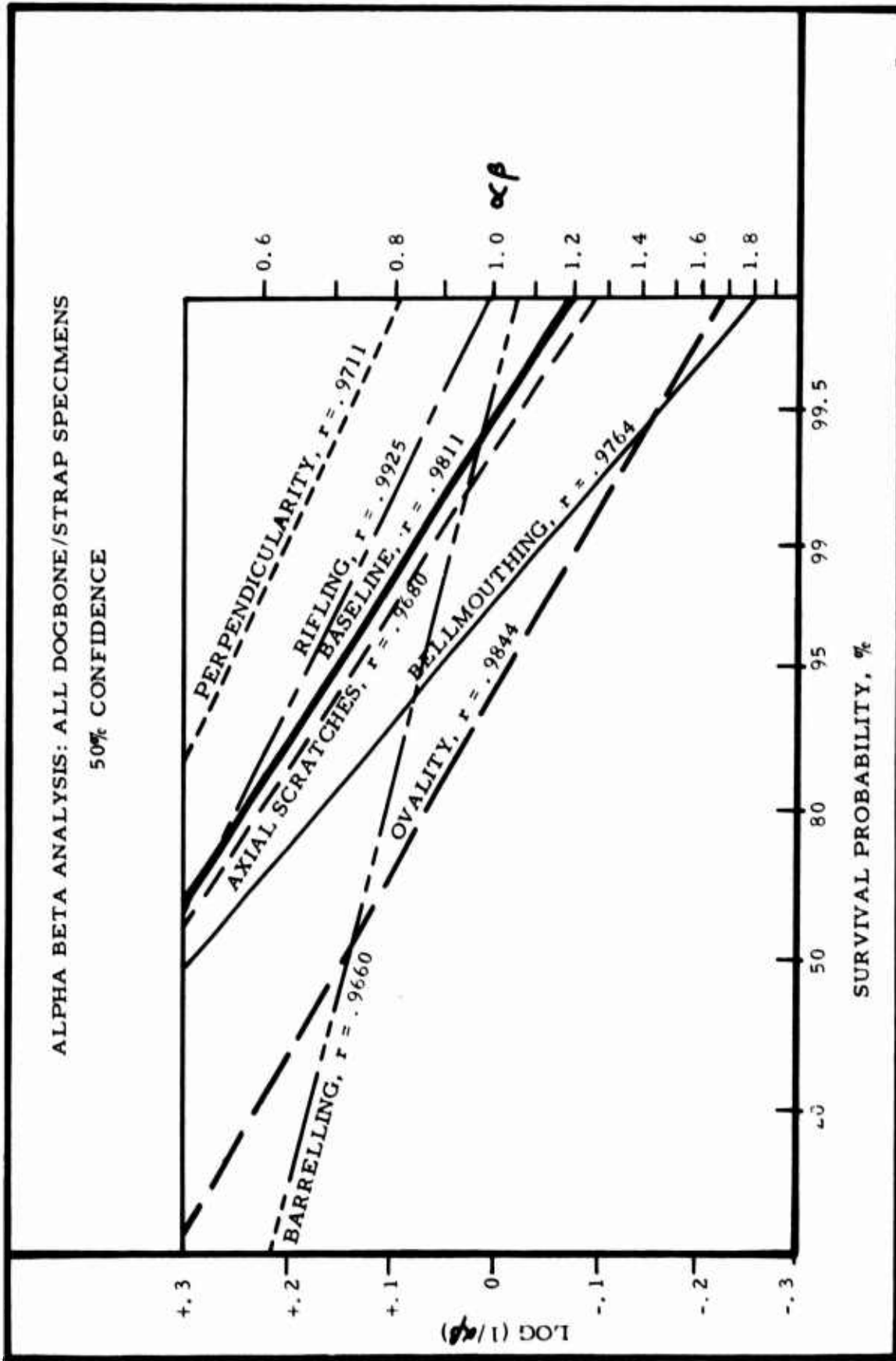


Figure 78 - ALPHA BETA ANALYSIS: ALL DOGBONE/STRAP SPECIMENS - 50% CONFIDENCE

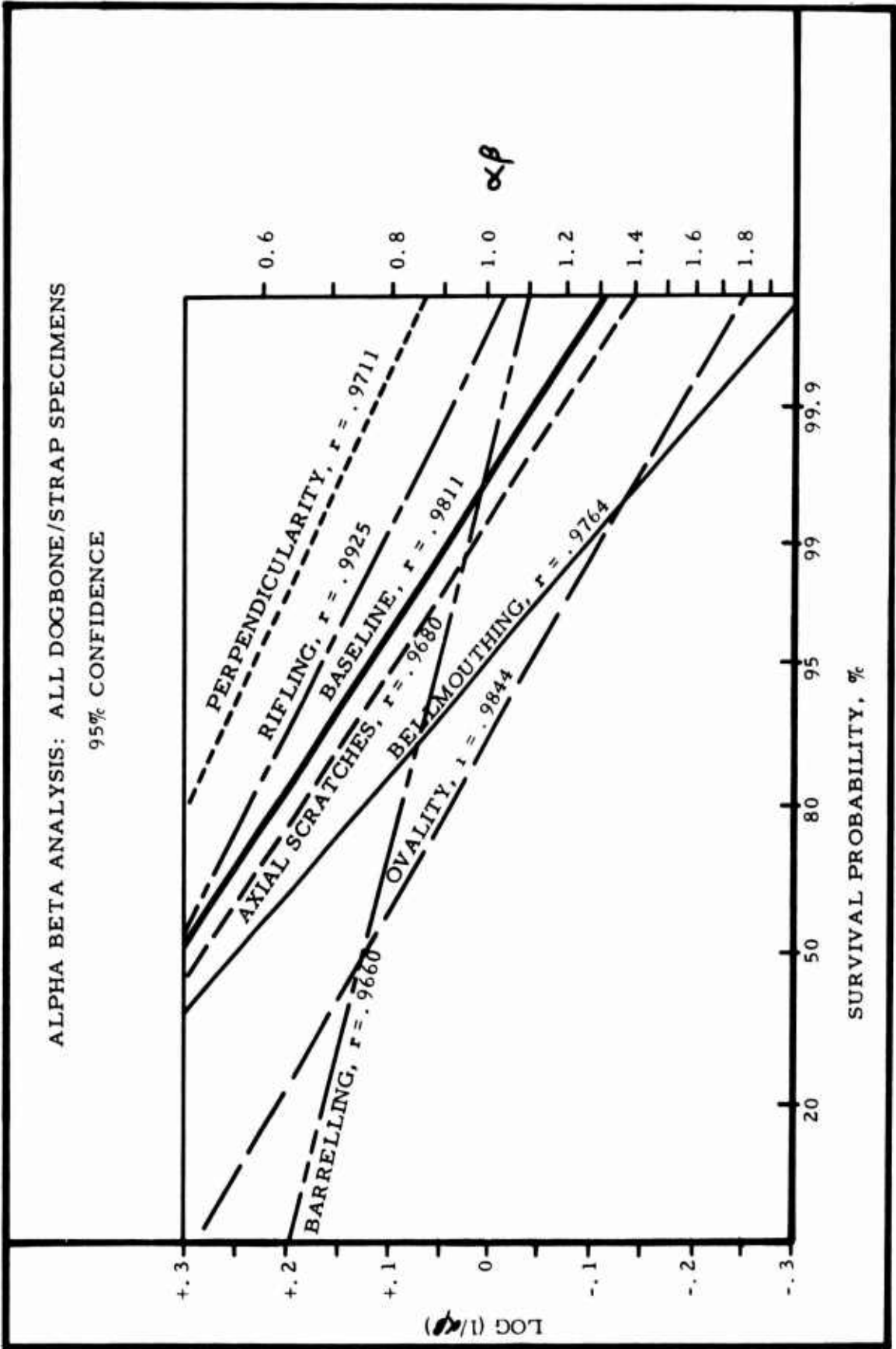


Figure 79 - ALPHA BEAT ANALYSIS: ALL DOGBONE/STRAP SPECIMENS - 95% CONFIDENCE

### 3. LLT Testing - Reverse Dogbone Specimen

#### a. Fatigue Testing

Fatigue tests were conducted on a reverse dogbone specimen of the design shown in Figure 8 at 1200 to 1800 cycles per minute. Stress ratios of  $R = 0.1$  and also  $-0.33$  were used on the reverse dogbone specimens. This specimen exhibited a level of load transfer in the range of 0.5 to 8.0%.

The selection of the particular combinations of hole quality variables used in the reverse dogbone specimens was based on the results obtained on previous tests, particularly Test Series 19. The stress conditions used for testing the reverse dogbone were based on calculations made by the Lockheed-Georgia Company. Having determined that a peak stress of 22,000 psi would yield a cyclic life of between .5 and 1.0 million cycles on a "standard" specimen, Lockheed-Georgia Company calculations selected a peak cyclic stress of 20,500 psi for testing the reverse dogbone specimens. This peak stress was used for both of the stress ratios involved. At a stress ratio of  $+0.1$  the minimum stress was 2.05 ksi in tension. Where the stress ratio of  $-0.33$  was used, the minimum cyclic stress was approximately 6.8 ksi in compression.

In developing the test schedule, Test Series 20 and 21 which had been defined separately in the various progress reports on this program were combined to form a single series. All specimens from series 20/21 were tested at the  $R = 0.1$  stress ratio. Likewise all specimens had an initial hole roughness of 100/125 AA; interference was targeted at the minimum specified level, .0035 in.

The data obtained on Test Series 20/21 is summarized in Figure 80. Note that the baseline specimens, which contained no intentional defects, and those specimens containing both an axial scratch and a rifled groove all behaved in a similar fashion. In other words, neither scratching nor rifling to the extent evaluated in this program caused a detriment in fatigue life under the test conditions. In the case of the specimens containing ovality in the tapered holes, however, a degradation in fatigue life was observed as indicated in Figure 80. This behavior was consistent with the behavior of oval holes when evaluated with the dogbone/strap specimen, Test Series 17.

FATIGUE SUMMARY OF REVERSE DOGBONE TESTING - COMBINED VARIABLES

TEST SERIES 20, 21 AND 22

MODE: AXIAL      MAXIMUM TEST STRESS: 20.5 KSI      TEMPERATURE: 75°F  
 FREQUENCY: 15-30 Hz      ORIENTATION: LONGITUDINAL

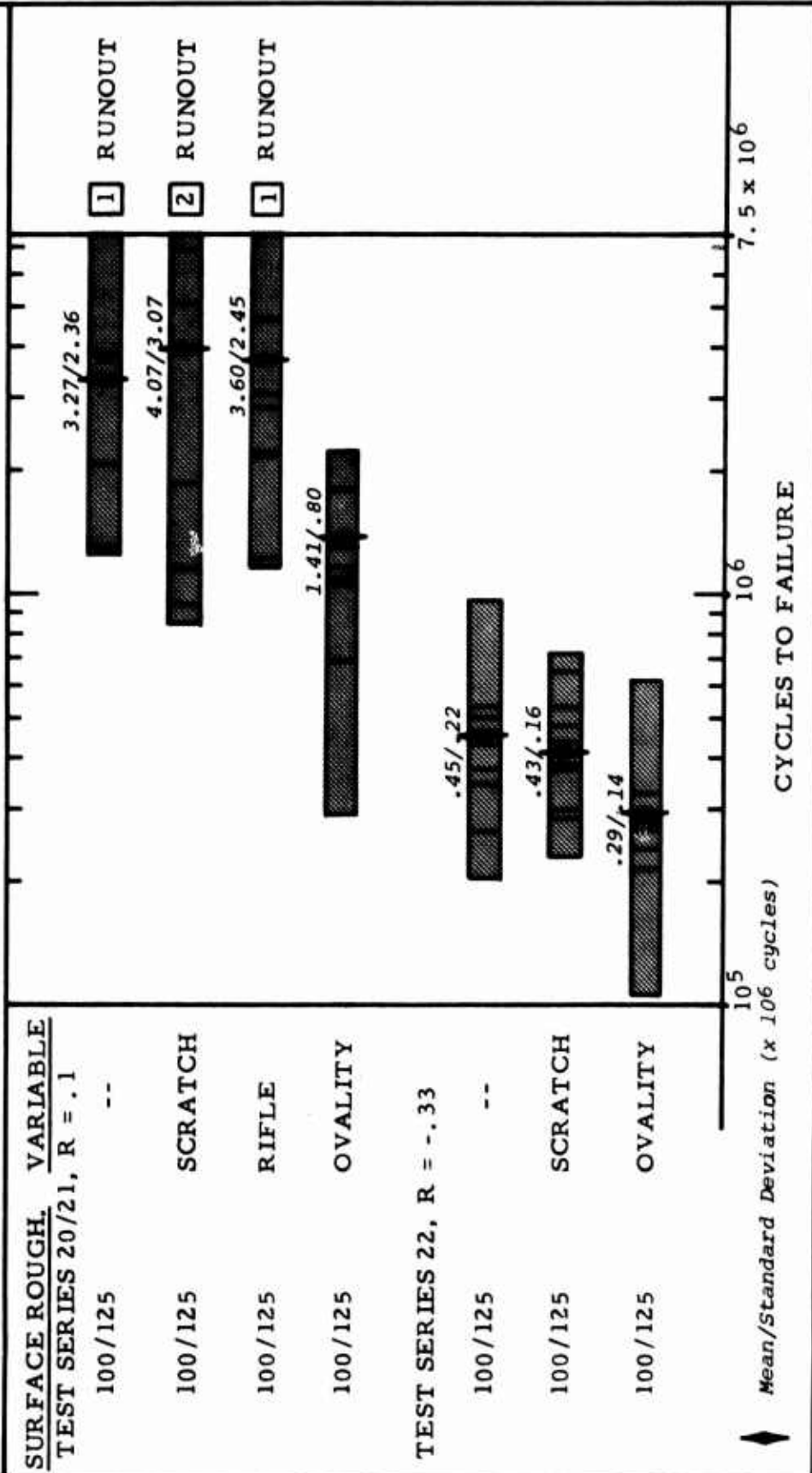


Figure 80 - FATIGUE SUMMARY OF REVERSE DOGBONE TESTING - COMBINED VARIABLES

Test Series 22 involves the same type of specimens as Series 20/21, all of which had the same initial surface roughness and level of interference between the specimen and the fasteners. In Test Series 22, however, the specimens were cyclically loaded at the stress ratio of -0.33. All of these specimens exhibited a lower fatigue life which would be expected because of the greater stress range involved. Both the scratched and the standard specimens behaved as a single group (rifling was not tested at this stress ratio), while the specimens containing oval holes again exhibited a degradation in fatigue properties. The relative magnitude of these differences is evident in Figure 80.

b. Fractography

Each of the failed reverse dogbone specimens was examined in order to determine the point at which failure nucleation took place. Again referring to the code presented in Figure 48, a summary of the observed behavior is as follows:

<u>Test Series</u>	<u>Failure Origin per Figure 48</u>
21 Combined variables, R = +0.1	
100/125 AA	3 at B, 1 at C, 1 at L, 1RO
100/125 AA + scratch	9 at B, 3 RO
100/125 AA + ovality	4 at B, 1 at E, 1 at F, 2RO
22 Combined variables, R = -0.33	
100/125 AA	5 at B, 2 at G
100/125 AA + scratch	5 at B, 4 at G, 1 at H
100/125 AA + ovality	1 at B, 3 at F, 2 at G, 3 at J

In reviewing the locations of failure, it should be noted that these reverse dogbone specimens for the most part failed at locations associated with normal fastener performance. Referring to Figure 48, these would be locations A, B, C, G, H and M. And in the same terms, the reverse dogbone specimens, insofar as the discrepancies are concerned, exhibited lives compatible with the baseline or standard specimens, indicating that the fasteners were performing effectively in these particular specimens. In the case of oval holes in both test series, however, substandard fatigue behavior was observed. Likewise a similar number of failures in the F

location (indicating fastener ineffectiveness) were observed. Here again, the origin of failure was consistent with the observed fatigue behavior.

### Evaluation

Two series of low-load transfer reverse dogbone specimens having specific defects were manufactured and fatigue tested in the tension-tension and tension-compression modes. The specific defects, the maximum applied stress and the test series numbers follow.

<u>Defect</u>	<u>Stress (ksi)</u>	<u>Test</u>
Baseline, scratches, rifling, and ovality with hole surface roughness constant at 100-125 AA; median interference of 0.0035"	20.5 tension-tension mode	20/21
Baseline, scratches, and ovality with hole surface roughness constant at 100-125 AA; median interference of 0.0035"	20.5 tension-compression mode	22

Figure 8 gives a description of the low load transfer specimen. The data evaluation is performed using the statistical analysis method outlined in Section VI.6. The analysis is presented for the dependent variable  $1/\alpha \beta$  only. A discussion of  $\alpha \beta$  method is contained in Section VII.2.c.

### Interpretation

The recorded data and test demonstrated values of  $\alpha \beta$  are listed in Tables 16 and 17. The test demonstrated values of  $\alpha \beta$  are obtained using the data presented in Figure 81.

Figures 82 and 83 and Table 18 present the reduced results for Test Series 21. The reduced results for Test Series 22 are presented in Figures 84 and 85 and Table 18. Since  $\alpha \beta$  is independent of stress level, it is possible to combine the results of Test Series 21 and 22. The results of combining these test series are presented in Figure 85 and 86 and also Table 18.

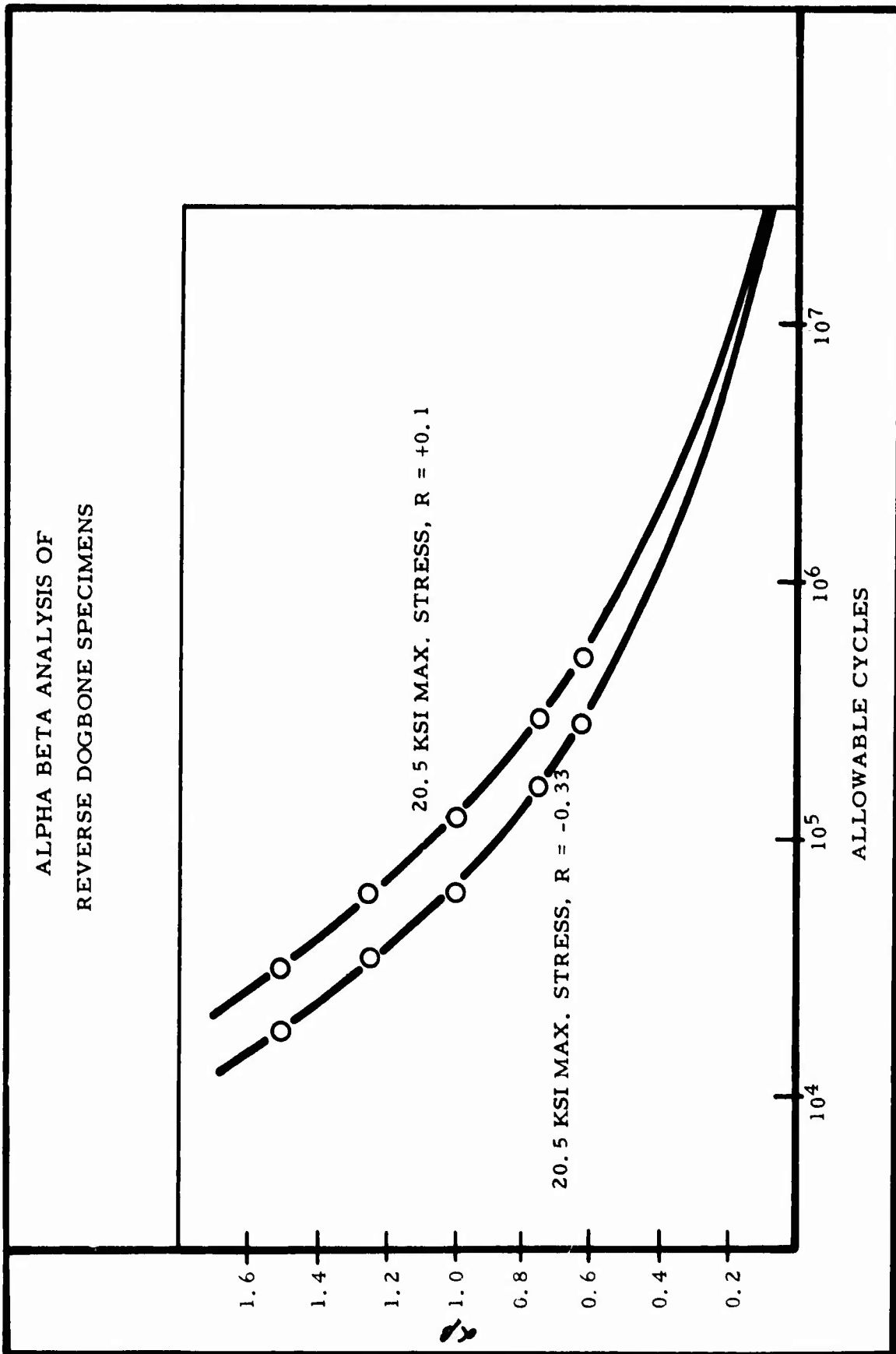


Figure 81 - ALPHA BETA ANALYSIS OF REVERSE DOGBONE SPECIMENS



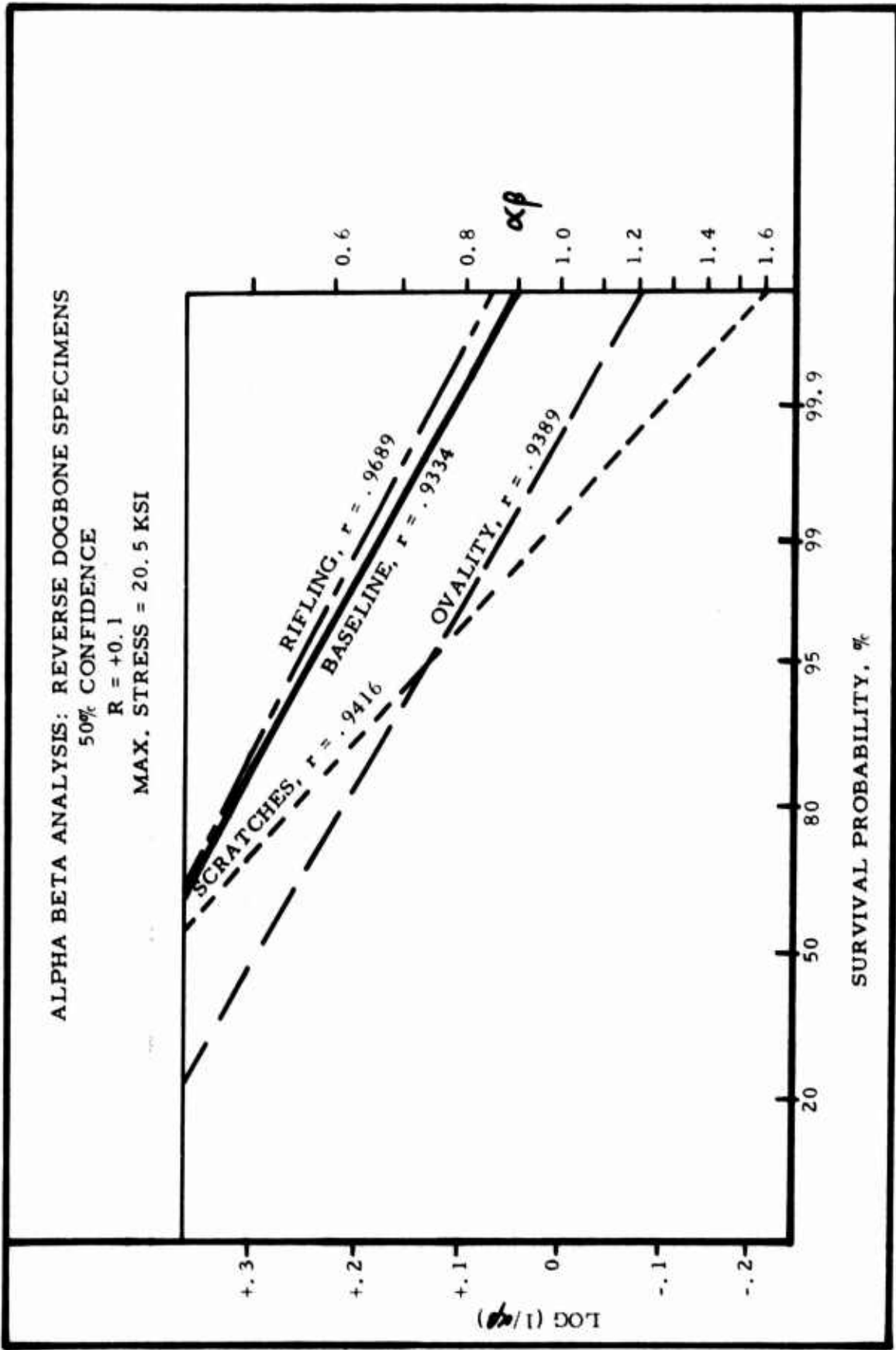


Figure 82 - ALPHA BETA ANALYSIS: REVERSE DOGBONE SPECIMENS - 50% CONFIDENCE

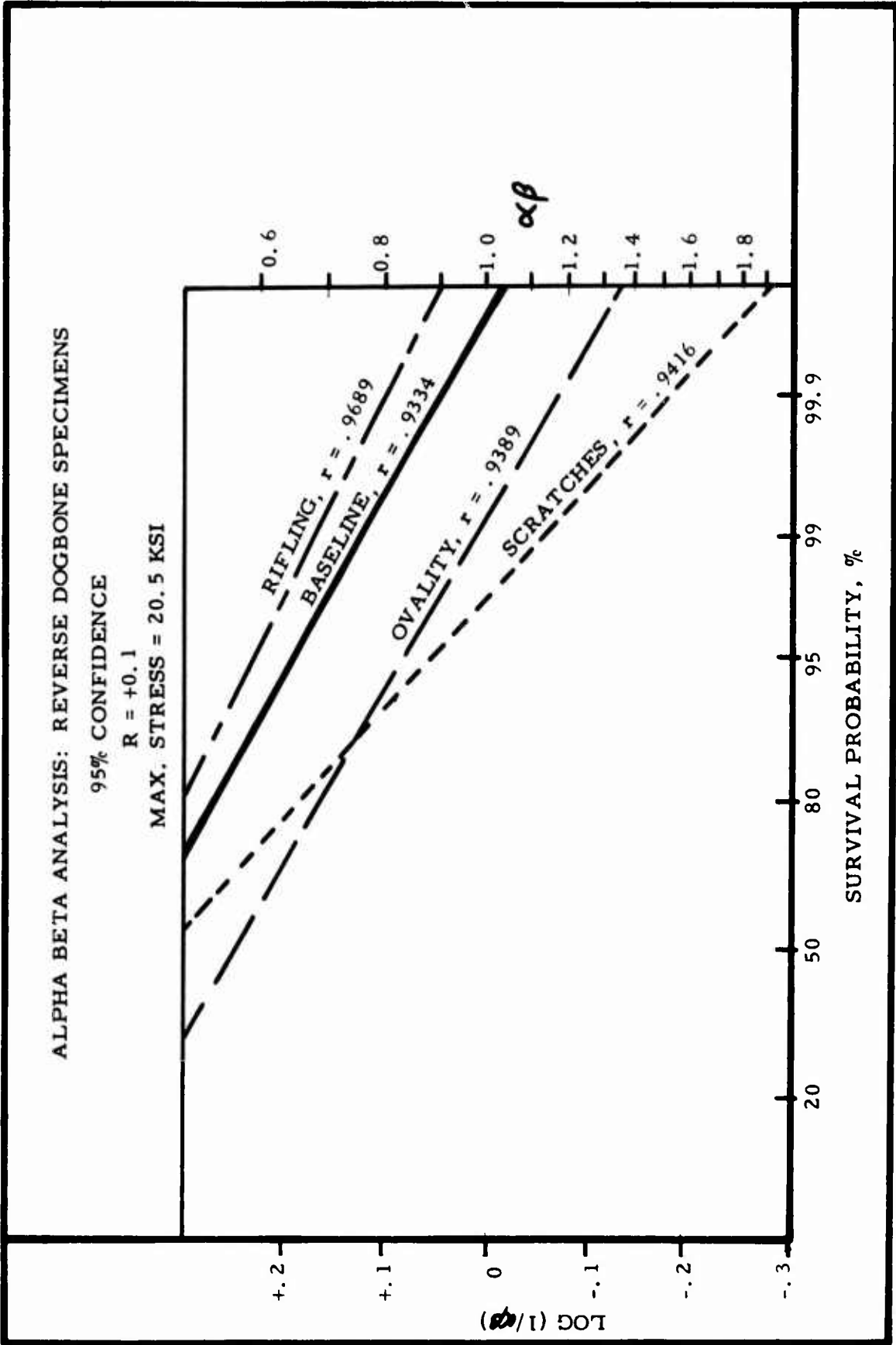


Figure 83 - ALPHA BETA ANALYSIS: REVERSE DOGBONE SPECIMENS - 95% CONFIDENCE

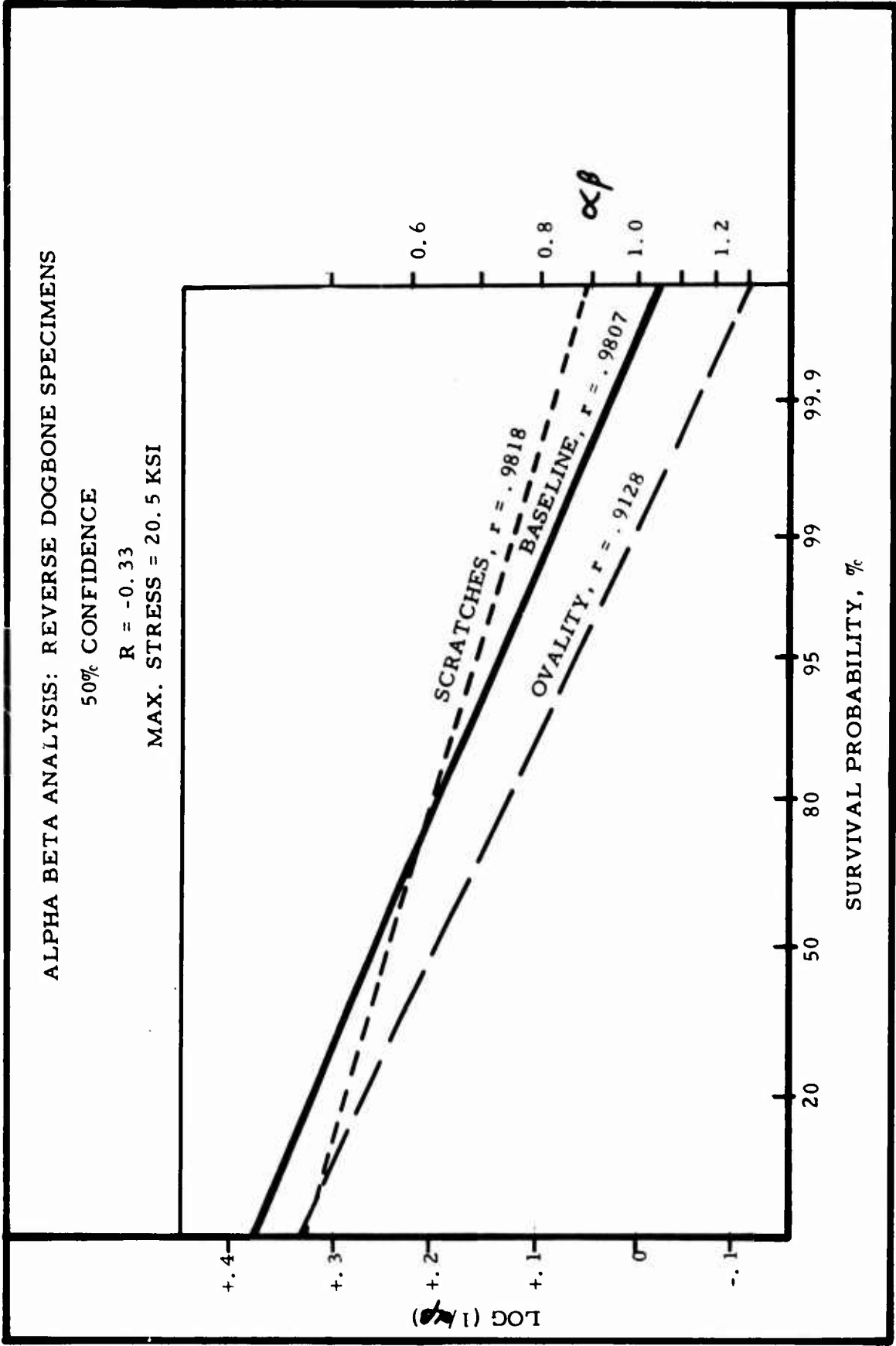


Figure 84 - ALPHA BETA ANALYSIS: REVERSE DOGBONE SPECIMENS - 50% CONFIDENCE

ALPHA BETA ANALYSIS: REVERSE DOGBONE SPECIMENS

95% CONFIDENCE

R = -0.33

MAX. STRESS = 20.5 KSI

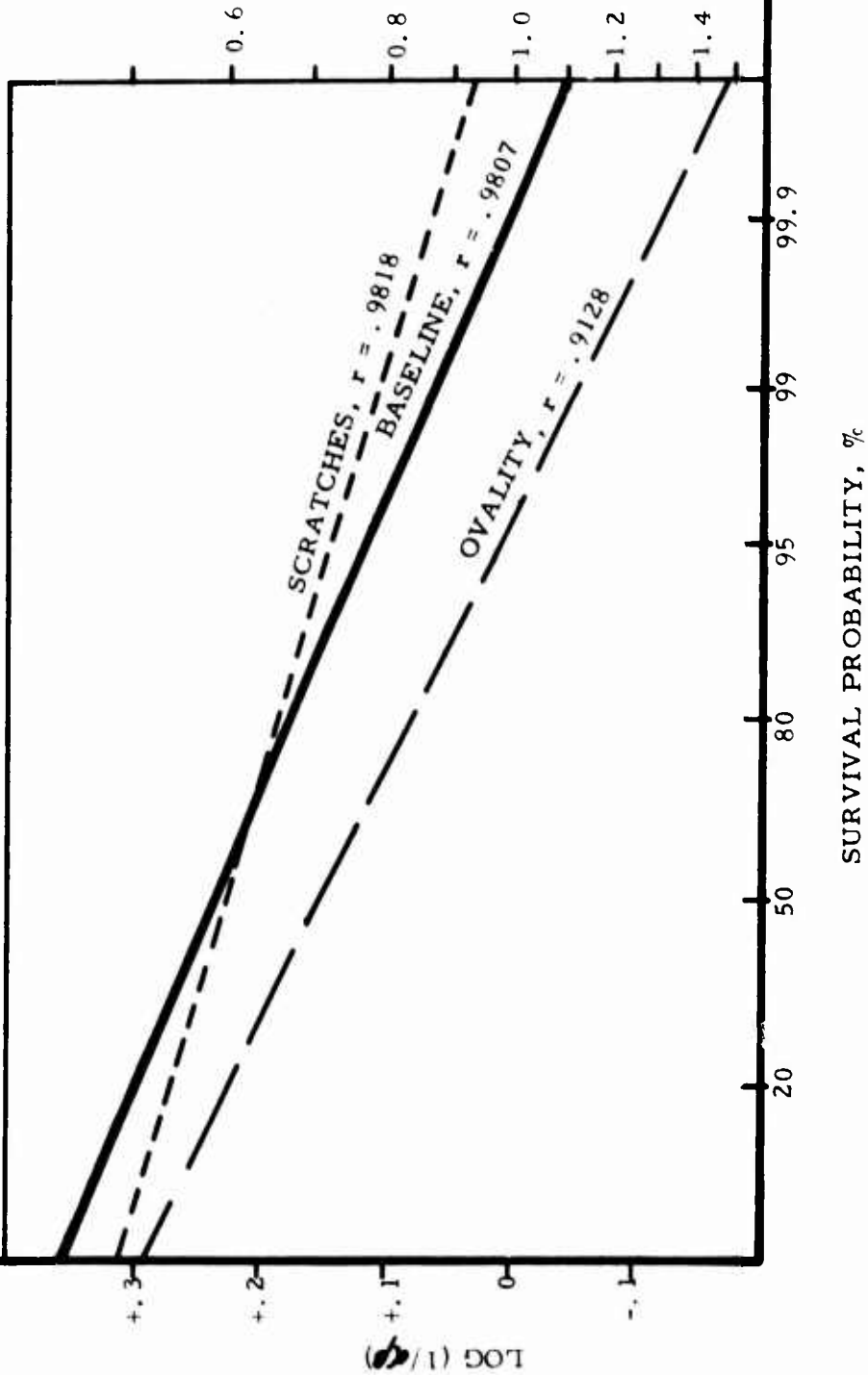


Figure 85 - ALPHA BETA ANALYSIS: REVERSE DOGBONE SPECIMENS - 95% CONFIDENCE

ALPHA BETA ANALYSIS: ALL REVERSE DOGBONE SPECIMENS

50% CONFIDENCE

MAX. STRESS = 20.5 KSI

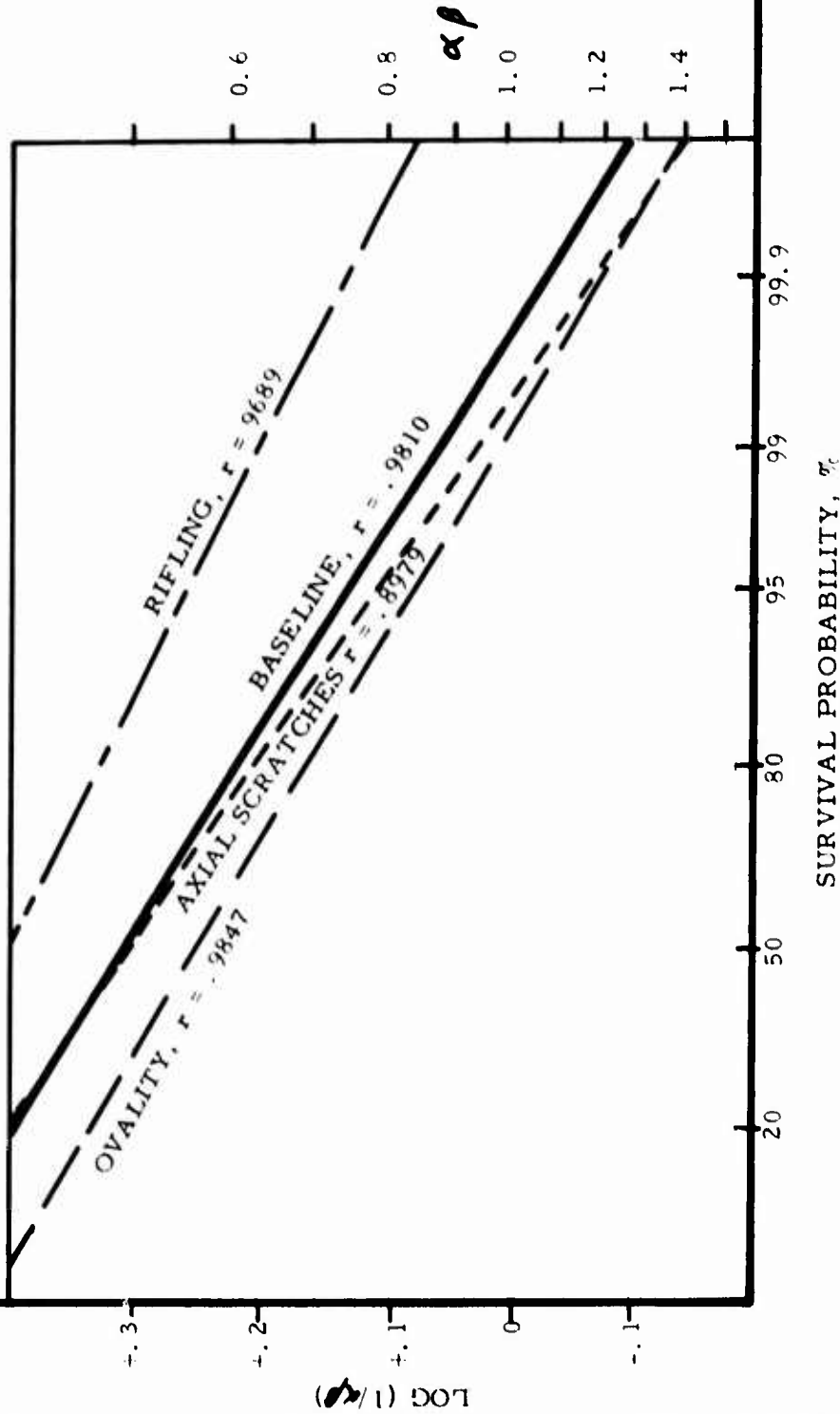


Figure 86 - ALPHA BETA ANALYSIS: ALL REVERSE DOGBONE SPECIMENS - 50% CONFIDENCE

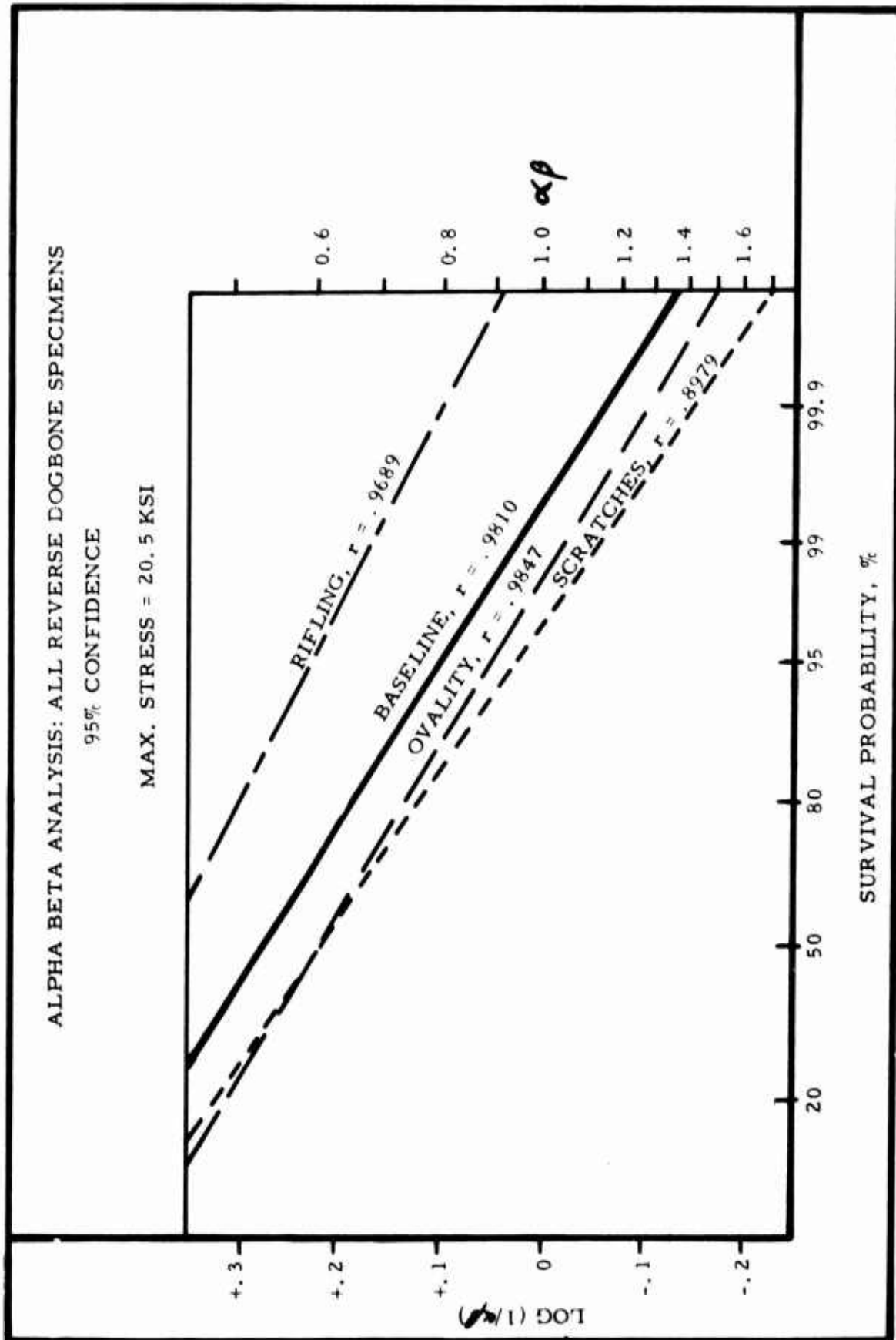


Figure 87 - ALPHA BETA ANALYSIS: ALL REVERSE DOGBONE SPECIMENS - 95% CONFIDENCE

Comparing the results shown in Table 18 with the dogbone plus strap results in Table 15 shows the values to be similar. Therefore, they could be pooled without adversely affecting the correlation. Figures 88 and 89 and Table 19 present the results of pooling the data together with the results of the dogbone plus strap tests not repeated in Test Series 21 and 22.

Included in Table 19 is the effect of pooling Test Series 18 burr results with the baseline results. From Table 19 using 99,95 values, the ranking of hole defects, starting with the most severe, is as follows:

- Bellmouthing
- Ovality
- Axial Scratches
- Barrelling
- Rifling
- Perpendicular Deviation (3°)

#### 4. Discussion: Crack Growth Testing

##### a. Specimen Manufacturing and Precracking

A total of nine specimens were employed for fatigue crack propagation evaluation: three of the open hole (OH) type (Test Series 4), three of the zero load transfer (ZLT) type (Test Series 5) and three of the low-load transfer (LLT) type (Test Series 6). In all cases no manufacturing discrepancies were introduced into the holes. A zero level of interference was used for the ZLT and LLT specimens.

The crack geometry employed in all three test series was a quarter circular crack emanating from the fastener hole intersection with the fay surface as shown in Figure 90. As illustrated, each specimen initially was manufactured with a conventionally drilled 3/16 in. diameter hole. To facilitate initiation of a fatigue crack, a notch of the indicated geometry was introduced at one corner of the hole by electrical discharge machining, EDM.

Fatigue precracking was performed on the specimens in the same test apparatus employed for all other fatigue testing in this program. A maximum stress level of 16.5 ksi was employed in precracking OH Series 4 specimens and a level of 22.0 ksi was

COMBINED ALPHA BETA ANALYSIS OF ALL SPECIMENS  
50% CONFIDENCE

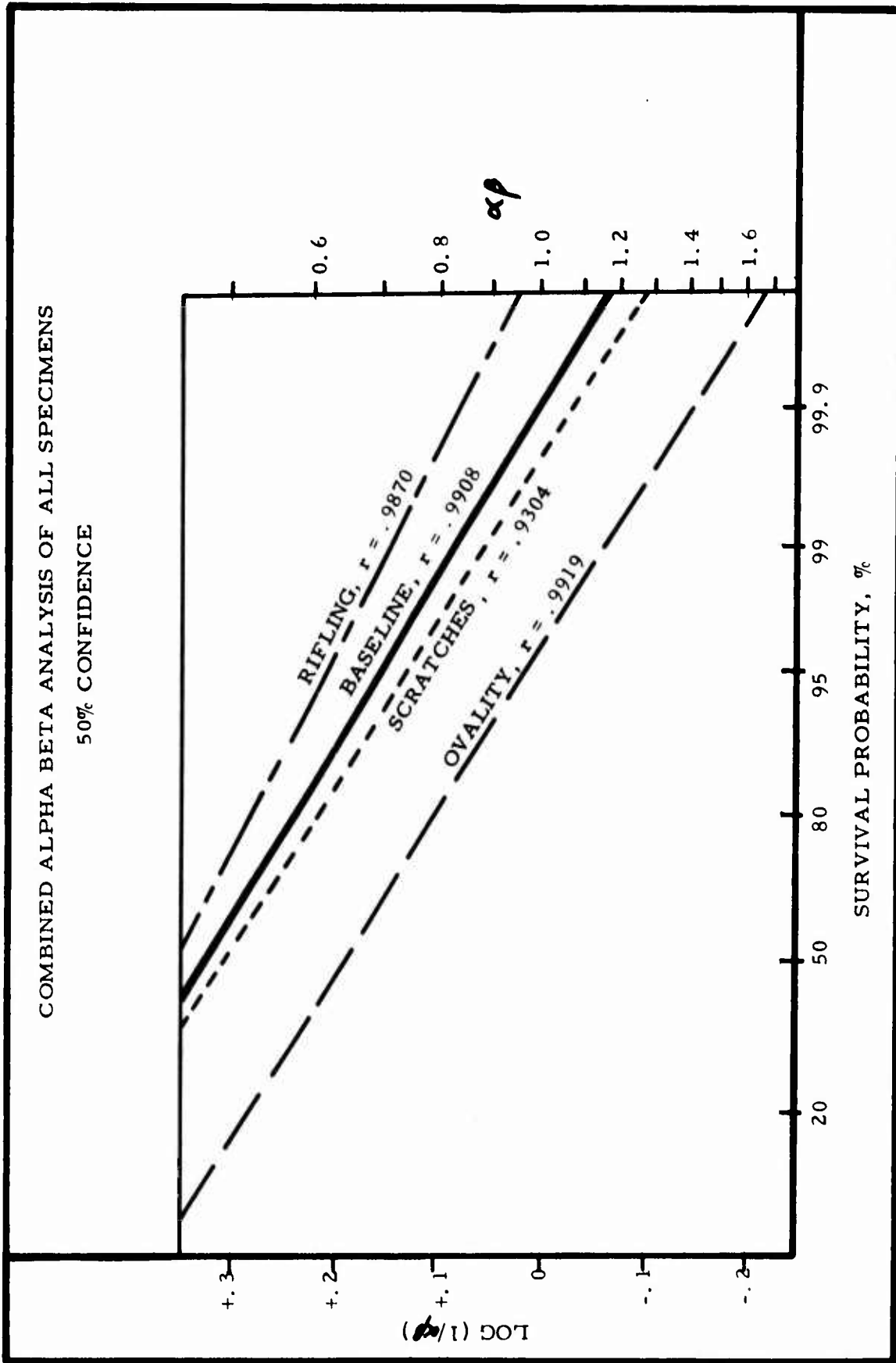


Figure 88 - COMBINED ALPHA BETA ANALYSIS OF ALL SPECIMENS - 50% CONFIDENCE



COMBINED ALPHA BETA ANALYSIS OF ALL SPECIMENS  
95% CONFIDENCE

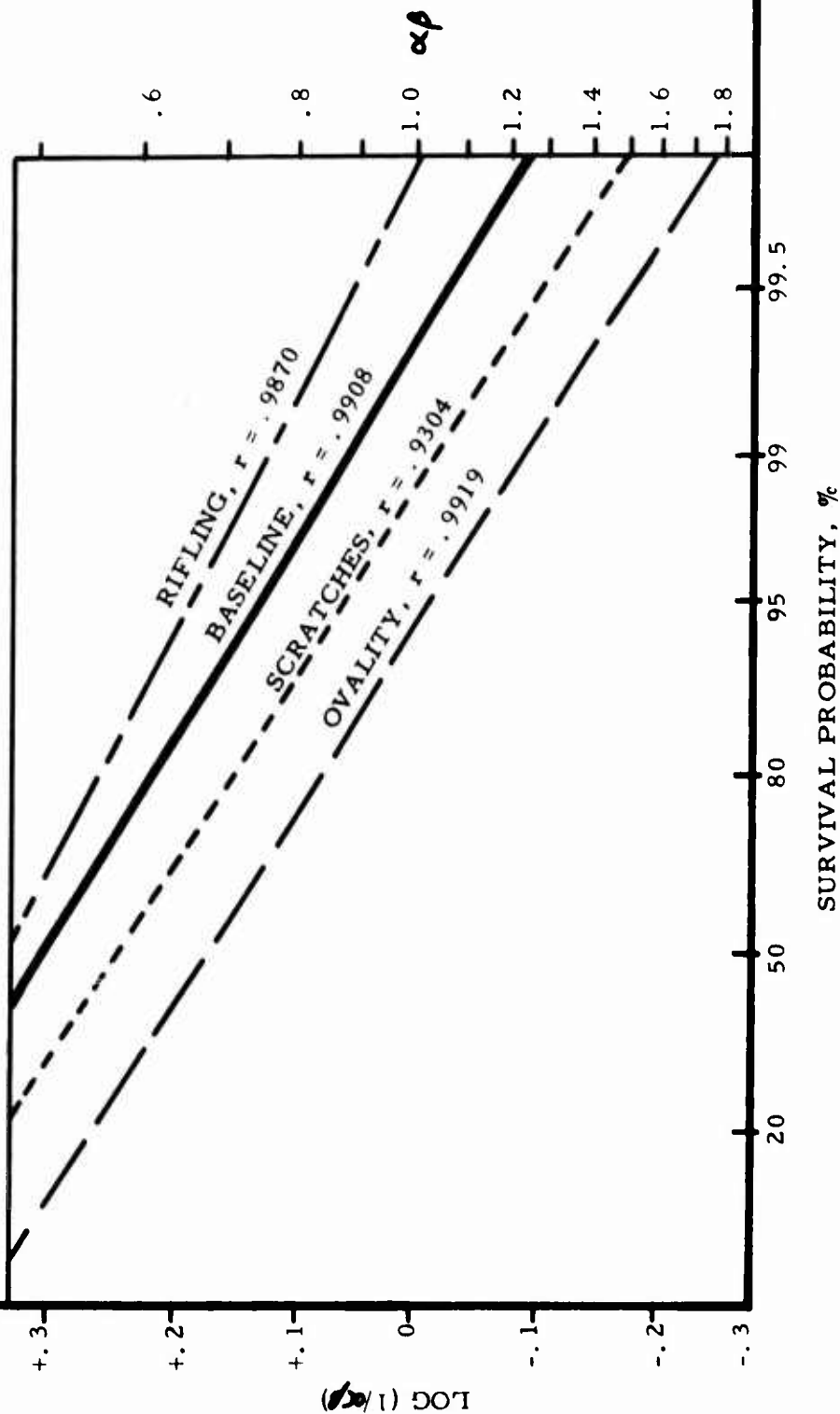
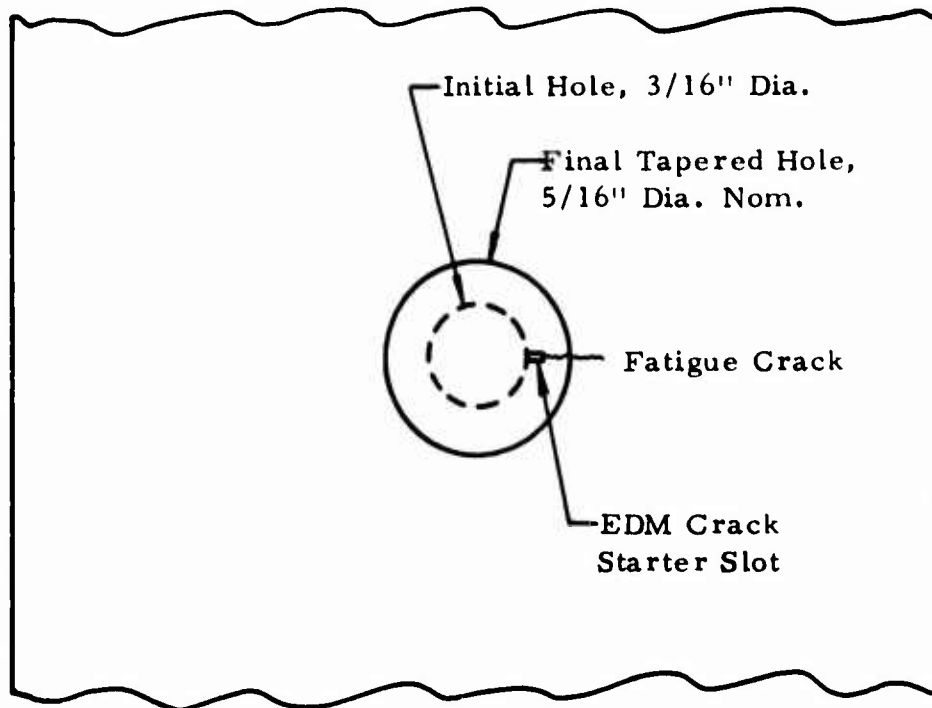
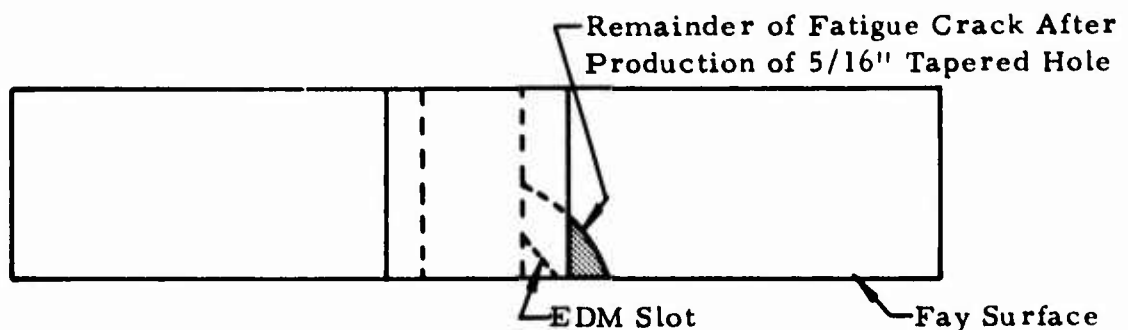


Figure 89 - COMBINED ALPHA BETA ANALYSIS OF ALL SPECIMENS - 95% CONFIDENCE



FRONT VIEW



TOP VIEW

(Section Through Crack Plane)

Figure 90 - SCHEMATIC ILLUSTRATION OF FASTENER HOLE/CRACK GEOMETRY FOR FATIGUE CRACK PROPAGATION SPECIMENS

employed in precracking ZLT Series 5 and LLT Series 6 specimens. These stress levels were chosen to be the same as those employed in fatigue testing after precracking. These stresses were also the same as those used for evaluation of similar specimens in the majority of test series in this program. Fatigue cracks were initiated from the EDM notches in each specimen and allowed to propagate to predetermined sizes. The crack length,  $a$ , on the surface, was monitored via a 20X traveling microscope. Fatigue precracking results are presented in Table 22.

After fatigue precracking, each of the specimens was finish machined by drilling and reaming a standard 5/16 in. nominal diameter tapered hole. Introduction of this hole resulted in removal of the EDM crack starter notch and a portion of the fatigue crack as may be seen from Figure 90.

b. Fatigue Crack Growth Testing

Subsequent to fatigue precracking and introduction of 5/16 in. nominal diameter tapered holes, the ZLT Series 5 and LLT Series 6 specimens were assembled with fasteners at a zero interference level (neat fit). Testing of Series 5 and 6 specimens was performed at a maximum stress level of 22.0 ksi and a cyclic frequency of 30 Hz. Cyclic life results as a function of initial crack size are presented in Table 23. No crack growth data were obtained from these specimens since the crack was inaccessible for visual observation during most of the specimen life.

Cyclic life results for the OH Series 4 specimens are also presented in Table 23. In addition, crack propagation data for these specimens were obtained since visual access to the crack location was available throughout the test. To facilitate crack extension measurements, the cyclic frequency during testing was varied from 0.5 to 5 Hz. All testing was conducted at a maximum stress level of 16.5 ksi. Crack propagation results in terms of crack length versus cycles for each of the three specimens tested are presented in Table 24.

Unfortunately, observation of the crack tip was found to be difficult until the crack grew to a size of about 30% of the hole diameter, i.e., of the order of 0.1 in. in length. Thus, relatively little data were obtained during the period in which the crack could be presumed to have a quarter-circular shape. Laboratory observers during the experiments reported that the anodized and lacquered surface roughness inhibited optical resolution of the crack tip until the crack grew to the indicated size. In contrast, it is interesting to note that considerably smaller than 0.1 in. cracks could be resolved when growing out of the EDM slot during the precracking phase of the experiments.

c. Evaluation of Results

It is emphasized that the objective for performing these relatively few crack propagation tests was to provide some background information whereby the cyclic life results from specimens with various fastener hole manufacturing "defects" could be compared to results from specimens with cracked holes. This limited amount of crack growth testing should not be viewed as having the intent of generation of fastener cyclic life design data. Subject to additional analysis of these results, it may be possible via fracture mechanics methodology to relate typical manufacturing defects to "equivalent" crack/flaw sizes.

Fracture Surface Examination

After testing each of the fracture surfaces, the specimens were examined visually and optically at magnifications up to 42X using a stereo binocular microscope. In each case, it could easily be seen that fatigue cracking had progressed from the location of the initial fatigue precrack; however, the boundary of the initial crack was not delineated by any fracture surface markings. While the precracking and subsequent test stresses were the same, it was hoped that the change in cyclic stress intensity resulting from the changes in hole diameter (and hence crack size) between precracking and crack growth testing would have resulted in a fatigue "beachmark" as the crack resumed growing. This effect, however, did not

produce the desired evidence. Additionally, the lack of fatigue "beachmarkings" on the fracture surfaces precluded obtaining direct information regarding crack shape as a function of crack size. This information would be necessary input for proper calculation of stress intensity factors. The lack of such information is a significant hindrance to analysis of the data in terms of crack growth rate as a function of cyclic stress intensity factor. No further testing is contemplated in this program; however, the advisability of using a fracture surface marking technique to delineate crack contours in any future work of this type is clearly indicated.

### Cyclic Life Results

Although fatigue crack growth rate data were not derived from the results of these experiments, the cyclic life data offer opportunity for some interesting comparisons. The cyclic life results from each specimen, previously presented in Table 23, are shown graphically in Figure 91. From these results it is apparent that the cyclic life of precracked OH specimens was sensitive to initial crack size. In contrast, it also appears that the life of LLT and ZLT was relatively insensitive to initial crack size. This apparent conclusion should be tempered, however, based on the limited number of results and the obvious scatter in life of ZLT and LLT specimens having about the same crack size. Reasons for the observed scatter are not clear. It may be simply that there was some delay in reinitiating fatigue progression from the original precrack. Another possibility is variation in interference level of the fasteners from specimen to specimen. As stated previously, the nominal level of interference was zero. It is recommended for further work that the variable of interference level be thoroughly investigated as to its influence on the propagation of cracks from fastener holes.

## 5. Fracture Mechanics Analysis

The fatigue analysis of test data contained in Sections VI and VII of this report was accomplished by the structures design group at the Lockheed-Georgia Company. In addition, a fracture mechanics group at Lockheed was asked to perform an overview analysis of the same data from a fracture control standpoint. A summary of their work is contained in this part of Section VII.

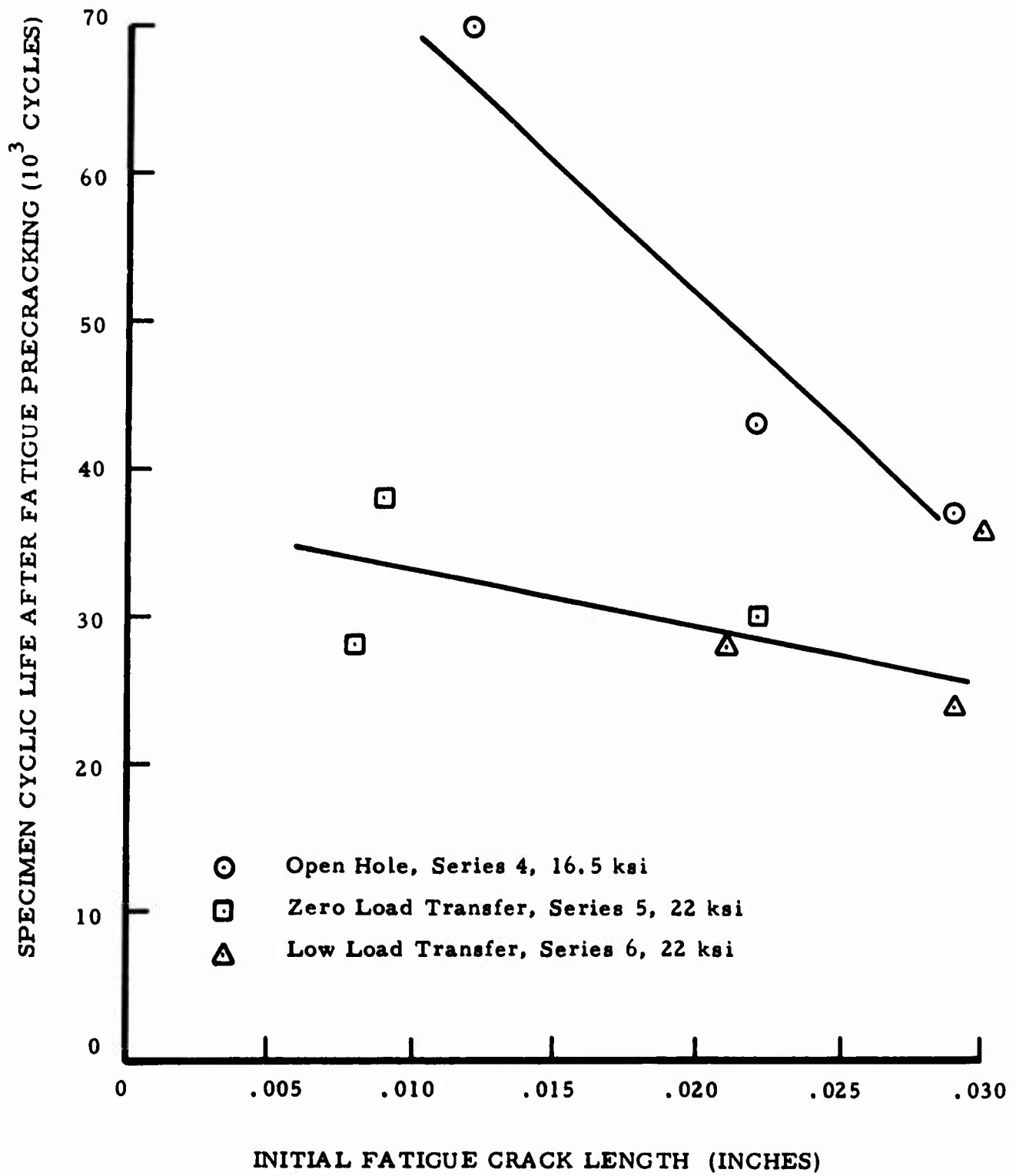


Figure 91 - SPECIMEN CYCLIC LIFE AS A FUNCTION OF INITIAL CRACK LENGTH ON FAY SURFACE

## Objective

To evaluate equivalent initial flaws corresponding to various defect conditions in fastener holes.

## Procedure

Test data were analyzed to give far field and fastener loads. Standard Lockheed fracture analysis methodology was used to calculate cycles for crack growth from an assumed small flaw to failure.

To obtain the equivalent initial flaw, the test failure cycles were subtracted from the calculated cycles to failure. The computer printout was then entered with the difference to find the equivalent initial flaw. The calculated cycles from the equivalent initial flaw to failure were thus equal to the test cycles to failure.

Equivalent initial flaws so obtained are shown for each group of tests in Figure 92. For each group of tests, the mean and standard deviation was calculated. The solid bar line spans one standard deviation each side of the mean. The individual calculated equivalent initial flaws are shown by check marks. Four charts are shown, two for low-load transfer specimens and one each for open hole and reverse dogbone specimens.

## Discussion

The calculated equivalent flaw represented the initial flaw which is calculated to give the same crack growth life as the test specimen. The results are comparative only and cross comparison of the different specimen types is not meaningful. The calculated data presented in the charts can, however, be used to compare the relative effects of the defects introduced into the specimens and the benefits to be obtained, if any, from fastener interference.

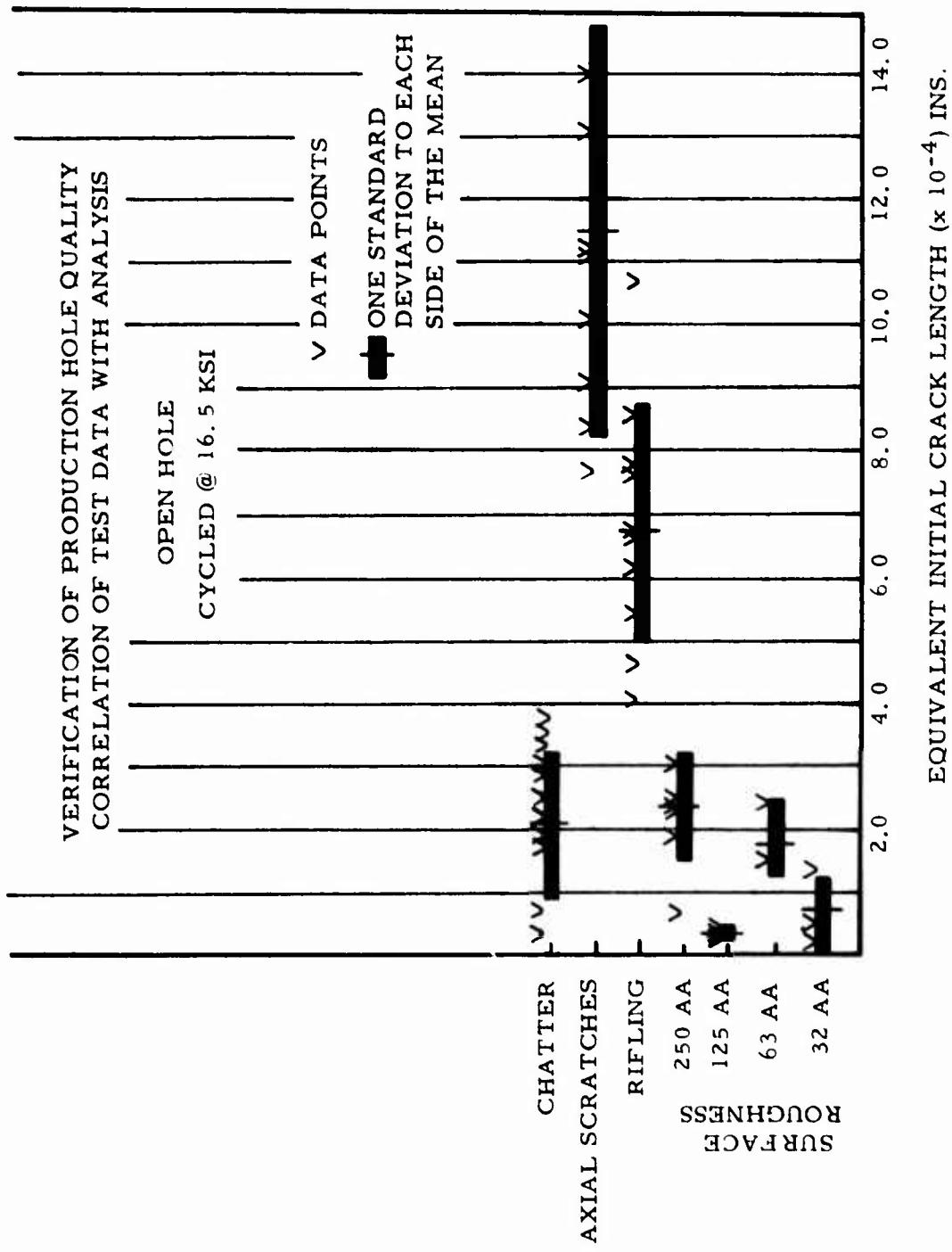


Figure 92 - VERIFICATION OF PRODUCTION HOLE QUALITY - CORRELATION OF TEST DATA WITH ANALYSIS



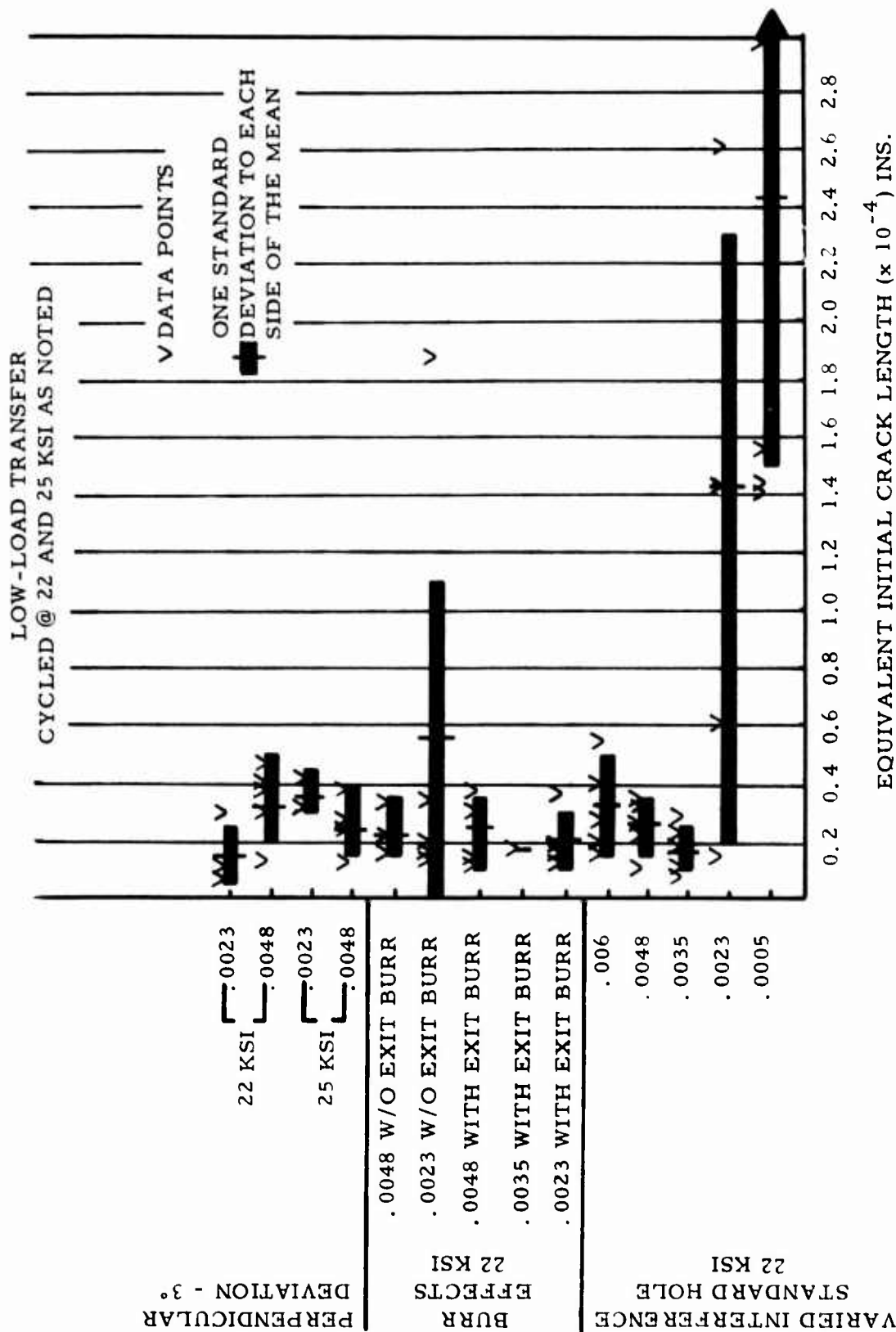


Figure 92 - VERIFICATION OF PRODUCTION HOLE QUALITY - CORRELATION OF TEST DATA WITH ANALYSIS

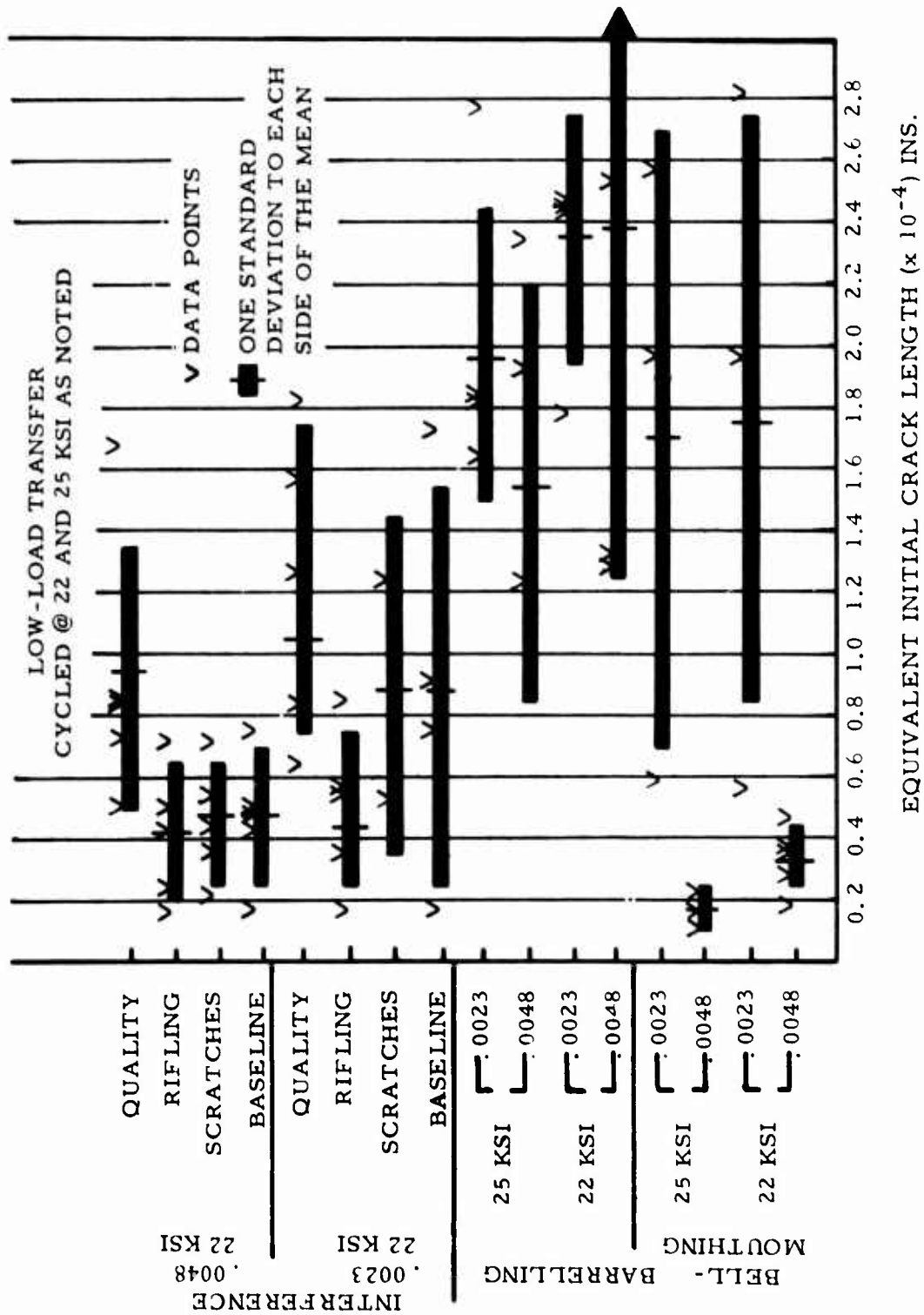


Figure 92 - VERIFICATION OF PRODUCTION HOLE QUALITY - CORRELATION OF TEST DATA WITH ANALYSIS

## Conclusions

- For standard holes, equivalent flaws are considerably greater and more scattered for interference levels of .0023" and less (Test Series 2).
- Perpendicular deviation of 3° and exit burrs are not significant (Tests Series 7 and 18).
- Barrelling and bellmouthing are significantly detrimental at low fastener interference. High fastener interference has a less detrimental effect on a bellmouthed hole than on a barrelled hole or on a bellmouthed hole with low interference (Test Series 8).
- Axial scratches and rifling are detrimental for open holes (Test Series 10 and 11) but are apparently not so significant for filled holes with interference fasteners (Test Series 19). Here again, higher interference appears to be less detrimental than lower interference (Test Series 19).
- Hole ovality is significantly detrimental with no improvement from high interference (Test Series 17, 19 and 22).
- Surface roughness had a significant effect for open holes but surprisingly low results for the 125 AA specimens (Test Series 9). Additional testing for loaded holes with varying surface roughness is recommended.

TABLE 1

MATERIAL DOCUMENTATION

Nominal Gage Section: 0.50" diameter x 2.0" long  
 Temperature: Room Temperature  
 Strain Rate through 0.2% Yield: 0.005 in./in./min.  
 Head Rate thence to Failure: 0.05 in./min.

<u>Specimen No.</u>	<u>Location</u>	<u>U.T.S. (ksi)</u>	<u>.2% Y.S. (ksi)</u>	<u>Elong. (%)</u>	<u>R.A. (%)</u>
5D2T-1	Top Transverse	72.6	61.4	10.5	25.7
5D2T-2	Top Transverse	72.4	61.4	10.9	26.4
5D2B-1	Bottom Transverse	74.6	64.2	11.8	32.8
5D2T-L-1	Top Longitudinal	74.9	64.7	11.9	37.0
5D2T-L-2	Top Longitudinal	74.1	63.7	13.6	38.1
5D2B-L-3	Bottom Longitudinal	75.1	64.9	12.7	42.8
5D2B-L-5	Bottom Longitudinal	76.0	65.7	12.8	41.9

TABLE 2

Fatigue Data Summary: Test Series I  
 Specimen Type: Parent Metal  
 Mode: R = 0.1, Room Temperature

<u>Specimen Number</u>	<u>Frequency (cps)</u>	<u>Max. Stress (ksi)</u>	<u>Cycles (x 10<sup>3</sup>)</u>	<u>Status</u>
<b><u>AS-MILLED SURFACES</u></b>				
5D4B	7	42	54	Failure
5D1B	7	40	66	Failure
5D3B	7	40	74	Failure
6A2B	7	37	103	Failure
6A4CB	7	32	191	Failure
5D1CT	7	27	1,494	Failure
5D3CB	30	29	1,073	Failure
5E1T	30	26	1,369	Failure-grip edge
<b><u>SHOT PEENED SURFACES</u></b>				
6A4T	30	46	108	Failure
6A4B	20	41	308	Failure
5E1CB	20	32	913	Failure-loading hole
5D2CT	20	35	932	Failure
6A4CT	30	31	10,185	Runout
5D2T	30	35	1,343	Failure
5D2B	30	33	12,672	Runout
5E1CT	30	35	10,068	Runout
5E1B	30	38.5	339	Failure
6A2C1B	30	37.5	719	Failure
6A3B	30	36	10,040	Runout
6A5T	30	37	7,266	Failure
5D4CB	30	36	10,246	Runout

TABLE 3

MACHINING CONDITIONS USED FOR MILLING THE SPECIMENS

	<u>Specimen Blank</u>	<u>Specimen Contour</u>
Cutter Diameter, in.	6	2-1/2
Tool Material	K68 Carbide	M2 HSS
Feed, in. /tooth	.004	.0014
Cutting Speed, ft. /min.	1200	1600
Tool Wear, max.	.006	.006
No. of Teeth	8	6
Fluid	20:1 Soluble Oil	Dry

TABLE 4

MANUFACTURING, INSPECTION AND FATIGUE SUMMARY

Test Series No. Low Load Transfer Baseline (Dogbone/Strap)

Test No.	Specimen No.	Inspection Results						Fatigue Results		
		Hole 1		Hole 2		Max. Stress	Cycles	Failure Hole Origin		
		Surf. Rough	Protru-sion	% Blue	Surf. Rough				Protru-sion	% Blue
38	5B3B	49	.188	70	53	.188	80	40	16	--
34	5A1T	55	.182	65	50	.180	70	35	63	--
33	6A6B	55	.176	70	55	.182	70	30	150	--
30	2A4B	59	.182	70	45	.179	70	25	254	--
39	5E5B	62	.187	80	36	.187	65	25	398	--
31	5C5B	41	.187	70	45	.178	70	23	493	--
32	2D2T	56	.187	60	45	.178	70	21	1,120	--
35	5B4B	57	.184	80	50	.184	70	20	1,108	--
36	5A6T	29	.185	70	30	.183	70	18	2,431	--
37	5B5B	41	.183	70	44	.178	70	17	10,000	--

Notes: Fatigue Testing at R=.1 ; Failure Origin Coding in Figure 48 ; Cycles expressed in thousands

TABLE 5  
MANUFACTURING, INSPECTION AND FATIGUE SUMMARY

Test Series No. 9, Surface Roughness

Test No.	Specimen No.	Inspection Results						Fatigue Results			
		Hole 1		Hole 2		Max. Stress	Cycles	Failure Hole	Origin		
		Surf. Roughness	Protru- sion	% Blue	Surf. Roughness					Protru- sion	% Blue
BASELINE											
83	5D5CT	52	.169	--	56	.172	--	22	112	2	E
84	2E1T	58	.174	--	61	.172	--	18	10,197	--	RO
85	5C6B	52	.189	--	65	.169	--	20	153	2	E
86	5A6B	50	.174	--	65	.170	--	19	219	2	F
88	5B1CT	53	.204	--	55	.201	--	27.4	35	1	E
89	5D5B	56	.193	--	46	.201	--	18.0	174	2	F
90	5D6CB	44	.199	--	48	.201	--	16	10,516	--	RO
91	2A6B	45	.138	--	55	.155	--	18	271	2	F
92	5E5CT	45	--	--	50	--	--	17	292	2	F
100	2C3T	62	.161	--	55	.181	--	24	40	1	F
93	5C4CB	63	.140	--	54	.146	--	15	1,270	2	F
94	5A5CT	66	.150	--	60	.151	--	12	8,068	--	RO
63 MICRONS											
95	5B9CB	48	.160	--	52	.163	--	16.5	377	2	F
96	5A2CT	65	.146	--	56	.162	--	16.5	377	2	F
97	5A5B	65	.169	--	55	.177	--	16.5	268	1	F
245	4C5T	48	.157	--	53	.154	--	16.5	361	2	D
247	3A5B	62	.148	--	57	.155	--	16.5	295	1	F
246	4D6B	77	.118	--	57	.139	--	16.5	427	2	F
249	4E2T	67	.152	--	77	.148	--	16.5	451	2	E
248	4C1B	62	.130	--	70	.155	--	16.5	341	1	F

Notes: Fatigue Testing at R = .1 ; Failure Origin Coding in Figure 48 ; Cycles expressed in thousands



TABLE 5 (continued)

MANUFACTURING, INSPECTION AND FATIGUE SUMMARY

Test Series No. 9, Surface Roughness

Test No.	Specimen No.	Inspection Results				Fatigue Results					
		Hole 1	Hole 2	Surf. Roughness	Max. Stress	Cycles	Failure Hole Origin				
		Surf. Roughness	Protru- sion	% Blue	Surf. Roughness	Protru- sion	% Blue				
32 MICROINCHES											
98	3C4T	34	.183	--	34	.182	--	16.5	10,139	--	RO
105	4C3B	17	.191	--	16	.188	--	16.5	444	2	F
107	5C2CB	22	.198	--	25	.198	--	16.5	3,823	1	F
110	5B4CB	22	.195	--	22	.197	--	16.5	10,048	--	RO
114	4B3T	35	.161	--	30	.183	--	16.5	1,318	1	F
125 MICROINCHES											
101	3C6T	115	.190	--	105	.183	--	16.5	12,940	--	RO
106	4B2T	95	.178	--	103	.200	--	16.5	13,018	--	RO
111	3C5T	118	.173	--	115	.186	--	16.5	2,125	--	RO
112	2E6T	100	.200	--	105	.192	--	16.5	2,390	--	RO
113	5A4CB	120	.208	--	108	.195	--	16.5	2,523	--	RO

Notes: Fatigue Testing at P = .1 ; Failure Origin Coding in Figure 48 ; Cycles expressed in thousands

TABLE 5 (continued)

MANUFACTURING, INSPECTION AND FATIGUE SUMMARY

Test Series No. 9, Surface Roughness

Test No.	Specimen No.	Inspection Results						Fatigue Results			
		Hole 1			Hole 2			Max. Stress	Cycles	Failure Hole Origin	
		Surf. Roughness	Protru- sion	% Blue	Surf. Roughness	Protru- sion	% Blue				
250 MICRONS											
102	6A1T	260	.230	--	265	.236	--	19.5	121	1	E
103	3B4B	250	.205	--	245	.205	--	16.5	814	2	F
104	4E2B	275	.203	--	270	.200	--	16.5	219	1	E
108	2E2T	260	.191	--	240	.223	--	16.5	318	2	E
109	3B3B	170	.192	--	170	.190	--	16.5	261	2	E
115	4A6B	265	.220	--	260	.225	--	16.5	279	2	F
116	5E3CB	240	.210	--	260	.210	--	16.5	4,477	--	RO
117	5A4CT	265	.240	--	220	.242	--	16.5	244	2	E
118	4D3T	220	.216	--	250	.204	--	16.5	227	2	E
119	2A5T	270	.210	--	270	.220	--	16.5	224	1	F

Notes: Fatigue Testing at R=.1 ; Failure Origin Coding in Figure 48 ; Cycles expressed in thousands

TABLE 6  
 MANUFACTURING, INSPECTION AND FATIGUE SUMMARY  
 Test Series No. 10

Test No.	Specimen No.	Inspection Results						Fatigue Results			
		Hole 1		Hole 2		Max. Stress	Cycles	Failure Hole Origin			
		Surf. Rough	% Blue	Surf. Rough	% Blue						
RIFLING											
120	2C4B	45	.183	70	40	.195	90	16.5	110	1	F
123	5E5T	60	.185	70	62	.186	80	16.5	91		E
126	2E3T	30	.181	90	32	.183	90	16.5	122	1	E
127	2E5T	45	.182	70	40	.183	80	16.5	121	1	E
132	4E6B	22	.167	70	19	.181	80	16.5	172	2	D
133	2B4T	20	.174	70	20	.172	80	16.5	140	2	E
134	3B2B	50	.183	70	40	.180	80	16.5	111	2	E
140	2B1T	30	.174	80	30	.175	70	16.5	158	1	E
141	3B6T	26	.175	70	22	.173	70	16.5	129	1	D
143	2B3B	30	.177	70	25	.175	70	16.5	103	2	E

Notes: Fatigue Testing at R = .1 ; Failure Origin Coding in Figure 48 ; Cycles expressed in thousands

TABLE 7  
 MANUFACTURING, INSPECTION AND FATIGUE SUMMARY  
 Test Series No. 11

Test No.	Specimen No.	Inspection Results							Fatigue Results						
		Hole 1			Hole 2				Max. Stress	Cycles	Failure Hole Origin				
		Surf. Rough	Protru- sion	% Blue	Surf. Rough	Protru- sion	% Blue								
SCRATCHES															
121	4A2B	47	. 173	80	33	. 169	80	16.5	90	2	E				
124	3D1T	37	. 168	80	48	. 170	90	16.5	99	2	E				
128	3D2T	35	. 169	80	40	. 177	70	16.5	105	2	D				
129	4B1T	40	. 171	80	30	. 170	80	16.5	93	2	E				
135	5C4B	40	. 172	90	45	. 173	80	16.5	88	2	D				
136	2A3T	40	. 171	90	41	. 168	90	16.5	65	1	E				
137	4C1T	41	. 171	70	40	. 168	80	16.5	85	2	D				
138	4D2B	39	. 176	80	31	. 175	90	16.5	77	2	D				
142	3A6T	41	. 169	90	30	. 169	80	16.5	80	2	D				
145	4C4T	45	. 190	70	41	. 176	70	16.5	111	2	D				

Notes: Fatigue Testing at R = .1 ; Failure Origin Coding in Figure 48 ; Cycles expressed in thousands

TABLE 8  
 MANUFACTURING, INSPECTION AND FATIGUE SUMMARY  
 Test Series No. 12

Test No.	Specimen No.	Inspection Results						Fatigue Results			
		Hole 1			Hole 2			Max. Stress	Cycles	Failure Hole Origin	
		Surf. Rough	% Blue	Protru-sion	Surf. Rough	% Blue	Protru-sion				
CHATTER											
122	3B2T	125	--	.155	90	.130	--	16.5	1,410	2	F
125	5D5T	132	--	.146	135	.135	--	16.5	508	1	F
130	5A3CT	75	--	.170	110	.162	--	16.5	2,656	--	RO
131	5A1B	155	--	.178	170	.135	--	16.5	2,018	--	RO
139	6A1CT	170	--	.141	170	.130	--	16.5	316	2	F
144	5C1CT	165	--	.131	210	.161	--	16.5	223	1	F
146	5A3T	195	--	.158	185	.136	--	16.5	2,087	--	RO
155	6A1CB	210	--	.152	190	.161	--	16.5	3,390	--	RO
156	3A2B	145	--	.185	150	.196	--	16.5	655	2	F
157	5A2CB	170	--	.182	195	.133	--	16.5	3,540	--	RO
TEARS AND LAPS, PLASTIC DEFORMATION											
147	3B4T	20	--	.224	102	.218	--	16.5	1,181	2	F
148	5B2CB	118	--	.225	75	.221	--	16.5	206	2	F
149	4A3BC	85	--	.222	109	.200	--	16.5	191	1	E
150	4B6B	56	--	.226	72	.213	--	16.5	201	2	E
151	3B1B	50	--	.227	102	.115	--	16.5	232	2	D
152	5E4CT	85	--	.215	92	.220	--	16.5	349	2	F
153	4E6T	30	--	.227	102	.210	--	16.5	288	2	F
154	3A1B	106	--	.144	104	.223	--	18.4	235	1	E
234	5E6CT	40	--	.190	102	.231	--	16.5	652	1	F
235	3A3T	142	--	.221	128	.225	--	16.5	265	2	F

Notes: Fatigue Testing at R = .1 ; Failure Origin Coding in Figure 48; Cycles expressed in thousands

TABLE 9  
 MANUFACTURING, INSPECTION AND FATIGUE SUMMARY  
 Test Series No. 2, Interference Level

Test No.	Specimen No.	Inspection Results						Fatigue Results				
		Hole 1		Hole 2		Max. Stress	Cycles	Failure Hole	Origin	$\sigma/\beta$		
		Surf. Rough	% Blue	Protru- sion	% Blue							
.0005 INTERFERENCE												
49	4C2B	22	.033	80	40	.028	80	22	58	2	F	--
48	5C1B	45	.015	70	45	.026	65	22	81	2	F	--
47	5B5CT	31	.028	85	34	.039	80	22	144	2	F	--
52	5A3CT	22	.026	90	19	.022	80	22	155	2	F	--
51	5E6CB	33	.018	70	41	.030	65	22	156	1	F	--
.0023 INTERFERENCE												
71	4E3B	34	.118	70	36	.125	65	22	93	1	F	.774
75	4A3T	31	.111	90	46	.104	70	22	154	2	F	.654
73	4D4B	25	.116	90	41	.108	90	22	304	1	F	.533
70	5C1T	25	.112	80	38	.115	70	22	961	1	B	.376
72	3B1T	31	.125	70	40	.112	70	22	1,004	2	G	.371
.0035 INTERFERENCE												
42	4A4B	50	.180	70	40	.185	80	22	675	2	G	.414
41	5C4T	35	.186	60	32	.186	80	22	824	2	G	.392
40	5C5CB	55	.182	70	35	.182	60	22	925	1	G	.379
44	6A6T	55	.187	60	50	.197	70	22	1,258	2	B	.348
43	5C6T	62	.193	70	35	.202	70	22	1,458	2	D	.332

Notes: Fatigue Testing at R=.1 ; Failure Origin Coding in Figure 48 ; Cycles expressed in thousands

TABLE 9 (continued)

MANUFACTURING, INSPECTION AND FATIGUE SUMMARY

Test Series No. 2, Interference Level

Test No.	Specimen No.	Inspection Results							Fatigue Results			
		Hole 1			Hole 2				Max. Stress	Cycles	Failure Hole Origin	$\alpha \beta$
		Surf. Rough	Protru-sion	% Blue	Surf. Rough	Protru-sion	% Blue					
.0048 INTERFERENCE												
82	2E4T	40	.233	80	40	.235	80	22	544	1	G	.458
78	5B6T	60	.236	70	50	.227	80	22	591	2	G	.450
87	5E2B	55	.222	80	40	.238	80	22	717	1	G	.436
76	5C5CT	40	.225	90	40	.242	85	22	788	2	B	.432
80	3B5T	41	.235	90	40	.242	90	22	1,398	1	F	.336
.006 INTERFERENCE												
79	5B6B	30	.292	80	45	.291	70	22	353	1	G	--
77	4C6T	40	.306	75	40	.292	70	22	450	1	G	--
74	4A5T	42	.292	85	45	.296	80	22	663	2	F	--
99	2D1T	40	.297	90	41	.292	85	22	865	2	G	--
81	3A1T	41	.291	90	41	.284	80	22	1,180	2	G	--

Notes: Fatigue Testing at R=.1 ; Failure Origin Coding in Figure 48 ; Cycles expressed in thousands

TABLE 10  
 MANUFACTURING, INSPECTION AND FATIGUE SUMMARY  
 Test Series No. 7, Perpendicularity

Test No.	Specimen No.	Inspection Results						Fatigue Results				
		Hole 1			Hole 2			Max. Stress	Cycles	Failure Hole Origin	$a/\beta$	
		Surf. Rough	Protru- sion	% Blue	Surf. Rough	Protru- sion	% Blue					
<b>MINIMUM INTERFERENCE</b>												
185	5BIT	32	.148	70	28	.157	80	22	1,793	2	G	.312
190	5D5CB	26	.143	75	65	.130	70	22	2,075	2	G	.298
191	5A4T	22	.141	70	35	.143	75	22	3,036	--	RO	--
196	4D6T	21	.140	70	22	.145	80	22	638	2	G	.422
198	5A4B	60	.143	70	28	.138	70	22	583	2	G	.434
213	2B6T	40	.137	70	140	.145	80	25	278	1	F	.463
201	5C3T	32	.152	70	105	.152	70	25	686	1	G	.361
203	5C3CB	30	.156	70	30	.155	70	25	555	1	G	.381
204	5E4CB	18	.156	70	80	.142	70	25	588	1	G	.377
214	6A1B	38	.150	70	28	.154	70	25	1,477	1	E	.292
<b>MAXIMUM INTERFERENCE</b>												
187	5B2T	28	.253	70	80	.225	60	22	468	1	G	.462
192	5B3CT	36	.253	75	32	.246	70	22	472	2	G	.460
193	5D6CT	28	.242	70	32	.248	80	22	628	1	G	.424
194	5A6CT	25	.239	70	30	.236	75	22	1,399	1	G	.337
195	4E1B	24	.238	75	15	.243	70	22	704	1	G	.410
242	5C3B	36	.266	70	28	.279	70	25	234	1	G	.479
202	5C6CT	22	.243	70	35	.250	80	25	223	1	G	.490
205	5C4CT	25	.257	80	30	.248	80	25	269	1	G	.466
206	4C5B	34	.232	70	35	.240	70	25	207	2	G	.508
215	5A1CT	36	.255	70	52	.249	80	25	568	2	G	.381

Notes: Fatigue Testing at R = .1 ; Failure Origin Coding in Figure 48 ; Cycles expressed in thousands



TABLE 11  
 MANUFACTURING, INSPECTION AND FATIGUE SUMMARY  
 Test Series No. 8, Barrelling

Test No.	Specimen No.	Inspection Results						Fatigue Results			
		Hole 1			Hole 2			Max. Stress	Cycles	Failure Hole Origin	$\alpha \beta$
		Surf. Rough	Protru- sion	% Blue	Surf. Rough	Protru- sion	% Blue				
MINIMUM INTERFERENCE											
166	4D2I	55	.126	20	55	.117	25	22	98	1	.759
160	3A6B	60	.121	30	50	.106	30	22	92	1	.776
161	2C5T	45	.126	25	50	.125	25	22	119	1	.709
164	3D2B	65	.121	30	55	.122	30	22	94	1	.770
165	3A2T	65	.119	20	45	.112	25	22	127	2	.696
182	2A6T	50	.124	25	60	.124	30	25	76	1	.704
171	2D4T	55	.122	30	50	.109	20	25	75	2	.706
176	5A6CB	50	.115	25	65	.119	25	25	54	2	.764
236	2C4I	60	.119	20	60	.120	20	25	83	1	.685
237	5C2CT	55	.112	30	50	.120	20	25	76	2	.704
MAXIMUM INTERFERENCE											
167	5E2CT	60	.243	25	60	.239	35	22	165	2	.640
158	5B2CT	50	.235	20	65	.233	30	22	84	1	.805
159	5B1CB	50	.235	20	55	.210	20	22	96	1	.766
162	5E5CB	60	.218	25	65	.238	20	22	161	2	.646
163	5E2CB	60	.239	25	50	.246	25	22	66	1	.870
181	2C5B	45	.239	25	55	.247	30	25	86	1	.680
239	2D3T	50	.245	25	50	.244	35	25	152	1	.560
174	5C3CT	60	.243	20	55	.246	25	25	62	1	.744
180	5A5CB	75	.221	20	60	.236	30	25	71	1	.716
238	4D4T	65	.238	20	45	.228	25	25	101	1	.652

Notes: Fatigue Testing at R = .1 ; Failure Origin Coding in Figure 48 ; Cycles expressed in thousands

TABLE 11 (continued)

MANUFACTURING, INSPECTION AND FATIGUE SUMMARY

Test Series No. 8, Bellmouthing

Test No.	Specimen No.	Inspection Results						Fatigue Results				
		Hole 1			Hole 2			Max. Stress	Cycles	Failure Hole Origin	$\sigma/\beta$	
		Surf. Rough	Protru- sion	% Blue	Surf. Rough	Protru- sion	% Blue					
<b>MINIMUM INTERFERENCE</b>												
241	2B1B	25	.118	35	55	.124	40	22	126	2	F	.698
207	3C2B	50	.125	40	42	.124	45	22	2,796	2	B	.271
208	2B5B	35	.125	40	28	.120	35	22	335	2	F	.509
209	3C5B	27	.125	35	35	.126	45	22	86	1	F	.797
210	3A4B	25	.124	40	15	.123	35	22	114	1	F	.711
240	4A4T	36	.100	45	40	.127	35	25	69	1	F	.720
211	2E2B	25	.126	35	20	.119	35	25	59	1	F	.750
212	2D5B	30	.125	35	38	.112	40	25	163	1	F	.557
265	2E5B	20	.120	45	35	.125	45	25	134	1	F	--
262	3A4T	30	.125	--	38	.114	45	25	105	1	F	--
<b>MAXIMUM INTERFERENCE</b>												
183	2D3B	45	.236	40	55	.243	45	22	609	1	G	.428
184	2A4T	40	.237	40	28	.244	45	22	411	1	G	.489
186	2E6B	35	.239	50	32	.200	40	22	950	2	G	.377
188	2C6T	80	.244	35	30	.241	40	22	515	1	G	.449
189	3C6B	40	.239	35	42	.245	40	22	537	1	C	.443
197	4B2BC	55	.230	40	35	.244	45	25	820	2	B	.343
199	3D3B	50	.245	35	32	.239	45	25	336	1	G	.440
200	3C1T	30	.244	40	75	.245	40	25	428	1	G	.411
261	4E4T	70	.243	50	80	.240	45	25	559	2	B	--
263	2D4T	30	.244	45	40	.241	40	25	289	1	G	--

Notes: Fatigue Testing at R = .1 ; Failure Origin Coding in Figure 48 ; Cycles expressed in thousands

TABLE 12  
 MANUFACTURING, INSPECTION AND FATIGUE SUMMARY  
 Test Series No. 17, Ovality

Test No.	Specimen No.	Inspection Results						Fatigue Results				
		Hole 1			Hole 2			Max. Stress	Cycles	Failure Hole Origin	$a \beta$	
		Surf. Rough	Protru- sion	% Blue	Surf. Rough	Protru- sion	% Blue					
MINIMUM INTERFERENCE												
230	3A3B	125	.127	60	97	.129	60	22	91	2	F	.781
222	3D1B	122	.133	55	88	.128	60	22	132	1	F	.688
223	4D5BC	92	.132	65	105	.125	55	22	52	1	F	.935
227	2A3B	97	.129	60	105	.131	60	22	78	2	F	.822
264	5D6B	97	.128	60	92	.129	55	22	74	1	F	.834
229	4E4TC	87	.130	65	98	.135	65	25	66	1	F	.870
221	4B2TC	87	.123	70	105	.132	60	25	45	1	F	.976
225	4A4BC	122	.128	60	128	.134	60	25	61	1	F	.891
226	4D3B	97	.126	60	122	.132	55	25	44	2	F	.983
260	2A1B	130	.133	55	87	.126	60	25	276	2	F	.549

Notes: Fatigue Testing at R=.1 ; Failure Origin Coding in Figure 48 ; Cycles expressed in thousands

TABLE 13  
 MANUFACTURING, INSPECTION AND FATIGUE SUMMARY  
 Test Series No. 18, Burrs

Test No.	Specimen No.	Inspection Results					Fatigue Results					
		Hole 1		Hole 2			Max. Stress	Cycles	Failure Hole	Origin	e β	
		Surf. Rough	Protru- sion	% Blue	Surf. Rough	Protru- sion						% Blue
MINIMUM INTERFERENCE, WITH BURR												
58	5E3T	45	.118	80	40	.115	80	22	499	2	F	.453
46	5D6T	--	.110	70	--	.115	70	22	1,035	2	G	.367
62	5B4T	33	.110	80	30	.119	80	22	1,143	1	B	.359
66	5C2T	30	.115	70	35	.120	65	22	1,396	2	C	.336
45	2D6T	35	.114	70	35	.110	80	22	1,885	1	B	.307
MINIMUM INTERFERENCE, WITHOUT BURRS												
61	5A5T	25	.122	85	30	.112	90	22	121	2	F	.707
69	5B6C	40	.120	70	30	.108	75	22	548	2	F	.440
57	6A6CT	35	.114	70	40	.104	70	22	910	1	E	.381
65	6A6CB	35	.119	80	40	.111	80	22	1,014	1	G	.370
54	5E2T	35	.113	90	40	.111	70	22	1,118	1	F	.360

Notes: Fatigue Testing at R = .1 ; Failure Origin Coding in Figure 48; Cycles expressed in thousands

TABLE 13 (continued)  
 MANUFACTURING, INSPECTION AND FATIGUE SUMMARY  
 Test Series No. 18, Burrs

Test No.	Specimen No.	Inspection Results						Fatigue Results				
		Hole 1			Hole 2			Max. Stress	Cycles	Failure Hole Origin	$\alpha \beta$	
		Surf. Rough	Protru-sion	% Blue	Surf. Rough	Protru-sion	% Blue					
MAXIMUM INTERFERENCE, WITH BURR												
67	3A5T	60	.225	80	60	.233	80	22	469	1	F	.460
63	5E6T	45	.226	70	50	.221	70	22	555	1	G	.439
50	4A1T	63	.227	80	40	.227	80	22	1,504	1	F	.330
55	2B5T	45	.230	80	45	.230	80	22	1,536	1	B	.327
59	5B5CB	35	.230	80	35	.228	80	22	1,831	1	G	.310
MAXIMUM INTERFERENCE, WITHOUT BURR												
60	5E4B	60	.230	85	35	.240	65	22	638	2	G	.421
53	2A5B	55	.230	85	55	.231	80	22	842	1	G	.391
56	5C1CB	50	.218	70	50	.220	70	22	1,210	2	G	.308
64	5C6CB	40	.227	80	40	.226	85	22	1,819	2	G	.311
68	5C2B	40	.230	70	45	.224	85	22	4,071	2	G	.226

Notes. Fatigue Testing at R = .1 ; Failure Origin Coding in Figure 48 ; Cycles expressed in thousands

TABLE 14

MANUFACTURING, INSPECTION AND FATIGUE SUMMARY

Series No. 19

Test No.	Specimen No.	Inspection Results						Fatigue Results				
		Hole 1			Hole 2			Max. Stress	Cycles	Failure Hole	Origin	α β
		Surf. Roughness	Protru-sion	% Blue	Surf. Roughness	Protru-sion	% Blue					
SURFACE ROUGHNESS 100-125μ in, MINIMUM INTERFERENCE												
255	4A3TC	125	.110	70	105	.118	70	22	218	2	F	.588
256	2A5TC	102	.125	70	100	.105	75	22	128	2	F	.693
257	4A5B	98	.105	80	122	.120	75	22	1,061	1	B	.364
259	4A6T	98	.115	85	105	.110	75	22	10,078	2	E	--
258	4D5T	110	.120	85	100	.100	90	22	236	2	F	.574
SURFACE ROUGHNESS 100-125μ in, MAXIMUM INTERFERENCE												
250	4C2BC	117	.222	90	105	.210	85	22	428	1	G	.483
251	3C3B	120	.223	75	115	.230	80	22	379	2	G	.500
253	4E4BC	110	.235	75	105	.223	70	22	1,027	2	G	.369
252	4B5B	117	.214	90	115	.235	70	22	395	1	G	.495
254	2C6B	122	.235	75	102	.228	85	22	240	1	F	.571
SURFACE ROUGHNESS 100-125μ in, MINIMUM INTERFERENCE, SCRATCH												
266	4B5TC	115	.102	65	125	.131	70	22	167	1	F	.640
268	4B5BC	102	.122	85	105	.127	75	22	1,764	1	F	.314
270	3B3T	100	.114	80	100	.128	75	22	2,792	--	RO	--
274	4E1T	115	.123	80	117	.121	75	22	2,192	--	RO	--
275	4C6B	115	.116	75	122	.130	80	22	347	1	F	.513

Notes: Fatigue Testing at R = .1 ; Failure Origin Coding in Figure 48 ; Cycles expressed in thousands

MANUFACTURING, INSPECTION AND FATIGUE SUMMARY  
Test Series No. 19

Test No.	Specimen No.	Inspection Results						Fatigue Results				
		Hole 1			Hole 2			Max. Stress	Cycles	Failure Hole Origin	$\sigma/\beta$	
		Surf. Roughness	Protrusion	% Blue	Surf. Roughness	Protrusion	% Blue					
SURFACE ROUGHNESS 100-125 $\mu$ in, MAXIMUM INTERFERENCE, SCRATCH												
267	2C3B	125	.215	65	122	.208	70	22	396	2	G	.494
269	4A3B	120	.225	70	100	.228	75	22	336	1	G	.519
271	4D5B	113	.222	75	120	.220	70	22	259	1	G	.559
272	3D6T	105	.230	85	122	.222	80	22	486	2	B	.455
273	2E1B	113	.221	70	105	.200	65	22	809	2	B	.393
SURFACE ROUGHNESS 100-125 $\mu$ in, MINIMUM INTERFERENCE, RIFLING												
315	4E4T	103	.121	80	103	.116	80	22	315	2	F	.528
316	2D6B	115	.109	75	103	.115	80	22	1,025	1	E	.369
332	4D1B	103	.116	70	122	.120	75	22	208	1	E	.596
331	4D1T	105	.108	70	112	.111	75	22	350	2	F	.512
322	4C2TC	122	.122	70	127	.118	85	22	522	2	E	.447
SURFACE ROUGHNESS 100-125 $\mu$ in, MAXIMUM INTERFERENCE, RIFLING												
317	2B4B	105	.210	70	130	.212	70	22	435	2	G	.481
334	2E3B	115	.211	75	103	.217	70	22	261	1	F	.558
333	2D2B	115	.210	65	122	.211	70	22	389	1	G	.497
330	3C1B	122	.212	65	115	.205	75	22	676	1	G	.415
319	2A1T	125	.218	70	105	.205	80	22	1,051	1	B	.364

Notes: Fatigue Testing at R = .1 ; Failure Origin Coding in Figure 48; Cycles expressed in thousands

TABLE 14 (continued)  
 MANUFACTURING, INSPECTION AND FATIGUE SUMMARY  
 Test Series No. 19

Test No.	Specimen No.	Inspection Results				Max. Stress	Fatigue Results		α β			
		Hole 1		Hole 2			Cycles	Failure Hole Origin				
		Surf. Roughness	Protrusion	% Blue	Surf. Roughness	Protrusion	% Blue					
SURFACE ROUGHNESS 100-125 μ in., MINIMUM INTERFERENCE, OVALITY												
318	4C3T	100	.125	55	103	.110	60	22	217	2	F	.590
329	4E5B	105	.121	60	127	.112	65	22	166	1	F	.639
326	3C2T	105	.118	70	125	.112	65	22	123	2	F	.703
328	2B3T	103	.128	70	120	.110	65	22	276	1	F	.549
321	4B2B	105	.118	70	105	.110	75	22	143	1	F	.669
SURFACE ROUGHNESS 100-125 μ in., MAXIMUM INTERFERENCE, OVALITY												
324	2E4B	110	.215	65	110	.221	70	22	257	1	F	.560
325	2C1T	93	.219	60	93	.230	65	22	136	2	F	.680
327	2A2B	95	.220	60	105	.226	70	22	209	1	F	.595
323	3D5T	95	.225	55	105	.228	70	22	355	1	F	.510
320	4B1B	120	.220	55	103	.214	65	22	206	1	F	.599

Notes: Fatigue Testing at R = .1 ; Failure Origin Coding in Figure 48; Cycles expressed in thousands



TABLE 15

 $\alpha\beta$  FACTOR

DOGBONE PLUS STRAP TEST DATA							
Condition	Number of Data Points	$\alpha\beta$ (50, 50)*	Equiv. Cycles	$\alpha\beta$ (99, 50)*	Equiv. Cycles	$\alpha\beta$ (99, 95)*	Equiv. Cycles
Baseline	24	0.4571	483,000	0.8356	78,000	0.9078	58,600
Ovality	20	0.7047	122,000	1.205	20,600	1.2912	15,300
Scratch	8	0.4753	430,000	0.877	65,300	0.9661	48,000
Rifling	10	0.4699	440,000	0.7551	101,000	0.7834	91,000
Barrelling	20	0.7178	118,000	0.9141	57,000	0.9528	50,700
Perpendicular Deviation - 3°	19	0.4074	730,000	0.6281	170,000	0.6653	142,000
Bellmouthing	16	0.5047	350,000	1.122	27,700	1.2589	17,500

Equivalent cycles are based on Dogbone Plus Strap 22 ksi data

\*(Survival Probability, Confidence)

TABLE 16

## MANUFACTURING, INSPECTION AND FATIGUE SUMMARY

Test Series No. 20/21

Test No.	Specimen No.	Inspection Results						Fatigue Results				
		Hole 1			Hole 2			Max. Stress	Cycles	Failure Hole	Origin	$\alpha$ $\beta$
		Surf. Rough	Protru- sion	% Blue	Surf. Rough	Protru- sion	% Blue					
SURFACE ROUGHNESS 100-125 $\mu$ in, .0035 INTERFERENCE												
277	4D1BC/6C3BC	98	.155	90	103	.166	85	20.5	(7, 675)	--	Grip	--
276	2B2BC/3C2BC	120	.174	75	105	.173	85	20.5	2, 029	1	L	.409
281	6C3T/3C6TC	95	.162	90	117	.166	85	20.5	3, 745	1	B	.331
282	3C3BC/6B3BC	100	.173	80	100	.170	90	20.5	(1, 434)	--	Grip	--
283	3C3BC/4E3TC	95	.181	85	102	.182	80	20.5	(1, 865)	--	Grip	--
339	6C3B/2B5TC	105	.171	75	90	.172	70	20.5	3, 758	2	B	.330
340	3C4TC/3E5BC	113	.172	80	113	.158	70	20.5	1, 281	2	B	.471
336	6D3TC/2C5TC	105	.163	75	100	.168	75	20.5	(1, 061)	--	Over- load	--
313	3B2TC/3C6BC	115	.170	75	95	.175	75	20.5	1, 285	1	C	.470
358	3E2B/6B4T	100	.178	70	110	.176	75	20.5	8, 198	--	RO	--
SURFACE ROUGHNESS 100-125 $\mu$ in, .0035 INTERFERENCE, SCRATCH												
286	2A6TC/4E6BC	95	.170	65	105	.188	75	20.5	1, 852	2	B	.420
287	6B2B/6D6T	100	.174	70	115	.188	70	20.5	5, 059	1	B	.297
290	6C5TC/2B2TC	103	.188	75	95	.179	85	20.5	8, 381	--	RO	--
304	2D6BC/6B5T	110	.174	65	125	.186	85	20.5	8, 216	--	RO	--
301	2A3BC/6C1B	122	.185	75	100	.188	75	20.5	1, 150	1	B	.489
353	3D6TC/4D3TC	100	.184	85	100	.168	75	20.5	958	2	B	.516
343	4D4TC/2C2TC	100	.182	75	120	.177	70	20.5	6, 933	2	B	.261
341	6C1T/6C6B	100	.180	75	110	.175	85	20.5	849	1	B	.536
361	3C1BC/4D3BC	105	.166	80	100	.171	80	20.5	7, 574	--	RO	--
364	2D2TC/2A3TC	110	.175	75	98	.181	70	20.5	1, 448	1	B	--

Notes: Fatigue Testing at R=.1 Failure Origin Codes in Figure 48; Cycles expressed in thousands

TABLE 16 (continued)  
 MANUFACTURING, INSPECTION AND FATIGUE SUMMARY

Test Series No. 20/21

Test No.	Specimen No.	Inspection Results						Fatigue Results			$\alpha$	$\beta$	
		Hole 1			Hole 2			Max. Stress	Cycles	Failure Hole			Origin
		Surf. Roughness	Protru- sion	% Blue	Surf. Roughness	Protru- sion	% Blue						
SURFACE ROUGHNESS 100-125 u in, .0035 INTERFERENCE, RIFLING													
294	4A2TC/6D1TC	115	.175	75	110	.160	70	20.5	1,218	1	B	.480	
302	3A2BC/2A5BC	120	.168	70	98	.174	70	20.5	2,178	1	F	.398	
303	2D3BC/3E6T	98	.174	80	100	.168	70	20.5	4,698	2	L	.304	
310	3C1TC/6B1B	100	.165	75	103	.163	80	20.5	(384)	--	Over- load	--	
306	4D2BC/4D6BC	103	.174	70	125	.167	85	20.5	1,176	2	B	.485	
314	6C3TC/3D4BC	100	.176	75	110	.170	85	20.5	2,858	1	E	.363	
354	6D6BC/3B5BC	98	.160	75	93	.175	80	20.5	3,099	1	B	.353	
350	6B1T/6B6BC	113	.173	80	117	.160	85	20.5	2,194	2	B	.397	
365	3E1BC/2B3BC	90	.175	75	100	.158	75	20.5	8,066	--	RO	--	
344	3E6B/6C4T	100	.175	85	100	.160	70	20.5	8,784	--	RO	--	
SURFACE ROUGHNESS 100-125 u in, .0035 INTERFERENCE, OVALITY													
300	3E6BC/6B3TC	120	.164	60	103	.160	75	20.5	1,064	2	F	.500	
305	3E2BC/4B6TC	125	.177	70	110	.178	65	20.5	292	1	F	.760	
309	3E1T/6C1BC	97	.168	60	110	.178	60	20.5	1,153	2	H	.489	
308	3C5BC/2C3BC	110	.155	65	103	.178	60	20.5	2,240	2	C	.394	
307	3D2BC/3E2T	110	.168	70	97	.171	60	20.5	685	2	F	.573	
347	6D4TC/3A5BC	110	.168	65	100	.164	55	20.5	1,295	2	F	.469	
348	3A1BC/4C3BC	93	.178	60	100	.162	70	20.5	1,058	2	B	.501	
352	6B6T/2A2TC	100	.171	60	110	.171	65	20.5	1,799	1	B	.423	
362	3C3TC/3E4TC	110	.171	65	110	.170	70	20.5	3,089	2	B	--	
363	6B2T/3A4BC	110	.178	55	98	.169	65	20.5	1,400	2	C	--	

Notes: Fatigue Testing at R=.1 ; Failure Origin Coding in Figure 48 ; Cycles expressed in thousands

TABLE 17  
 MANUFACTURING, INSPECTION AND FATIGUE SUMMARY  
 Test Series No. 22

Test No.	Specimen No.	Inspection Results						Fatigue Results				
		Hole 1			Hole 2			Max. Stress	Cycles	Failure Hole	Origin	$\alpha \beta$
		Surf. Rough	Protru- sion	% Blue	Surf. Rough	Protru- sion	% Blue					
SURFACE ROUGHNESS 100-125 $\mu$ in, .0035 INTERFERENCE												
278	6D3BC/6B5TC	117	.168	65	100	.182	85	20.5	379	1	B	.567
279	3D3BC/3A4TC	100	.170	80	105	.179	85	20.5	265	2	B	.632
280	4B1TC/2B6BC	113	.177	80	100	.172	75	20.5	467	2	B	.534
284	2E3BC/3B3TC	100	.165	75	105	.158	85	20.5	498	2	G	.524
285	4C1TC/6D6TC	105	.170	80	100	.164	90	20.5	973	--	G	.431
311	6D5TC/6C4TC	110	.176	70	100	.182	70	20.5	205	2	B	.689
357	6B2BC/4C1BC	95	.158	70	90	.171	70	20.5	430	1	B	--
335	4C4TC/6D3T	95	.170	85	105	.180	80	20.5	(59)	--	Over- load	--
342	6C5B/3B5TC	115	.176	85	110	.183	85	20.5	538	1	G	.512
312	3C2TC/3D5BC	95	.168	75	110	.173	85	20.5	348	1	G	.580
SURFACE ROUGHNESS 100-125 $\mu$ in, .0035 INTERFERENCE, SCRATCH												
288	3D6BC/3C4BC	117	.174	70	98	.178	75	20.5	285	2	B	.616
289	6B4TC/2E4TC	115	.174	65	90	.176	75	20.5	376	1	B	.568
291	3E6TC/2E2TC	100	.172	70	100	.168	70	20.5	645	2	G	.486
292	3B3BC/2B3TC	98	.177	65	115	.185	75	20.5	230	2	B	.661
293	2B1BC/6B3B	100	.188	80	100	.184	80	20.5	438	2	B	.543
351	6D6B/6C4BC	100	.182	75	110	.174	70	20.5	377	1	G	.568
356	3B4BC/4A1BC	110	.166	75	100	.176	80	20.5	524	1	G	--
355	6D5T/6B1BC	93	.174	70	103	.166	80	20.5	712	2	G	--
338	6D3B/4A5BC	100	.171	75	110	.174	80	20.5	298	1	B	--
337	2A1BC/4E5BC	115	.180	75	105	.178	75	20.5	479	1	H	.530

Notes: Fatigue Testing at R=, .33; Failure Origin Coding in Figure 48; Cycles expressed in thousands

TABLE 17 (continued)  
 MANUFACTURING, INSPECTION AND FATIGUE SUMMARY  
 Test Series No. 22

Test No.	Specimen No.	Inspection Results				Fatigue Results						
		Surf. Roughness	Hole 1 Protru-sion	% Blue	Surf. Roughness	Hole 2 Protru-sion	% Blue	Max. Stress	Cycles	Failure Hole Origin	$\alpha$	$\beta$
SURFACE ROUGHNESS 100-125 $\mu$ in, .0035 INTERFERENCE, OVALITY												
295	4A1TC/6C6TC	110	.178	70	100	.158	60	20.5	216	2	J	.675
296	4B1BC/2C4TC	103	.160	75	103	.164	65	20.5	269	2	B	.628
297	4E2BC/3E4T	105	.174	65	100	.162	55	20.5	288	2	G	.615
298	2B5BC/6C5BC	100	.185	60	125	.165	65	20.5	330	1	F	.590
299	6C6BC/6B2TC	110	.180	60	110	.177	55	20.5	621	2	G	.492
346	6C4B/3A5TC	100	.160	65	110	.173	70	20.5	103	1	F	.870
360	6D5BC/2D6TC	110	.165	75	90	.160	70	20.5	272	1	F	--
345	3B1BC/4E3BC	100	.172	75	100	.171	65	20.5	(534)	--	Over-load	--
359	4C6BC/2C2BC	105	.162	60	100	.168	65	20.5	240	1	J	--
349	4B6BC/4C4BC	90	.160	65	90	.174	60	20.5	283	1	J	.617

Notes: Fatigue Testing at R = .33; Failure Origin Coding in Figure 48; Cycles expressed in thousands

TABLE 18

 $\alpha\beta$  FACTOR

REVERSE DOGBONE TEST DATA							
<u>Condition</u>	<u>Number of Data Points</u>	$\alpha\beta$ (50, 50)*	<u>Equiv. Cycles</u>	$\alpha\beta$ (99, 50)*	<u>Equiv. Cycles</u>	$\alpha\beta$ (99, 95)*	<u>Equiv. Cycles</u>
<u>Test Series 20/21</u>							
Baseline	5	0.3981	2,000,000	0.6683	440,000	0.7499	300,000
Ovality	8	0.5035	1,000,000	0.871	200,000	1.0209	125,000
Scratch	6	0.4055	2,000,000	0.9594	140,000	1.1376	85,000
Rifling	7	0.3926	2,000,000	0.6383	500,000	0.6776	400,000
<u>Test Series 22</u>							
Baseline	8	0.5585	700,000	0.8279	222,000	0.867	195,000
Ovality	7	0.6368	490,000	0.9977	125,000	1.122	85,000
Scratch	8	0.5715	700,000	0.7551	300,000	0.7834	270,000
<u>Test Series 20/21 Combined</u>							
Baseline	13	0.4873	1,100,000	0.8874	175,000	0.9532	140,000
Ovality	15	0.5623	700,000	0.9908	125,000	1.0544	125,000
Scratch	14	0.4955	1,000,000	0.9462	140,000	1.1455	85,000
Rifling	7	0.3926	2,000,000	0.6383	500,000	0.6776	400,000

\*(Survival Probability, Confidence)

Equivalent cycles based on reverse dogbone 20.5 ksi

Max. stress R = 0.1, Figure 81

TABLE 19

 $\alpha\beta$  FACTOR

COMBINED DATA							
Test Series 2, 7, 8, 17, 18, 19, 21, 22							
Condition	Number of Data Points	$\alpha\beta$ (50, 50)*	Equiv. Cycles	$\alpha\beta$ (99, 50)*	Equiv. Cycles	$\alpha\beta$ (99, 95)*	Equiv. Cycles
Baseline	37	0.4685	472,000	0.8344	75,000	0.8790	65,000
Ovality	35	0.6396	162,000	1.162	24,200	1.2215	19,500
Scratch	22	0.4869	396,000	0.8839	63,700	1.0261	39,000
Rifling	17	0.4368	576,000	0.7112	120,000	0.7471	104,000
Barrelling	20	0.7178	117,000	0.9141	57,200	0.9528	50,500
Perpendicular Deviation - 3°	19	0.4074	727,000	0.6281	169,000	0.6653	145,000
Bellmouthing	16	0.5047	349,000	1.122	27,700	1.2589	17,300
Baseline with Burr Data	57	0.4313	570,000	0.8024	85,000	0.8562	66,000

Equivalent cycles are based on Dogbone Plus Strap 22 ksi data

\* (Survival Probability, Confidence)

TABLE 20  
SUMMARY OF LOAD TRANSFER DATA  
ON DOGBONE/STRAP SPECIMENS

Test Series	Test No.	% Load Transfer				
		Start	Quarter Life	Half Life	Last Reading	Nominal
2 - Interference Level: .0005"	51	13	14	14	13	13
	52	12	13	14	14	13
	.0023"	73	14	14	14	14
		75	14	14	14	13
	.0035"	42	15	15	14	15
		44	14	14	15	15
	.0048"	82	14	13	14	14
		87	14	14	14	14
	.0060"	81	14	14	14	14
		99	14	14	14	14
7 - Perpendicularity Min. Int.	185	14	14	14	14	14
	213	13	14	14	--	14
	Max. Int.	187	13	14	14	13
		242	13	14	14	14
8 - Barrelling Min. Int.	166	12	14	14	13	13
		182	14	14	14	14
	Max. Int.	167	14	14	14	14
		181	14	14	14	13
Bellmouthing Min. Int.	240	12	14	14	14	14
		241	13	14	14	14
	Max. Int.	183	14	14	14	14
		197	14	14	Gage Out	14



TABLE 20 (continued)  
 SUMMARY OF LOAD TRANSFER DATA  
 ON DOGBONE/STRAP SPECIMENS

Test Series	Test No.	% Load Transfer					
		Start	Quarter Life	Half Life	Last Reading	Nominal	
17 - Ovality	Min. Int.	229	13	14	14	14	14
		230	13	14	14	14	14
19 - Combined Variables							
100-125 AA	Min. Int.	258	14	15	15	15	15
	Max. Int.	254	14	14	14	14	14
100-125 AA with Scratch							
	Min. Int.	275	14	15	15	14	14
	Max. Int.	273	14	14	15	15	15
100-125 AA with Rifling							
	Min. Int.	322	14	14	14	14	14
	Max. Int.	319	14	14	14	14	14
100-125 AA with Ovality							
	Min. Int.	321	13	14	14	14	14
	Max. Int.	320	14	15	15	15	15

TABLE 21  
SUMMARY OF LOAD TRANSFER DATA  
ON REVERSE DOGBONE SPECIMENS

Test Series	Test No.	% Load Transfer				
		Start	Quarter Life	Half Life	Last Reading	Nominal
20/21 Combined Variables*						
Baseline	276	2.5	2.5	2.4	1.9	2.4
	277	1.6	2.0	2.5	4.8	2.5
	281	1.3	2.2	4.4	4.6	4
	282	.7	4.2	4.3	--	4
	283	3.0	5.2	5.2	--	5
	313	3.7	1.4	1.2	1.2	1.5
	336	5.7	2.4	5.4	5.8	5
	339	2.5	3.2	1.9	1.7	2.5
	340	3.1	3.5	4.1	4.5	4
	358	2.6	3.9	4.2	4.0	4
Scratches	286	5.4	5.4	5.4	6.2	5.5
	287	1.4	1.1	2.9	1.7	2
	290	1.6	2.8	3.2	1.9	2
	301	1.0	2.4	--	--	--
	304	.7	1.3	1.0	3.4	1
	341	2.1	3.8	2.0	--	2
	343	1	2	2.4	2.2	2
	353	.8	--	--	--	--
	361	2.4	--	4.1	5.6	4
	364	3.5	4.3	4.8	4.9	4

\*All tests at 100-125 AA finish and mid-spec interference (.0035")

TABLE 21 (continued)

SUMMARY OF LOAD TRANSFER DATA  
ON REVERSE DOGBONE SPECIMENS

Test Series	Test No.	% Load Transfer				
		Start	Quarter Life	Half Life	Last Reading	Nominal
20/21 Combined Variables*						
Rifling	294	4.8	5.9	6.0	--	6
	302	2.3	1.6	1.1	1.6	1.5
	303	1.6	2.5	3.4	3.5	3
	306	1.7	3.1	--	--	--
	310	1.9	2.9	--	--	--
	314	1.9	3.0	2.3	1.9	2
	344	2.1	3.3	2.7	4.5	3
	350	2.4	3.9	4.0	4.4	4
	354	1.1	2.9	2.3	1.1	2
	365	2.5	4.5	3.9	4.5	4
Ovality	300	1.6	3.6	--	--	--
	305	.7	4.0	--	--	--
	307	1.2	3.6	3.6	3.5	3
	308	.7	2.5	1.0	0.9	1
	309	0	--	--	--	--
	347	2.6	4.2	5.4	--	4
	348	2.0	5.2	5.4	--	4
	352	1.8	3.0	2.5	3.0	3
	362	3.7	6.3	5.9	5.7	5
	363	2.9	3.6	5.2	5.1	5

\*All tests at 100-125 AA finish and mid-spec interference (.0035")

TABLE 21 (continued)  
 SUMMARY OF LOAD TRANSFER DATA  
 ON REVERSE DOGBONE SPECIMENS

Test Series	Test No.	% Load Transfer				
		Start	Quarter Life	Half Life	Last Reading	Nominal
22 Combined Variables*						
Ovality	295	1.7	--	--	--	--
	296	1.4	2.5	3.7	3.7	3
	297	.5	1.8	1.6	1.8	1.5
	298	1.0	2.1	2.8	--	2
	299	1.7	1.9	1.7	4.5	2
	345	1.9	2.8	1.9	--	--
	346	1.6	--	--	--	--
	349	1.4	2.1	2.8	2.4	2
	359	5.3	7.2	7.1	7.2	7
	360	4.3	4.7	4.7	5.3	5

\*All tests at 100-125 AA finish and mid-spec interference (.0035")

TABLE 21 (continued)  
SUMMARY OF LOAD TRANSFER DATA  
ON REVERSE DOGBONE SPECIMENS

Test Series	Test No.	% Load Transfer				
		Start	Quarter Life	Half Life	Last Reading	Nominal
22 Combined Variables*						
Baseline	278	2.8	3.2	2.6	2.6	2.7
	279	4.7	4.8	4.7	4.6	4.7
	280	2.0	2.0	2.0	2.0	2.0
	284	3.4	3.0	2.7	3.0	3
	285	2.4	4.6	4.3	2.2	3
	311	1.3	2.2	4.5	--	--
	312	3.3	2.7	2.5	2.5	3
	335	4.7	3.2	4.5	4.5	4
	342	7.8	7.8	8	8.5	8
	357	4.8	6.4	6.6	6.3	6
Scratches	288	2.9	3.7	3.6	2.6	3
	289	2.8	3.1	3.9	--	3
	291	2.3	4.2	4.3	2.6	3
	292	2.3	3.9	5.4	--	4
	293	1.4	2.0	2.2	2.9	2
	337	6.1	4.4	2.8	--	4
	338	4.1	2.9	5.4	5.7	5
	351	4.1	5.1	6.7	6.5	5
	355	4.9	6.1	6.8	--	6
	356	5.1	5.9	6.7	6.5	6

\*All tests at 100-125 AA finish and mid-spec interference (.0035")

TABLE 22

FATIGUE PRECRACKING RESULTS

<u>Test No.</u>	<u>Specimen No.</u>	<u>Test Series</u>	<u>Specimen Type*</u>	<u>Max. Stress (ksi)</u>	<u>Fatigue Cycles (<math>\times 10^3</math>)</u>	<u>Surface Crack Length, a (in.)</u>
177	3C3T	4	OH	16.5	55	.0858
178	5A2T	4	OH	16.5	48	.0806
179	5B1CT	4	OH	16.5	43	.0689
168	4E3T	5	ZLT	22	22	.0657
172	5B1B	5	ZLT	22	16	.0654
173	3B6B	5	ZLT	22	19	.0791
169	3D5B	6	LLT	22	16	.0779
170	3D4B	6	LLT	22	21	.086
175	4C2T	6	LLT	22	23	.0866

\* All specimens were precracked as open hole (3/16 in. dia.) specimens. Specimen type refers to specimen geometry for testing subsequent to precracking.

TABLE 23

CYCLIC LIFE RESULTS, PRECRACKED SPECIMENS

<u>Test No.</u>	<u>Specimen No.</u>	<u>Initial Crack Length, a (in.)</u>	<u>Stress (ksi)</u>	<u>Freq. Hz</u>	<u>Cyclic Life (x 10<sup>3</sup>)</u>
SERIES 4, OPEN HOLE					
233	5B1CT	.012	16.5	(a)	70
243	5A2T	.024	16.5	(a)	43
244	3C3T	.029	16.5	(a)	37
SERIES 5, ZERO LOAD TRANSFER					
217	5B1B	.008	22	30	28
218	4E3T	.009	22	30	38
231	3B6B	.022	22	30	30
SERIES 6, LOW LOAD TRANSFER					
219	3D5B	.021	22	30	28
220	3D4B	.029	22	30	24
232	4C2T	.030	22	30	36

Test crack size  $\pm$  .002 in.

(a) da/dn crack growth data taken. Frequency varied from 5 to .5 Hz.

TABLE 24

FATIGUE CRACK PROPAGATION RESULTSOPEN HOLE SPECIMENS - SERIES 4

16.5 ksi max. stress, 0.5-5 Hz cyclic frequency

<u>Specimen No.</u>	<u>Crack Length, a (in.)</u>	<u>Fatigue Cycles (x 10<sup>3</sup>)</u>
5B1CT	.113	36.5
	.128	38.5
	.131	39.3
	.134	39.5
	.136	40.0
	.137	40.1
	.142	40.4
	.148	40.7
	.150	43.7
	.169	44.0
	.170	44.3
	.183	45.7
	.184	48.1
	.198	49.5
	.209	53.5
	.213	54.2
	.219	54.8
	.232	55.4
	.243	56.0
	.246	56.5
	.267	57.0
	.277	58.2
	.294	58.9
	.299	59.5
	.303	60.0
	.328	60.5
.341	61.0	
.362	62.0	
.377	62.5	
.395	63.0	
.398	63.5	
.415	64.0	
.444	65.0	
.500	66.5	



TABLE 24 (continued)

<u>Specimen No.</u>	<u>Crack Length, a (in.)</u>	<u>Fatigue Cycles (<math>\times 10^3</math>)</u>
5B1CT	.540	67.5
	.561	68.0
	.603	68.5
	.608	68.9
	.632	69.25
	.650	69.4
	.673	69.65
	.755	70.05
		70.948 (fracture)
	5A2T	.112
.142		23.5
.151		24.5
.167		25.46
.185		26.42
.201		27.32
.201		27.85
.213		28.4
.238		29.6
.260		30.65
.281		31.38
.296		32.25
.316		33.06
.346		34.0
.365		34.81
.392		35.5
.415		36.23
.445		36.91
.458		37.45
.487		38.03
.504		38.43
.524		38.82
.548		39.28
.568		39.63
.584		39.9
.610		40.13
.630		40.4
.653	40.63	
.679	40.84	
.701	40.96	
	42.81 (fracture)	

TABLE 24 (continued)

<u>Specimen No.</u>	<u>Crack Length, a (in.)</u>	<u>Fatigue Cycles (x 10<sup>3</sup>)</u>
3C3T	.147	18.4
	.153	19.3
	.164	20.5
	.182	21.5
	.205	22.72
	.223	23.48
	.244	24.46
	.264	25.5
	.274	26.2
	.299	27.5
	.351	28.5
	.359	29.38
	.367	30.07
	.388	30.5
	.428	31.5
	.466	32.5
	.499	33.4
	.536	34.0
	.574	34.5
	.609	35.0
	.653	35.4
	.676	35.62
		36.9 (fracture)

A P P E N D I X

	<u>Page</u>
MANUFACTURE OF STRAP SPECIMENS	192
STATISTICAL EVALUATION OF FATIGUE TEST DATA	195
AGARD SMP SUBCOMMITTEE ON CRITICALLY LOADED HOLE TECHNOLOGY	200
EVALUATION OF TAPERED BLADE CUTTER	225

**MANUFACTURE OF STRAP SPECIMENS**

## MANUFACTURE OF STRAP SPECIMENS

### OPERATION SHEET

1. Insert strap and clamp specimen in drilling fixture.
2. Center drill (#2) two holes.
3. Drill (19/64 in. dia.) two holes.
4. Taper ream and countersink (Omark drill-reamer).
5. Check depth of countersink with flushness gage.
6. Check protrusion using fastener and tag fastener with the hole number.
7. Check perpendicularity using same fasteners.
8. Remove specimen from drilling fixture and wipe off chips and cutting fluid with naphtha and wipe with dry rag.
9. Reposition strap on specimen and press fasteners firmly into holes to locate strap.
10. Clamp specimen in inspection fixture and remove fasteners.
11. Visually inspect each hole.
12. Measure hole surface finish (Clevite Surfanalyzer 7100 System).
13. Insert capacitance gage probe in each hole and record gage setting (Omark capacitance gage).
14. Insert air gage probe in each hole and rotate probe recording high and low readings at each orifice location.
15. Perform blueing check on each hole (Prussian blue).
16. Remove blueing from holes and wipe specimen surfaces with a naphtha soaked rag then wipe with a clean dry rag.

17. Apply sealant (STM40-112, Class B-12) to fay surfaces at each end of strap and to hole surfaces.
18. Apply sealant (STM 40-112, Class B-12) to fasteners.
19. Position strap and install fasteners.
20. Torque fasteners to 80% of specified torque and let stand for 30 minutes.
21. Torque fasteners to specified torque.
22. Store specimens for 120 hours or until sealant is tack free.
23. Specimen is now ready for test.

STATISTICAL EVALUATION OF FATIGUE TEST DATA

## Notation

P	Probability
$P_F$	Probability of failure
$P_S$	Probability of survival ( $1 - P_F$ )
$n_S$	Number of specimens in test series
N	Dependent variable (load cycles to failure, cyclic test hours, events, etc.)
X	Logarithmic transformation of dependent variable (Log N)
u	Standardized variate in normal distribution function
$\phi(u)$	Standardized normal distribution function
i	Order ranking subscript
$t_c$	Number of standard deviations corresponding to specified confidence level

The following equivalence relations between probability and normal distribution function values are used in the following analysis:

$$P = \phi(u_p), \quad P \geq .5; \quad u_p \geq 0$$

$$u_p = \phi^{-1}(P), \quad u_p \geq 0; \quad P \geq .5$$

## Analysis

Consider a test series of  $n_S$  identical specimens. The probability of failure is

hence 
$$P_{Fi} = i / (n_S - 1) \quad (1)$$

$$P_{Si} = 1 - P_{Fi} = 1 - i / (n_S - 1) \quad (2)$$



The test and computed data can be displayed in a table as shown below:

<u>Failure Rank Order No.</u>	<u>Dependent Variable</u>	<u>Log Ni</u>	<u>Probability of Survival</u>	<u>Standardized Variate</u>
i	N <sub>i</sub>	X <sub>i</sub>	P <sub>Si</sub>	u <sub>Si</sub>
1 low	--	--	--	--
2	--	--	--	--
.	--	--	--	--
.	--	--	--	--
n <sub>S</sub> high	--	--	--	--

We compute next quantities required for linear regression analysis:

$$\bar{X} = \frac{1}{n_S} \sum_{i=1}^{i=n_S} X_i \quad (3)$$

$$S_X = \left[ \left( \frac{1}{n_S} \sum_{i=1}^{i=n_S} X_i^2 \right) - \bar{X}^2 \right]^{1/2} \quad (4)$$

$$\bar{u}_S = \frac{1}{n_S} \sum_{i=1}^{i=n_S} u_{Si} \quad (5)$$

$$S_U = \left[ \left( \frac{1}{n_S} \sum_{i=1}^{i=n_S} u_{Si}^2 \right) - \bar{u}_S^2 \right]^{1/2} \quad (6)$$

$$C_{XU} = \left[ \left( \frac{1}{n_S} \sum_{i=1}^{i=n_S} X_i u_{Si} \right) - \bar{X} \bar{u}_S \right] \quad (7)$$

$$r_{xu} = \left[ \text{CXU}, S_x S_u \right] \quad (8)$$

$$E_{S_x} = S_x \left[ (1 - r_{xu}^2) n_S / (n_S - 1) \right]^{1/2} \quad (9)$$

$$E_{S_u} = S_u \left[ (1 - r_{xu}^2) n_S / (n_S - 1) \right]^{1/2} \quad (10)$$

The quantity  $r_{xu}$  (equation 8) is the sample correlation coefficient

### Application of Data

The data developed in equations (3) through (10) can be used in two different ways.

- (1) To determine with specified confidence the value of the dependent variable which corresponds to a given probability of survival.

The number of normalized standard deviations which corresponds to the probability of survival  $P_S$  is

$$u_{S_r} = \phi^{-1} (P_S) \quad (11)$$

The number of standard errors of the estimate which corresponds to the specified confidence level  $P_c$  is

$$t_c = \phi^{-1} (P_c) \quad (12)$$

We have then

$$\text{LOG } N_r = X_{S_r} = S_x/S_u \cdot r_{xu} (u_{S_r} - \bar{u}_S) + \bar{X} - t_c E_{S_x} \quad (13)$$

- (2) To determine with specified confidence the probability of survival which corresponds to a given value of the dependent variable  $N$ ,  $X_N = \text{LOG } N$ .

The number of normalized standard deviations which corresponds to the unknown probability of survival  $P_{S_n}$  is

$$P_{S_n} = \phi(u_N) \quad (14)$$

We have then

$$u_N = S_u/S_x \cdot r_{xu} (X_N - \bar{X}) + \bar{u}_S - t_c E_{S_u} \quad (15)$$

AGARD SMP SUBCOMMITTEE ON CRITICALLY LOADED HOLE TECHNOLOGY

## INTRODUCTION

A pilot program has been initiated by the AGARD SMP Subcommittee on Critically Loaded Hole Technology in an effort to promote a mutual confidence in fatigue test data generated by participating countries. The successful completion of the program will lead to a more uniform quality of fatigue testing and evaluation of critically loaded hole parameters among its participants. The objectives of the three-phase program are as follows:

- Phase I:           Generate baseline open hole fatigue data in order to examine laboratory-to-laboratory variations
  
- Phase II:          Reaffirm the exchangeability of baseline data and investigate the effect of hole quality on open hole fatigue specimens
  
- Phase III:         Conduct independent fatigue evaluations of various fatigue improvement fasteners and exchange data.

Participants in the program included representatives from Belgium, France, Germany, Italy, Netherlands, Sweden, Turkey, United Kingdom, and the United States. All specimens for the program were prepared by Metcut Research Associates Inc. from a single heat of 7050 material procured from Alcoa in the form of 7050-T76 bare sheet, 0.196 in. (5 mm) thick. Battelle's Columbus Laboratories (BLC) were designated as the USA testing facility.

The report contained herein details the results of the Phase I effort.

## MANUFACTURE OF SPECIMENS

The material for the AGARD SMP Critically Loaded Hole Technology Program was 7050-T76 aluminum alloy. This material was received in sheets approximately .196 in. x 44.5 in. x 96 in. The chemical composition and mechanical properties, as supplied by the production facility (Aluminum Company of America), are given in Table A1.

Because the specimens were tested in the as-received or as-milled condition the sheets of aluminum alloy were procured with protective coating on each side to prevent scratching or other surface blemishes during shipment. A sketch showing the layout of the specimens is shown in Figure A1. The blanks were cut out per the sketch using a Grob bandsaw cutting at approximately 300 ft. per minute. After cutout, the edges were milled using the conditions given in Table A2. This was followed by contouring of the gage section per the conditions in Table A3. The hole located in the center of the gage section was produced in a three-step operation:

- Step 1: Drill at 660 rpm, .002 in. per revolution, 7/32 in. diameter hole
- Step 2: Ream at 660 rpm, hand feed, .243 in. diameter hole
- Step 3: Ream at 660 rpm, hand feed, .251 in. diameter hole

After drilling, the edges of the hole and gage area were radiused using a carbide form cutter having a 1/32 in. radius. This operation was followed by longitudinal polishing of the edges of the gage area and was accomplished by use of 180 grit aluminum oxide paper. The specimens were then packaged for shipment to the participants as specified in Table A4. Each country received the specimens, a letter and a packing slip identifying their specimens.

Residual stress readings were taken on the surfaces of three sample holes. (A sample hole was reamed in a coupon following the reaming of each specimen hole in order to duplicate the type hole in each specimen). Three of these holes (Nos. 10, 50 and 90) were used for surface stress identification.

Residual stress measurements by the x-ray diffraction method were required on the circumference of three holes that had been drilled and double reamed in a 7050-T76 aluminum test coupon. The determinations were made at a point at the mid-thickness of the coupon in the tangential direction with

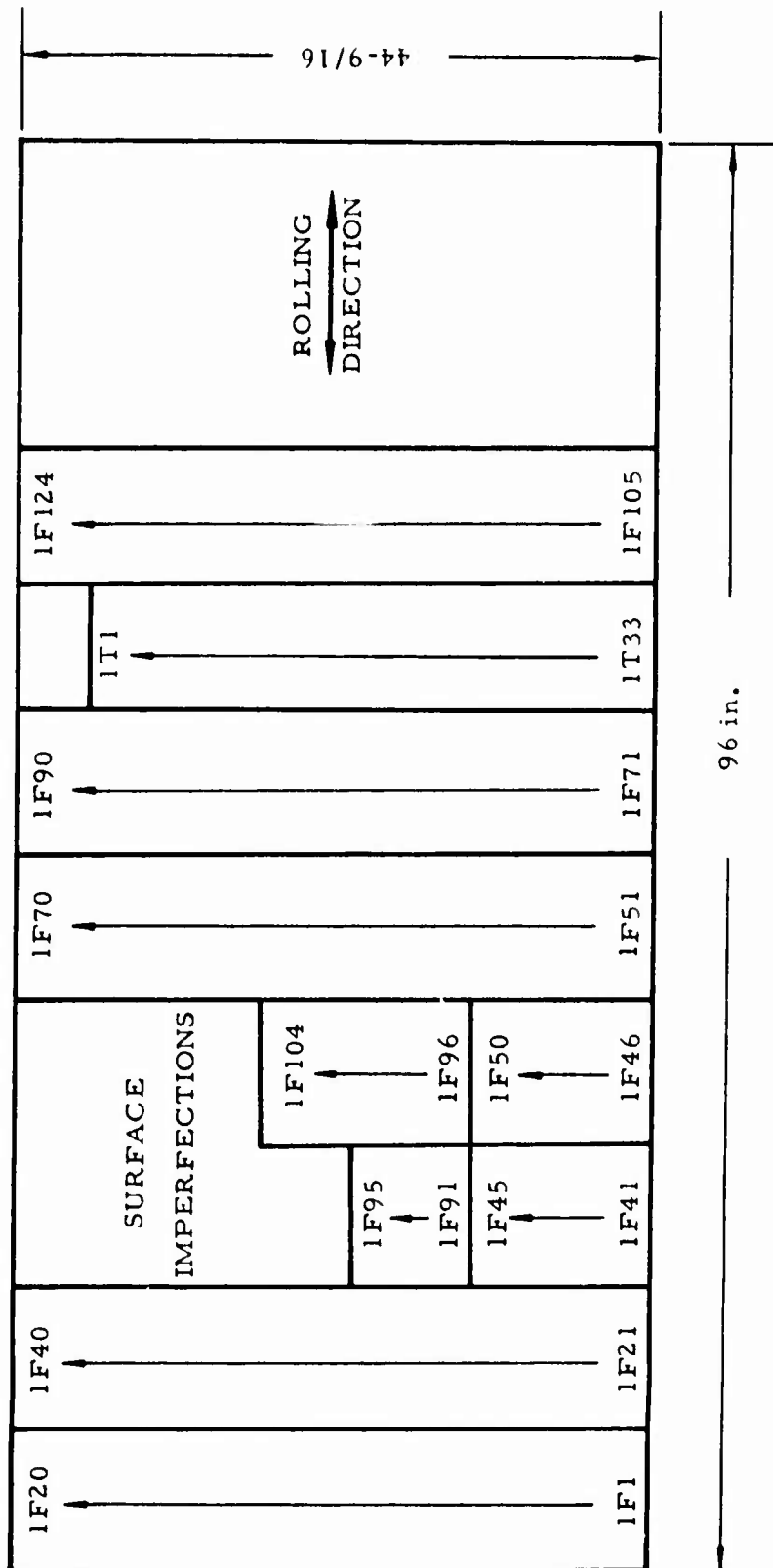


Figure A1 - AGARD SMP CRITICALLY LOADED HOLE TECHNOLOGY SPECIMEN LOCATION

respect to the hole periphery. In order to make these measurements, a wedge containing approximately 120 degrees of the hole periphery was sectioned from each coupon.

The size of the incident x-ray beam used to measure the stresses was approximately 0.1 x 0.1 inches. The value of the elastic constant  $E/(1 + \nu)$  in the direction normal to the (311) plane was obtained previously by calibration for 7075-T76 aluminum, an alloy similar to 7050-T6 in chemical composition and mechanical properties. Determination of the single crystal elastic properties for 7050-T6 aluminum alloy was outside the scope of this investigation.

Residual stresses measured in the three holes are listed below. Compressive stresses are reported as negative values.

<u>Hole No.</u>	<u>Residual Stress (x 10<sup>3</sup>psi)</u>
10	-5.8
50	-9.4
90	-5.6

Due to the limited scope of this stress analysis, the stress relaxation resulting from the sectioning of the test coupons was not monitored. Because of general systematic errors, the large beam size, and the lack of stress relaxation data, the measured stresses do not necessarily represent the total residual stress present in the holes before sectioning. Since the same measurement procedures were used on each sample, a relative comparison of results is considered to be meaningful.

The information obtained is contained in Figures A2, A3 and A4.



METCUT RESEARCH ASSOCIATES INC.  
CINCINNATI, OHIO

FIVE POINT PARABOLIC DIFFRACTION PEAK STRESS ANALYSIS

097C-22800 1 7708.29 HOLE #10,CIP,SURF

PSI	2 THETA	TIME	COR. TIME	D (A)	VERTEX +- ST.DEV.
0.000	138.400	120.730	244.982		
	138.500	114.950	231.834		
	138.900	102.670	204.600		
	139.100	116.720	236.511		
	139.300	121.400	247.527	1.22359	138.8273 +-0.0067
45.000	138.500	100.080	123.300		
	138.600	94.160	115.486		
	138.900	85.520	104.538		
	139.300	95.840	119.457		
	139.400	100.950	126.798	1.22319	138.9273 +-0.0069

E/(1+V) = 8830. +- 71. (KSI) STRESS = -5.8 +- 0.8 (KSI)

DELTA D = -0.00040 (A) STRAIN = -0.000327 (IN./IN.)

Figure A2 - PARABOLIC DIFFRACTION PEAK STRESS ANALYSIS OF HOLE 10

FIVE POINT PARABOLIC DIFFRACTION PEAK STRESS ANALYSIS

0970-22800 1		7708.29 HOLE #50, CIR, SURF			
PSI	Z THETA	TIME	COR. TIME	D (A)	VERTEX +- ST.DEV.
0.000	138.400	175.380	379.461		
	138.600	158.290	335.832		
	138.900	143.490	299.574		
	139.300	157.760	335.549		
	139.400	179.100	391.016	1.22328	138.9058 +-0.0056
45.000	138.600	115.120	144.537		
	138.700	108.290	135.197		
	139.000	99.410	123.642		
	139.400	105.330	132.947		
	139.600	116.930	150.133	1.22263	139.0696 +-0.0078
E/(1+V) = 8830. +- 71. (KSI)		STRESS = -9.4 +- 0.8 (KSI)			
DELTA D = -0.00065 (A)		STRAIN = -0.000534 (IN./IN.)			

Figure A3 - PARABOLIC DIFFRACTION PEAK STRESS ANALYSIS OF HOLE 50

METCUT RESEARCH ASSOCIATES INC.  
CINCINNATI, OHIO

FIVE POINT PARABOLIC DIFFRACTION PEAK STRESS ANALYSIS

0970-22800 1 7708.29 HOLE #90, CIR, SURF

PSI	2 THETA	TIME	COR. TIME	D (A)	VERTEX +- ST.DEV.
0.000	138.300	229.860	532.280		
	138.400	219.490	501.738		
	138.900	198.630	443.228		
	139.200	221.280	508.816		
	139.400	232.770	543.739	1.22363	138.8183 +-0.0078
45.000	138.300	143.920	185.626		
	138.400	133.190	170.010		
	139.000	110.580	139.262		
	139.400	129.830	168.485		
	139.600	147.040	195.457	1.22325	138.9144 +-0.0060
E/(1+V) = 8830. +-		71. (KSI)		STRESS = -5.6 +- 0.8 (KSI)	
DELTA D = -0.00038 (A)		STRAIN = -0.000314 (IN./IN.)			

Figure A4 - PARABOLIC DIFFRACTION PEAK STRESS ANALYSIS OF HOLE 90

## GENERATION OF THE FALSTAFF SPECTRUM

In order to insure that all participants apply the same cyclic loads, each country was to test specimens under the FALSTAFF (Fighter Aircraft Loading STAndard for Fatigue) This spectrum was developed in Europe and is in common use among the AGARD participants in this program.

The BCL fatigue load control program was generated using the computer program detailed in the definitive description of the FALSTAFF spectrum, dated March 1976. The flight-by-flight load steps were generated on the BCL CDC 6400 main computer and stored on magnetic tape. The load steps were also printed out and checked carefully against the above noted FALSTAFF description. Zero load was defined to be at load step 7.5269 of the 32 available load steps. A second magnetic tape was generated (compatible with the fatigue laboratory's Hewlett Packard 2100 computer) converting the loadsteps to percentages of full-scale load. This information was also stored on the laboratory computer disc unit.

### PROGRAM CONTROL

This section describes the BCL system and equipment used to apply and control FALSTAFF program loads. In general, the HP 2100 computer provides load steps to a hybrid unit which generates a constant ramp rate function for the MTS 20,000-pound (88,960 N) closed-loop electrohydraulic fatigue machine. A null pacing unit makes a constant comparison of programmed load to load cell output and signals the hybrid unit when the programmed load has been reached, at which time the ramp direction is reversed and a new load is called from the computer. This procedure continues until a preprogrammed number of flights has been reached or until the test specimen fails. A graphic presentation of the program control cycle is presented in Figure A5. A secondary computer subrouting, STATS, makes it possible to determine the flight number, total number of cycles, and percent of a pass through the spectrum completed at the moment of questioning.

### Pretest Checks

Prior to initiating the fatigue test program, a spare specimen (without a hole in the test section) was instrumented with two strain gages located near the specimen edge on each face of the specimen. The output of the four strain gages made

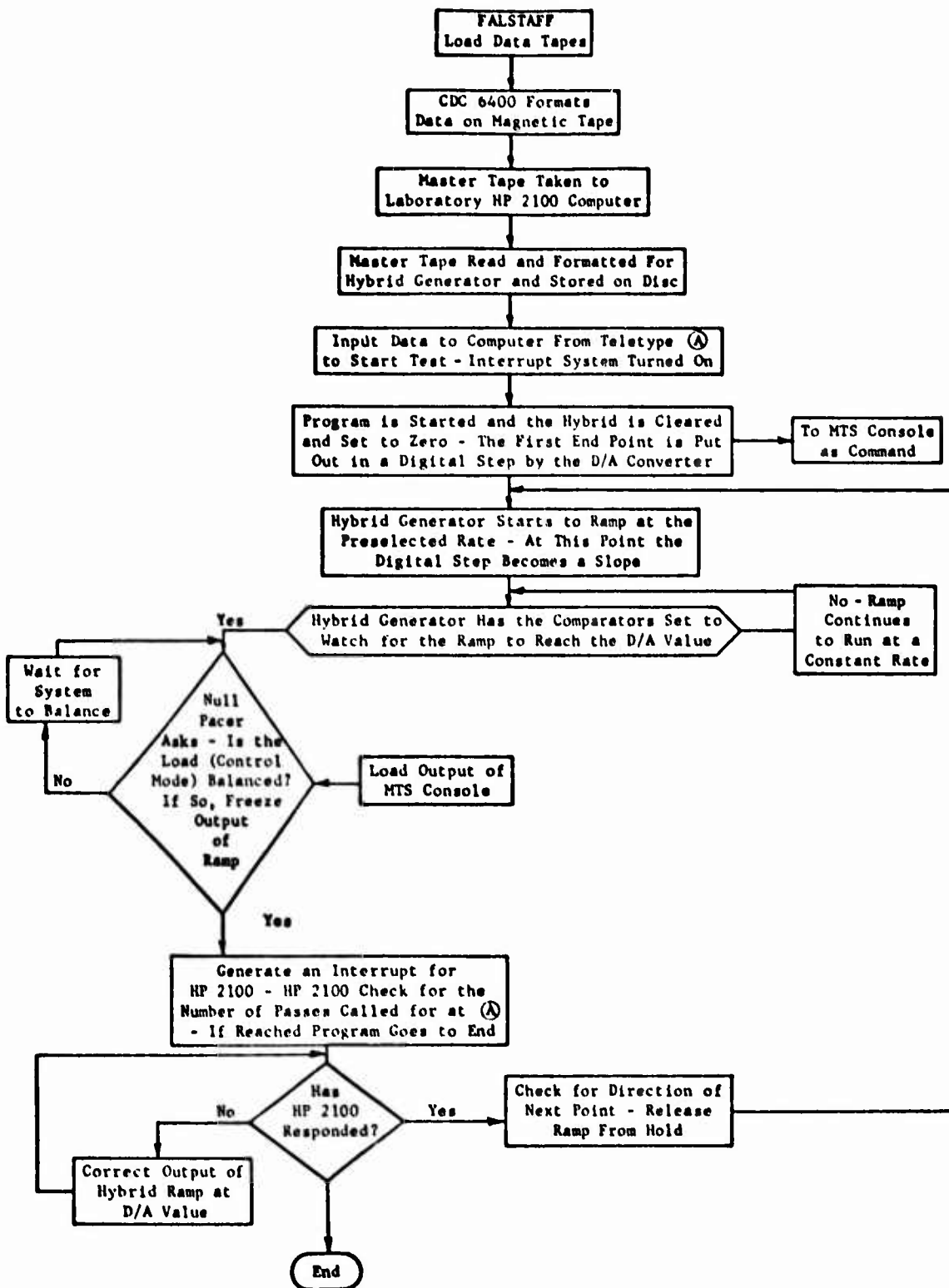


Figure A5 \_ PROGRAM CONTROL CYCLE

it possible to determine specimen bending and buckling (if any existed) and to confirm that dynamic loads matched static calibration loads.

#### Bending Check

Strain gage data were obtained at incremental load steps for loads to an equivalent of 38 ksi (262 MPa) maximum and -19 ksi (131 MPa) minimum. Data were obtained for three loading cycles. The strain-load data were submitted to a linear regression analysis with resulting  $R^2$  static values ranging from 1.000 to .9994. Strain values were computed for the load equivalent of 30 ksi (206.85 MPa) gross stress. Analysis of the strain values indicated that the maximum error due to specimen bending was 1.45 percent. Analysis of the compressive load data indicated that no buckling could be detected.

#### Static-Dynamic Loads Check

Comparison of strain gage output and calibrated load cell output indicated a maximum axial load error of 1.33 percent at 38 ksi (262 MPa) static load. Application of cyclic loads at the same level provided the same strain outputs.

#### FALSTAFF Loads Check

The specimen was subjected to FALSTAFF loads cycling and ramp rate and MTS unit controls were adjusted so that fatigue machine load output matched the command signal (reference Figure A6). The controls were not changed during the rest of the test program and the mean cyclic rate was determined to be 10.5 Hz.

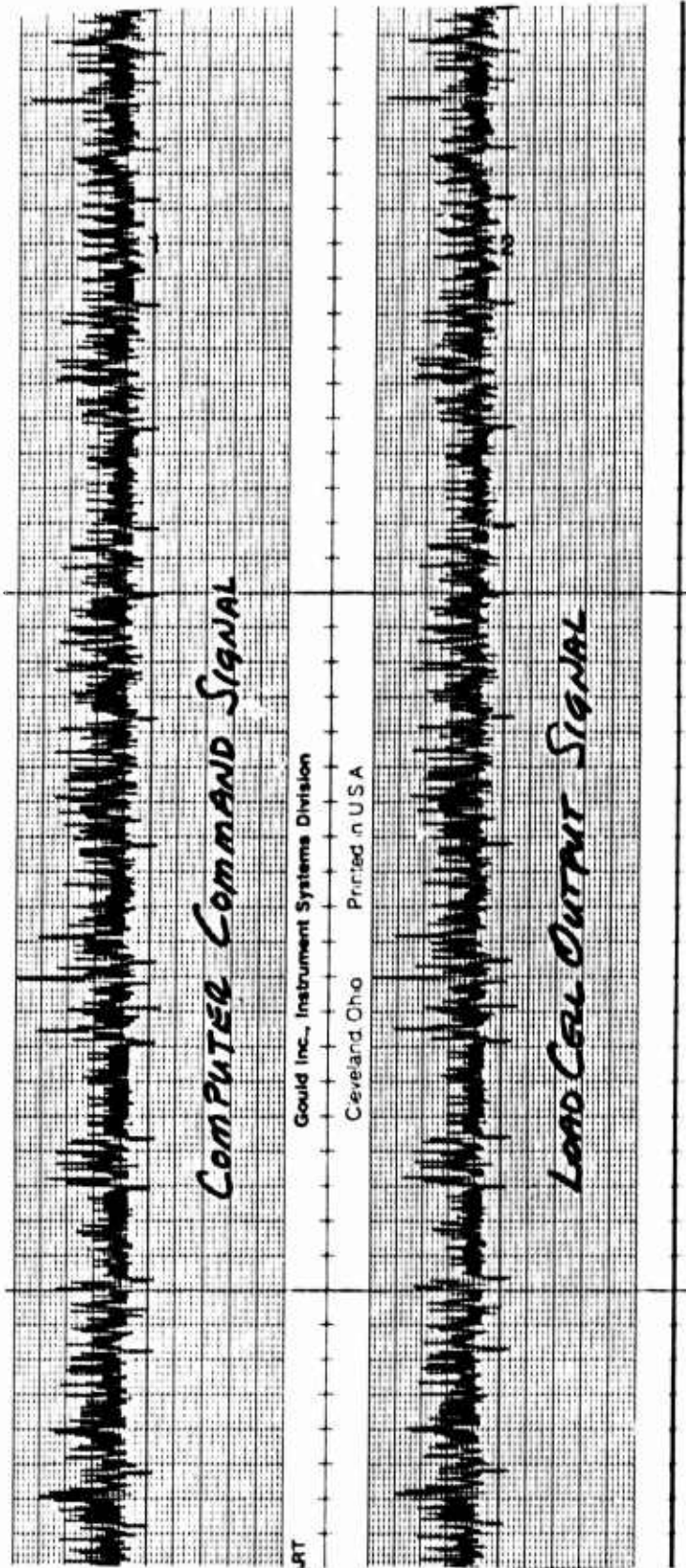


Figure A6 - COMPUTER COMMAND AND LOAD CELL SIGNAL COMPARISON FOR A PORTION OF THE TEST ON SPECIMEN 1F40

## TEST RESULTS

### Fatigue Test Program

Fatigue test specimens, as supplied by Metcut Research Associates Inc. were selected at random. The initial specimen 1F37 was cycled at a reference (gross) stress level of FALSTAFF spectrum (Step 32) of 31 ksi (213.7 MPa) and testing was discontinued with no failure after 11,285 flights. Specimen 1F40 was cycled at a reference stress of 34 ksi (234.4 MPa) and failed at 9728 flights. The latter reference stress was then approved by the Project Monitor for use on the remaining five fatigue specimens. A summary of the fatigue test data is presented in Table A5 and detailed data sheets are included as Figure A9. Examples of typical failure surfaces are shown in Figures A7 and A8. In all cases, fatigue failures initiated at the open hole near the sheet mid-thickness.

### Tensile Test Program

Tensile coupons provided by Metcut Research were tested in the Mechanical Test Laboratory on August 4, 1977. Tests were conducted in a Baldwin 60,000-pound (266.890 N) capacity Universal test machine. Room temperature was 69 F (21 C) and the relative humidity was 60 percent. The loading rate was controlled at 100 ksi/min. (689.5 MPa/min). The results of the tensile tests are presented in Table A6.

## SUMMARY AND CONCLUSIONS

Because of the care taken to insure that the FALSTAFF spectrum had been carefully reproduced and continuous checks made during the setup procedure, it is believed that the fatigue data are truly representative of the lives that can be expected for this test condition. This is confirmed by the low standard deviation for the data (well within normally obtained values). It is expected that the Phase II results will yield results of similar quality. As a result of this phase, all participating nations should be encouraged to continue with Phase II of the program.



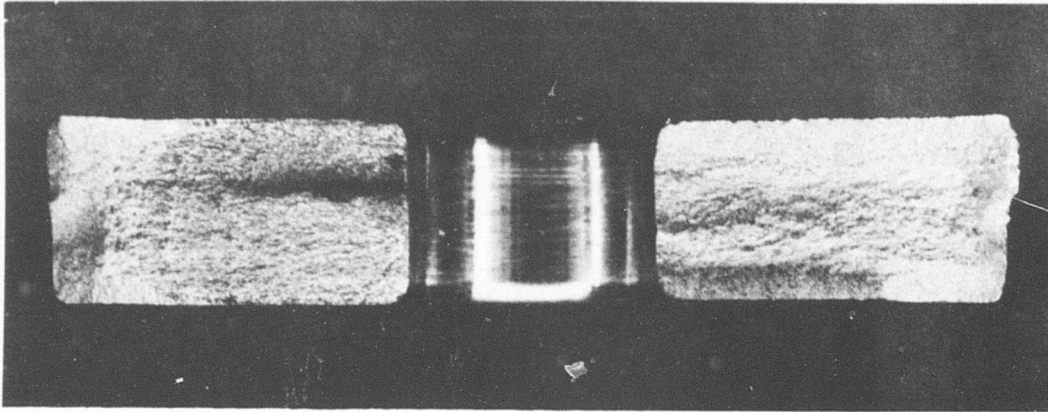


Figure A7 - FAILURE SURFACE OF SPECIMEN 1F64

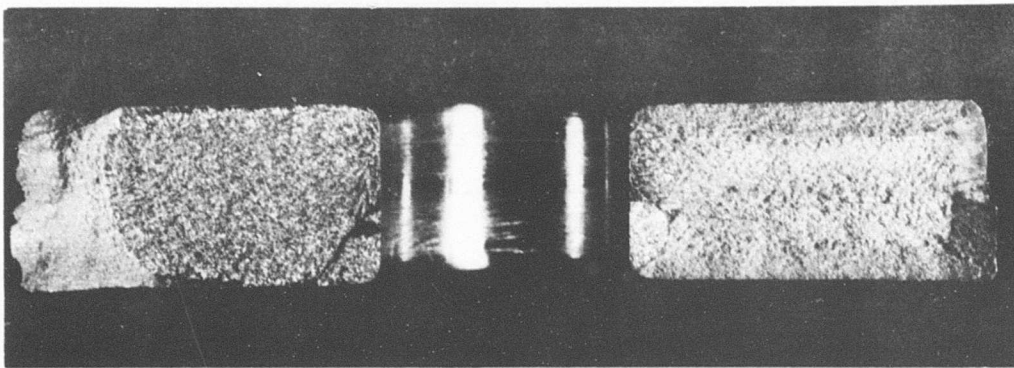
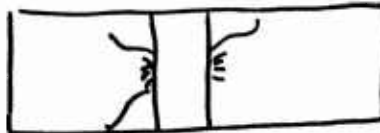


Figure A8 - FAILURE SURFACE OF SPECIMEN 1F10

**AIR FORCE/AFML - METCUT RESEARCH SPONSORED  
AGARD CRITICALLY LOADED HOLE TECHNOLOGY PROGRAM**

**TESTS CONDUCTED BY: BATTELLE'S COLUMBUS LABORATORIES  
STRUCTURAL MATERIALS AND TRIBOLOGY SECTION  
STRUCTURAL FATIGUE LABORATORY**

1. Date of Test: Start 7/12/77 End 7-14-77
2. Manufacture/Model of Fatigue Test Machine: MTS 20KIP
3. Test Temperature: 68 °F (~~20~~ °C)
4. Relative Humidity: 56 (%)
5. Reference (Gross) Stress Level of FALSTAFF Spectrum (Step 32)  
34 ksi (234.4 MPa)
6. Specimen Identification: 1-F-40
7. Specimen Bending at Minimum Load: NONE %
8. Specimen Bending at RMS Mean Load: 1.45 %
9. RMS Mean Cyclic Frequency: 10.5 Hz
10. Number of Flights to Initial Visible Crack: 9128 Flights
11. Size of Initial Visible Crack: 0.25 (1/4) in. (1.27 mm)
12. Number of Flights to Catastrophic Failure: 9728 Flights
13. Fatigue-Crack-Initiation Site: IN HOLE AT MID THICKNESS  
- BOTH SIDES



Sketch

14. Description of Abnormalities: \_\_\_\_\_
15. Description of Buckling Restraint (If Used): NONE

Figure A9 - DATA SHEETS

AIR FORCE/AFML - METCUT RESEARCH SPONSORED  
AGARD CRITICALLY LOADED HOLE TECHNOLOGY PROGRAM

TESTS CONDUCTED BY: BATTELLE'S COLUMBUS LABORATORIES  
STRUCTURAL MATERIALS AND TRIBOLOGY SECTION  
STRUCTURAL FATIGUE LABORATORY

1. Date of Test: Start 7-14-77 End 7/16/77
2. Manufacture/Model of Fatigue Test Machine: MITS. 20KIP
3. Test Temperature: 68 °F ( 20 °C)
4. Relative Humidity: 55 (%)
5. Reference (Gross) Stress Level of FALSTAFF Spectrum (Step 32)  
34 ksi ( 234.4 MPa)
6. Specimen Identification: 1 F 23
7. Specimen Bending at Minimum Load: NONE %
8. Specimen Bending at RMS Mean Load: 1.45 %
9. RMS Mean Cyclic Frequency: 10.5 Hz
10. Number of Flights to Initial Visible Crack: — Flights
11. Size of Initial Visible Crack: — in. ( — mm)
12. Number of Flights to Catastrophic Failure: 9373 Flights
13. Fatigue-Crack-Initiation Site: IN HOLE NEAR MID THICKNESS



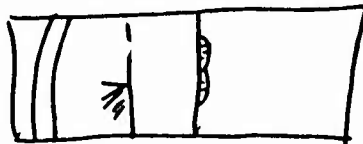
Sketch

14. Description of Abnormalities: \_\_\_\_\_
15. Description of Buckling Restraint (If Used): \_\_\_\_\_

AIR FORCE/AFML - METCUT RESEARCH SPONSORED  
AGARD CRITICALLY LOADED HOLE TECHNOLOGY PROGRAM

TESTS CONDUCTED BY: BATTELLE'S COLUMBUS LABORATORIES  
STRUCTURAL MATERIALS AND TRIBOLOGY SECTION  
STRUCTURAL FATIGUE LABORATORY

1. Date of Test: Start 7/18/76 End 7/20/76
2. Manufacture/Model of Fatigue Test Machine: MTS 20KIP
3. Test Temperature: 68 °F ( 20 °C)
4. Relative Humidity: 55 (%)
5. Reference (Gross) Stress Level of FALSTAFF Spectrum (Step 32)  
34 ksi ( 234.4 MPa)
6. Specimen Identification: IF64
7. Specimen Bending at Minimum Load: NONE %
8. Specimen Bending at RMS Mean Load: 1.45 %
9. RMS Mean Cyclic Frequency: 10.5 Hz
10. Number of Flights to Initial Visible Crack: — Flights
11. Size of Initial Visible Crack: — in. ( — mm)
12. Number of Flights to Catastrophic Failure: 8824 Flights
13. Fatigue-Crack-Initiation Site: IN HOLE NEAR MID THICKNESS



Sketch

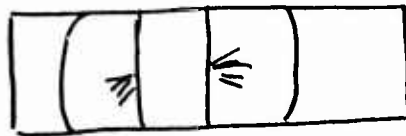
14. Description of Abnormalities: \_\_\_\_\_
15. Description of Buckling Restraint (If Used): NONE

Figure A9 - DATA SHEETS (continued)

AIR FORCE/AFML - METCUT RESEARCH SPONSORED  
AGARD CRITICALLY LOADED HOLE TECHNOLOGY PROGRAM

TESTS CONDUCTED BY: BATTELLE'S COLUMBUS LABORATORIES  
STRUCTURAL MATERIALS AND TRIBOLOGY SECTION  
STRUCTURAL FATIGUE LABORATORY

1. Date of Test: Start 7/20/77 End 7/22/77
2. Manufacture/Model of Fatigue Test Machine: M.T.S. 20K1P
3. Test Temperature: 68° °F ( 20 °C)
4. Relative Humidity: 55 (%)
5. Reference (Gross) Stress Level of FALSTAFF Spectrum (Step 32)  
34 ksi ( 234.4 MPa)
6. Specimen Identification: 1 F 77
7. Specimen Bending at Minimum Load: NONE %
8. Specimen Bending at RMS Mean Load: 1.45 %
9. RMS Mean Cyclic Frequency: 10.5 Hz
10. Number of Flights to Initial Visible Crack: 9297 Flights
11. Size of Initial Visible Crack: 0.03 in. ( 0.76 mm)
12. Number of Flights to Catastrophic Failure: 9572 Flights
13. Fatigue-Crack-Initiation Site: IN HOLE NEAR MID THICKNESS



Sketch

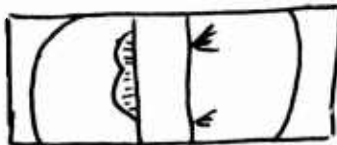
14. Description of Abnormalities: \_\_\_\_\_
15. Description of Buckling Restraint (If Used): NONE

Figure A9 -DATA SHEETS (continued)

**AIR FORCE/AFML - METCUT RESEARCH SPONSORED  
AGARD CRITICALLY LOADED HOLE TECHNOLOGY PROGRAM**

**TESTS CONDUCTED BY: BATTELLE'S COLUMBUS LABORATORIES  
STRUCTURAL MATERIALS AND TRIBOLOGY SECTION  
STRUCTURAL FATIGUE LABORATORY**

1. Date of Test: Start 7/27/77 End 7/29/77
2. Manufacture/Model of Fatigue Test Machine: MTS 20 K1/2
3. Test Temperature: 68° or (20 °C)
4. Relative Humidity: 55 (%)
5. Reference (Gross) Stress Level of FALSTAFF Spectrum (Step 32)  
34 ksi (234.4 MPa)
6. Specimen Identification: IF 85
7. Specimen Bending at Minimum Load: NONE %
8. Specimen Bending at RMS Mean Load: 1.45 %
9. RMS Mean Cyclic Frequency: 10.5 Hz
10. Number of Flights to Initial Visible Crack: 9835 Flights
11. Size of Initial Visible Crack: 0.20 in. (0.51 mm)
12. Number of Flights to Catastrophic Failure: 10929 Flights
13. Fatigue-Crack-Initiation Site: IN HOLE NEAR MIDTHICKNESS



Sketch

14. Description of Abnormalities: \_\_\_\_\_

15. Description of Buckling Restraint (If Used): NONE

Figure A9 - DATA SHEETS (continued)

AIR FORCE/AFML - METCUT RESEARCH SPONSORED  
AGARD CRITICALLY LOADED HOLE TECHNOLOGY PROGRAM

TESTS CONDUCTED BY: BATTELLE'S COLUMBUS LABORATORIES  
STRUCTURAL MATERIALS AND TRIBOLOGY SECTION  
STRUCTURAL FATIGUE LABORATORY

1. Date of Test: Start 7-30-77 End 8-1-77
2. Manufacture/Model of Fatigue Test Machine: M.T.S. 20 KIP
3. Test Temperature: 68 °F ( 20 °C)
4. Relative Humidity: 56 (%)
5. Reference (Gross) Stress Level of FALSTAFF Spectrum (Step 32)  
34 ksi ( 234.4 MPa)
6. Specimen Identification: 1-F-10
7. Specimen Bending at Minimum Load: NONE %
8. Specimen Bending at RMS Mean Load: 1.45 %
9. RMS Mean Cyclic Frequency: 10.5 Hz
10. Number of Flights to Initial Visible Crack: — Flights
11. Size of Initial Visible Crack: — in. ( — mm)
12. Number of Flights to Catastrophic Failure: 8,364 Flights
13. Fatigue-Crack-Initiation Site: IN HOLE NEAR MIDTHICKNESS



Sketch

14. Description of Abnormalities: \_\_\_\_\_
15. Description of Buckling Restraint (If Used): NONE

TABLE A1

MECHANICAL PROPERTIES

<u>Lot No.</u>	<u>No. of Tests</u>	<u>Tensile Strength, ksi</u>		<u>Yield Strength, ksi</u> **		<u>Elong. in 2 in. or 4D</u>		<u>Conductivity (Min.)</u>
		<u>Max.</u>	<u>Min.</u>	<u>Max.</u>	<u>Min.</u>	<u>Max.</u>	<u>Min.</u>	
302-791	3	85.9	85.4	80.2	79.3	12.0	12.0	35.4

\* When two or more tests per lot are made, the highest and lowest values are reported for each property determined. Single tests are reported in minimum columns.

\*\* Kips per square inch one Kip equals one thousand pounds.

CHEMICAL COMPOSITION FOR 7050-T76 ALLOY

	<u>Maximum</u>	<u>Minimum</u>
Silicon	0.12	
Iron	0.15	
Copper	2.6	2.0
Manganese	0.10	
Magnesium	2.6	1.9
Chromium	0.04	
Zinc	6.7	5.7
Titanium	0.06	
Zirconium	0.15	0.08
Others, each total	0.05	0.15



TABLE A2

MACHINING CONDITIONS USED FOR  
MILLING THE SPECIMEN BLANKS

Cutter Diameter, in.	6
Tool Material	K68 Carbide
Feed, in./tooth	.004
Cutting Speed, ft./min.	1200
Tool Wear, max.	.006
No. of Teeth	8
Fluid	20:1 Soluble Oil

TABLE A3

MACHINING CONDITIONS USED FOR  
MILLING THE SPECIMEN CONTOUR

Cutter Diameter, in.	1
Tool Material	M2 HSS
Feed, in./tooth	.0014
Cutting Speed, rpm	950
Tool Wear	.006
No. of Teeth	6
Fluid	Dry

TABLE A4

## AGARD SMP CRITICALLY LOADED HOLE TECHNOLOGY SPECIMEN NUMBER IDENTIFICATION

	<u>Belgium</u>	<u>France</u>	<u>Germany</u>	<u>Italy</u>	<u>Netherlands</u>	<u>Sweden</u>	<u>Turkey</u>	<u>United Kingdom</u>	<u>United States</u>	
Tensile	1T4	1T6	1T1	1T22	1T2	1T9	1T27	1T3	1T19	
	1T10	1T11	1T8	1T23	1T13	1T12	1T29	1T5	1T24	
	1T17	1T14	1T21	1T26	1T15	1T16	1T33	1T18	1T30	
Fatigue (with hole)	1F17	1F48	1F6	1F35	1F31	1F9	1F4	1F20	1F23	
	1F32	1F50	1F16	1F43	1F33	1F29	1F62	1F22	1F40	
	1F38	1F74	1F54	1F57	1F34	1F73	1F63	1F28	1F64	
	1F45	1F101	1F100	1F61	1F47	1F96	1F72	1F83	1F77	
	1F81	1F109	1F103	1F65	1F67	1F97	1F75	1F113	1F85	
	1F99	1F118	1F105	1F82	1F92	1F107	1F78	1F115	1F95	
	1F112	1F119	1F106	1F84	1F108	1F114		1F121	1F104	
	1F123	1F120	1F124		1F117	1F116		1F122		
	Fatigue (without hole)	1F94	1F42	1F12	1F98	1F66	1F52		1F93	1F36
	Extra									1F37
									1F10	
									1F24	

TABLE A5  
FATIGUE TEST RESULTS\*

Specimen Number	Flights to Initial Crack	Initial Crack Size, inch (mm)	Flights to Failure
1F40	9128	0.05 (1.27)	9728
1F23	--	--	9373
1F64	--	--	8824
1F77	9297	0.03 (0.76)	9572
1F85	9835	0.02 (0.51)	10929
1F10	--	--	8364
Mean Life			9465
Standard Deviation			878

\* FALSTAFF reference stress - 34 ksi (234.4 MPa).

TENSILE TEST RESULTS

Specimen Number	Yield Strength, ksi (MPa)	Ultimate Strength, ksi (MPa)	Elongation, percent (2-inch gage)
1T24	80.79 (557.0)	84.40 (581.9)	11.5
1T30	80.60 (555.7)	84.34 (581.5)	11.5
1T19	80.22 (553.1)	84.15 (580.2)	11.0
Average	80.54 (555.3)	84.30 (581.2)	11.33
Standard Deviation	.29	.13	.29

EVALUATION OF TAPERED BLADE CUTTER

## INTRODUCTION

The production of tapered holes is a principal cost in airframe construction using tapered interference-fit fasteners. A tapered blade cutter has been designed and produced by Deutsch as a means of producing a tapered hole in a single operation. This tapered blade cutter represents a possible approach toward producing interference fit fastener holes of the required dimensional and metallurgical quality at a lower cost than can be accomplished with currently used tooling.

This program evaluated a one-piece cutter designed to produce in a single operation a tapered hole with an integral countersink to closely controlled dimensional and quality limits. The material used was 7175-T73511 aluminum alloy, 5/16 in. thick. The holes were drilled into two panels, each 5/16 in. thick for a total material thickness of 5/8 in. This material and fastener geometry represented a major application for fasteners in the C-5A wing structure design.

## DISCUSSION

In the drilling of tapered holes, the blade cutter consistently produced chatter in both the tapered portion and countersink area of the hole. A picture of this condition can be seen in Figure A10. The drilling conditions used to produce the hole in Figure A10 were:

Cutting Speed: 1800 rpm  
Feed Rate: .002 ipr  
Coolant: Forced Air, 80 psi

During the testing phase of the cutter evaluation, various speeds and feeds were used. In each case, the surface produced was similar to the surface shown in Figure A10.

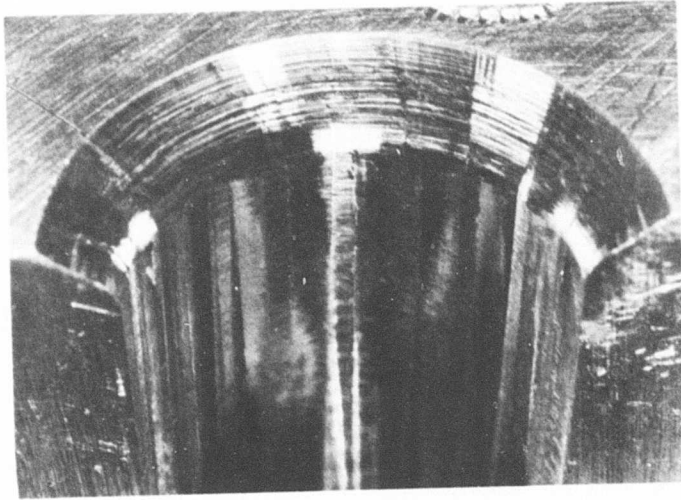
Figure A11 shows a hole produced by the drill and taper ream procedure currently used for producing tapered holes. There was no evidence of other surface irregularities using the current techniques.

During the drilling tests, the tapered blade cutter was etched approximately every 100 holes to remove build up of the aluminum material. After etching, the cutter would produce approximately five holes of an acceptable visual surface condition (without chatter). Starting with hole

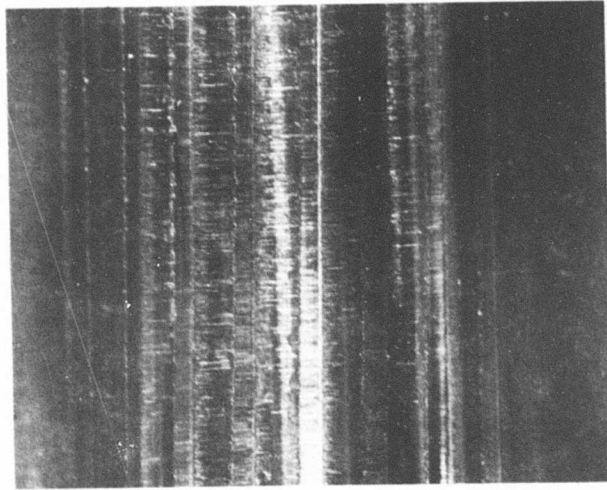
five or six, the blade cutter would begin to chatter in a manner similar to Figure A10. After drilling and etching 400 holes, the blade cutter was photographed both before and after etching. Figure A.2 shows the blade cutter before etching and Figure A13 after the aluminum build up had been removed. Metallurgically, the surface condition of the holes produced with the blade cutter immediately prior to etching did not show a great deal of distortion or deformation. Figure A14 shows the metallurgical condition of hole 400 both parallel and perpendicular to the hole axis.

#### SUMMARY

Due to the high degree of chatter produced during the drilling operation with the tapered blade cutter, it is not recommended for use in a production environment. Because of the acceptable nature of the metallographic examination as seen in Figure A14, further work should be done in the area of cutter geometry to eliminate the chatter condition. The holes produced seem to be acceptable except for the chatter produced during manufacturing.



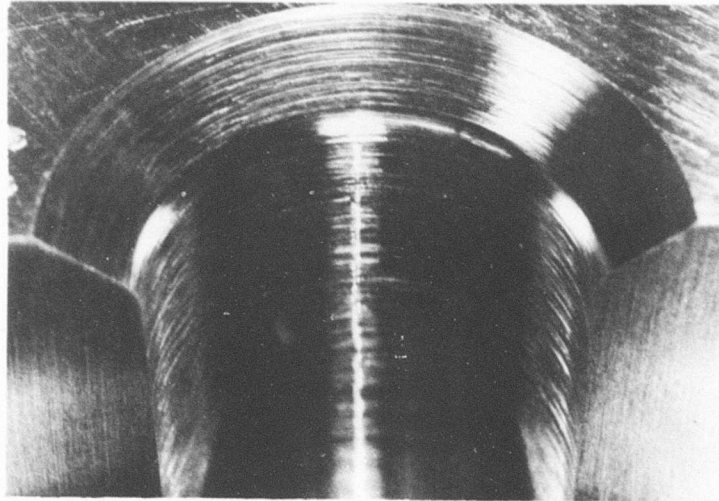
Countersink + Transition Radius



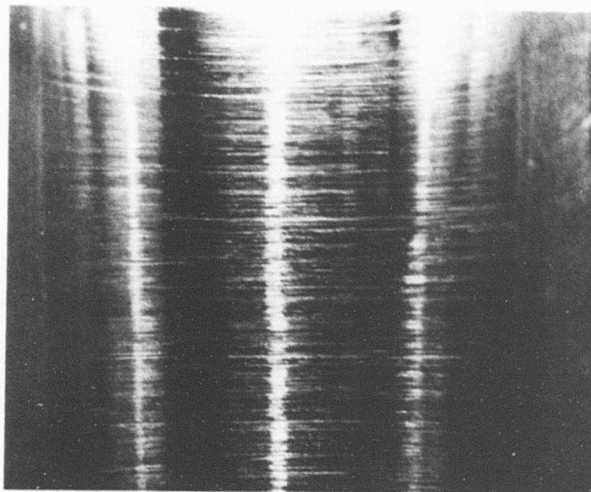
Tapered Hole Surface

Figure A10 - TYPICAL SURFACE CONDITION PRODUCED  
BY TAPER BLADE CUTTER



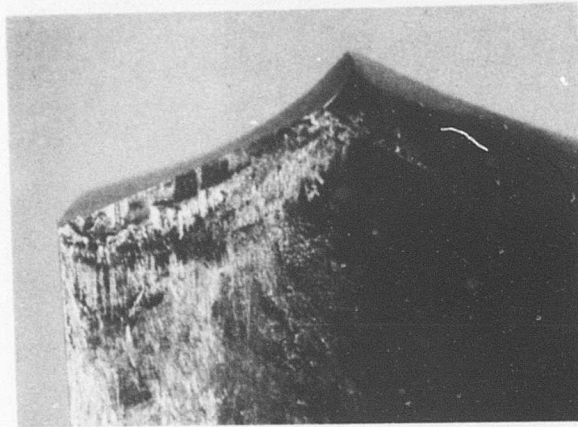


Countersink + Transition Radius

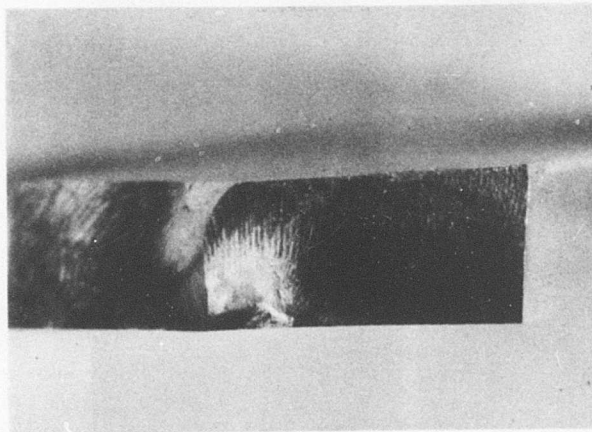


Tapered Hole Surface

Figure A11 - TYPICAL SURFACE CONDITION PRODUCED  
BY STANDARD TECHNIQUES

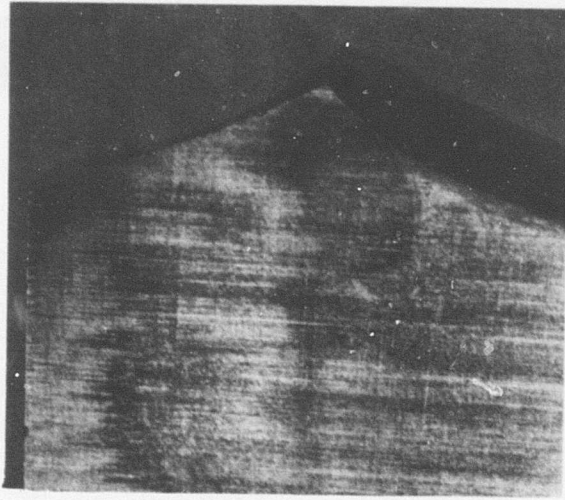


Side View

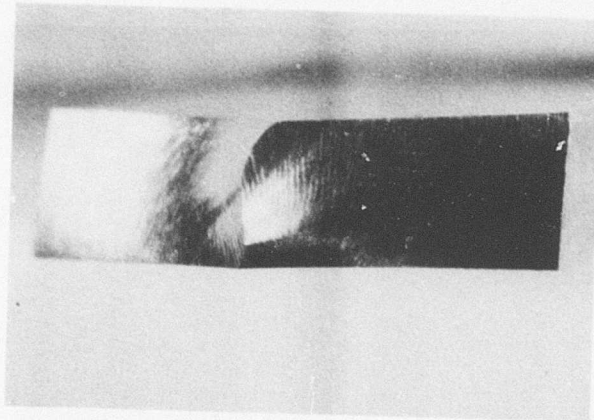


Top View

Figure A12 - PHOTOGRAPHS OF BLADE CUTTER PRIOR TO ETCHING SHOWING BUILDUP

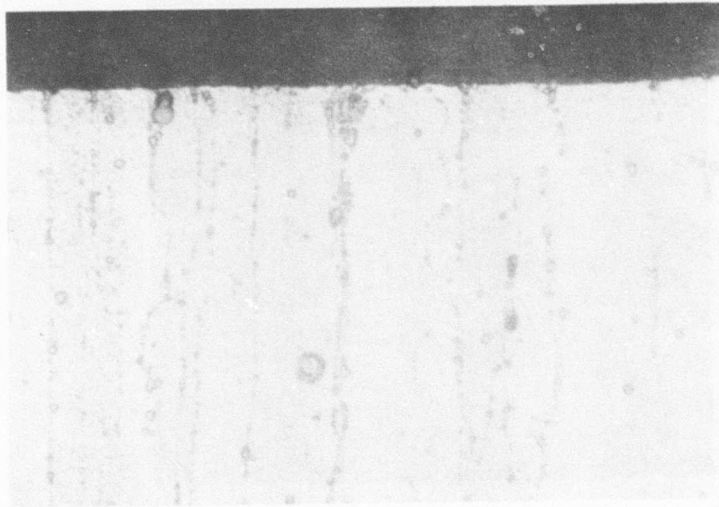


Side View

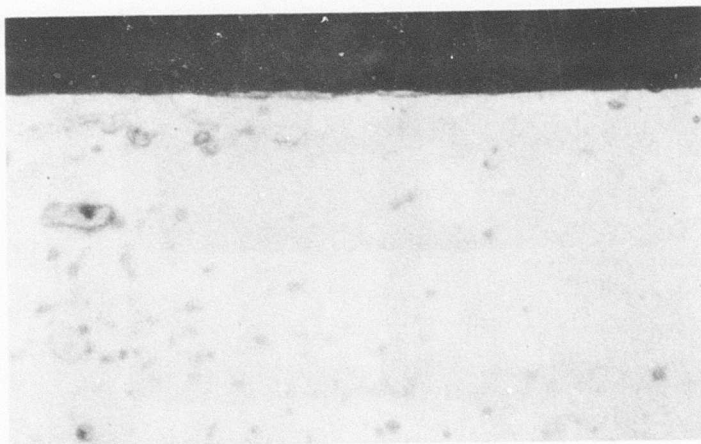


Top View

Figure A13 - PHOTOGRAPHS OF BLADE CUTTER AFTER  
ETCHING OF BUILDUP



Parallel to Hole Axis



Perpendicular to Hole Axis

Figure A14 - PHOTOMICROGRAPHS OF A HOLE PRODUCED  
BY A TAPERED BLADE CUTTER



UNCLASSIFIED

AD BD 29580

AUTHORITY:

AFWA L

6 OCT 81



UNCLASSIFIED